



University of
Nottingham

UK | CHINA | MALAYSIA

Structure-Function Relationship of DEF6

By

Huaitao Cheng BSc

Thesis submitted to the University of Nottingham for
the degree of Doctor of Philosophy

September 2017

Acknowledgements

First and foremost, I would like to express my sincere gratitude to my supervisor Prof. Fred Sablitzky. His support, guidance and encouragement were essential and over the years he protected me like a father.

I would also like to thank Dr. Peter Jones, Dr. Martin Gering and Dr. Sally Wheatley for their kind help and guidance.

My dear colleagues Deniz, Maha, Chen, Tamil, Kerry, Naz, Xiaou, and our project students Mike, George, Sara and Chris, thanks for you supporting me when I was down and weary. You made my PhD life cheerful.

To my mum and dad, thanks is not enough to express my gratitude. Your unconditional love, trust and support motivated me and helped me to overcome so many difficulties.

Finally, I would like to dearly cherish my memory of my grandpa. He left us when I was in the first year of my PhD study. In order to make me study without worries, my family hid this terrible news from me just telling me he is fine in his home. I'm sorry grandpa, I know that people will die but I didn't know one day you would leave us. I will never forget you and I will always love you!

Abstract

DEF6 (Differentially Expressed in FDCP 6, also known as IBP and SLAT) is critical for the development of autoimmune disease and cancer. In T cells, DEF6 participates in TCR-mediated signalling determining T helper cell-mediated immune responses. In addition, DEF6 acts as a guanine nucleotide exchange factor (GEF) for Rho GTPases facilitating F-actin assembly and stabilisation of the immunological synapse (IS). However, DEF6 is also a component of mRNA processing bodies (P-bodies) linking it to mRNA metabolism. DEF6 and its only relative switch-associated protein-70 (SWAP70) share a common domain structure that is highly conserved from human to *trichoplax adhaerens* suggesting an ancestral function that is distinct from its role in T cell immunity. To further dissect the structure-function relationship of DEF6, a comprehensive analysis of wild type and mutant DEF6 proteins expressed in either COS7 or Jurkat T cells was conducted. The results demonstrate that DEF6 can adopt multiple conformations that result in different cellular localisations and functions. Post translational modifications such as phosphorylation result in conformational change liberating functional domains that are masked in the native state of DEF6. ITK phosphorylation of Try210/222 liberates the N-terminal end and to a certain extent also the C-terminal coiled coil domain of DEF6 resulting in P-body colocalisation. In fact, the N-terminal 45 amino acids of DEF6 that forms two Ca²⁺-binding EF hands are sufficient to target P-bodies. The coiled coil domain in conjunction with the N-terminal end is facilitating dimerisation and oligomerisation of DEF6 likely to be essential for GEF activity which was mapped to amino acids 537-590, a region that includes the C-terminal end of the coiled coil domain. Mutant proteins that unleashed the coiled coil domain spontaneously aggregated forming large structures in the cytoplasm. These aggregates trapped proteins such as the P-body component DCP1. In some cases, aggregates appeared to function like prions enforcing conformational change onto wild type as well as mutant DEF6 proteins. Ectopically expressed DEF6 colocalised with F-actin in cell protrusions as well as with P-bodies in resting Jurkat T cells. Upon TCR-mediated activation, wild type and several

mutant DEF6 proteins were recruited to the IS. However, while wild type DEF6 localised to the central supramolecular activation cluster (cSMAC), mutant DEF6 with disrupted coiled coil domain were present in the outer ring of IS suggesting that recruitment of DEF6 to the cSMAC depends upon a functional coiled coil domain. In contrast, recruitment to the IS of DEF6 that seemed to be mediated through cellular protrusion contacting the antigen presenting cell was independent of both the N-terminal end and a functional coiled coil domain. Taken together, the data presented provide evidence that DEF6 is more than a GEF linking TCR-mediated signalling with F-actin organisation and control of mRNA metabolism.

Abbreviations

Ago	Argonaute Protein
APC	Antigen-Presenting Cell
ARP2/3	Actin-Related Protein 2/3 complex
BSA	Bovine Serum Albumin
CC	Coiled coil
Cdc42	Cell division cycle 42
DCP1	Decapping protein one
DEF6	Differentially Expressed in FDCP 6
DH domain	Dbl homology domain
DHL	Dbl homology-like domain
DHR	Dock homology region
Dock	Dedicator of cytokinesis
DSH	DEF6-SWAP70 homology
EAE	Experimental Autoimmune Encephalomyelitis
EAU	Experimental Autoimmune Uveitis
EDC3	Enhancer of mRNA-decapping protein 3
EDC4	Enhancer Of MRNA Decapping 4
F-actin	Filamentous Actin
FBS	Foetal Bovine Serum
FH domain	Formin Homology domain
GAP	GTPase-activating protein
GDI	Guanine nucleotide-dissociation inhibitor
GDP	Guanosine Diphosphate

GEF	Guanine nucleotide exchange factor
GTP	Guanosine Triphosphate
GTPase	Guanosine Triphosphate Hydrolase
IBP	IRF-4-binding protein (alternative name for DEF6)
ICAM	Intercellular Adhesion Molecules
IgG	Immunoglobulin G
IL-	Interleukin
IP ₃	Inositol 3,4,5-triphosphate
IRF-4	Interferon regulatory factor-4
IS	Immunological Synapse
ITAM	Immunoreceptor tyrosine-based activation motif like
ITK	IL2-INDUCIBLE T-cell kinase
LCK	Lymphocyte specific tyrosine kinase
LFA	Leukocyte Function-associated Antigen
LIMK	LIM domain kinase
MAPK	Mitogen-activated protein kinase
MHC	Major Histocompatibility Complex
MIP	Macrophage Inflammatory Protein
MRCK	Myotonic dystrophy kinase-related CDC42-binding kinase
NFAT	Nuclear Factor of Activated T cells
NLS	Nuclear Localization Sequence
O/N	Overnight
OSCC	Oral Squamous Cell Carcinoma
P-body	Processing Body
PAK	p21-activated kinase
PBS	Phosphate-Buffered Saline

PH domain	Pleckstrin homology domain
PI3K	Phosphatidylinositol 3-kinase
PIP ₃	Phosphatidylinositol 3, 4, 5, Triphosphate
RA	Rheumatoid Arthritis
Rac1	Ras-Related C3 Botulinum Toxin Substrate 1
RhoA	Ras Homolog Gene Family, member A
ROCK	Rho-associated Serine/Threonine Kinases
SDS-PAGE	Sodium Dodecyl Sulphate–Polyacrylamide Gel Electrophoresis
SLAT	SWAP70-like attenuator of T cells (alternative name for DEF6)
SLE	Systemic Lupus Erythematosus
SMAC	Supramolecular Activation Cluster
cSMAC	Central SMAC
pSMAC	Peripheral SMAC
dSMAC	Distal SMAC
SWAP70	Switch-Associated Protein-70
TCR	T cell receptor
TNF	Tumor Necrosis Factor
WASP	Wiskott–Aldrich Syndrome Protein
WAVE	WASP-family Verprolin-homologous Protein

List of Contents

Chapter 1 Introduction	1
1.1 DEF6 functions as a guanine nucleotide exchange factor for Rho-GTPases.	2
1.1.1 DEF6 and Rho-GTPases	2
1.1.2 A general mechanism of guanine nucleotide exchange by GEFs to Rho GTPases	4
1.1.3 DEF6 functions as a GEF protein	5
1.1.4 DEF6 protein structure	7
1.1.4.1 DEF6 and its only relative SWAP70 are highly conserved	7
1.1.4.2 DEF6 and SWAP70 are atypical GEFs	7
1.1.4.3 PH and DH domain function	8
1.1.5 Vav, a prototype Dbl GEF, is activated through conformational change.....	10
1.1.5.1 Is the model of VAV also applicable to DEF6?	11
1.2 DEF6 function in the immune system	13
1.2.1 DEF6 localises to and enhances stability of immunological synapse	13
1.2.2 DEF6 is critical for the development of autoimmune diseases.....	16
1.3 DEF6 is highly expressed in cancer cells and promotes its development	18
1.4 DEF6 phosphorylation at Tyr210/222 results in colocalisation with P- bodies.....	21
1.4.1 Core function of P-bodies is mRNA degradation	21
1.4.2 Assembly of P-body components requires EDC4 as a scaffold for the decay machinery and Q/N rich protein interactions	22
1.4.3 P-body size and abundance varies during cell cycle.....	24
1.5 Aims and Objectives	25
Chapter 2 Materials and Methods	26

2.1 Mammalian cell culture	26
2.1.1 Cell lines	26
2.1.2 Cell culture media and solution	26
2.2 Bacterial cell culture	28
2.2.1 Competent Cells	28
2.2.2 Bacteria culture broth/agar	29
2.3 Antibiotics	29
2.4 DNA Materials.....	29
2.5 Bacteria technology	33
2.5.1 Bacteria freezing	33
2.5.2 Recovery of frozen bacteria	33
2.5.3 Cell transformation	33
2.5.4 Plasmid Miniprep (Sigma)	34
2.5.5 Plasmid Maxiprep (Sigma)	35
2.6 Nucleotide technology	37
2.6.1 DNA restriction enzyme digestion	37
2.6.2 DNA gel electrophoresis.....	37
2.6.3 DNA extraction from agarose gel	37
2.6.4 DNA ligation	38
2.6.5 Q5 Polymerase Chain Reaction (PCR), and StrataClone Blunt PCR Cloning (Agilent Technologies) to establish recombinant plasmids	38
2.6.6 QuikChange Lightning Multi Site-Directed Mutagenesis PCR (Agilent)	40
2.7 Mammalian cell culture.....	42
2.7.1 Passaging of Adherent Cells (COS7).....	42
2.7.2 Passaging of Cells growing in Suspension (Jurkat T cells and Raji B cells)	43
2.7.3 Cryopreservation of mammalian cell lines	43

2.7.4 Recovery of cells after cryopreservation	43
2.7.5 Transfection of COS7 cells	44
2.7.6 Transfection of Jurkat T cells	44
2.7.7 Jurkat T and Raji B cells conjugation	45
2.7.8 Cell fixation	45
2.7.9 Phalloidin staining of f-actin	46
2.7.10 Cell imaging	46

Chapter 3 Study of DEF6 Granule Formation: Colocalisation with P-bodies

versus DEF6 aggregation47

3.1 The N-terminal part of the DHL domain contains a Q-rich coiled coil domain.....	48
3.2 Substitution of highly conserved amino acid residues in the “a” and “d” position with prolines disrupt the coiled coil structure of DEF6.....	51
3.3 Proline mutants exhibited three types of distinct phenotypes but none of them colocalises with P-body.....	55
3.4 Arsenate treatment failed to induce colocalisation of the proline mutants with P-bodies	59
3.5 The coiled coil domain is dispensable for DEF6 granule formation and colocalisation with DCP1	61
3.6 N-terminal 45 amino acids of DEF6 are necessary and sufficient to spontaneously colocalise with P-bodies	65
3.7 The coiled coil domain facilitates DEF6 aggregation	68

3.8 Coiled coil-mediated DEF6 aggregations can be classified into three distinct groups according to structure/morphology and association with DCP1	75
3.8.1 Differential response of DEF6 aggregates to cellular stress	77
3.8.2 ITAM and coiled coil domains are both required for colocalisation with P-bodies under cellular stress conditions	82
3.8.3 Introduction of Y210/222E or Y210/222F mutations into $\Delta 0-104$ did not alter the morphology of aggregates but prevented the mutant proteins to completely colocalise with P-bodies under cellular stress condition.	85
3.9 The N- and C-terminal of DEF6 mediate interactions	88
3.10 LCK phosphomimic mutant Y133-144D forms aggregates that interact with DEF6 N-terminal truncated mutants	95
3.11 Summary of main findings.....	100
Chapter 4 Mapping DEF6 GEF function	101
4.1 Molecular organisation of actin assembly	102
4.1.1 F-actin polymerisation	102
4.1.2 The signalling network of CDC42, Rac1 and RhoA	104
4.1.3 Lamellipodia, Filopodia, Invadosome and Stress fibre.....	106
4.2 Proline mutations on several <i>a/d</i> positions within the coiled coil domain of DEF6 resulted in colocalisation with F-actin	108
4.3 Truncation mutants containing amino acids 537 to 590 of DEF6 are sufficient to label F-actin	110
4.3.1 F-actin colocalisation is dependent on the coiled coil domain suggesting that oligomerisation is required for F-actin binding	114

4.4 Coiled coil-mediated aggregation prevents DEF6 from colocalising with F-actin	115
4.5 H ₂ O ₂ treatment inducing PI3K activation resulted in DEF6/mutants labelling F-actin.....	118
4.5.1 H ₂ O ₂ treatment altered WT DEF6 and Δ0-104 to overlap with F-actin	118
4.5.2 Conformation of phosphomimic DEF6 mutants are resistant to H ₂ O ₂ -mediated protein modifications	120
4.5.3 Conformation of proline mutants Q407P-M410P and I428P-L431P are resistant to H ₂ O ₂ -mediated protein modifications but localisation of Q371P-A374P and K491P-L494P was altered.....	122
4.6 Summary of main finding.....	125
Chapter 5 DEF6 function in T cells.....	126
5.1 GEFs and F-actin are important for immunological synapse formation and function.....	127
5.2 WT DEF6, L533P-A536P, All-10 and Δ0-216-All-10 labelled F-actin in Jurkat T cells.....	130
5.3 Δ0-104, Δ0-216, DH2 and Y133/144D exhibited divers phenotypes in Jurkat T cells.....	133
5.4 The ITK phosphormimic mutant, Y210E/Y222E, formed granules co-localising with P-bodies but also appeared diffuse overlapping with F-actin.	135
5.5 Upon TCR-mediated activation, WT DEF6 is recruited to the IS concentrating in cSMAC.....	137
5.6 All-10, Δ0-216-All-10, L533P-A536P, DH2 and Δ0-216 mutants translocate to the IS but don't concentrate in cSMAC	139

5.7 WT DEF6 seems to be recruited to the IS through cell protrusion ruffling	143
5.8 Spontaneous granule formation and colocalisation of Y210E/Y222E with P-bodies in resting T cells seems reversed in activated T cells	145
5.9 Summary of main finding	147
Chapter 6 Discussion	148
6.1 Coiled coil-mediated aggregation	149
6.2 Coiled coil-mediated interaction of wild type DEF6	150
6.3 Coiled coil-mediated trapping or enforced conformational change	150
6.4 The coiled coil domain is dispensable for both granule formation and P-body localisation	151
6.5 The N-terminal 45 amino acids of DEF6 are sufficient for spontaneous P-bodies colocalisation	152
6.6 ITAM, PH and/or coiled coil domains facilitate cellular stress-induced P-body colocalisation	153
6.7 Both, N-terminal end and the coiled coil domain are mediating dimerisation and/ or oligomerisation of DEF6	154
6.8 F-actin labelling of DEF6 is regulated through the coiled coil domain	154
6.9 Amino acids 537 to 590 of DEF6 are sufficient to label F-actin in cell protrusions	155
6.10 How is the GEF activity of DEF6 controlled?	155
6.11 Overexpressed DEF6 in resting Jurkat T cells localises in cell protrusions	156

6.12 ITK phosphomimic mutant Y210/222E colocalises with P-bodies and F-actin in resting Jurkat cells	156
6.13 LCK phosphomimic mutant Y133/144D forms aggregates in Jurkat T cells	157
6.14 The coiled coil domain is important for DEF6 localisation in the cSMAC of the IS	157
6.15 Neither N-Terminus nor coiled coil domain is necessary for IS recruitment of DEF6	158
6.16 DEF6 recruitment to the IS appears to be mediated through cell protrusions initiated by APC conjugation with T cells	158
Conclusion	160
Reference	161
Appendix	179
8.1 Plasmid map	179
8.2 Wild Type DEF6 Full Length sequence	181
8.3 DNA sequencing results of DEF6 mutants	184-193
8.4 Additional images	194-216
8.5 Summary of DEF6/Mutants phenotypes	217-226

List of Figure

Fig. 1.1.0 The mechanism of Rho-GTPases' GDP- and GTP- binding state cycle	3
Fig. 1.2.0 GEFs accelerate GTPases nucleotide exchange	5
Fig. 1.3.0 Domain structure of GEFs.	9
Fig. 1.4.0 The activation module of Vav1.....	11
Fig. 1.5.0 Schematic of DEF6 signalling network in CD4+ T cells.....	15
Fig. 1.6.0 DEF6 protein expression in different cancer tissues	19
Fig. 1.7.0 Schematic diagram of P-body assembly	23
Fig. 3.1.1 Schematic diagram of zenithal and lateral view of a two- stranded coiled coil motif.....	49
Fig. 3.1.2 Predicted coiled coil domain of DEF6.....	50
Fig. 3.2.1 Comparison of the “a” and “d” positions within the coiled coil domain of DEF6 and SWAP70 across species from human to trichoplax	53
Fig. 3.2.2 Insertion of proline residues at selected a/d positions disrupts the coiled coil domain of DEF6	54-55
Fig. 3.3.0 GFP-tagged DEF6 proline mutants exhibited three types of cellular localisation in COS7 cells	57
Fig. 3.3.1 Q371P-A374P mutant granules are not colocalising with P- bodies ...	57
Fig. 3.4.0 Disruption of the coiled coil domain prevented arsenate induced granule formation	60

Fig. 3.5.0 Introduction of the ITK phosphomimic mutations Y210/222E results in colocalisation of proline mutants with P-bodies	62-63
Fig. 3.5.1 Y210/222E-L505P-A508P and Y210/222E-All-10 form granules that colocalise with DCP1	64
Fig. 3.6.0 The N-terminal 45 amino acids of DEF6 are necessary and sufficient for colocalisation with P-bodies	66
Fig. 3.6.1 The N-terminal 45 amino acids of DEF6 are sufficient for colocalisation with P-bodies	67
Fig. 3.7.1a Schematic representation of DEF6 N-terminal truncation and deletion mutants	69
Fig. 3.7.1b DEF6 N-terminal truncation and deletion mutants form large aggregates	70
Fig. 3.7.2a Schematic representation of DEF6 N-terminal truncation and deletion mutants	72
Fig. 3.7.2b The coiled coil domain of DEF6 facilitates aggregation	73
Fig. 3.7.3 Formation of large aggregates of DEF6 is abolished through proline mutations in the coiled coil domain	74
Fig. 3.8.0 Coiled coil-mediated aggregates of DEF6 form large structure that 'trap' DCP1	76-77
Fig. 3.9.0 Cellular stress induced through nocodazole treatment results in WT DEF6 colocalising with DCP1	79

Fig. 3.10.1 Cellular stress had no effect on formation of vesicle-like structures of DH2 and their ability to ‘trap’ DCP1	80
Fig. 3.10.2 Cellular stress had no effect on formation of large structures of Δ 0-216 and their ability to ‘trap’ DCP1	81
Fig. 3.10.3 Cellular stress results in complete colocalisation of Δ 0-104 structures with DCP1	82
Fig. 3.10.4 Cellular stress did not alter localisation of the ITAM or All-10 mutants	84
Fig. 3.11.1 Introduction of Y210/222E or Y210/222F mutations into Δ 0- 104 did not alter the morphology of aggregates that still partially overlapped with DCP1	86
Fig. 3.11.2 Introduction of Y210/222E or Y210/222F mutations into Δ 0- 104 prevented complete overlap with DCP1 under cellular stress conditions	87
Fig. 3.12.0 Interaction of DEF6 molecules through dimerisation and or oligomerisation	91
Fig. 3.12.1 Dimerisation and or oligomerisation of DEF6 can also be mediated through its N-terminal 108 amino acids.....	92
Fig. 3.13.0 DEF6 mutants Q371P-A374P, L442P-E445P, All-10 and DHL- N did not interact with mCherry-NLS-DEF6	94
Fig. 3.14.0 LCK phosphomimic mutant Y133/144D formed aggregates that partially overlapped with DCP1 in untreated and nocodazole treated cells.....	96
Fig. 3.15.0 Aggregates formed by the LCK phosphomimic mutant Y133/144D interact with DH2, Δ 0-216 and Δ 0-104	98-99

Fig. 4.1.0 Schematic of actin polymerisation	103
Fig. 4.2.0 Schematic of RAC1, CDC42 and RhoA interacting network	105
Fig. 4.3.0 F-actin dynamics	106
Fig. 4.4.0 Disruption of the coiled coil domain results in conformational change and colocalisation of some proline mutants with F-actin	109-110
Fig. 4.5.0 Amino acids 537 to 590 of DEF6 colocalise with F-actin	113
Fig. 4.6.0 Y133/144D aggregates enforce aggregation of mutant proteins 537 to 590 and 537-550	115
Fig. 4.7.0 Coiled coil-mediated aggregation prevents colocalisation of mutant proteins with F-actin	117
Fig. 4.8.1 H ₂ O ₂ treatment alleviates Δ 0-104 aggregates	119
Fig. 4.8.2 Conformation of phosphomimic DEF6 mutants are resistant to H ₂ O ₂ - mediated protein modifications	121
Fig. 4.8.3 Proline mutants that exhibited a diffuse localisation in the cytoplasm react differently to H ₂ O ₂ -mediated protein modifications	123
Fig. 5.1.0 Immunological synapse (IS) and its “bull’s eye” pattern	128
Fig. 5.2.1 GFP-tagged wild type DEF6 colocalises with F-actin in resting Jurkat T cells	131
Fig. 5.2.2 GFP-tagged DEF6 mutants L533P-A536P, All-10 and Δ 0-216- All-10 colocalised with F-actin in resting Jurkat T cells	132
Fig. 5.2.3 Cellular localisation of GFP-tagged Δ 0-104, Δ 0-216 and DH2 mutants in resting Jurkat T cells	134

Fig. 5.2.4 GFP-tagged Y133D/Y144D formed aggregates in Jurkat T cells	134
Fig. 5.2.5 ITK phosphomimic mutant Y2210E/Y222E colocalises with DCP1 but also colocalised with F-actin in cell protrusions	136
Fig. 5.3.1 Recruitment and localisation of GFP-tagged WT DEF6 to the cSMAC of the IS	138
Fig. 5.3.2 Selected DEF6 mutants are recruited to the IS but their localisation is distinct from WT DEF6	140-141
Fig. 5.3.3 DEF6 mutants DH2 and Δ 0-216 are recruited to the IS but their localisation is distinct from WT DEF6.....	142
Fig. 5.4.0 Dynamic of WT DEF6 in Jurkat T cells forming conjugations with Raji B cells	144
Fig. 5.5.0 Spontaneous granule formation and colocalisation with P-bodies of Y210E/Y222E in resting Jurkat T cells is reversed upon activation	146
Fig. 8.1.1 Plasmid map of eGFP tagged DEF6	179
Fig. 8.1.2 Plasmid map of mCherry and SV40 NLS tagged DEF6.....	180
Fig. 8.2.0 DNA sequence of DEF6	181-183
Fig. 8.3.1 DNA Sequencing results of DEF6 Proline mutants.....	184-187
Fig. 8.3.2 DNA sequencing result of mCherry-NLS-DEF6	188
Fig. 8.3.3 DNA sequencing results of DEF6 phosphomimic and phosphor preventing mutants	188
Fig. 8.3.4 DNA sequencing results of DEF6 C-terminal truncated mutants.....	189
Fig. 8.3.5 DNA sequencing results of DEF6 N-terminal truncated mutants	190

Fig. 8.3.6 DNA sequencing results of $\Delta 45-108$, $\Delta 79-108$ and $\Delta 45-79$	191
Fig. 8.3.7a DNA sequencing result of DEF6 mutants 537-590aa, 537-550aa	192
Fig. 8.3.7b DNA sequencing result of DEF6 mutants 551-590aa and ITAM.....	193
Fig. 8.4.0 DCP1 and DEF6 Y210/222E did not form granules in COS7 cells mitosis phase	194
Fig. 8.5.1 Coiled coil-mediated aggregates ($\Delta 0-311$) of DEF6 form large structure that 'trap' DCP1	195
Fig. 8.5.2 Coiled coil-mediated aggregates ($\Delta 0-45$) of DEF6 form large structure that 'trap' DCP1	196
Fig. 8.5.3 Coiled coil-mediated aggregates ($\Delta 0-79$) of DEF6 form large structure that 'trap' DCP1	197
Fig. 8.5.4 Coiled coil-mediated aggregates ($\Delta 45-79$) of DEF6 form large structure that 'trap' DCP1	198
Fig. 8.5.5 Coiled coil-mediated aggregates ($\Delta 45-108$) of DEF6 form large structure that 'trap' DCP1	199
Fig. 8.5.6 Coiled coil-mediated aggregates ($\Delta 79-108$) of DEF6 form large structure that 'trap' DCP1	200
Fig. 8.6.1 Cellular stress (Arsenate) had no effect on formation of large structures of $\Delta 0-311$ and their ability to 'trap' DCP1	201
Fig. 8.6.2 Cellular stress (Arsenate) results in complete colocalisation of $\Delta 45-$ 108 structures with DCP1	202
Fig. 8.6.3 After arsenate treatment, few samples of $\Delta 45-108$ remained in partially overlapping with DCP1	203

Fig. 8.7.1 Cellular stress (Nocodazole) had no effect on formation of large structures of $\Delta 0$ -311 and their ability to 'trap' DCP1	204
Fig. 8.7.2 Cellular stress (Nocodazole) results in complete colocalisation of $\Delta 45$ -79 structures with DCP1.....	205
Fig. 8.8.1 Disruption of the coiled coil domain of R407P-M410P did not results in colocalisation with F-actin.....	206
Fig. 8.8.2 Disruption of the coiled coil domain of I428P-L431P did not results in colocalisation with F-actin	207
Fig. 8.8.3 Disruption of the coiled coil domain of K491P-L494P did not results in colocalisation with F-actin	208
Fig. 8.8.4 Disruption of the coiled coil domain of L463P-E466P results in conformational change and colocalisation with F-actin	209
Fig. 8.8.5 Disruption of the coiled coil domain of L470P-E473P results in conformational change and colocalisation with F-actin	210
Fig. 8.8.6 Disruption of the coiled coil domain of L505P-A508P results in conformational change and colocalisation with F-actin	211
Fig. 8.8.7 Disruption of the coiled coil domain of L512P-V515P results in conformational change and colocalisation with F-actin	212
Fig. 8.8.8 Disruption of the coiled coil domain of Q371P-A374P-L505P-A508P results in conformational change and colocalisation with F-actin	213
Fig. 8.9.0 $\Delta 0$ -104 formed aggregations in less than 2% transfected Jurkat T cells	214

Fig. 8.10.0 Formation of large aggregates of DEF6 is abolished through proline mutations in the coiled coil domain	215
Fig. 8.11.0 Cellular stress did not alter localisation of the 105-312aa or Δ 0-104-All-10 mutants.....	216

List of Tables

Table 1: DNA oligonucleotides used for site-directed mutagenesis, PCR amplification or sequencing as indicated	30
Table 2. The setting up of DNA digestion reaction	37
Table 3. The PCR reaction system for inserting and amplify DNA fragment	39
Table 4. The Cycling Parameters for inserting and amplify DNA fragment	40
Table 5 The PCR reaction system of the QuikChange Lightning Multi Site-Directed Mutagenesis	41
Table 6. The Cycling Parameters for the QuikChange Lightning Multi Site-Directed Mutagenesis	41
Table 7: Cellular localisation of wild type and mutant DEF6 proteins coexpressed with mCherry-NLS-DEF6.....	90
Table 8: DEF6/Mutants in COS7 cells	217-222
Table 9: Cellular localisation of wild type and mutant DEF6 proteins coexpressed with mCherry-NLS-DEF6.....	223
Table 10: mCherry-Y133/144D coexpression with DEF6 mutants.....	224
Table 11: DEF6/Mutants in resting Jurkat T cells	225

Table 12: DEF6/Mutants in conjugated Jurkat T cells226

Chapter 1

Introduction

1.1 DEF6 functions as a guanine nucleotide exchange factor for Rho-GTPases

1.1.1 DEF6 and Rho-GTPases

Initially, DEF6 (Differentially Expressed in FDCP 6; Hotfilder *et al.*, 1999) was shown to act as a Guanine nucleotide exchange factor (GEF) that activated Rho-GTPases (Cdc42, RhoA and Rac1) (Gupta *et al.*, 2003b; Mavrakis *et al.*, 2004). Rho-GTPases are tightly regulated signalling proteins, which bind GDP when inactive and GTP when activated. Rho-GTPases are part of the RAS superfamily GTPases and more than 22 members have been identified in the human genome (Johnson *et al.*, 2009; Rossman *et al.*, 2005). Rho-GTPases regulate actin polymerisation and cellular morphogenesis, and are also involved in the regulation of cell proliferation, cell survival and gene transcription. Downstream targets affect cell movement, adhesion, phagocytosis, cytokinesis, and polarisation. Such widespread functions of Rho-GTPases are vital for cell homeostasis and misregulation or loss of function promotes tumorigenesis (Sahai and Marshall, 2002; Rossman *et al.*, 2005).

The function of Rho-GTPases as bi-molecular switches depend on two different conformational states: GDP- or GTP-binding, which correspond to inactive and active conformation respectively (Fig. 1.1.0). Three molecules regulate the cycling between these two states: guanine nucleotide exchange factors (GEFs), such as DEF6, regulate the exchange of GDP to GTP, GTPase-activating proteins (GAPs) promote the intrinsic hydrolytic activity of GTPase from GTP state to GDP, and guanine nucleotide-dissociation inhibitors (GDIs), which inhibit GDP dissociation

and sequester GDP-bound GTPases in the cytoplasm. Moreover, GDIs might be necessary before the engagement of GEFs (Fig. 1.1.0) (Sahai and Marshall, 2002; Rossman *et al.*, 2005; Alan and Lundquist, 2013).

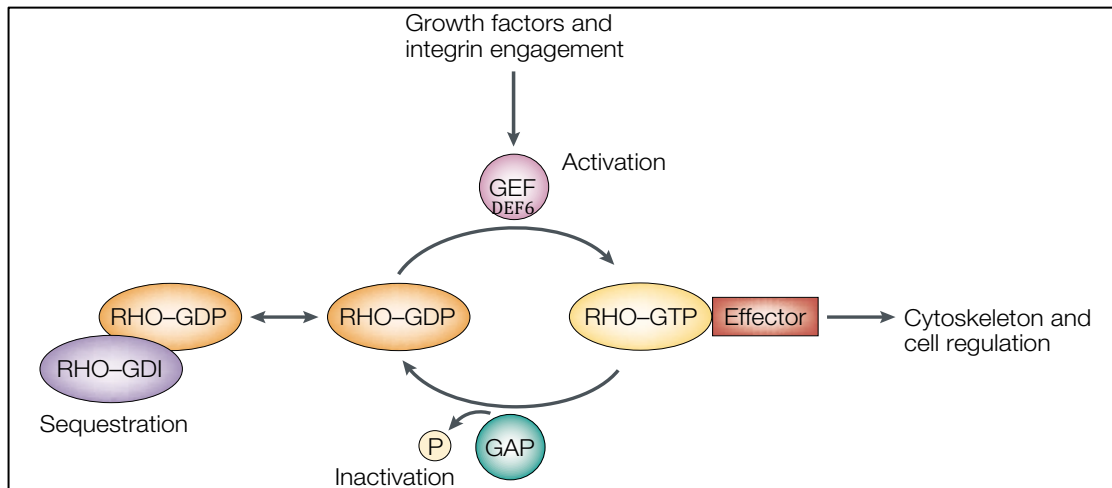


Fig. 1.1.0 The mechanism of Rho-GTPases' GDP- and GTP- binding state cycle.

Guanine nucleotide exchange factors (GEFs) such as DEF6 promote GDP-bound Rho-GTPases to change conformation releasing GDP and binding GTP. Most Rho-GTPases have an intrinsic hydrolytic action from GTP-bound to GDP-bound form, which can be accelerated by GTPase-activating proteins (GAPs). Guanine nucleotide-dissociation inhibitors (GDIs) sequester GDP-bound Rho-GTPases in the cytoplasm, which might be necessary before the GEF function (Figure adapted from Sahai and Marshall, 2002).

1.1.2 A general mechanism of guanine nucleotide exchange by GEFs to Rho GTPases

Rho GTPases have an ability to intrinsically dissociate their GDP and altering to GTP-bound form. However, GEFs accelerate switching 10^5 fold. The structure of nucleotide binding and hydrolysis in Rho GTPases is called G-domain (Fig. 1.2.0). Within the G-domain, two confined primarily switch regions (I, II) and a conserved phosphate-binding loop (P-loop) together with a Mg^{2+} -binding site contribute to the nucleotide binding and exchange. Although the two switch regions exhibit a large structural variation in GDP-bound form, they demonstrate remarkable similarity in GTP-bound phase. GEFs respectively interact with these two regions, which subsequently results in a series of conformational changes that move switch I region away and push switch II region toward the P-loop. Within the switch II region, a highly conserved glutamate residue (E) in DxxGQE motif contacts a lysine residue in the P-loop (e.g. Glu64 of Rho and Glu62 of Rac/CDC42 of their switch II region toward Lys16/18 of their P-loop). Consequently, these conformational changes push out the Mg^{2+} , reducing the nucleotide affinity, thereby releasing GDP and shifting GTPases to nucleotide free phase and allowing GTP-binding due to its high concentration in cells (Fig. 1.2.0) (Vetter and Wittinghofer, 2001; Thomas *et al.*, 2006; Dong *et al.*, 2007; Gasper *et al.*, 2008; Guo *et al.*, 2013).

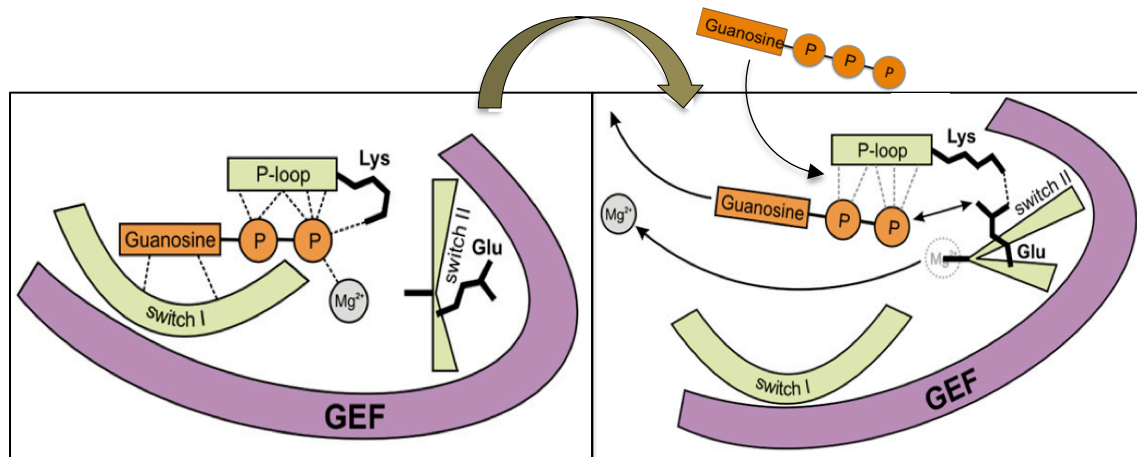


Fig. 1.2.0 GEFs accelerate GTPases nucleotide exchange.

GEFs interact with GTPases switch I and II regions, which removes the switch I region from its normal position and pushes the switch II region towards the P-loop. A conserved lysine residue forms the P-loop subsequently contacts a conserved glutamic acid residue from the switch II region, which result in the release of Mg²⁺ reducing the affinity of the nucleotide. Subsequently, GDP is released and GTP binds to the vacant position (Figure adapted from Tomas *et al.*, 2006).

1.1.3 DEF6 functions as a GEF protein

DEF6 was first isolated in a screen to identify differentially expressed genes during haematopoiesis (Hotfilder *et al.*, 1999). Utilising the FDCP-mix cell line that was derived from the mouse and can be directed to differentiate into various haematopoietic cells (Spooner *et al.*, 1986; Heyworth *et al.*, 1990; Kan *et al.*, 1993), a gene-trap approach identified several differentially expressed genes, one of which was DEF6. Subsequently, it was shown that DEF6 functions as a GEF activating Rho-GTPases (Gupta *et al.*, 2003b; Mavrakis *et al.*, 2004). Furthermore, Gupta *et al.* (2003b) showed that DEF6 is phosphorylated by LCK in T cells upon TCR-mediated activation, liberating its GEF function and translocation to the junction between T cells and antigen presenting cells, termed as immunological synapse (IS). This synapse formation and function is critically depended on F-

actin polymerisation and thus Rho GTPases activity (Dustin *et al.*, 2000). Similarly, Mavrakis *et al.* (2004) demonstrated upon PI3K signalling, DEF6 localised to lamellipodia, membrane ruffling and filopodia in COS7 cells, all of which are hallmarks of GEF activity and actin polymerisation.

Indeed, both of these reports demonstrated biochemical interactions between CDC42, Rac1 and DEF6 (Gupta *et al.*, 2003b and Mavrakis *et al.*, 2004). Mavrakis *et al.* (2004) detected *in vivo* interaction between DEF6 and RhoA, however, *in vitro* data from Gupta *et al.* (2003b) did not support this result, which might suggest the interaction between DEF6 and RhoA is indirect. Moreover, comparing to wild type (WT) T cells, T cells deficient of DEF6 or loss of DEF6 GEF function exhibited lower F-actin content and less IS stability. In contrast, a constitutively active Rho GTPase, Rac2 (G12V), partially rescued the actin polymerisation in DEF6-deficient cells (Fanzo *et al.*, 2006). Similarly, as reported from Mavrakis *et al.* (2004), DEF6 lamellipodia, membrane ruffling and filopodia localisation would be abolished by overexpression of dominant negative Rac1, Cdc42 and RhoA. Additionally, as report by Mavrakis *et al.* (2004), a DEF6 C-terminal fragment (DHL domain) was sufficient to trigger lamellipodia, membrane ruffling and filopodia formation, consistent with Gupta *et al.* (2003b) who reported that DEF6 C-terminal fragment could directly activate CDC42 and Rac1 *in vitro*. Bécart *et al.* in 2008 further demonstrated DEF6 GEF functions showing that DEF6 promotes NFAT signalling in CD4⁺ T cells via Cdc42/Rac1 activation, regulating Th1 and Th2 differentiation.

1.1.4 DEF6 protein structure

1.1.4.1 DEF6 and its only relative SWAP70 are highly conserved

DEF6 exhibits strong homology to only one other protein namely SWAP70 (Borggreffe *et al.*, 1998; Gupta *et al.*, 2003a; Ripich *et al.*, 2006 Ripich *et al.*, 2016; Manni *et al.*, 2017). Both proteins are highly conserved exhibiting the same domain structure and originate from a common ancestor gene present in *tricolox adhaerens* (Shuen, MRes 2010). Two Ca²⁺ binding EF hands at the N-terminus are followed by DEF6-SWAP70 homology (DSH) domain. DSH domain is strongly conserved between DEF6 and SWAP70, which contains an immunoreceptor tyrosine-based activation motif like (ITAM) sequence. A central pleckstrin-homology (PH) domain, which acts as a PI (3,4,5) P3 anchor is followed by the C-terminal Dbl homology-like (DHL) domain that contains a coiled coil domain and exhibits GEF activity (Fig. 1.2.0 A) (Mavrakis *et al.* 2004; Bécart *et al.*, 2008; Hey *et al.* 2012).

1.1.4.2 DEF6 and SWAP70 are atypical GEFs

Up to date, more than 84 GEFs have been reported, which belong to three families. Among them, Dbl family functions for RhoA, Rac1 and Cdc42, and constitutes the largest group of approximately 69 distinct homologues (Rossman *et al.*, 2005). Dbl proteins contain diverse structural motifs but all share a Dbl homology (DH) domain and a tandem pleckstrin homology (PH) domain (Fig. 1.3.0B, Zheng, 2001). The second group of GEF proteins form the Dock (dedicator of cytokinesis) family, which contains 11 members in mammalian cells, and function as GEFs for

Rac and/or Cdc42. Unlike Dbl family, Dock GEFs lack DH-PH module, but possess a Dock homology region-1 and -2 (DHR-1, -2) to respectively play roles as PH and DH domains (Shi, 2013; Zheng, 2001).

As described above, DEF6 and SWAP70 also have a DH-like domain (DHL) and a PH domain but while all other Dbl proteins feature a PH domain C-terminal to the DH domain, DEF6 and SWAP70 are different in that their PH domain is N-terminal of the DHL domain (Fig. 1.3.0B). Due to this difference in domain structure, DEF6 and SWAP70 are atypical GEFs and build a third group of GEFs (Gupta *et al.*, 2003a; Mavrakis *et al.* 2004; Bécart *et al.*, 2008; Hey *et al.* 2012; Ripich *et al.*, 2016; Manni *et al.*, 2017).

1.1.4.3 PH and DH domain function

In general, the DH domain of Dbl family members interacts with the switch regions of Rho-GTPases to facilitate nucleotide exchange, whereas the PH domain acts as a membrane anchor (Rossman *et al.*, 2005). However, the PH domains of Dbs and LARG directly contact the bound GTPases, whereas Tiam1 and ITSN-L do not have interaction between their PH and DH domains (Rossman *et al.*, 2005). In addition, Sos1 has an interface formed by its PH domain's helix and DH domain's seat-back region, which occludes the GTPase-binding surface and prohibits the binding and exchanging of its downstream Rho-GTPases (Rossman *et al.*, 2005). As for DEF6, the DHL domain that exhibits only weak homology with the DH domain, still functions as a GEF even in the absence of the PH domain (Gupta *et al.*, 2003b; Mavrakis *et al.*, 2004), suggesting that the PH domain of DEF6 does not directly participate in maintaining DEF6-GTPases interaction.

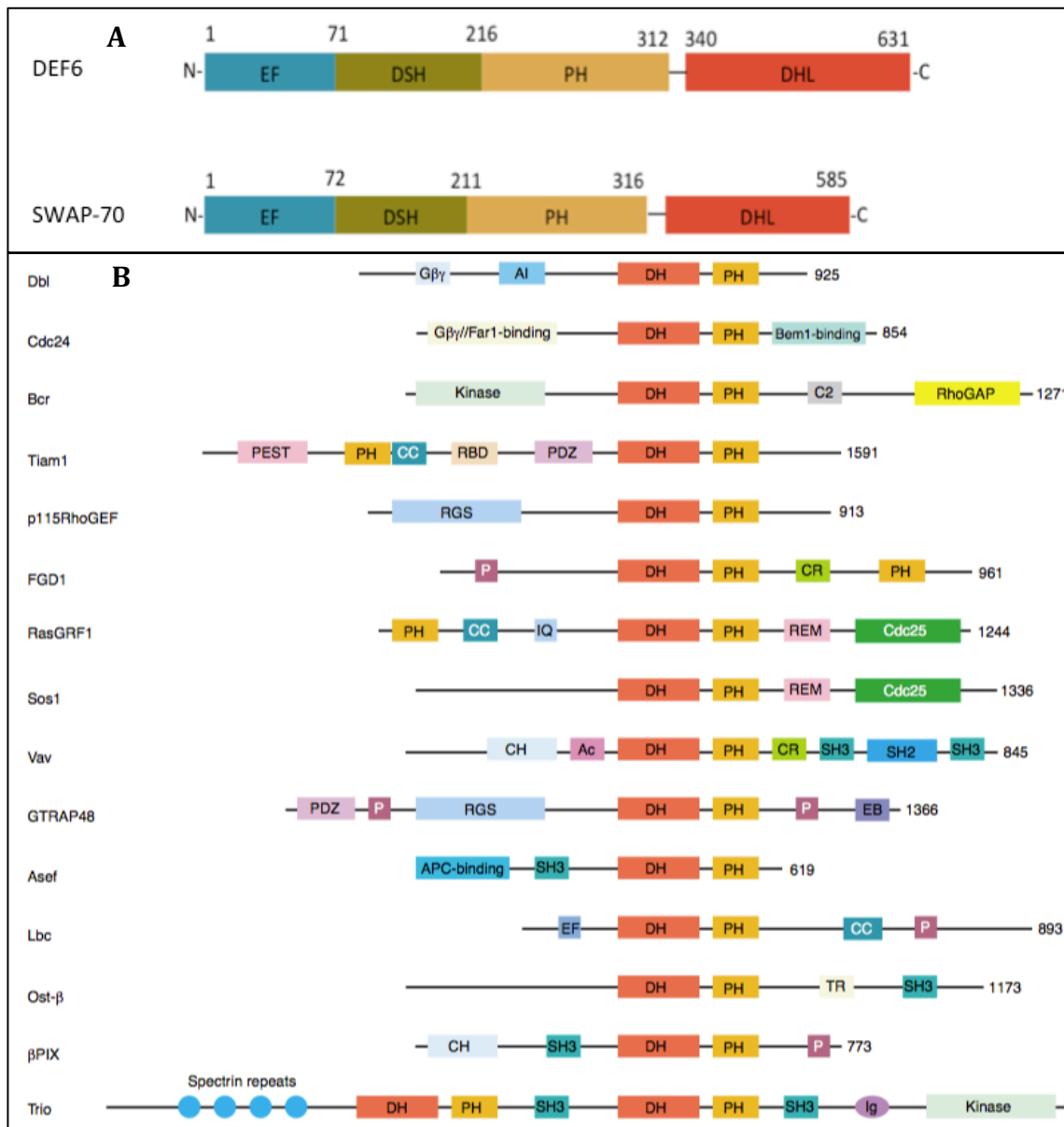


Fig. 1.3.0 Domain structure of GEFs.

(A) Schematic diagram of DEF6 and SWAP70 domain structure. EF: Ca²⁺-binding EF-hand; DSH: DEF6-SWAP70 homology; PH: pleckstrin homology domain and DHL: Dbl homology like domain **(B)** Domain structure of Dbl family GEFs highlighting the conserved DH-PH configuration. (Figure adapted from Zheng 2001).

1.1.5 Vav, a prototype Dbl GEF, is activated through conformational change

Vav1 is a Dbl family GEF, which is required for TCR induced signalling in T cells. From the N- to C-terminal, Vav1 contains a calponin homology domain (CH), acidic domain (Ac), DH domain, PH domain, cysteine-rich C1 domain and several SH domains (Fig. 1.4.0). In its inactive form, GEF activity of vav1' DH domain is inhibited by the Ac, CH, PH and C1 domains. In this phase, its Tyr-174 within Ac domain binds to the DH domain, and CH domain also binds to C1 domain. These bindings cover the DH domain inhibiting the GEF activity. TCR-mediated activation results in phosphorylation of Try-147, which in turn results in disassociation of the CH domain from the C1 domain, and in the Ac domain releasing the DH domain resulting in GEF activity. In addition, PIP3 binding by the PH domain might also be important for GEF activity as indicated by experiments in mice showing that prevention of PIP3 binding reduced Rac1 activation. Post-translational modification inducing conformational change are thus key to activate vav1' GEF function (Fig. 1.4.0) (Tybulewicz, 2005).

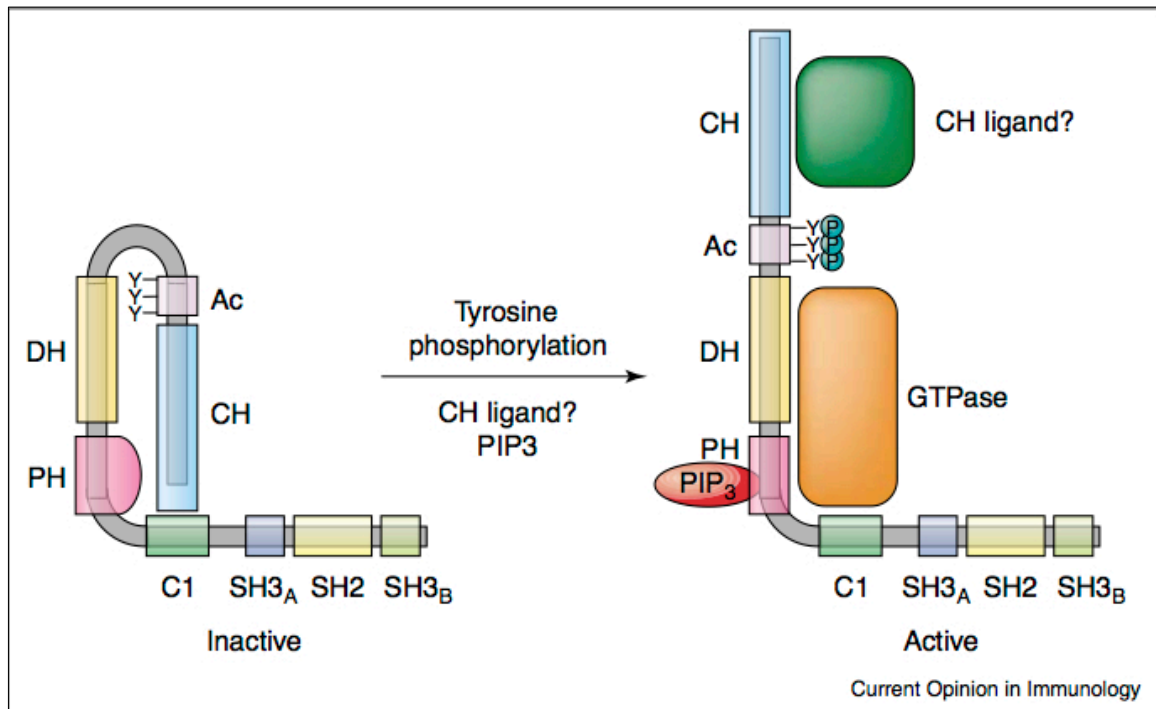


Fig. 1.4.0 The activation module of Vav1.

Phosphorylation of Tyr residues within the acidic domain (Ac) releases the binding between Ac domain and DH domain. This modification in turn disassociates the binding between the calponin homology (CH) and C1 domains, opening the molecule and unmasking the DH domain. PIP₃ binding to the PH domain might also contribute to the conformational change and activation of GEF function. (Figure adapted from Tybulewicz, 2005).

1.1.5.1 Is the model of VAV also applicable to DEF6?

DEF6 like vav1 is highly expressed in T cells and upon TCR-mediated signalling DEF6 is phosphorylated on Tyr 210 by LCK, binds PIP₃, is recruited to the IS and exhibits GEF activity (Gupta *et al.*, 2003b). However, Bécart *et al.* (2008) showed that LCK is actually phosphorylating Tyr 133 and 144 within the ITAM motif of DEF6, but both groups concluded that similar to vav1, phosphorylation resulted in conformational change of DEF6 essential for GEF activity. However, Mavrakis *et al.* (2004) showed that H₂O₂ treatment that results in enhanced PI3K signalling was sufficient to confer GEF activity to GFP-DEF6 overexpressed in COS7 cells and that

this could be prevented by the addition of a PI3K inhibitor. COS7 cells lack LCK expression, suggesting that other post-translational modifications of DEF6 can also activate its GEF activity.

1.2 DEF6 function in the immune system

1.2.1 DEF6 localises to and enhances stability of immunological synapse

Immunological synapse (IS) is the junction between T cells and antigen presenting cells (APCs), which plays critical roles in immune response. The IS is formed as a consequence of TCR-mediated activation upon binding to peptides presented by major histocompatibility complex (MHC) of APCs (More details in Chapter 5). In CD4⁺ T cells, DEF6 is recruited to the IS after T cell activation (Gupta *et al.*, 2003b; Bécart *et al.*, 2008) and lack of DEF6 resulted in reduced stabilisation of the IS (Fanzo *et al.*, 2006).

Gupta *et al.* (2003b) showed that the phosphorylation of residue Try210 of DEF6 by LCK upon TCR stimulation mediates DEF6 translocation into the IS, and prevention of this modification abolished this recruitment. However, Bécart *et al.* (2008) demonstrated that LCK phosphorylation positions are Try133 and Try144 of DEF6, rather than Try210. Interestingly, Hey *et al.* (2012) reported that Try210 together with residue Try222 are actually phosphorylated by ITK, which resulted in DEF6 colocalising with P-bodies.

Gupta *et al.* (2003b) also demonstrated that PI3K signalling is indispensable for DEF6 localising to the IS. They showed translocation of DEF6 was prevented by a treatment of a PI3K inhibitor, wortmannin. However, Bécart *et al.* (2008) described that pretreatment of Jurkat T cells with PI3K inhibitors wortmannin or LY294002 did not affect the translocation of endogenous DEF6 to cell membrane upon TCR stimulation, and that DEF6 can still be recruited to IS. However, Hey (2012, PhD thesis) showed that wortmannin did significantly reduce the

detectable amount of DEF6 from the cell membrane in Jurkat T cells, which supports the conclusion from Gupta *et al.* (2003b) to some extent.

Finally, DEF6 binding to the activated small GTPase, Rap1 (Rap1-GTP) might be also critical for the recruitment of DEF6 to the IS (Côte *et al.*, 2015). According to this study, DEF6 and Rap1-GTP are interdependent, which either deficiency of DEF6 or Rap1 will inhibit the other one to relocate to the IS. The evidence did not show DEF6 has a function to alter Rap1 from GDP to GTP binding, but the constitutively active Rap1 mutant can rescue DEF6-deficient T cells. Rap1 activates β 2 integrin leukocyte function-associated antigen (LFA-1) resulting in binding to its endothelial ligand, intercellular adhesion molecules (ICAMs). This interaction guides T cell trafficking and antigen recognition in the IS (T cell adhesion and inside-out signalling) (Hogg *et al.*, 2002 and 2011). Therefore, as an upstream activator of Rap1, DEF6 indirectly regulates LFA-1 activation and further downstream functions (Côte *et al.* 2015, Fig. 1.5.0).

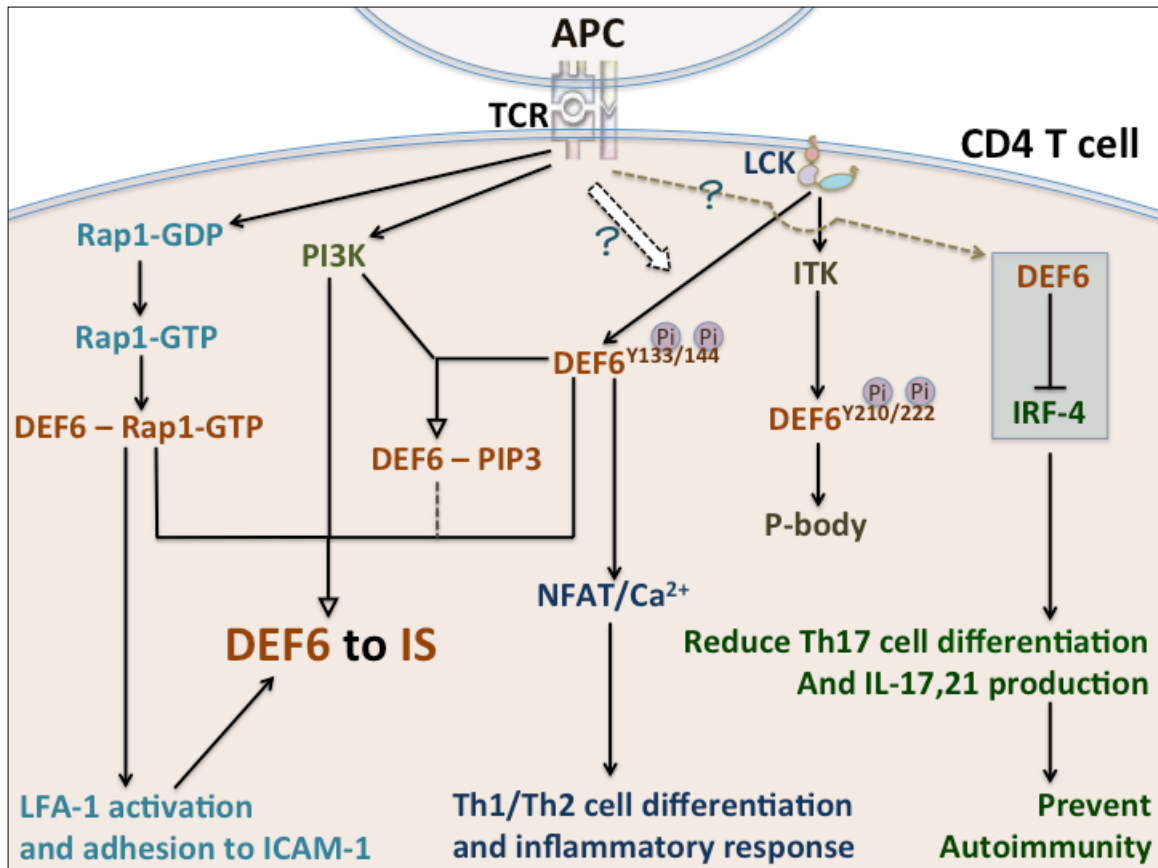


Fig. 1.5.0 Schematic of DEF6 signalling network in CD4⁺ T cells.

TCR-mediated signalling results in the recruitment of DEF6 to the IS. **1)** LCK phosphorylates DEF6 on Tyr133/144, also resulting in activation of the NFAT/Ca²⁺ signalling pathway. LCK is constitutively active in T cells, however, it is unknown if TCR activation promoted the interaction between LCK and DEF6. ITK phosphorylates DEF6 at Try210/222, which results in DEF6 colocalising with P-bodies. LCK theoretically participates in this modification because LCK is also responsible for ITK activation, however, this possibility has not been tested so far. **2)** Activation of PI3K signalling cooperates with LCK modification and will result in DEF6 binding to PIP3 enhancing DEF6 relocation to the IS (but is not a necessary condition). **3)** DEF6 binds to the activated GEF protein Rap1 (Rap-GTP) resulting in LFA-1 activation and ICAM-1 adhesion. **4)** DEF6 is required for NFAT activation, Th1/Th2 differentiation and IL-2, IL-4 and IFN γ expression. **5)** DEF6 inhibits IRF-4 activation resulting in reduced Th17 differentiation, reduced IL-17 and IL21 expression and preventing autoimmunity. (Figure based on information from citations given in the text).

1.2.2 DEF6 is critical for the development of autoimmune diseases.

Initial study of knockout mice lacking DEF6 revealed that DEF6 deficiency resulted in deregulation of Th17 cell function causing autoimmune disease (Chen *et al.*, 2009). Th17 cells are a subset of CD4⁺ T helper distinct from other T helper cells such as Th1 and Th2, by the production of cytokines IL-17 (A, F), IL-21 and IL-22. Overexpression of IL-17 promotes autoimmune disease, such as rheumatoid arthritis (RA), systemic lupus erythematosus (SLE), experimental autoimmune uveitis (EAU) and experimental autoimmune encephalomyelitis (EAE). Anti-IL-17 antibody treatment has been demonstrated to significantly relieve autoimmune disease symptoms (Park *et al.*, 2005; Komiyana *et al.*, 2006; Yang *et al.*, 2014; Tabarkiewicz *et al.*, 2015). The mechanism of IL-17 function is still unclear, but it seems that IL-17 stimulates and synergizes with other cytokines, i.e. tumor necrosis factor (TNF)- α and macrophage inflammatory protein (MIP)-2. (Khan *et al.*, 2015; Zhu *et al.*, 2012)

Even though excessive IL-17 results in high risk of autoimmune disease, IL-17 deficiency will also increase bacteria and fungal infection and tumor growth (Welch *et al.*, 2015). Thus, the expression level of IL-17 needs to be precisely controlled. IRF-4 (IFN regulatory factor-4) is a transcriptional factor that promotes IL-17 expression and Th17 cell differentiation (Brüstle *et al.*, 2007, Huber *et al.*, 2008). IRF-4 is activated upon ROCK-2 (Rho-associated serine/threonine kinases) -mediated phosphorylation. DEF6 can bind and thereby inhibit the phosphorylation of IRF-4, which results in deregulation of Th17 cells and its cytokine production (Chen *et al.*, 2009).

Fanzo *et al.* (2006) described that DEF6-deficient mice developed a lupus-like

syndrome starting at 5 month of age exhibiting a series of serologic symptoms, such as high level of IgG, antinuclear antibodies, anti-double-stranded DNA and anti-Smith antibodies. In addition, similar to human systemic lupus erythematosus (SLE), symptoms were more prevalent in female (60%) than in male (10%) DEF6-deficient mice. Subsequently, Chen *et al.* (2009) showed that DEF6 deficiency altered IRF-4 function increasing Th17 cells differentiation and IL-17, 21 expressions, resulting in autoimmune disease.

However, Altman and Bécart (2009) doubted DEF6 deficiency causes autoimmunity because their analysis of DEF6-deficient mice did not reveal signs of autoimmunity. In the following dispute, Chen and Pernis (2009) responded that DEF6 gene deletion related lupus-like syndrome only happened in particular mouse strains dependent upon the genetic background. Soon, Canonigo-Balancio *et al.* (2009) demonstrated that DEF6-deficient mice were resistant to MOG induced EAE, and DEF6 positively regulated Th17 cells differentiation *in vitro*. Similar results were also reported from Vistica *et al.* (2012) in the EAU model. Recently, a bioinformatics analysis reported that SNP (rs10807150) in an intron of the DEF6 gene has a very high correlation with SLE in East Asia (Sun *et al.*, 2016) but it remains to be seen what specific role DEF6 plays in the prevention and/or development of autoimmune diseases and whether it would be a potential target for therapy.

1.3 DEF6 is highly expressed in cancer cells and promotes cancer development

Li and their colleagues in 2009 reported that DEF6 is highly expressed in human invasive breast carcinoma tissue and breast cancer lines. In contrast, the expression level of DEF6 was low or undetectable in normal or low-risk breast tumour tissue. Moreover, overexpression of DEF6 significantly increased proliferation and invasiveness of a non-DEF6 breast cancer cells, and reduction of DEF6 in DEF6 abundant breast cancer cell lines resulted in the opposite outcome (Li *et al.*, 2009). Similar results were reported in murine tumour endothelial cells and in human colorectal, oral squamous and ovarian cancer cells (Otsubo *et al.*, 2014; Jian *et al.*, 2015 and Liew *et al.*, 2016). In fact, DEF6 has been shown to be highly expressed in different types of cancer tissue (Fig. 1.8.0). Based on the analysis of breast cancer cells, the high expression of DEF6 might be attributed to the abnormal expression of p53 (Yang *et al.*, 2012). P53 is largely known as a transcriptional factor that triggers a variety of anti-proliferation cellular programs, and insufficiency of p53 function is commonly found in breast cancer cells (Gasco *et al.*, 2002, Zilfou and Lowe, 2009). The relations between DEF6 and p53 are reflected on two levels. Firstly, DEF6 expression is negatively regulated by p53, which is probably through p53 binding to DEF6 promoter (Yang *et al.*, 2012). Second, DEF6 could bind and inactivate p53 protein (Yang *et al.*, 2012). Hence, the defective p53 expression in these cancer cells increases the expression of DEF6, and high level of DEF6 further reduces p53 function. Consequently, this regulatory loop promotes the development of breast cancers.

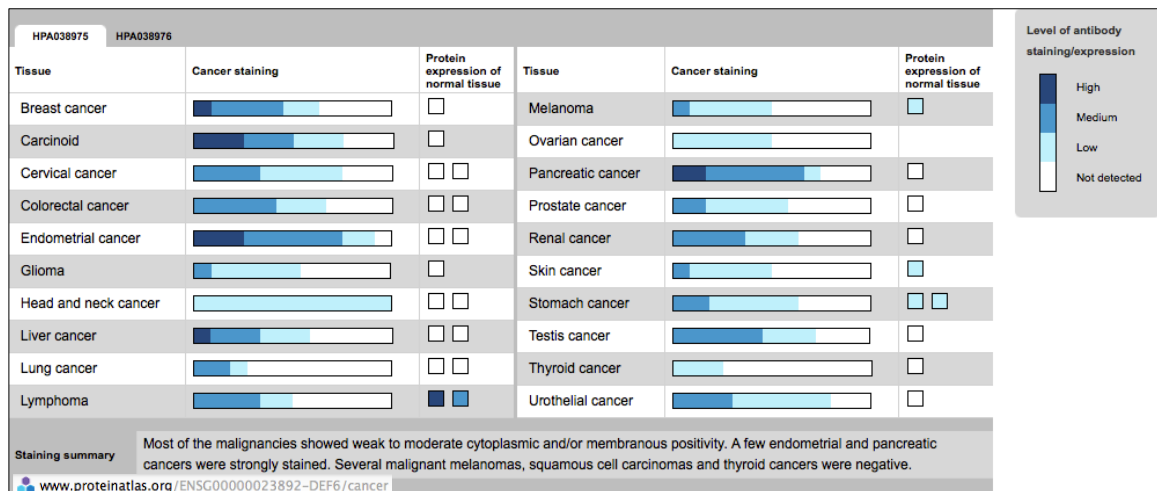


Fig. 1.6.0 DEF6 protein expression in different cancer tissues.

DEF6 is widely expressed in cancers, but hardly detected in majority of normal tissues (www.proteinatlas.org/ENSG00000023892-DEF6/cancer).

DEF6 might also contribute to cancer development through other routes. For example, in OSCC cells (oral squamous cell carcinoma cells), DEF6 overexpression shortened the G1 phase and G1 was prolonged by DEF6 knockdown. Furthermore, the expression level of DEF6 in these cells positively correlated with the expression of cyclin D1, a key regulator of G1/S phase transition. Hence, the interaction of DEF6 and cyclin D1 might be the reason for the shortening of the G1 phase (Jian *et al.*, 2012). DEF6 has also been shown to inhibit autophagy reaction in cancer cells probably through interfering with FoxO3 pathway. FoxO3 is a transcription factor, which is necessary and sufficient to induce autophagy. This protein can be suppressed by Akt ser473 phosphorylation. Interestingly, DEF6 overexpression correlated with this phosphorylation and subsequent suppression of autophagy in breast cancer cells. This is consistent with later research showing that DEF6 activates mTORC2 acting upstream of Akt, and further mediates suppression of autophagy in breast cancer cells. Taken together, it seems, therefore, that DEF6 functions via the mTORC2/Akt/FoxO3 pathway to inhibit

autophagy and to promote cancer development (Yang *et al.*, 2012; Chen *et al.*, 2013). However, mTORC1 signalling was also activated by DEF6 in breast cancer cells implying that DEF6 can suppress autophagy in multiple ways (Chen *et al.*, 2013).

1.4 DEF6 phosphorylation at Tyr210/222 results in colocalisation with P-bodies.

In addition to LCK phosphorylation, DEF6 is also a substrate of the kinase ITK, phosphorylating Tyr^{210/222} of DEF6 in Jurkat T cells. DEF6 ITK phosphomimic mutant, Y210/222E, overexpressed in COS7 cells changed its cellular localisation forming DEF6 foci that overlapped with the P-body marker decapping enzyme 1 (DCP1). Endogenous DEF6 in Jurkat cells has also been observed to colocalise with P-bodies (Hey *et al.*, 2012 and Mollett, 2014 PhD thesis). Moreover, arsenate (Hey *et al.*, 2012) or nocodazole treatment can also induce WT DEF6 and several DEF6 mutants to localise into P-bodies in COS7 cells. Interestingly, COS7 cell line, however, is lacking expression of ITK, thereby indicating that ITK phosphorylation is not the only modification of DEF6 resulting in P-body colocalisation (Hey *et al.*, 2012).

1.4.1 Core function of P-bodies is mRNA degradation

P-body is a major type of messenger ribonucleoproteins (mRNP) granule, which is non-membranous and dynamic cytoplasmic foci (Anderson and Kedersha, 2008 and 2009). P-body is a supermolecular organelle that, including DEF6, contains more than 34 types of proteins (Parker and Sheth, 2007; Hey *et al.*, 2012). Even though the components of P-bodies vary in different tissues, generally, the core of each P-body unit is mRNA decay machinery. The decay core can be simplified into two molecules, decapping enzyme 2 (DCP2) and XRN1. DCP2 responds to remove mRNA 5'-cap by catalyzing the hydrolysis of the cap structure, and subsequently, XRN1, an exonuclease, degrades mRNA from 5' to 3'. Even though DCP2 is capable to perform its function *in vitro*, its activity is stimulated and regulated by several

other proteins termed decapping coactivators, which include DCP1, EDC3, EDC4, LSM1-7 complex, LSM14A, Dhh1 and Pat1. These proteins are highly conserved in eukaryotes, and all have been observed to be localised in P-bodies and function in 5' to 3' mRNA decay (Eulalio *et al.*, 2007 and cited in Chang *et al.*, 2014).

In addition, small interfering RNAs (siRNA) induced RNA interference (RNAi) is also carried out in P-bodies by Argonaute-2 (Ago2), GW182 and/or the mRNA decay core (Jakymiw *et al.*, 2005). Moreover, mRNAs returning from P-bodies to polysomes has also been observed in Yeast (Bregues *et al.*, 2005), which indicates P-bodies could also function as mRNA storage. DEF6 function in P-bodies is unknown and it remains to be seen which role DEF6 plays in this organelle.

1.4.2 Assembly of P-body components require EDC4 as a scaffold for the decay machinery and Q/N rich protein interactions

How P-bodies assemble is still not fully understood. Many factors are involved in this process, such as Ago, GW182 and mRNAs. This implies P-bodies formation is a complicated and multilevel process. Among them, EDC4 is a scaffold for the decay machinery (Chang *et al.*, 2014). In P-bodies, EDC4 provides binding sites for DCP1, DCP2 and XRN1, where three DCP1 molecules gather as a trimer to activate DCP2 and subsequently perform the decapping. Without EDC4, DCP1 and DCP2 can still interact, however, the binding force between them is too weak to maintain their function. Moreover, the binding of DCP2 and XRN1 to the same EDC4 molecule ensures that the decapped mRNAs are transferred to XRN1 for further decay. Each of the decay machinery could be considered as a working unit.

Assembly of these units to so-called microscopically visible P-body is also little understood. Decker and Parker (2012) summarised a possible model of P-body assembly in yeast, which depends on EDC3 self-interaction domain (Yjef-N) and Lsm4 Q/N rich domain. Although in *Drosophila* S2 cells, P-body assembly is not blocked by EDC3 depletion, to deplete some P-bodies Q/N rich proteins, such as GW182, would decrease P-body formation in *Drosophila* and human. It is possible therefore that assembly through interaction of Q/N rich domains/proteins is the first step in P-body formation. Hence, a simple model of P-body formation can be summarised as following: in the first step, DCP1, DCP2, XRN1 rely on EDC4 as a scaffold to assemble as P-bodies units. Then these units gather to be microscopically visible P-bodies through the interactions of Q/N rich components (Fig. 1.7.0). Q/N rich proteins tend to form coiled coil structure (Fiumara *et al.*, 2010). DEF6 has a Q-rich coiled coil domain in its C terminal end. Thus, it educes a possibility that DEF6 location in P-bodies is mediated via its coiled coil domain.

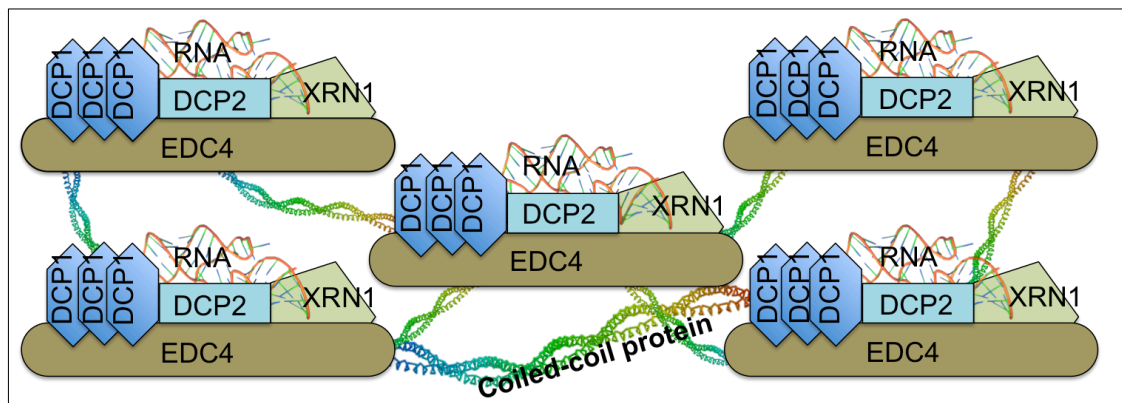


Fig. 1.7.0 Schematic diagram of P-body assembly.

EDC4 functions as a scaffold to support DCP1 (trimer), DCP2, XRN1 and RNA to interact. This complex is termed P-body functional unit. Then, these units associate via interactions among their coiled coil domains to form microscopically visible P-bodies (Chang *et al.*, 2014; Decker and Parker, 2012).

1.4.3 P-body size and abundance varies during cell cycle

P-bodies are flexible and dynamic structures varying in size and abundance during the cell cycle. Yang *et al.* (2004) observed in HeLa cells that the microscopically visible P-bodies could hardly be detected during the mitotic phase of the cell cycle, but reassembled at the start of the G1 phase. Until early S phase, P-bodies were still small and less abundant, but bigger and more abundant in late S phase and G2 phase. A similar phenomenon was also observed for DEF6 P-bodies dynamic: both DEF6 and DCP1 did not form granules but were diffuse in the cytoplasm in cells undergoing mitosis (Appendix 8.4, Fig. 8.4.0). Yang and their colleagues (2004) further discovered that P-bodies start to reform slightly later than nucleoli in mitotic phase, and become more abundant from the late stage of telophase when more nucleoli were also detectable. The dynamic of P-body size (100nm-300nm) is due to fusion of small P-bodies to form large one (Yang *et al.*, 2004). Moreover, P-bodies were described as “liquid-like” assemblies, which can be dissolved in cells through hexanediol treatment disassociating weak hydrophobic interactions among molecules. In contrast, other non-liquid-like foci, such as stress granule, would not display this phenomenon. Thereby, it suggests the assembling of P-body units does not rely on chemical bonds but hydrophobic interactions. This feature might also endow a flexibility to P-bodies for a rapid reaction of mRNA metabolism (Becker and Gitler, 2015).

1.5 Aims and Objectives

To establish a comprehensive functional map of the DEF6 protein

- **Establish GFP-tagged mutant DEF6 proteins using site-directed mutagenesis and recombinant DNA technology and establish their cellular localisation in COS7 and Jurkat T cells under various culture conditions using fluorescent and confocal microscopy**
- **Determine the regions of DEF6 that facilitate granule formation and P-body colocalisation**
- **Determine the role of the coiled coil domain in DEF6 aggregation**
- **Determine the regions of DEF6 that facilitate GEF activity**
- **Determine the role of post-translational modification through phosphorylation of DEF6 by LCK and ITK**

Chapter 2

Materials and Methods

Materials

2.1 Mammalian cell culture

2.1.1 Cell lines

COS7 cells: African Green Monkey Kidney Fibroblast cells

Jurkat T cells: Jurkat E6.1 human leukemic T cell lymphoblasts (ECACC #88042803)

Raji B cells: Raji human B cell lymphoblasts (Sigma #85011429)

2.1.2 Cell culture media and solution

Dulbecco's Modified Eagle's Medium (DMEM) (Sigma, #D6429) supplemented with 10% (v/v) FBS (Sigma, #F9665) and stored at 4°C.

RPMI-1640 Medium (Sigma, #R8758) supplemented with 10% (v/v) FBS (Sigma, #F9665) and stored at 4°C.

1X Trypsin/EDTA was obtained by diluting **10x Trypsin/EDTA** (Sigma, #59418C) with 1x PBS.

Ringer's Buffer (RB): NaCl 9.058g, KCl 0.370g, CaCl₂ 0.294g, MgCl₂•6H₂O 0.204g, HaH₂PO₄•H₂O 0.276g, HEPES 2.384g and Glucose 1.800g was dissolved in 1L dH₂O and adjust pH to 7.2 by dropping NaOH or HCl solution under measure of pH meter (NANNA instrument pH210 Microprocessor pH Meter). This buffer was stored at -20°C, and filter sterilized before using.

Fetal Bovine Serum (FBS) (Sigma, #F9665)

Freezing Mix: 10% (v/v) DMSO in FBS

Alexa Fluor 568 Phalloidin and **Rhodamine Phalloidin** (ThermoFisher, #A12380 and #R415)

Genejuice Transfection Reagent (Novagen, #70967-3)

Sodium Arsenite (Sigma 50mM stock solution, #35000)

Nocodazole (Sigma, #M1404-2MG): dissolved in DMSO (1mg/ml) and stored at -20°C.

1x PBS; 1x PBS was prepared as 8g NaCl, 0.2g KCl, 1.44g Na₂HPO₄, and 0.2g KH₂PO₄ were dissolved in about 800ml dH₂O, and then adjust the pH to 7.4 to 7.6, finally made up to 1 liter and autoclaved.

4% paraformaldehyde (PFA): 0.8g paraformaldehyde was dissolved in 10ml dH₂O with 10µl 10M NaCl by 60°C heating in a 50ml-falcon tubes and once dissolved, 10ml 2x Tris Buffered Saline (TBS) was added. Per 10ml TBS was made by mixing 0.2ml 1M pH8-Tris solution and 0.6ml 5M NaCl in a final volume of 10ml.

Poly-L-lysine solution (Sigma, #P4832)

2.2 Bacterial cell culture

2.2.1 Competent Cells

Subcloning Efficiency DH5α Competent Cells (*E.coli*) (ThermoFisher, #18265017)

NEB High Efficiency 5- α Competent Cells (*E.coli*) (New England Biolabs, #2987)

XL10-Gold ultracompetent cells (Agilent Technologies, come with QuikChange Lightning Multi Site-Directed Mutagenesis Kit)

2.2.2 Bacteria culture broth/agar

Luria Bertani (LB) broth/agar: 1% (w/v) tryptone, 0.5% (w/v) yeast extract and 0.5% (w/v) were dissolved by dH₂O, for the LB agar, 1.5% (w/v) was added and then autoclaved at 121°C for 20mins. Before using, antibiotic as appropriate would be added.

Super Optimal Broth with Catobolite Repression broth (SOC), 2% (w/v) tryptone, 0.5% (w/v) yeast extract and 0.5% (w/v), 8.6mM NaCl, 2.5mM KCl, 20mM MgSO₄ and 20mM glucose were dissolved by dH₂O and autoclaved at 121°C for 20mins. No antibiotic has been used for SOC broth.

2.3 Antibiotics

Kanamycin (sodium salt, Sigma, #P0781), the stock solution was dissolved in dH₂O to obtain 30mg/ml concentration and then filter sterilized before stored at -20°C. It was used in LB broth/agar at final concentration: 30 μ g/ml.

Ampicillin (sodium salt, Sigma, #A2804), the stock solution was dissolved in dH₂O to obtain 100mg/ml and then filter sterilized before stored at -20°C. It was used in LB broth/agar at final concentration: 100 μ g/ml.

2.4 DNA Materials

Agarose gel (Sigma, #A9539-500)

10x TBE buffer: it was dissolved by 108g Tris, 55g Boric Acid and 9.3g EDTA in about 800ml dH₂O, and then adding dH₂O to one liter. The 1x TBE buffer was directly diluted from this 10x buffer by dH₂O.

DNA Restriction Enzymes and Buffers (New England Biolabs)

QuikChange Lightning Multi Site-Directed Mutagenesis Kit (Agilent Technologies, #210516)

dNTP Mix (Promega, #0000233460)

Q5 Hot Start High-Fidelity DNA Polymerase and Q5 Reaction Buffer (New England BioLabs, #M0493)

GenElute HP Plasmid Miniprep Kit (Sigma, #NA0150)

GenElute HP Endotoxin-Free Plasmid Maxiprep Kit (Sigma, #NA0410-1KT)

StrataClone Blunt PCR Cloning Kit (Agilent Technologies, #240207)

NucleoSpin Gel and PCR clean-up (MACHEREY-NAGEL, #740609.50)

Table 1: DNA oligonucleotides used for site-directed mutagenesis, PCR amplification or sequencing as indicated (Thermo Fisher Scientific)

Name	Sequence 5'-3'	Application
Q371P-A374P	ggaggcgcccgaggagcccgagcgg	All-10
R407P-M410P	gagcaggccccggcctccccgaggctgag	R407P-M410P
L442P-E445P	gttgcaggaggccccgcaactaccgggtgaaagctcggc	L442P-E445P
L463P-E466P	cttcagcttcttccggcttccggcagctgtgctgagc	L442P-E445P
L470P-L473P	gaggaggaagagaagccgaagcagccgatgcagctgaagg	All-10
K491P-L494P	ggcgcagcaggagccggaagaggcgcagcaggagatg	L470P-L473P

Name	Sequence 5'-3'	Application
L505P-A508P	gccgctccccgcagcagccccagcagc	L505P-A508P
L512P-V515P	ccagcagcagccggaggagccgcggcagaacc	All-10
L533P-A536P	ggggagagaaaaccgcgccagcccagcaccaa	L533P-A536P
Y133D	ccatgatcagagggtccttgcctcagac	Y133/144D
Y144D	ccttttcagcaggtcttcacctcatc	Y133/144D
Y133F	ccatgatcagagggaacttgcctcagac	Y133/144F
Y144F	ccttttcagcaggaattccacctcatc	Y133/144F
Y210E	gccatccacgagggtcgaacaggagctcatc	Y210/222F-Px
Y222E	tcctgaagcagggcgagctgtggaagcgagg	Y210/222F-Px
30-stop	ctccaagtcccagtagaagggtgtgtcccac	N-30
45-stop	cctgcacatcccctaggaccccgtggccc	N-45
79-stop	agtacatcctggacaagtaggaggagggggcctttg	N-79
216-stop	gagctcatccaataggctcctgaagcag	N-216
550-stop	ccagatgaaccggctgtagtagccaattgagcctggag	537aa-550aa
S-EcoRI-45	acacggctctgcacatcgaattcgaccccgtggcctgga	Δ 45-79
S-EcoRI-79	caacaagtacatcctggaattcgtggaggagggggcctttt	Δ 45-79
Sa-Final	ggtcctgcacatcgtggaggaggggg	Δ 45-79
G-EcoRI-108	agaagaactatcggcagatgaattcggggaacagtttgc	Δ 45-108 Δ 79-108
C-EcoRI-108	cgggcagaggaattcggggaacagt	Δ 45-108 Δ 79-108
C-EcoRI-0-79	tacatcctggaattcgtggaggag	Δ 0-79
78-EcoRI-79	aagtacatcctggacgaattcaaggtggaggagggg	Δ 79-108
EcoRI-216	gagctcatccaagatgaattcgtcctgaagcagggt	Δ 0-216
G-EcoRI-45	acacggctctgcacatcgaattcgaccccgtggcctgga	Δ 0-45
G-EcoRI-45	tgtacacggctctgcacgaattccatgaccccgtggccc	Δ 45-108

Name	Sequence 5'-3'	Application
EcoRI-311	gccatccagatggaattccggctgcaggccgagg	Δ 0-311
550-EcoRI-551	ccagatgaaccggctggaattcatgcatccaattgagc	550aa-590aa
535-EcoRI	gagaaaactgcgcaattcagcaccaacgtg	537aa-590aa 537aa-550aa
MSC-EcoRI-de	ctcgagctcaagcttcaaatgtgcagtcgacggtac	Destroy MSC EcoRI site
mCherry-sense	taccggtcgccaccatggtgagcaagggcgaggaggataa	Amplify mCherry
mCherry-anti-sense	cgagatctgctgtacagctcgtccatgccgccggtgg	Amplify mCherry
NLS-sense	agcttaccaaaaaagaagagaaaggtag	mCherry-NLS- DEF6
NLS-anti-sense	aattctacctttctctcttttttgg	mCherry-NLS- DEF6
Prom-sequencing	tgacgtcaatgacggtaaag	Sequencing
GFP-d-sequencing	gccctgagcaaagacccaacgagaag	Sequencing
DEF6-m-sequencing	acagctgccatccagatg	Sequencing
210/220-sequencing	ggcccaggtggcccagaccaccggg	Sequencing
C-half-sequencing	gaagctgaagcagttgatgcagctgaag	Sequencing
mCherry-d-sequencing	gcgctacaacgtcaacatcaagttgga	Sequencing

Methods

2.5 Bacteria technology

2.5.1 Bacteria freezing

A single colony of the bacteria was picked and cultured overnight in 5ml selective LB broth at 37°C with 220rpm shaking. The next day, the bacteria were be mixed with same volume of 80% glycerine (Sigma #SZBG020FV), aliquot into 0.5ml - Eppendorf tubes, cooled at 4°C for 1 to 2 hours and finally frozen at -80°C.

2.5.2 Recovery of frozen bacteria

Frozen bacteria were thawed at room temperature, and 20µl aliquots incubated in 1ml LB or SOC broth (without antibiotics) for an hour at 37°C with 220rpm shaking. Subsequently, 100µl bacteria solution was spread on selective LB agar and plates were incubated O/N at 37°C.

2.5.3 Cell transformation

20µl of competent cells were aliquoted in 1.5 ml eppendorf tubes and stored at -80°C. Before transformation, competent cells were thawed on ice and gently 1µl plasmid ($\geq 100\text{ng}$) added (avoiding pipetting them up and down). For XL10-Gold ultracompetent cells, 1µl β -ME (supplied with the kit) was added to the cells before adding plasmid DNA, incubating them on ice for 10 minutes with gently swirling every 2 minutes. Subsequently, the mixture was incubated on ice for 30 minutes and then heat-shocked in 42°C water bath. The time for heat-shock was different dependent upon which competent cells were used: for DH5 α subcloning efficiency and NEB High Efficiency 5- α competent cells, the time was 45 seconds;

and for XL10-Gold ultracompetent cells, the time was 30 seconds. After heat-shock, the tube of the cells was rapidly placed in ice for 2 minutes, and then 500 μ l per-warmed (42°C) SOC or LB broth without antibiotics was added to the cells and incubated for an hour at 37°C with 220rpm shaking. Following this incubation, 50 μ l of transformed bacteria was spread on selective (Kanamycin or Ampicillin) LB agar and plates incubated for overnight at 37°C.

2.5.4 Plasmid Miniprep (Sigma)

At the first day, a single bacterial colony was collected with a sterile bacterial loop, inoculated in 5ml selective LB broth and cultured overnight (13~16 hours) at 37°C with 220rpm shaking. The next day, bacteria from the O/N culture were harvested by centrifugation (1min, 13,000 x g) in a 1.5ml eppendorf tube, discarding supernatant if necessary, this step was repeated 2 to 3 times to collect sufficient number of bacteria. The bacteria pellet was resuspended in 200 μ l of resuspension solution, and 78 μ l RNase A was added and stored at 4°C. The resuspended bacteria cells were lysed by adding 200 μ l lyses buffer immediately mixing the solution by inverting the tube several times until the content appeared to be clean and viscous. Following this step, 350 μ l of S3 Neutralization/Binding Solution was added, the tube inverted about 6 times to mix the content, and then centrifuged for 10 minutes at 13,000 x g speed.

After centrifugation, the cleared supernatant was transferred to a prepared spin column (column preparation was adding 500 μ l column preparation solution into the column and then centrifuging for 1 minute at 13,000 x g speed) and the column was placed in a collection tube, which was subsequently centrifuged for 1

minute at 13,000 x g speed. After this step, 500µl optional-wash solution and 750µl wash solution were successively and respectively adopted to wash the column by 1 minute centrifuge at 13, 000 x g speed. The centrifuge step was repeated again for further removing the wash solution.

Finally, plasmid DNA was eluted from the column by adding 50µl of the elution solution. The column was incubated at room temperature for one minute and then centrifuged for one minute at 13,000 x g speed to collect the eluted plasmid DNA. The concentration of the plasmid DNA was determined using Nanodrop machine.

2.5.5 Plasmid Maxiprep (Sigma)

Maxiprep of plasmid DNA was essentially based on the same principle as miniprep procedure and hence only the differences are listed here. To prepare a large volume of bacteria culture the initial 5ml O/N culture was inoculated in 200ml selective LB broth using a 500ml flask and incubated overnight at 37°C with 220rpm shaking. Bacteria were harvested by centrifugation at 5, 000 x g for 10 minutes using 4 x 50ml-falcon tubes. The pellet was subsequently resuspended in 12ml resuspension/RNase A solution and lysis solution, followed by the addition of 12ml chilled neutralization solution. Cleared lysate was collected by filtration through vacuum rather than centrifugation. 9ml binding solution was added to the filtered lysate and subsequently passed through a prepared binding column again using vacuum to bind the plasmid DNA. After repeated washing steps using 12ml Wash Solution 1 and 2, which was also by vacuum the column

was air-dry for several hours and the plasmid DNA was eluted by centrifugation (5, 000 x g for 5 minutes) using 3ml endotoxin-free water. The binding column was prepared by adding 5ml column preparation solution in a 50ml-falcon tube and centrifuged at 5, 000 x g speed for 5 minutes.

2.6 Nucleotide technology

2.6.1 DNA restriction enzyme digestion

Restriction enzyme digestions were set up for small-scale or larger-scale digestion as indicated in Table 2.

Table 2. The setting up of DNA digestion reaction

Incubating Time	1h	3h
dH ₂ O	2.5µl	0
Buffer	0.5µl	2µl
DNA	1µl	15µl
Enzyme(s)	1µl	3µl

2.6.2 DNA gel electrophoresis

Agarose gel powder (Sigma, #A9539-500) was melted in 1x TBE buffer by microwave oven, and then cooled to ~40°C in a water bath. The range of agarose concentration was from 0.5% to 2% depending on the size of the DNA fragments analysed. 0.5% gels were used for extraction of DNA from the agarose. SafeViwe (source) was mixed to the agarose solution (1‰ final concentration) before preparing the gel. DNA samples and DNA marker ladders were mixed with 6x loading dye (final 1x) and samples loaded into wells. After electrophoresis under a constant suitable voltage (90-120V) the results were visualized using UV trans-illumination.

2.6.3 DNA extraction from agarose gel

The NucleoSpin Gel and PCR clean-up Kit (MACHEREY-NAGEL, #740609.50) were used to isolate DNA fragments from agarose gels essentially according to the protocols provided. The gel slice containing the DNA fragment was excised under UV light (Bio-Red Molecular Imager Gel Doc™ XR+ System #1708195EDU) and

dissolved in NTI buffer in a volume according to the weight of the gel slice; 200µl NTI buffer for each 100mg agarose gel. The mixture was incubated at 50°C and vortexed every 2 to 3 minutes until the gel was completely dissolved. This solution was transferred to a spin column and centrifuged for 30 seconds at 11,000 x g discarding the flow-through. 700µl Buffer NT3 was added to the column and the column was centrifuged for 30 seconds at 11,000 x g. This washing step was repeated and the column air dried for 1 min. Subsequently, the column was inserted into a new 1.5-ependorf tube, and the DNA was eluted by adding 20µl Buffer NE followed by another centrifugation step as before. The concentration of the eluted DNA was determined using Nanodrop.

2.6.4 DNA ligation

To clone DNA fragments into plasmid vectors, DNA ligation reactions were set up as following:

2µl 10X T4 DNA Ligase Buffer, 50ng digested vector DNA, relative amount insert DNA (3 molar times of the vector DNA), 1µl T4 DNA Ligase, and adding dH₂O to final volume of 20µl. After incubation at room temperature for 10 minutes 5µl of the reaction was used for transformation as described above.

2.6.5 Q5 Polymerase Chain Reaction (PCR), and StrataClone Blunt PCR Cloning (Agilent Technologies) to establish recombinant plasmids

Following on Q5 PCR amplification, StrataClone Blunt PCR Cloning kit was used to establish new recombinant plasmids. Q5 PCR reaction system and cycling were prepared as indicated in Tables 3 and 4.

To amplify DNA appropriate for subsequent subcloning, specific primers were designed (see Table 1). DNA was amplified by PCR (Table 3 and 4) and successful amplification was monitored by gel electrophoreses using 5 μ l of the PCR product. The PCR product was diluted 10 x with dH₂O and 2 μ l of this was mixed with 3 μ l Blunt Cloning Buffer and 1 μ l StrataClone Blunt Vector. After incubation for 5 minutes at room temperature, 3 μ l of the mixture was used to transform NEB 5 α high efficiency competent cells. For blue-white selection, bacterial cells were cultured on LB agar plates containing 100 μ g/ml ampicillin and 20 mg/ml X-gal. Several white (or light blue) colonies were selected to isolate plasmid DNA and aliquotes analysed by restriction enzymes digestion and gel electrophoresis to ensure successful cloning. To transfer the subcloned fragments from the StrataClone Blunt Vector into expression vectors, DNA fragments after appropriate restriction enzyme digestion were isolated and ligated as described (2.6.3 and 2.6.4). Expression vectors **mCherry-Dcp1**, **mCherry-DEF6** and **mCherry-Y133/144D** were generated and partly sequenced to verify in-frame cloning (vector maps and nucleotide sequences are listed in the appendix 8.1 and 8.3).

Table 3. The PCR reaction system for inserting and amplify DNA fragment

Template DNA	0.5μl (50ng)
Q5 Reaction Buffer	5 μ l
dNTP (10mM of each dNTP)	0.5 μ l
Sense Primer	0.5 μ l (10pmol)
Anti-sense Primer	0.5 μ l (10pmol)
Q5 Hot Start High-Fidelity DNA Polymerase	0.25 μ l
dH ₂ O	17.75 μ l

Table 4. The Cycling Parameters for inserting and amplify DNA fragment

Segment	Cycles	Temperature	Time
1	1	98°C	2 minutes
2	30	98°C	30 seconds
		65°C	45 seconds
		72°C	30 seconds per 1 kb
3	1	72°C	5 minutes
4	~	4°C	~

To insert the SV40 nuclear localisation signal (NLS) into the mCherry-DEF6 vector to create mCherry-NLS-DEF6, sense and antisense oligonucleotides were designed that contained the NLS sequence flanked by HindIII (AAGCTT) and EcoRI (GAATTC) restriction enzyme recognition sites at their 5' and 3' end respectively (see Table1 and Appendix Fig. 8.1.2 and 8.3.2 Fig for nucleotide sequence), and purchased from Thermo Fisher Scientific. The two oligos were dissolved in dH₂O, mixed 1:1 and incubated to 90°C for 30 seconds before letting the mixture cool down to room temperature. The annealed NLS DNA was then subcloned into mCherry-DEF6 that had been digested with HindIII and EcoRI and successful in-frame cloning was verified by partial sequencing (vector map and sequence see appendix).

2.6.7 QuikChange Lightning Multi Site-Directed Mutagenesis PCR (Agilent)

To create mutant GFP-tagged DEF6 proteins, site-directed mutagenesis was employed essentially following the protocol provided by Agilent. Oligonucleotides were designed that contained the desired mutations and used to introduce the mutation into the wild-type DEF6 cDNA using GFP-DEF6 as a template for amplification (Tables 5 and 6). After incubation with 1.5µl Dpn-I to digest the

methylated template plasmid DNA, the amplified single-stranded DNA was transformed into XL 10-Gold ultracompetent cells. Mutant plasmid DNAs were isolated as described (2.5.4) and partially sequenced to verify successful introduction of the desired mutations (for sequences see appendix 8.3).

Table 5 The PCR reaction system of the QuikChange Lightning Multi Site-Directed Mutagenesis

dH ₂ O	17.75µl
10× QuikChange Lightning Multi reaction buffer	2.5µl
QuikSolution	0.75µl
ds-DNA template	1µl (100ng)
Mutagenic primers	1µl (100ng)
dNTP mix	1µl
QuikChange Lightning Multi enzyme blend	1µl

Table 6. The Cycling Parameters for the QuikChange Lightning Multi Site-Directed Mutagenesis

Segment	Cycles	Temperature	Time
1	1	95°C	2 minutes
2	30	95°C	20 seconds
		55°C	30 seconds
		65°C	3.5 minutes
3	1	65°C	5 minutes
4	~	4°C	~

The following mutant plasmids were established using three strategies.

Method A: amino acid replacement with the desired new amino acid or with a stop codon. The mutants established by this method were: **Q371P-A374P**

(Mollett, 2014), **R407P-M410P, I428P-L431P** (Mollett, 2014), **L442P-E445P, L463P-E466P, L470P-L473P** (Mollett, 2014), **K491P-L494P, L505P-A508P, L512P-V515P** (Mollett, 2014), **L533P-A536P, Q371P-A374P-L505P-A508P, R407P-M410P-L505P-A508P, I428P-L431P-L505P-A508P, the All-10 mutants, 537aa-590aa, Y133/144D, Y133/144F, Y210/222E-Q371P-A374P, Y210/222E-I428P-L431P, Y210/222E-L505P-A508P, Y210/222E-Q371P-A374P-L505P-A508P, Y210/222E-I428P-L431P-L505P-A508P, Y210/222E-All-10, N-30, N-45, N-79, N216, N-312, Δ 0-104-Y210/222E, and Δ 0-104-Y210/222F.**

Method B: introduction of EcoRI restriction enzyme sites at various positions of the GFP-DEF6 vector to create truncation mutants **Δ 0-311, Δ 0-216, Δ 0-79, Δ 0-45, 537aa-590aa, 551aa-590aa, ITAM and Δ 0-216-All-10.**

Method C: to first destroy the EcoRI site in the multiple cloning site between eGFP and DEF6 and to subsequently insert two new EcoRI restriction enzyme sites at appropriate positions in the GFP-DEF6 vector. After deletion of the EcoRI-flanked sequence, the left-over EcoRI site was changed with an appropriate primer to provide in-frame deletion mutants **Δ 45-79, Δ 79-108 and Δ 45-108.**

For vector maps see appendix 8.1.

2.7 Mammalian cell culture

2.7.1 Passaging of Adherent Cells (COS7)

COS7 cells were cultured in 10% FBS supplemented DMEM at 37°C, 5% CO₂ and humidified atmosphere using 10cm² petri dishes. At 70~90% confluency, medium

was removed and the attached cells washed with 5ml 1x PBS. Cells were then rinsed with 2ml 1x Trypsin-EDTA and incubated for 2-5 minutes at 37°C. Detached cells were resuspend in 10ml fresh full culture medium and aliquots of 2ml added to 10ml fresh full culture medium in a new petri dish. COS7 cells were passaged about every 2-3 days.

2.7.2 Passaging of Cells growing in Suspension (Jurkat T cells and Raji B cells)

Jurkat T cells and Raji B cells were incubated at 37°C, 5% CO₂ and humidified atmosphere as above. However, these cells were cultures in RPMI-1640 with 10-15% FBS using 75cm² or 150cm² flasks (Corning #431464 and #431465). Number of viable cells was determined using trypan blue staining (Sigma #42K2360) and passaged by either adding fresh medium or dilution to keep a cell density of 3-5 x 10⁵ cells/ml.

2.7.3 Cryopreservation of mammalian cell lines

Cells were harvested in their logarithmic growth phase by centrifugation (3 minutes at 300 x g) and resuspended in 1ml 10% FBS in DMSO, incubated at 4°C for 10 mins, at -20°C for 20 mins, at -80°C overnight and finally stored in liquid nitrogen.

2.7.4 Recovery of cells after cryopreservation

Frozen cells were thawed instantly at 37°C either transferred into prewarmed 10 ml DMEM medium (COS7) or diluted in a small volume (about 2 ml) of RPMI-1640 medium and after determination of viable cell count further diluted to obtain a cell concentration of 2 x 10⁵/ml (Jurkat T and Raji B cells).

2.7.5 Transfection of COS7 cells

COS7 cells were seeded (about 1×10^5 /ml and 2 ml each) on clean and sterilized coverslips in a 6-well plate one day before the transfection. At 50 to 70% confluency, 1ng plasmid DNA was used for each well. Prior to transfection, plasmid DNA was mixed with 1% volume of 2M NaCl and 2.5x volume of -20°C 100% ethanol in a 1.5-ependorf tube, and then incubated at -20°C for at least 10mins. Precipitated plasmid DNA was recovered by centrifugation (10mins at 4°C and 13000rpm speed), the pellet washed by 150µl 70% ethanol at -20°C and again recovered by centrifugation as above. After removal of the ethanol, DNA pellet was air dried in a biosafety cabinet (class II) and then dissolving in 100 µl of FBS and antibiotics free culture medium was added. 3µl Genejuice transfection reagent (Novagen, #70967-3) was added and the mixture incubated at room temperature for 10mins. Finally, the mixture was evenly dropped onto the cells of each well and incubated for either 24 hrs or 48 hrs as described above.

2.7.6 Transfection of Jurkat T cells

Jurkat T cells were transfected using square-wave electroporation (BTX Elector Square Porato T820). 50µg plasmid DNA was prepared as described in 2.6.5 and the DNA dissolved in 150µl FBS free and antibiotics free RPMI-1640 medium. 2×10^7 Jurkat cells were collected by centrifugation (3mintues at 300x g speed), resuspended in 150µl FBS and antibiotics free RPMI-1640 medium, mixed with the plasmid DNA in a 4mm-gap electroporation cuvette and electroporated (310V voltage, 10ms pulse length and 1 pulse). Then, transfected cells were diluted and cultured in 10 ml 10% FBS contained RPMI-1640 medium for 24 hrs.

2.7.7 Jurkat T and Raji B cells conjugation

Raji B cells were incubated with *Staphylococcus aureus* enterotoxin A/B and mixed with Jurkat T cells. At B/T conjugations, super antigen presentation by Raji B cells triggered TCR-mediated signalling and IS formation in Jurkat T cells. 6.6×10^6 Raji cells were collected by centrifugation (3mins at 300x g), resuspended in 1 ml full culture medium containing $1\mu\text{g}/\text{ml}$ calcein blue and incubated at 37°C for 20mins. Calcein blue diffuses into the B cells marking them and with blue fluorescence so that they could be distinguished from T cells. Marked B cells were harvested (300x g, 3mintues), washed twice in $100\mu\text{l}$ fresh medium and resuspended in 1ml fresh medium containing $1\mu\text{g}/\mu\text{l}$ *Staphylococcus aureus* enterotoxin A/B. After 30mins incubation at 37°C the antigen presenting B cells were collected by centrifugation and resuspended in $250\mu\text{l}$ fresh medium. 3.3×10^6 Jurkat T cells were prepared at same time by centrifuge and also resuspended in $250\mu\text{l}$ fresh medium. Subsequently, both cell types were mixed and incubated at 37°C for 1 hour to allow them conjugate. 1ml fresh medium was added to the conjugated cells and $500\mu\text{l}$ each were seeded onto poly-L-lysine coated coverslips. Cells were fixed after 5mins (see 2.6.8).

To prepare coverslips, $300\mu\text{l}$ poly-L-lysine solution was distributed over the coverslip and after 10mins, coverslips were rinsed twice with sterilized distilled water and air dried.

2.7.8 Cell fixation

After removal of the culture medium, cells on the coverslips were fixed adding 1ml pre-warmed (37°C) 4% PFA (prior to fixation of COS7 cells, cells were washed once with 1x PBS at 37°C before adding PFA). Coverslips were covered

with aluminium foil and after 10 to 15mins fixation in the tissue culture cabinet, PFA was removed and the fixed cells washed three times with 1ml 1x PBS at 37°C. If no further processing was required, FluoroGen mounting medium (GeneTex) was dropped onto a glass slide and coverslip placed upside-down onto the drop. Glass slide were labelled, air dried and stored in a dark place.

2.7.9 Phalloidin staining of f-actin

The stock phalloidin (300U) solution (ThermoFisher, #A12380) was dissolved in 1.5µl methanol and stored at -20°C. The stock solution was diluted in 1x PBS by 1:100 and 50µl was used for each slide to stain f-actin. For COS7 cells, 50µl working solution was dropped onto a piece of parafilm, and coverslip was placed upside-down onto the solution. Slides with fixed Jurkat T cells and Raji B cells were placed onto a piece of parafilm 100µl working solution was dropped onto each slide. After incubation cells at room temperature for about an hour covered in foil stained cells were washed and mounted as described above.

2.7.10 Cell imaging

Cells were imaged using either a conventional fluorescent (Zeiss AxioSkop MOT) or a confocal Zeiss LSM710 microscope with 40x, 63x and 100x objectives (SLIM facility). Fiji software was used for image analysis.

The red fluorescent protein, mCherry, can also be excited to fluorescent green light. It was therefore essential to adjust the range of wavelength the camera of the confocal Zeiss LSM710 microscope can receive to eliminate the potential of green fluorescence by mCherry.

Chapter 3

Study of DEF6 Granule Formation: Colocalisation with P-bodies versus DEF6 aggregation

3.1 The N-terminal part of the DHL domain contains a Q-rich coiled coil domain

The coiled coil domain is a left-handed alpha helix that can interact with other coiled coil domains to form a right-handed supercoil structure. Typically, these supercoiled structures contain two coiled coil domains, but up to seven have been noted (Liu *et al.*, 2006). The coiled coil motif is characterised by a heptad (seven) repeat denoted as $(a-b-c-d-e-f-g)_n$, where “a” and “d” positions are occupied by nonpolar amino acids, which interact with “a” and “d” positions of another coiled coil domain forming a hydrophobic core (Fig. 3.1.1). In addition, de novo-designed and native coiled coil studies demonstrated that “a” and “d” positions of the coiled coil are critical for folding and stability endowing a thermodynamic driving force (Tripet *et al.*, 2000; Mason & Arndt, 2004). Frequently, “e” and “g” positions are charged amino acids that interact with the other chain’s “e” and “g” amino acids through interhelical ionic interactions influencing the preference of helix orientation, partner specificity and the stability of the structure. The “b”, “c” and “f” positions are normally polar or charged (Fig. 3.1.1; Tripet *et al.*, 2000; Mason & Arndt, 2004; Deng *et al.*, 2007).

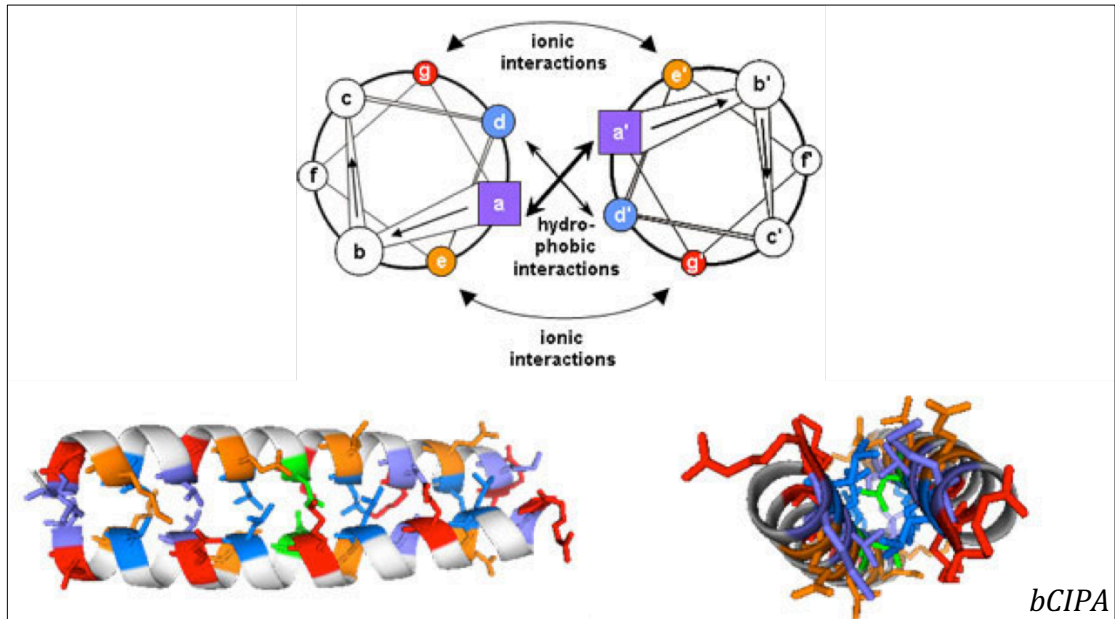


Fig. 3.1.1 Schematic diagram of zenithal and lateral view of a two-stranded coiled coil motif.

Heptad of one coiled coil domain is denoted as a-b-c-d-e-f-g, the other as a'-b'-c'-d'-e'-f'-g'. Interaction of a, d with a', d' forms a hydrophobic core and g, e and g', e' are normally charged and their ionic interactions stabilises the coiled coil oligomerisation (Mason & Arndt, 2004).

Ferdinando *et al.* reported in 2010 that Q/N-rich and polyQ containing proteins tend to form coiled coil structures. Similarly, the N-terminal part of the DHL domain of DEF6 contains a 28-heptad Q-rich repeat region (Fig. 3.1.2 A) that was predicted by bioinformatics analysis using Paircoil2 (Hey *et al.*, 2012; see also Fig. 3.2.2) and through Circular Dichroism spectra analysis (Fig. 3.1.2 B; Mollett, 2014) to form a coiled coil structure.

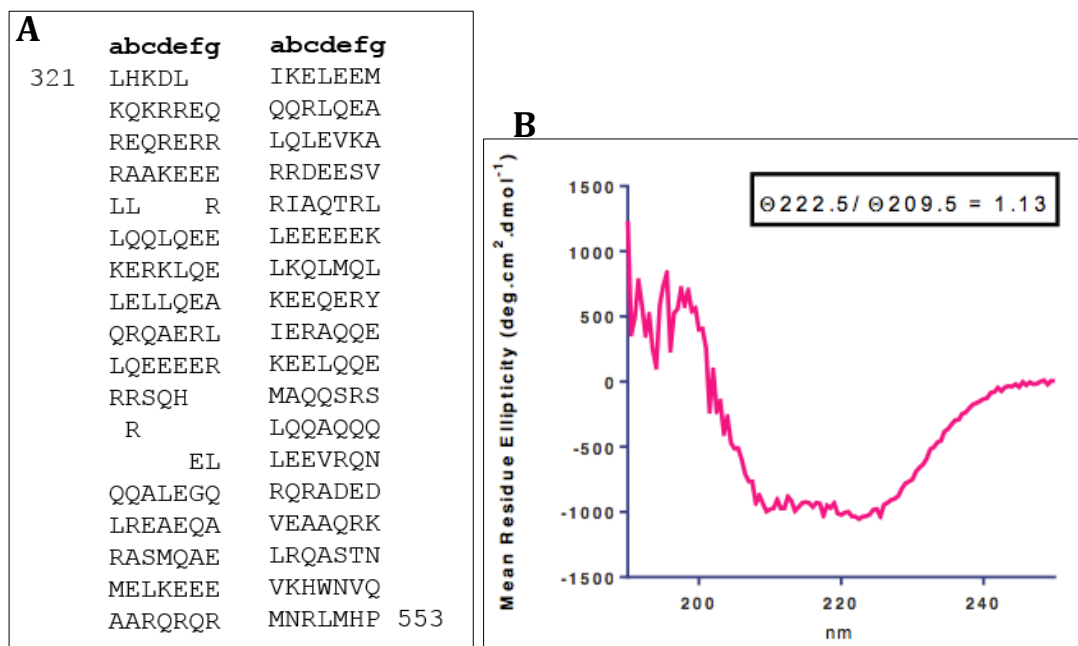


Fig. 3.1.2 Predicted coiled coil domain of DEF6

(A) Heptad repeat of DEF6 from amino acid 321 to 553 (Hey *et al.*, 2012).

(B) Circular Dichroism spectra analysis of amino acids 321 to 553 of DEF6. The mean residue ellipticity is consistent with a coiled coil structure (Mollett PhD thesis, 2014).

3.2 Substitution of highly conserved amino acid residues in the “a” and “d” position with prolines disrupt the coiled coil structure of DEF6

Hey *et al.* (2012) described that phosphorylation of DEF6 by ITK caused a conformational change resulting in DEF6 granule formation, colocalising with the P-body marker DCP1. Given that P-body components often are proteins with coiled coil domains such as EDC3 and GW182 (Reijns *et al.*, 2008; Chang *et al.*, 2014), it was suggested that the conformational change released the coiled coil domain of DEF6 facilitating colocalisation and perhaps interaction with P-body components. To test this hypothesis, amino acids in ten “a” and “d” positions within the coiled coil domain were exchanged with proline residues. It had been shown that introduction of prolines disrupts the formation of coiled coil domains (Chang *et al.*, 1999). Amino acid sequences alignments of DEF6 and its only related protein SWAP70 indicated that amino acids in the “a” and “d” positions are highly conserved across species from human to trichoplax (Fig. 3.2.1; Spencer and Sablitzky, unpublished; Shuen, 2010). Based on these analyses, 10 a/d positions as indicated in Fig. 3.2.1 and Fig. 3.2.2 were selected and the amino acids exchanged with prolines using site-directed mutagenesis (Chapter 2, 2.5.2). Initially, 10 mutant DEF6 proteins with a single set of a/d mutations were established (Q371P-A374P, R407P-M410P, I428P-L431P, L442P-E445P, L463P-E466P, L470P-L473P, K491P-L494P, L505P-A508P, L512P-V515P and L533P-A536P), and subsequently, multiple sets of a/d mutations were combined with one DEF6 protein containing all 10 sets of a/d mutations (Q371P-A374P-L505P-A508P, R407P-M410P-L505P-A508P, I428P-L431P-L505P-A508P and All-10 mutant) (Fig. 3.2.2). Sequence analysis of all mutants confirmed exchange of codons at the a/d positions chosen with no other apparent changes of the DEF6 coding region (Appendix 8.3, Fig. 8.3.1). COIL2

analysis shown in Fig. 3.2.2 C suggested that introduction of proline residues indeed disrupts the coiled coil domain.

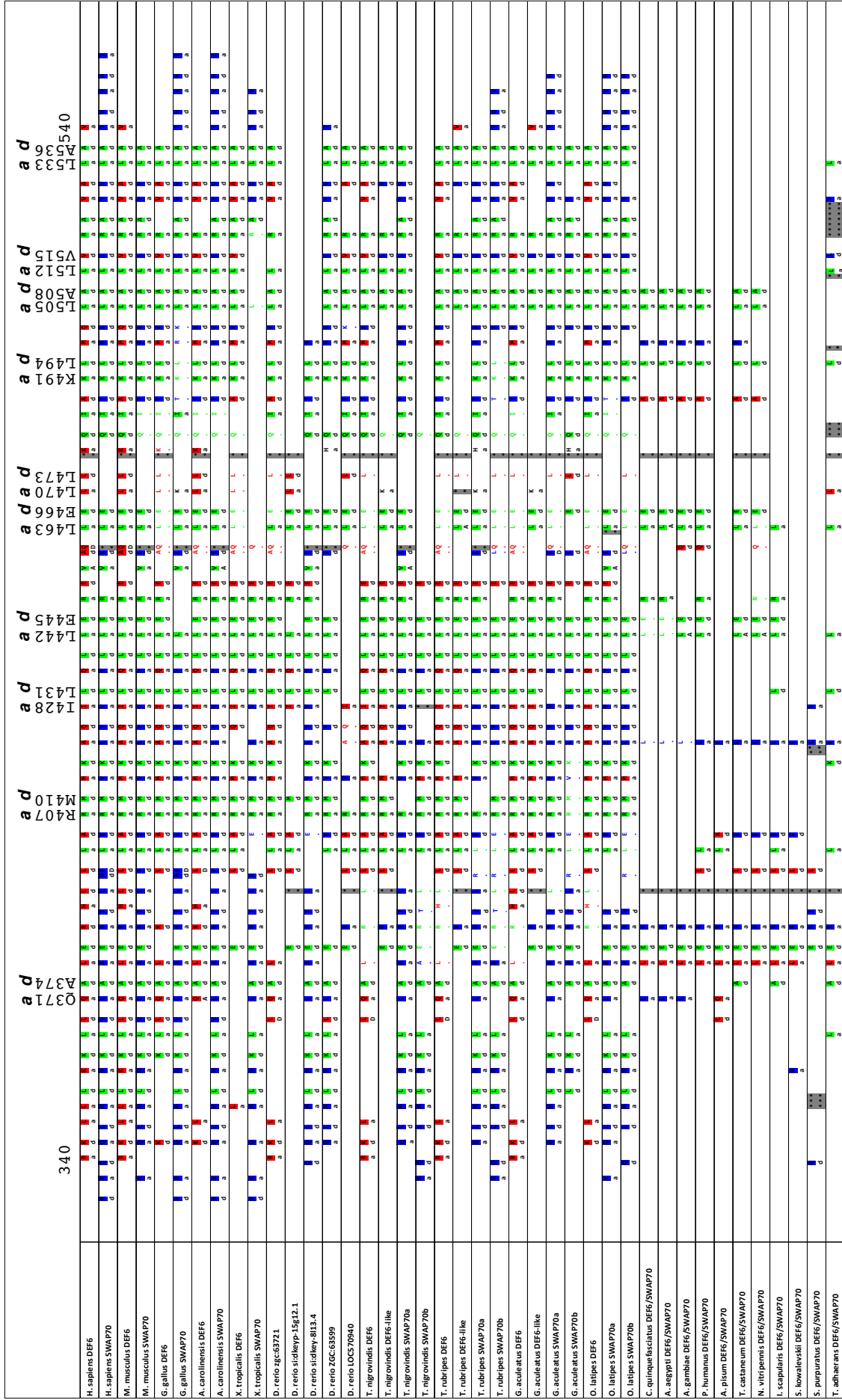
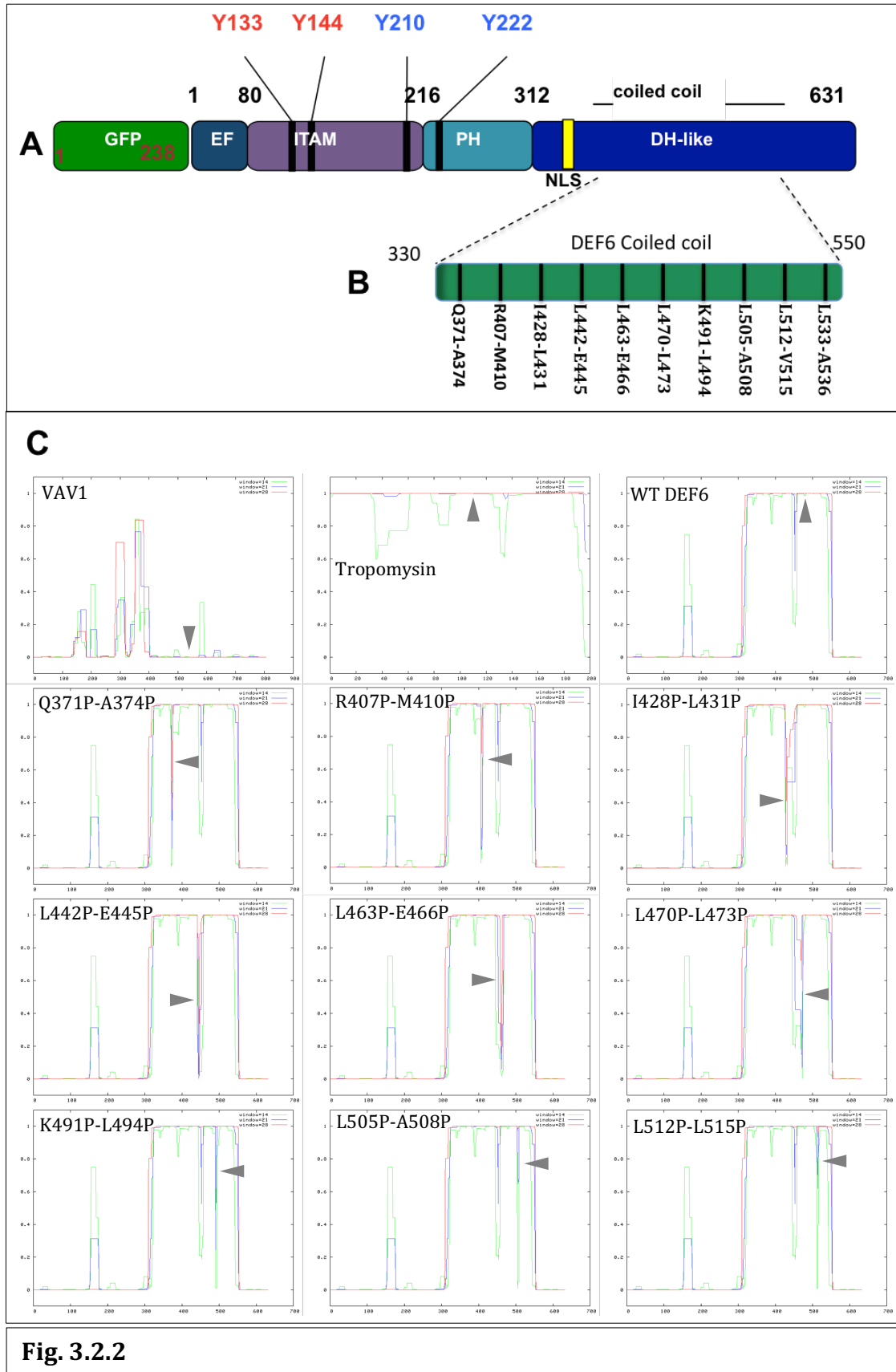


Fig. 3.2.1 Comparison of the ~ a ~ and ~ d ~ positions within the coiled coil domain of DEF6 and SWAP70 across species from human to trichoplax
 Colour coding of amino acid residues indicates identity: red – amino acids identical to the ones in human DEF6; blue – amino acid identical to the ones in human SWAP70; green – amino acids identical to both human DEF6 and SWAP70 (Spencer and Sablitzky, personal communication).



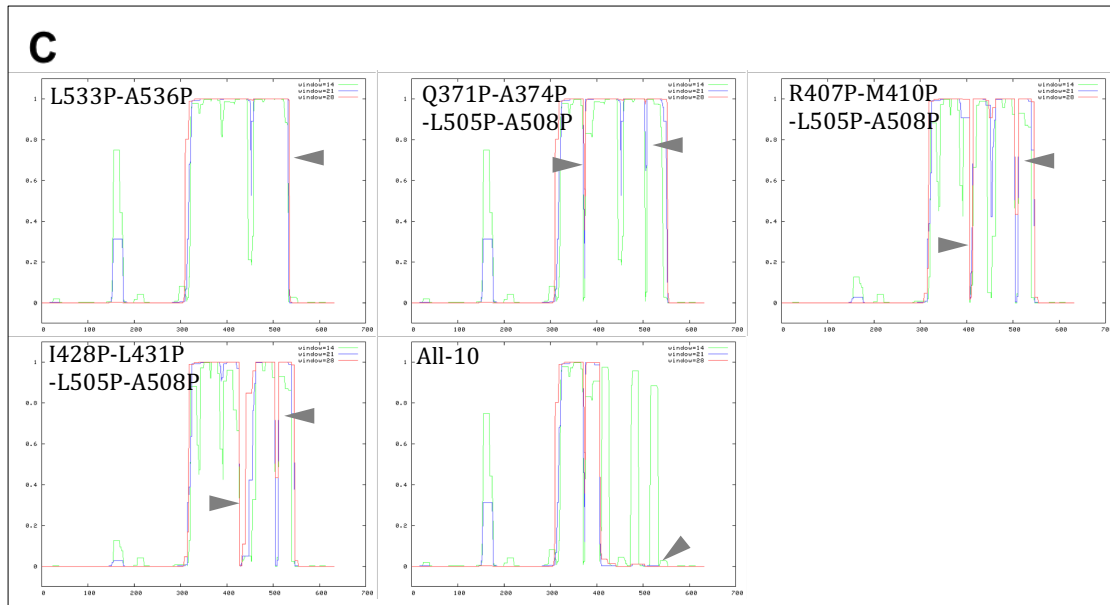


Fig. 3.2.2 Insertion of proline residues at selected a/d positions disrupts the coiled coil domain of DEF6

(A) Schematic representation of the domain structure of DEF6 fused to GFP. EF: Ca²⁺-binding EF-hand; ITAM: immunoreceptor tyrosine activation motifs within the DEF6-SWAP70 homology domain; PH: pleckstrin homology domain; DHL: Dbl homology like domain (see Figure 1.3.0). Within the ITAM and PH domains, Try-133/144 are phosphorylated by LCK and Try-210/222 by ITK. DHL domain contains a nuclear localisation sequence (NLS) and a coiled coil structure.

(B) 10 highly conserved *a/d* positions within coiled coil sequence of DEF6 were selected and amino acids replaced by prolines (P) as indicated.

(C) Coil2 analysis predicted disruption of the coiled coil domain in proline mutants compared to wild type DEF6. *a/d* double P mutants and ALL-10 predictions are shown as indicated. Vav1, lacking a coiled coil domain, served as a negative control and tropomyosin that consists entirely out of a coiled coil structure as a positive control.

3.3 Proline mutants exhibited three types of distinct phenotypes but none of the mutant proteins colocalised with P-bodies.

GFP-tagged DEF6 wild type and proline mutants were transfected into COS7 cells and the cellular localisation of the proteins was determined after 24h by fluorescent and/or confocal microscopy. COS7 cells do not express LCK nor ITK, two kinases known to phosphorylate DEF6 in T cells (Hey et al., 2012) but it cannot be ruled out that other unknown modifications of DEF6 might occur. Nevertheless, changes in cellular localisation in non-treated COS7 cells are likely

a consequence of conformational change due to the introduction of the proline residues rather than post-translational modifications. Compared to wild type DEF6 and GFP alone, that are diffuse in cytoplasm and in the case of GFP also in the nucleus, proline mutants exhibited three types of distinct phenotypes. R407P-M401P, I442P-E445P and K491P-L494P exhibited a diffuse localisation in the cytoplasm similar to wild type DEF6 (Fig. 3.3.0). Apart from Q371P-A374P, all other single set of a/d mutants as well as combined sets including the ALL-10 mutant seemed to mainly localise in filopodia, lamellipodia and podosomes suggesting colocalisation with F-actin (see also Fig. 3.3.0 and chapter 4). Q371P-A374P was mainly diffuse in the cytoplasm and somewhat localised with F-actin on lamellipodia but it also occasionally formed granules in the cytoplasm (Fig. 3.3.0). To test whether Q371P-A374P granules colocalise with P-bodies, a cotransfection with a P-bodies maker, DCP1 tagged with mCherry was carried out. Confocal analysis with Z-stack images shown in both vertical and side versions (X and Y coordinates) to provide a 3D view, revealed clearly that Q371-A374P granules did not colocalise with DCP1 (Fig. 3.3.1). It is not clear whether Q371-A374P granules are associated with other known cytoplasmic granules such as stress granules or just aggregation of the mutant protein. This was not further analysed given that Q371-A374P granules were less common than the mutant protein being diffuse in the cytoplasm.

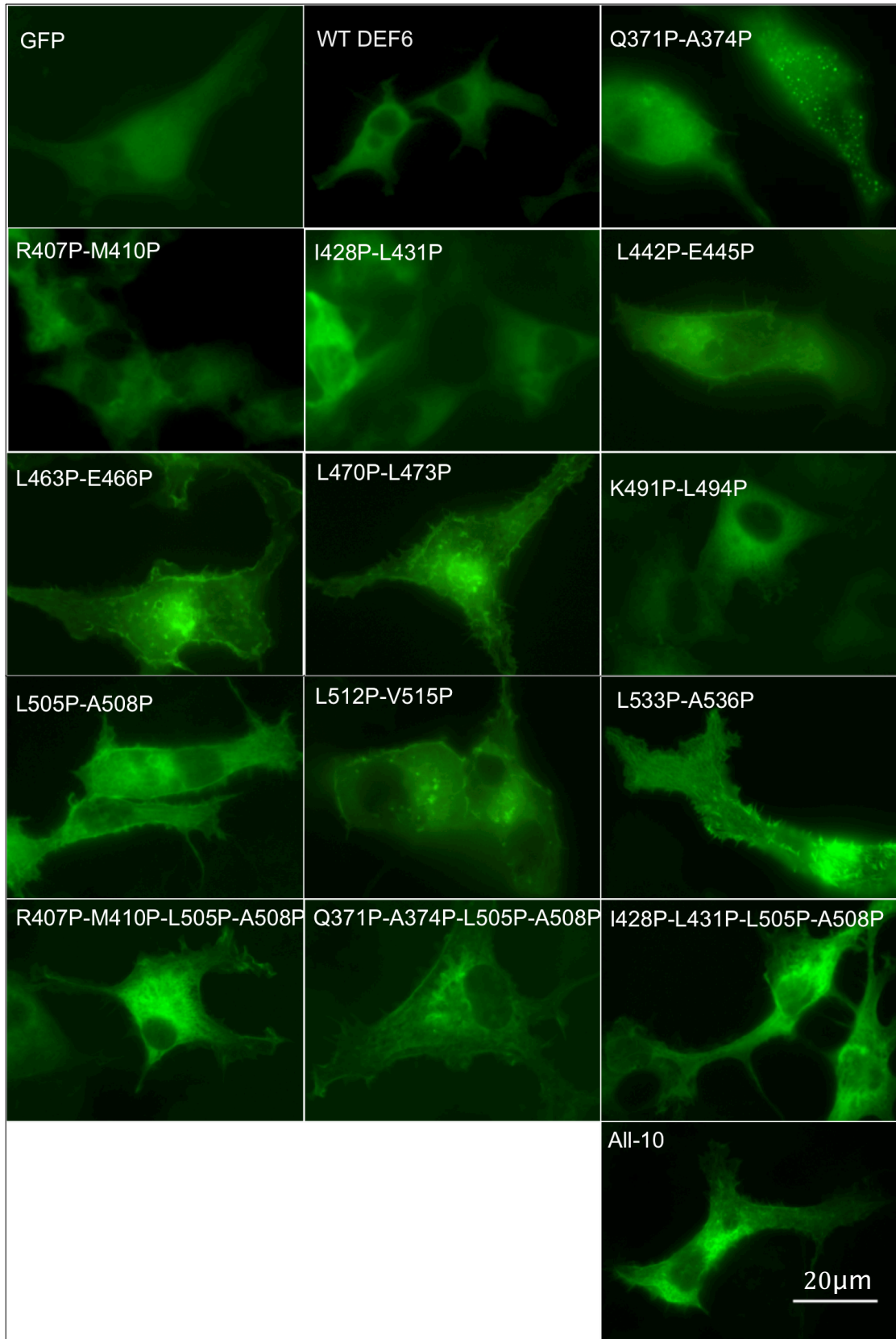


Fig. 3.3.0

Fig. 3.3.0 GFP-tagged DEF6 proline mutants exhibited three types of cellular localisation in COS7 cells.

Type 1: Q371P-A374P was mainly diffuse in the cytoplasm but occasionally exhibited granules

Type 2: R407P-M410P, I428P-L431P and K491P-L494P were localised diffuse in the cytoplasm similar to WT DEF6

Type 3: All other mutant proteins as indicated localised in lamellipodia, filopodia and podosome (see also Chapter 4).

GFP alone localised diffuse in the cytoplasm and nucleus.

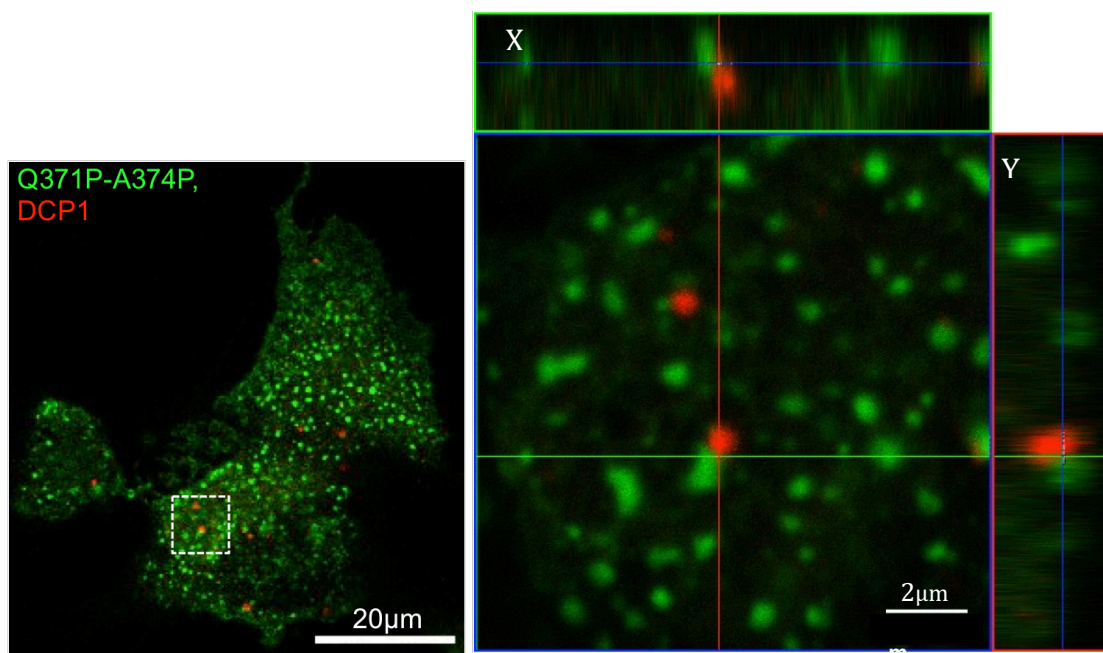


Fig. 3.3.1 Q371P-A374P mutant granules are not colocalising with P-bodies

Confocal Z-stack image analysis of Q371P-A374P (green) and P-body marker DCP1 tagged with mCherry (red) cotransfected in COS7 cells. Boxed area in the left image is shown enlarged on the right. Vertical and side views (X and Y coordinates) are also shown indicating that Q371P-A374P did not colocalise with DCP1.

3.4 Arsenate treatment failed to induce colocalisation of the proline mutants with P-bodies.

Arsenate treatment of cells results in an oxidative condition that leads to arrest of mRNA translation and induction of stress granules and P-bodies (Anderson and Kedersha 2009). It was previously shown that wild type DEF6 relocates and colocalises with DCP1 in P-bodies, after arsenate treatment (Hey *et al.*, 2012) in COS7 cells. To test whether disruption of the coiled coil domain by the introduction of prolines would interfere with granule formation, COS7 cells were treated with 1mM arsenate (Sigma) for 40 mins 24 hrs after transfection. As shown in Fig. 3.4.0, wild type DEF6 formed granules in cytoplasm as expected. Apart from K491P-L494P mutant that exhibited granules in a subset of cells (~17%), all other single set as well as combined sets including the All-10 mutant did not form granules. These results are in line with the notion that the coiled coil domain is essential for granule formation and suggest that K491P-L494P mutation might be less disruptive to the coiled coil domain than the other proline mutations.

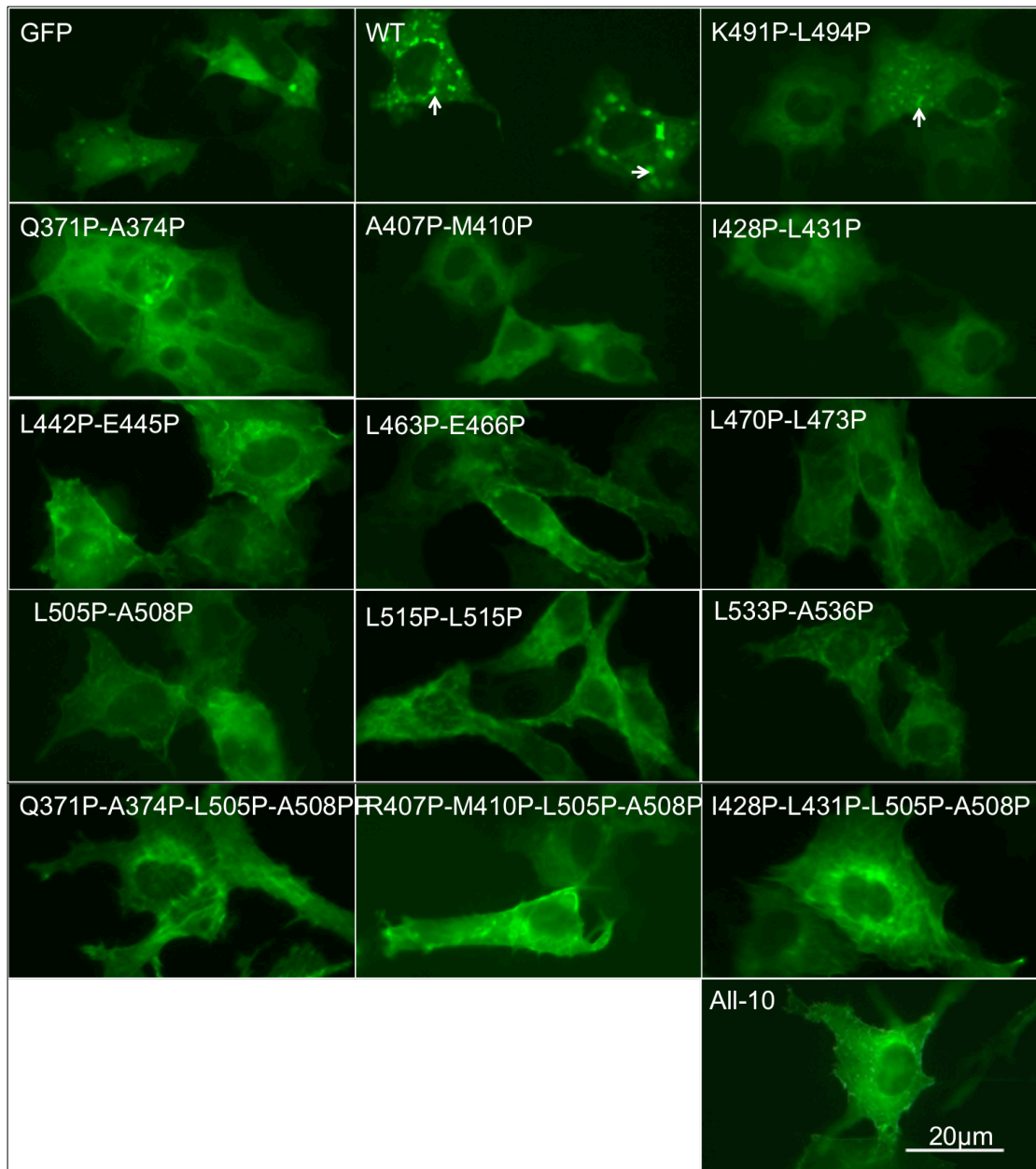


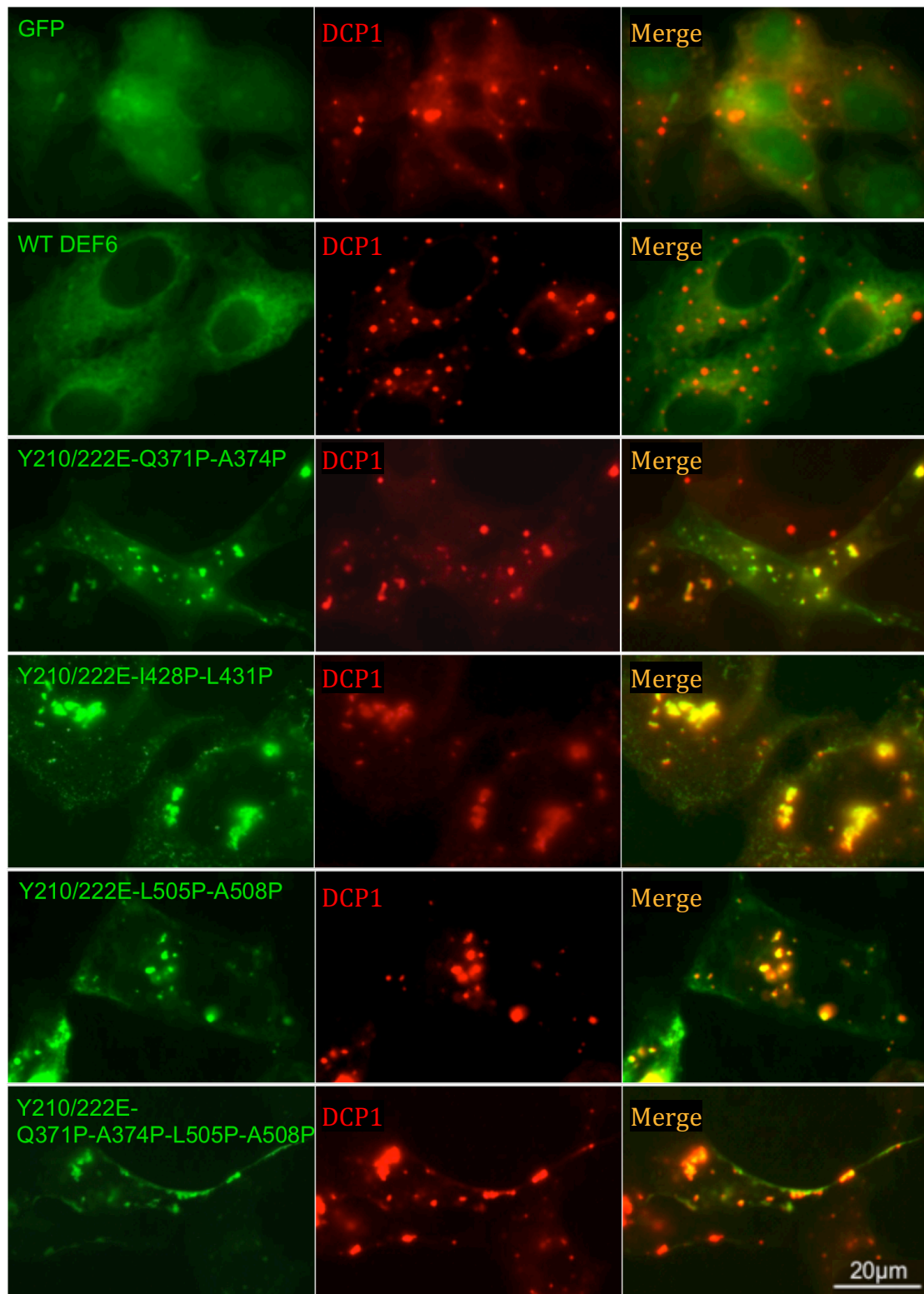
Fig. 3.4.0 Disruption of the coiled coil domain prevented arsenate induced granule formation

Analysis of proline mutants as indicated 24 h after transfection of COS7 cells treated with arsenate (1mM, 40mins). As previously shown, about 16% WT DEF6 formed granules. However, among the proline mutants, only K491P-L494P (17% cells) exhibited granules. Arsenate treatment had no effect on the other mutants exhibiting a cellular localisation as in untreated cells (compare with Figure 3.3.0).

3.5 The coiled coil domain is dispensable for DEF6 granule formation and colocalisation with DCP1

As described above, the data presented so far would suggest that the coiled coil domain is essential for granule formation of DEF6 in cells treated with arsenate. This is in line with data presented by Hey *et al.* (2012) who showed that DEF6 is phosphorylated by ITK at amino acid positions of Tyr 210 and Tyr 222 *in vitro* and that phosphomimic mutants in COS7 cells spontaneously relocated colocalising with P-bodies. Therefore, the Tyr (Y) residues 210 and 222 were changed to Glu (E) in selected proline mutant proteins to see whether the disrupted coiled coil domain prevents spontaneous granule formation of the phosphomimic Y210-222E mutant.

Mutant Y210-222E-Q371P-A374P, Y210-222E-I428P-L431P, Y210-222E-L505P-A508P, Y210-222E-Q371P-A374P-L505P-A508P, Y210-222E-I428P-L431P-L505P-A508P and Y210-222E-All-10 were established and transfected into COS7 cells. Surprisingly, all these combined mutants spontaneously formed granules in COS7 cells. Furthermore, cotransfections revealed that granules formed by the combined mutants colocalised with P-body marker DCP1 (Fig. 3.5.0). Confocal z-stack images also confirmed colocalisation of Y210-222E-L505P-A508P and Y210-222E-All-10 with DCP1 (Fig. 3.5.1). These results demonstrate that granule formation and P-body colocalisation of the phosphomimic Y210-222E mutant is independent of the coiled coil domain and suggests that instead another region of DEF6 is responsible for both.

**Fig. 3.5.0**

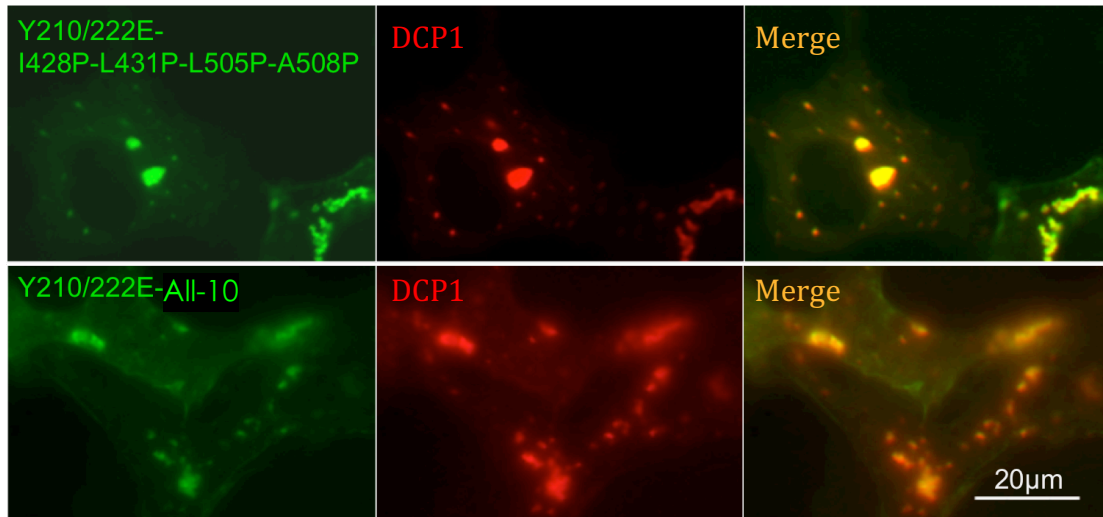


Fig. 3.5.0 Introduction of the ITK phosphomimic mutations Y210/222E results in colocalisation of proline mutants with P-bodies.

Y210/222E mutations were introduced into selected proline mutants as indicated and these combined GFP-tagged mutants (green) were cotransfected into COS7 with mCherry-tagged DCP1 (red). Images taken 24h after transfection. Merged images from the left and middle columns shown on the right indicate that the combined mutants formed granules that colocalised with DCP1.

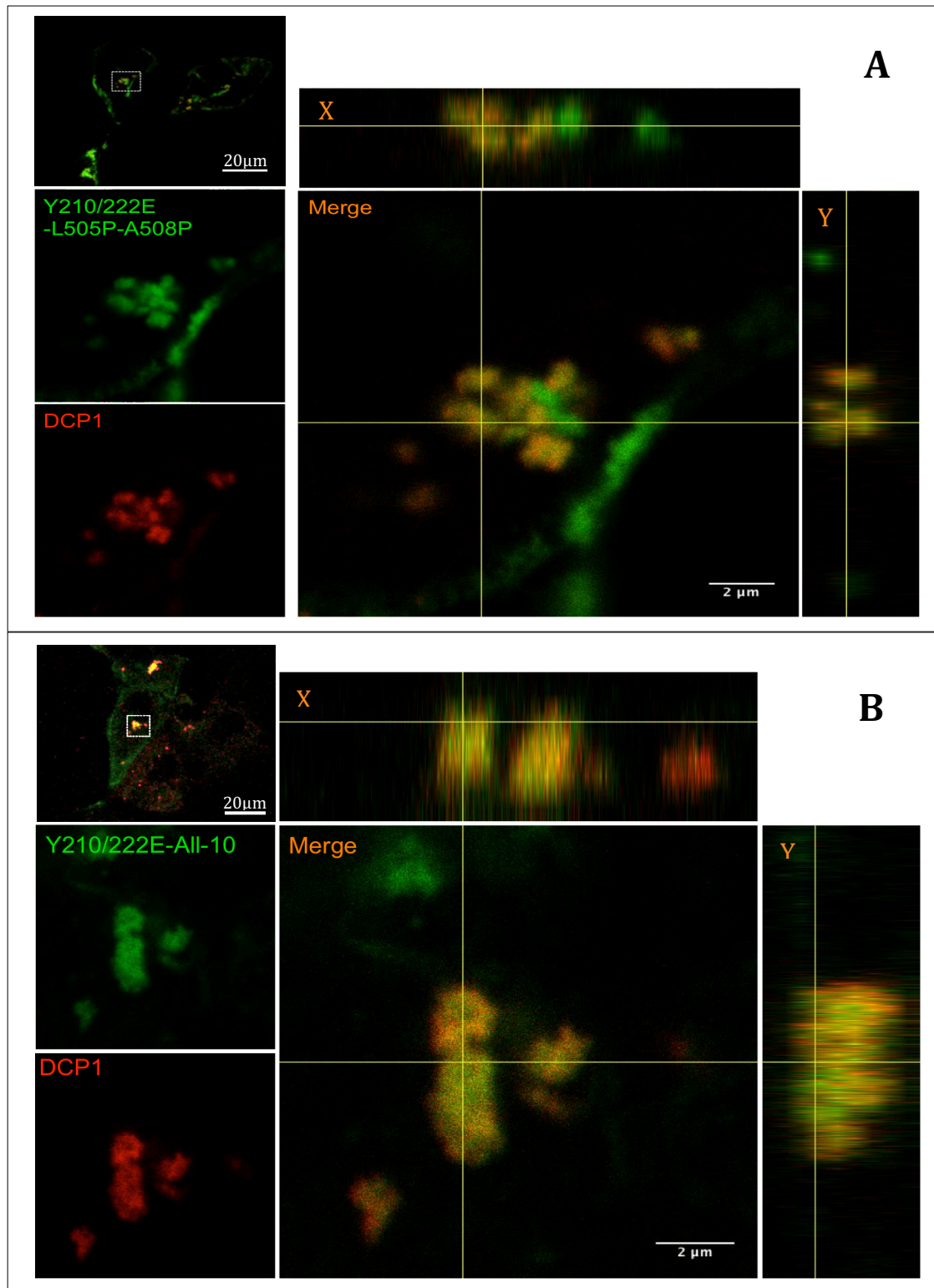


Fig.3.5.1 Y210/222E-L505P-A508P and Y210/222E-All-10 form granules that colocalise with DCP1

Confocal Z-stack analysis of GFP-tagged Y210/222E-L505P-A508P **(A)** and Y210/222E-All-10 **(B)** (green) cotransfected with mCherry-tagged DCP1 (red) 24 h after transfection of COS7 cells. Boxed area in the images on top left are enlarged on the left middle and bottom and further enlarged in the merged images on the right. Vertical and side views (X and Y coordinates) are also shown indicating colocalisation.

3.6 N-terminal 45 amino acids of DEF6 are necessary and sufficient to spontaneously colocalise with P-bodies

Having established that the coiled coil domain of DEF6 is dispensable for granule formation and colocalisation with P-bodies, C-terminal truncation mutants N-30, N-45, N-79, N-108, N-216 and N-312, N-590 were made as depicted in Fig. 3.6.0 and cellular localisation of these mutants tested in COS7 cells. All C-terminal truncation mutants but N-30 formed granules (Fig. 3.6.0) confirming earlier data for N-108 (Mollett, 2014) and N-590 (Theodore, 2011). In addition, N-590, N-312, N-216 (Alsayegh, personal communication) and N-108 (Mollett, 2014) as well as N-79 and N45 spontaneously colocalised with DCP1 (Fig. 3.6.2). Given that N-30 did not form granules these data establish that the first 45 amino acids of DEF6 are necessary and sufficient to spontaneously target P-bodies. It is worth mentioning, that the transfection efficiency of some of the C-terminal truncation mutants was low perhaps suggesting that expression of these mutant proteins is in some way detrimental to COS7 cell survival but further experiments are needed to firmly establish this idea.

Overall the data presented are consistent with the notion that the Y210-222E mutant mimicking ITK phosphorylation is liberating the N-terminal end of DEF6 rather than the coiled coil domain as initially proposed by Hey *et al.* (2012), resulting in targeting and colocalisation of DEF6 to/with P-bodies.

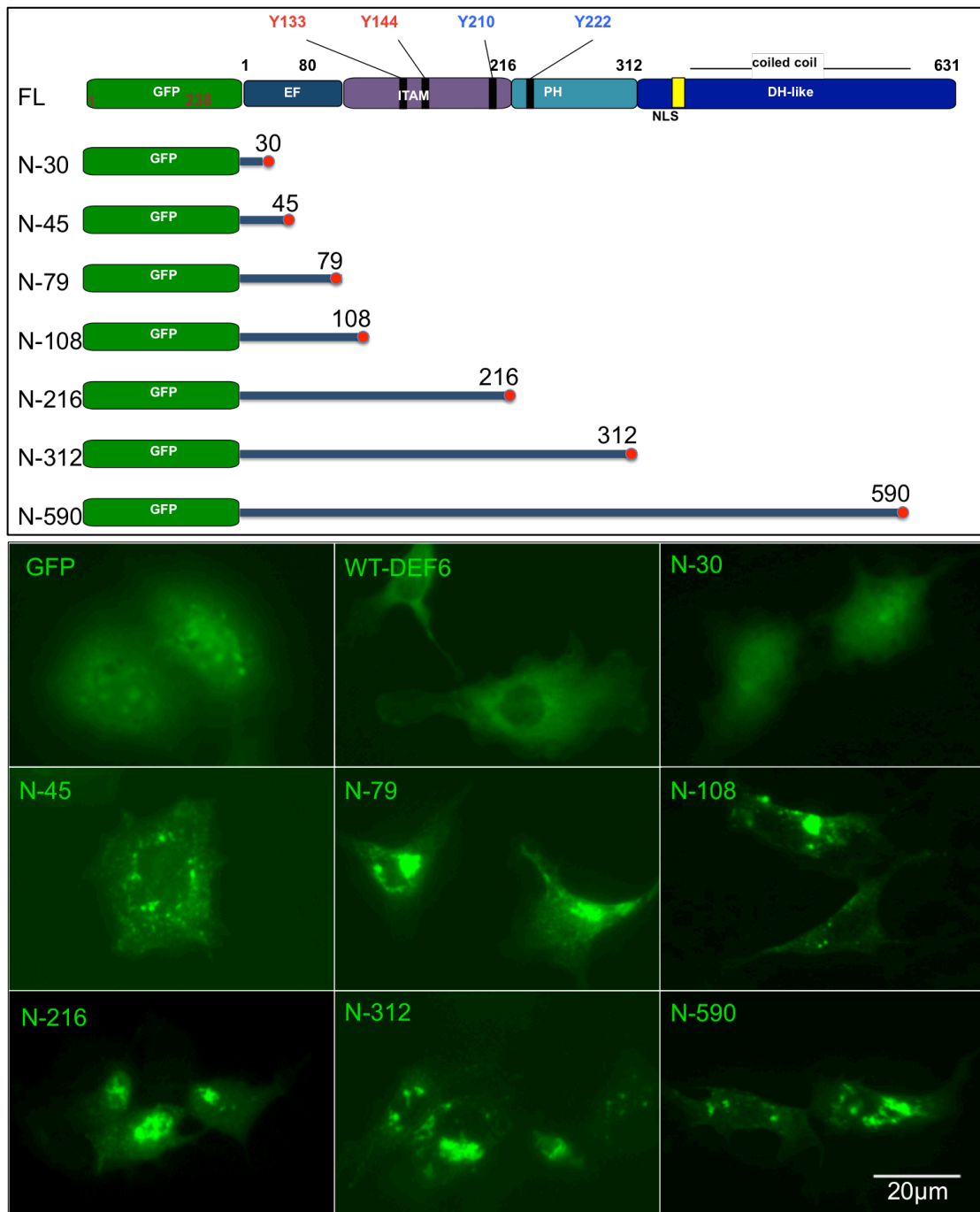


Fig. 3.6.0 DEF6 N-terminal domains form granules and aggregations

Upper panel: Schematic representation of C-terminal truncation mutants as indicated.

Lower panel: after 24h expression in COS7 cells, GFP-tagged N-45, 79, 108, 216, 312 and 590 exhibited cytoplasmic granules. N-30 however did not form any granules but was diffuse in the cytoplasm and cell nucleus. GFP and wild type DEF6 are shown for comparison.

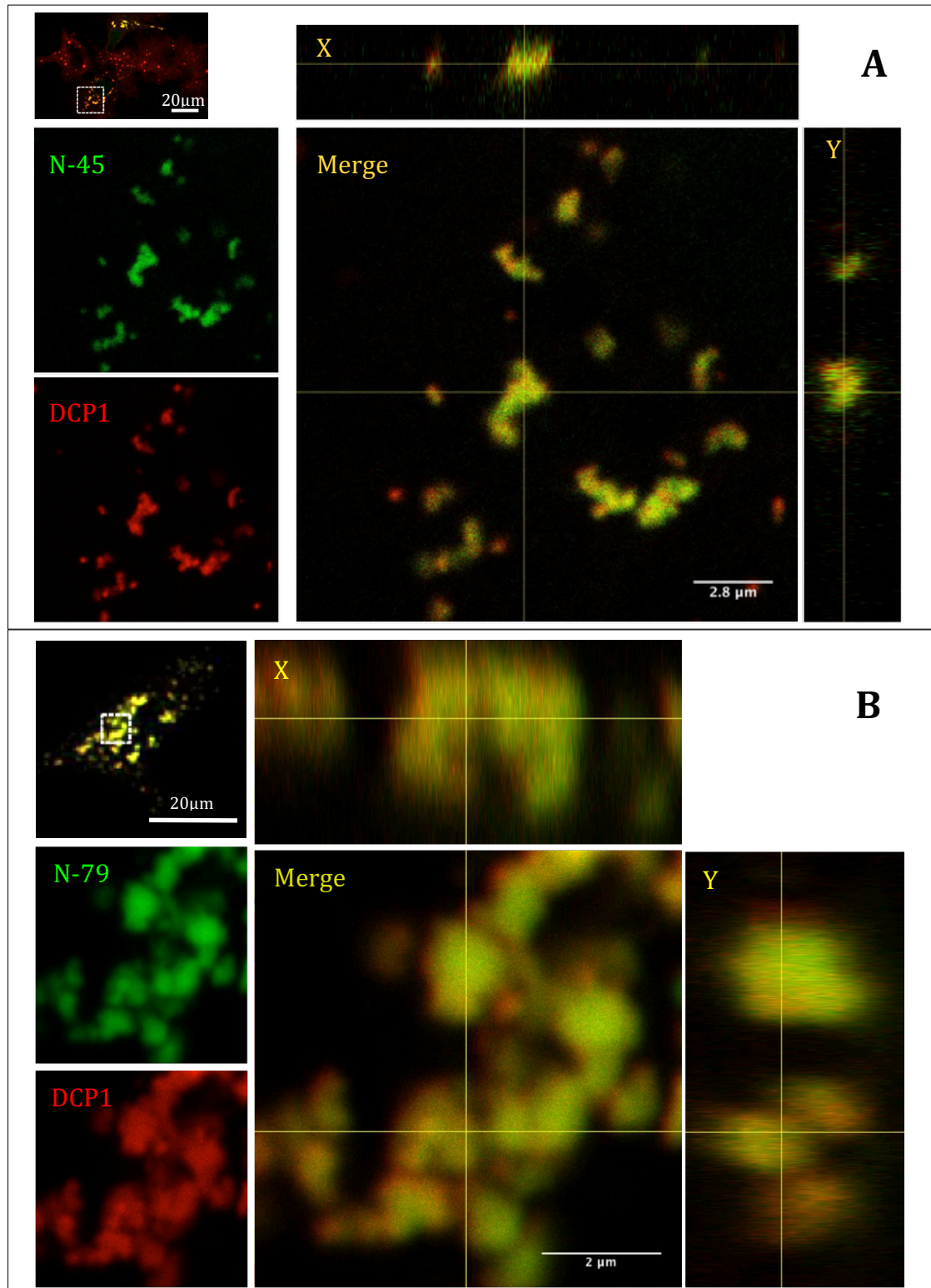


Fig. 3.6.1 The N-terminal 45 amino acids of DEF6 are sufficient for colocalisation with P-bodies

Confocal Z-stack analysis of GFP-tagged N-45 (A) and N-79 (B) (green) cotransfected with mCherry-tagged DCP1 (red) 24 h after transfection of COS7 cells. Boxed area in the images on top left are enlarged on the left middle and bottom and further enlarged in the merged images on the right. Vertical and side views (X and Y coordinates) are also shown indicating colocalisation.

3.7 The coiled coil domain facilitates DEF6 aggregation

Having established that the N-terminal end of DEF6 is necessary and essential whereas the coiled coil domain is dispensable for spontaneous P-body localisation, N-terminal truncation and deletion mutants were established to test which functional role the coiled coil domain of DEF6 plays. The structures of these N-terminal truncation mutants are schematically depicted in Figure 3.7.1a. In addition to the previously established mutants DH2 (Mollett, 2014) and $\Delta 0-104$ (Martin, 2007), all other mutants shown (referred to as $\Delta X-N$ indicating the amino acids missing from position X to N) were established as described in Chapter 2 (2.5.2). Cellular localisation of the N-terminal truncation and deletion mutants is summarised in Figure 3.7.1b showing that all 9 mutant DEF6 proteins formed aggregates regardless of which of the N-terminal amino acids were missing. These aggregates appeared different in shape and size from the previously described granules that colocalise with P-bodies and although not colocalising with P-bodies DEF6 aggregates altered the cellular localisation of P-bodies (as described below in more detail).

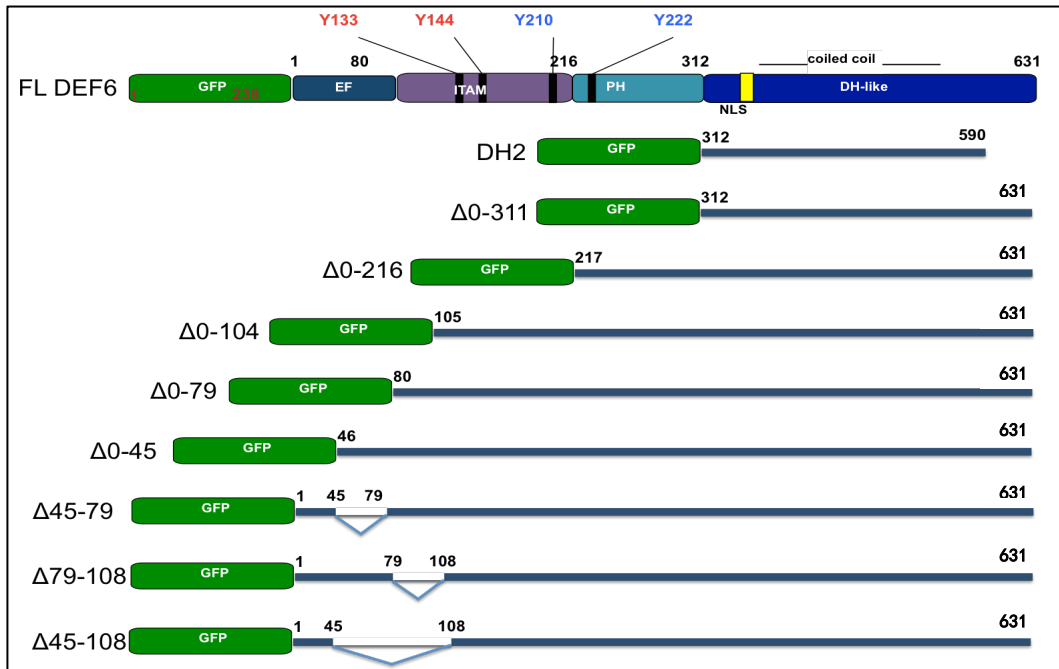


Fig. 3.7.1a Schematic representation of DEF6 N-terminal truncation and deletion mutants.

GFP-tagged N-terminal truncation and deletion mutants were established as indicated.

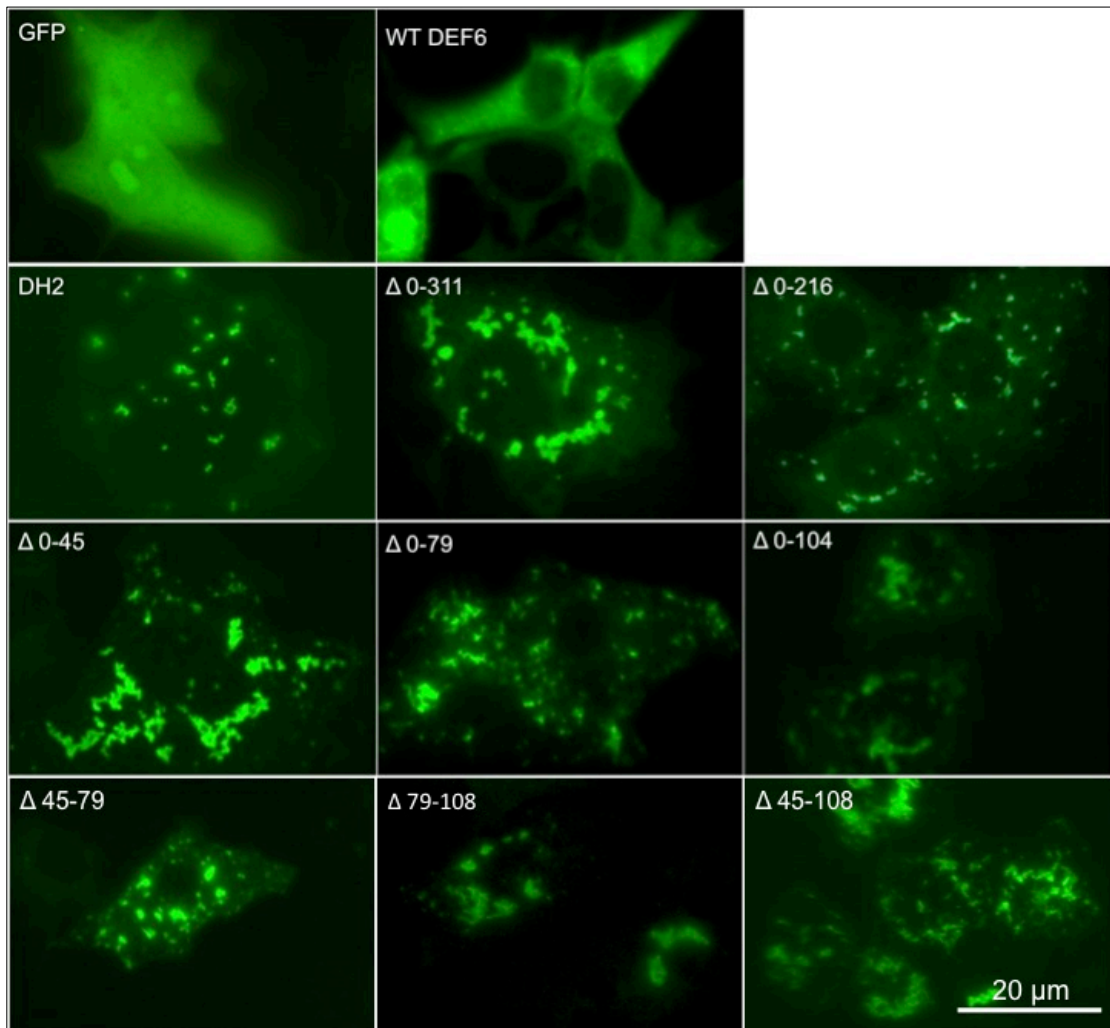


Fig. 3.7.1b DEF6 N-terminal truncation and deletion mutants form large aggregates

24h after transfection of COS7 cells, GFP-tagged N-terminal truncation and deletion mutants as indicated exhibited large cytoplasmic aggregations. GFP and wild type DEF6 are shown for comparison.

To further test the role of the coiled coil domain in aggregation formation, a series of DEF6 truncation mutants were established, which either contained the coiled coil domain entirely or partially or lacked it completely as indicated in Fig. 3.7.2a. To establish the ITAM containing mutant, a stop codon between amino acid 215 and 216 was introduced in the Δ0-104 construct, the other mutants had been previously established (PH1, PH2: Martin, 2007; DH1: Mavrakis *et al.*, 2004; DH2, DH2-N, DH2-C: Mollett, 2014).

As shown in Fig. 3.7.2b, DH2 that just contained the coiled coil domain formed aggregates. In contrast DH1 and DHL-C (partially containing the coiled coil domain), did not form aggregates. Instead, these mutant proteins labelled lamellipodia, filopodia and stress fibres (Fig. 3.7.2b) and as shown in chapter 4 colocalise with F-actin.

Mutant DEF6 proteins not containing the coiled coil domain (ITAM, PH1 and DHL-N) localised diffuse in cytoplasm and nucleus without any signs of aggregations. Nuclear localisation of ITAM and PH1 mutant are likely due to their small size. In contrast, PH2 which contains a predicted NLS region (amino acid positions 330 to 341) localised exclusively to the nucleus as previously shown (Martin, 2007).

DHL-N also partially contains the coiled coil region. As shown in Figure 3.7.2b, this mutant protein was mainly distributed diffuse in the cytoplasm and was absent from the nucleus. However, DHL-N did occasionally exhibit distinct cytoplasmic granules. These granules have three features: 1) only one or two are seen per cells; 2) they always localise next to the cell nucleus 3) if present as a pair, they usually localised on the opposite sides of the cell nucleus and it remains to be seen whether this localisation of DHL-N coincides with centrosomes.

To firmly establish that the coiled coil domain is indeed facilitating DEF6 aggregation, mutants $\Delta 0$ -216 and $\Delta 0$ -216-All-10 were established and tested (Fig. 3.7.3). $\Delta 0$ -216-All-10 contains the 10 sets of prolines in *a/d* positions of the coiled coil domain as discussed earlier. The N-terminal truncation mutant $\Delta 0$ -216 formed consistently large aggregations, whereas $\Delta 0$ -216-All-10 did not.

Instead, $\Delta 0-216$ -All-10 exhibited similar phenotype to the All-10 mutant (Fig. 3.7.3 and Fig. 3.3.0) localising to lamellipodia and filopodia.

Together the data established that the coiled coil domain facilitates DEF6 aggregation and this function is masked/inhibited in the wild type protein.

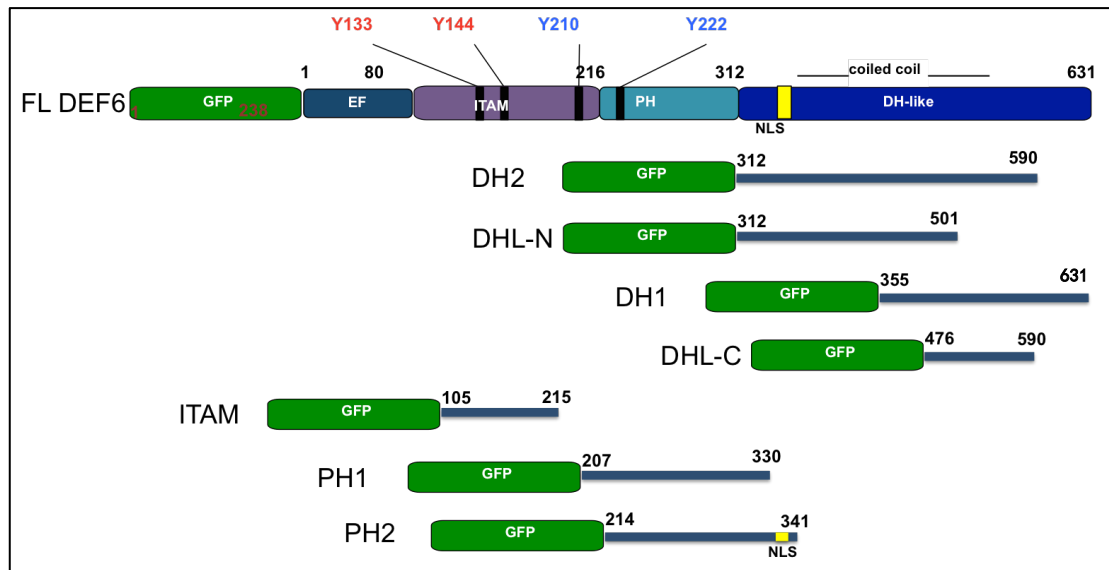


Fig. 3.7.2a Schematic representation of DEF6 N-terminal truncation and deletion mutants.

GFP-tagged N-terminal truncation and deletion mutants were established as indicated.

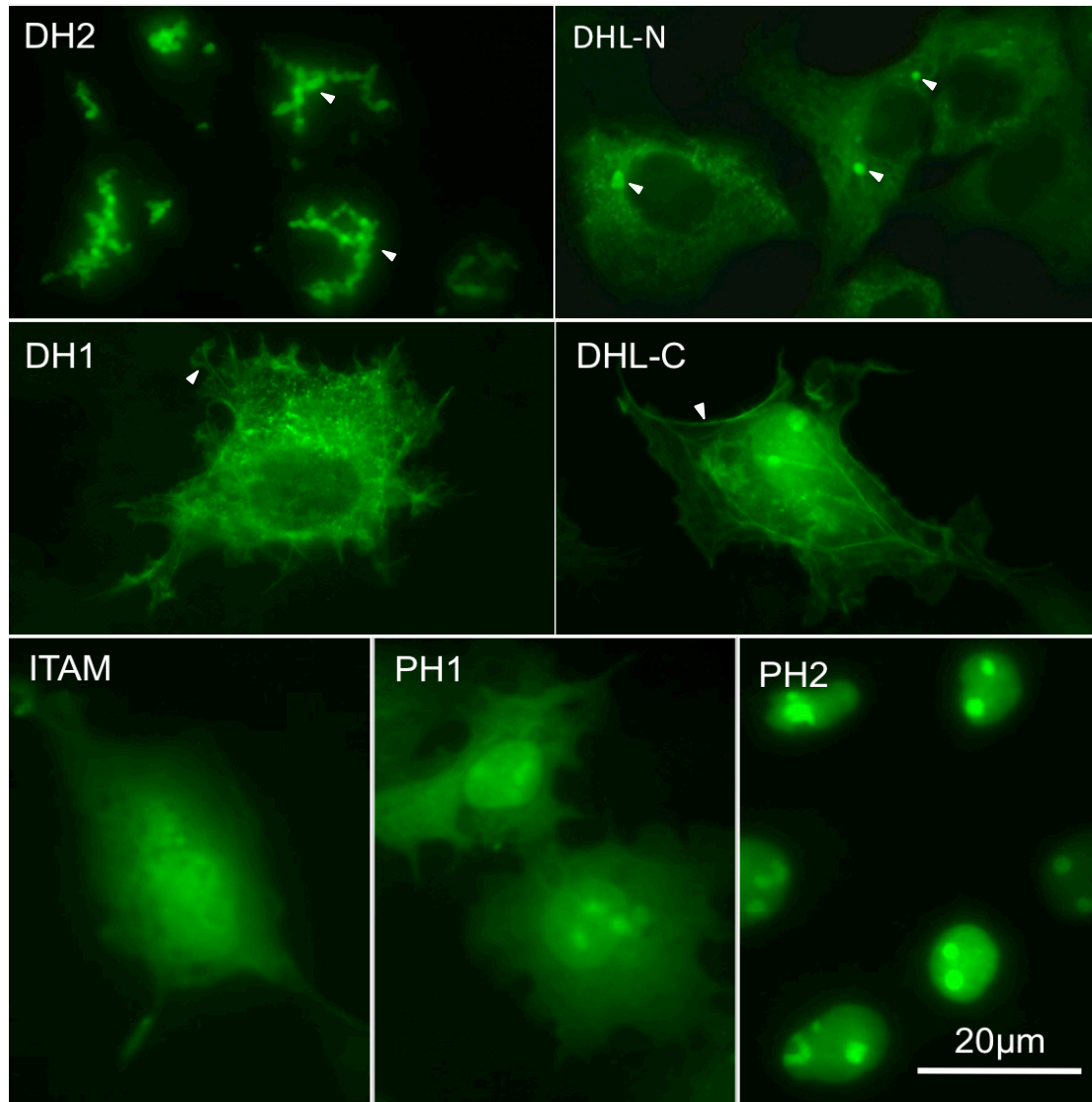


Fig. 3.7.2b The coiled coil domain of DEF6 facilitates aggregation

GFP-tagged mutants schematically depicted in Fig. 3.7.2a were transfected into COS7 cells and images taken 24h after transfection.

DH2 that contains the entire coiled coil region formed large aggregates in the cytoplasm.

DHL-N that partially contains the coiled coil region was mainly diffuse in cytoplasm. However, some large round granules were occasionally observed with the following features: only one or two granules were present in the cytoplasm that always localised next to and when present in pairs at opposite sides of the cell nucleus.

DH1 and **DHL-C** did not form large aggregates despite containing the C-terminal part of the coiled coil domain. Instead, they localised to lamellipodia filopodia and stress fibres.

The **ITAM** and **PH1** domain tagged to GFP were diffuse in cytoplasm and nucleus similar to GFP alone.

The **PH2** mutant that contained the predicted NLS sequence of DEF6 was exclusively localised in the nucleus as previously shown (Martin, 2007).

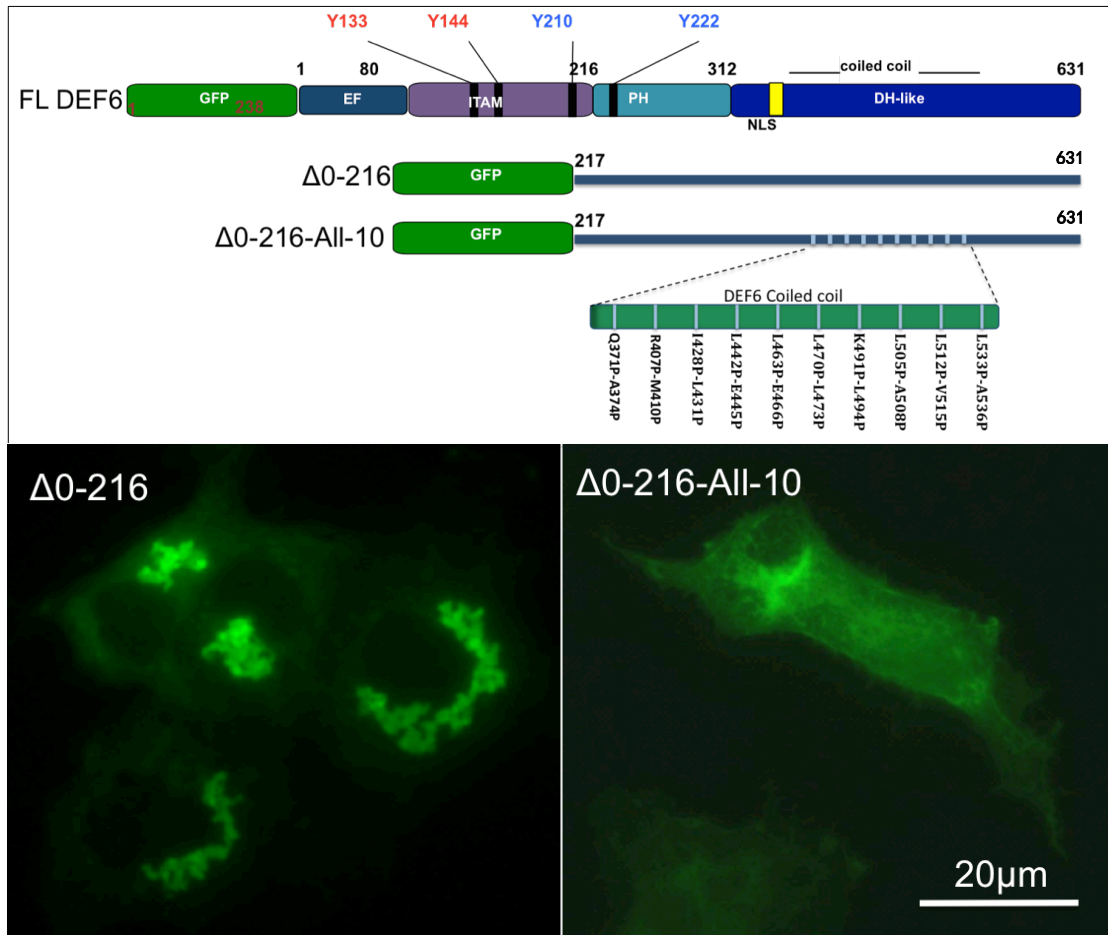


Fig. 3.7.3 Formation of large aggregates of DEF6 is abolished through proline mutations in the coiled coil domain

Upper panel: Schematic representation of GFP-tagged Δ0-216 and Δ0-216-All-10 DEF6 mutants.

Lower panel: 24 h after transfection of COS7 cells, GFP-tagged Δ0-216 mutant formed aggregates that seemed to interact with each other forming large structures. Aggregation and large structure formation was abolished when the coiled coil domain was disrupted through prolines at all 10 a/d positions.

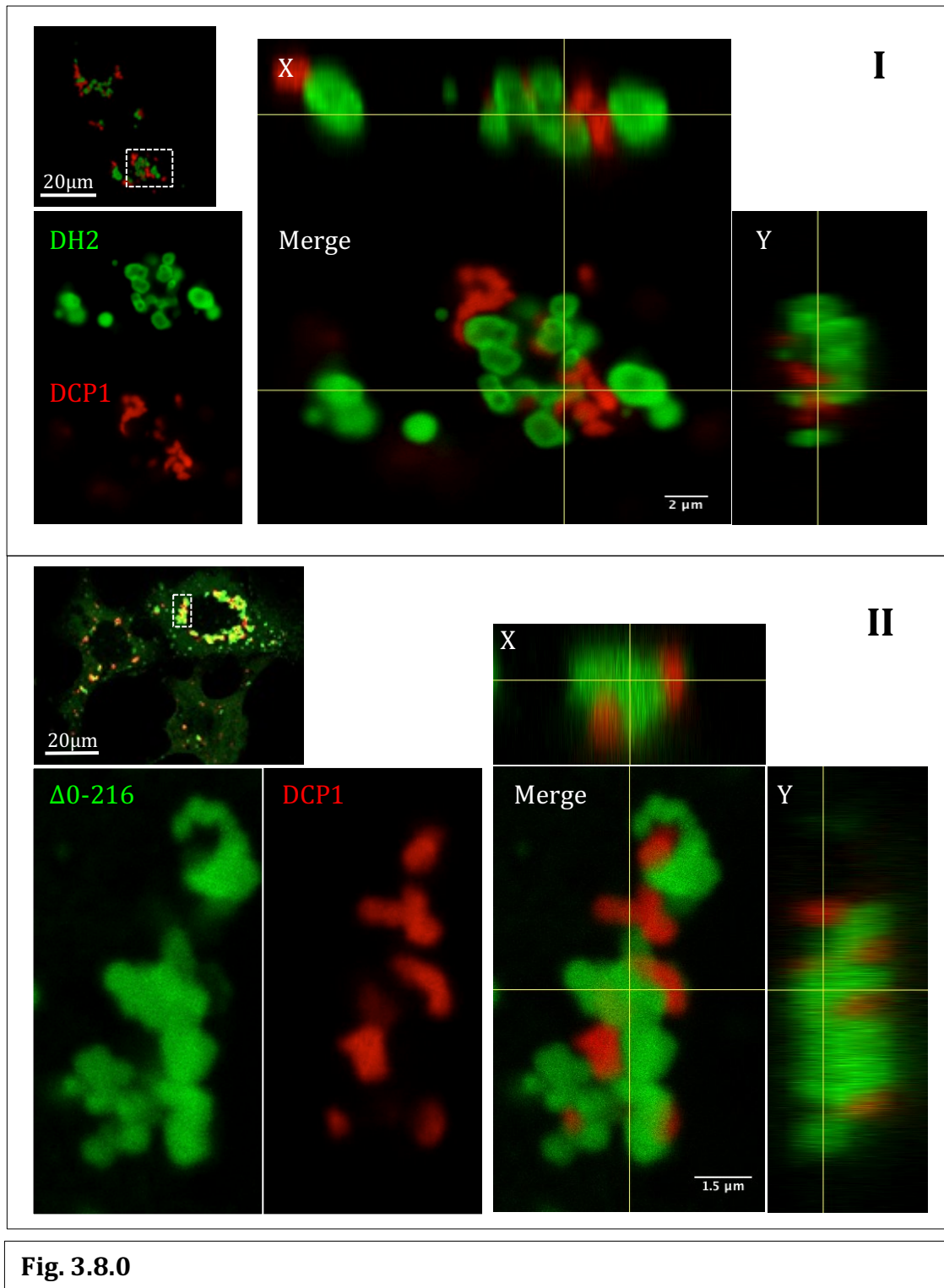
3.8 Coiled coil-mediated DEF6 aggregations can be classified into three distinct groups according to structure/morphology and association with DCP1

To further test the functional properties of DEF6 aggregates, cotransfection with DCP1 were performed. As shown in Figures 3.8.0 DEF6 aggregates differed in their shape and structure but were always associated with DCP1 albeit in various ways clearly distinct from the colocalisation with DCP1 described above.

(i) DH2 aggregates were unique in the sense that they formed vesicle-like tubular structures (Fig. 3.8.1 I). DCP1 was always associated with these aggregates but never colocalised. Furthermore, cellular localisation of DCP1 was clearly altered: the normal cytoplasmic distribution of DCP1/P-bodies was absent from the double transfected COS7 cells and all DCP1 was tightly 'bound' by the DEF6 aggregates. In addition, the normally round shape of DCP1/P-bodies was altered exhibiting shapes that appeared to be dependent upon the shape of DEF6 aggregates (Fig. 3.8.0). DH2 vesicle-like tubular aggregates somewhat resembled the structure of the Golgi apparatus but cotransfection of DH2 with several Golgi markers (Addgene: mCherry-GalT and mCherry-SiT-N-15) were inconclusive and it remains to be seen whether DH2 aggregates are associated with some cytoplasmic organelles or self-assembled.

(ii) $\Delta 0-216$ and $\Delta 0-311$ did not form vesicle-like aggregates as seen with DH2, but were also always associated with DCP1 altering its cytoplasmic localisation (Fig. 3.8.0 II and Appendix 8.4, Fig. 8.5.1).

(iii) All other mutant proteins tested fall into the 3rd group (e.g. $\Delta 0-104$): their aggregates were also not vesicle-like but did partially overlapped with DCP1 (Fig. 3.8.0 III and Appendix 8.4, Fig. 8.5.2 to 8.5.6).



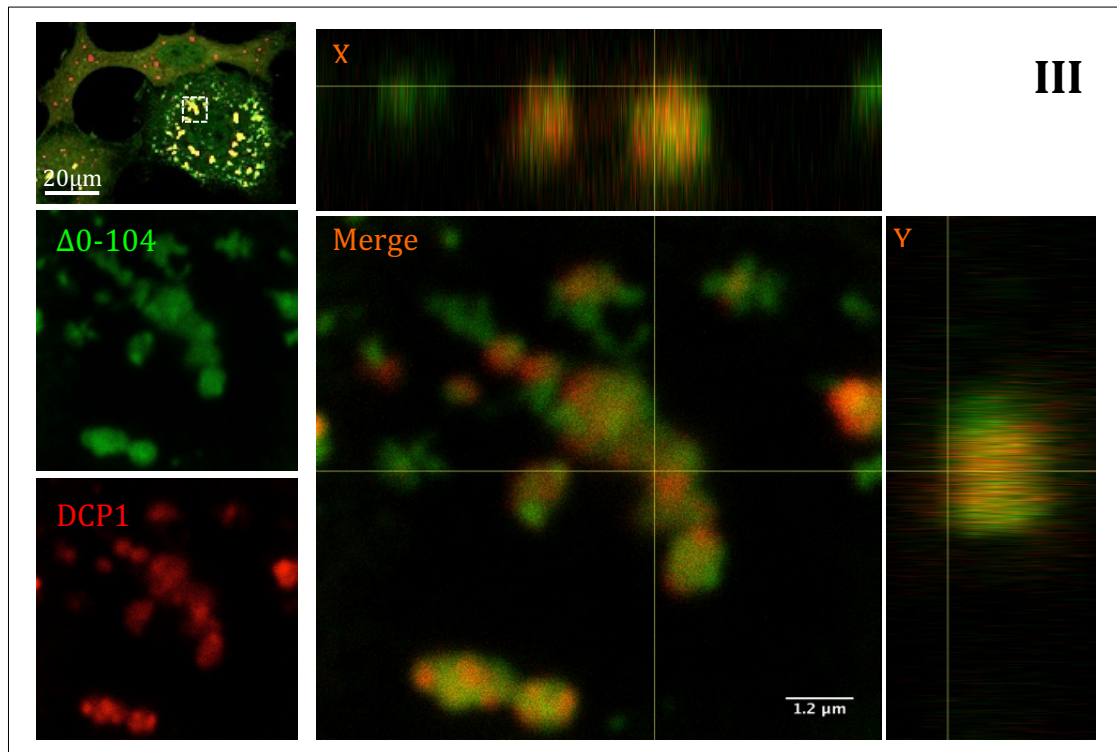


Fig. 3.8.0 Coiled coil-mediated aggregates of DEF6 form large structure that 'trap' DCP1

Confocal analysis of transfected COS7 cells as described before.

(I) GFP-tagged DH2 aggregates formed vesicle-like structures that did not colocalise with DCP1. Instead, localisation of DCP1 was altered and always adjacent to DEF6 structures (see merged images on the right).

(II) GFP-tagged $\Delta 0-216$ and $\Delta 0-311$ (Appendix Fig. 8.5.1) aggregates also formed large structures but these did not appear vesicle-like. However, these structures also altered the localisation of DCP1 that was always associated with DEF6 structures (see merged images on the right).

(III) GFP-tagged $\Delta 0-104$ is representative for all other N-terminal truncation mutants tested. GFP-tagged $\Delta 0-104$ formed aggregates and larger structures but in this case these structures partially overlapped with DCP1; again altering the normal cellular localisation of DCP1 (see merged images on the right).

3.8.1 Differential response of DEF6 aggregates to cellular stress

Arsenate treatment of COS7 cells caused wild type DEF6 to relocate colocalising with P-bodies (as shown above and Hey *et al.*, 2012). To test other stress conditions, cells were treated with nocodazole, a microtubule inhibitor. As shown in Figure 3.9.0, wild type DEF6 formed granules that colocalised with DCP1 in response to nocodazole treatment similar to arsenate treatment. This is consistent with the studies showing that inhibiting microtubules promote P-body formation and might suggest that cellular relocation of DEF6 into P-bodies is also independent of microtubules.

Coiled coil-mediated DEF6 aggregates responded to cellular stress in distinct fashion. Neither arsenate nor nocodazole treatment influenced aggregates formed by DH2 (group 1) or mutant proteins of group 2 like $\Delta 0-216$ and $\Delta 0-311$. They still were associated with DCP1 as observed in untreated cells and never colocalised with DCP1 (Fig. 3.10.1, Fig. 3.10.2 and Appendix 8.4, Fig. 8.6.1 and Fig. 8.7.1). In contrast, aggregates of mutant proteins of the 3rd group (e.g. $\Delta 0-104$) that partially overlapped with DCP1 in untreated cells mostly colocalised with DCP1 when treated with arsenate (Fig. 3.10.3 A and Appendix 8.4, Fig. 8.6.2 and Fig. 8.6.3) and completely colocalised with DCP1 after nocodazole treatment (Fig. 3.10.3 B and Appendix 8.4, Fig. 8.7.2).

It seems therefore that coiled coil-mediated aggregates that are formed by mutant DEF6 proteins either just containing the coiled coil domain (DH2) or in addition the PH domain ($\Delta 0-216$) are non-responsive to cellular stress. In contrast, in the presence of the ITAM domain ($\Delta 0-104$), aggregates partially overlap with DCP1 and can be induced to completely colocalise with DCP1 under

stress conditions.

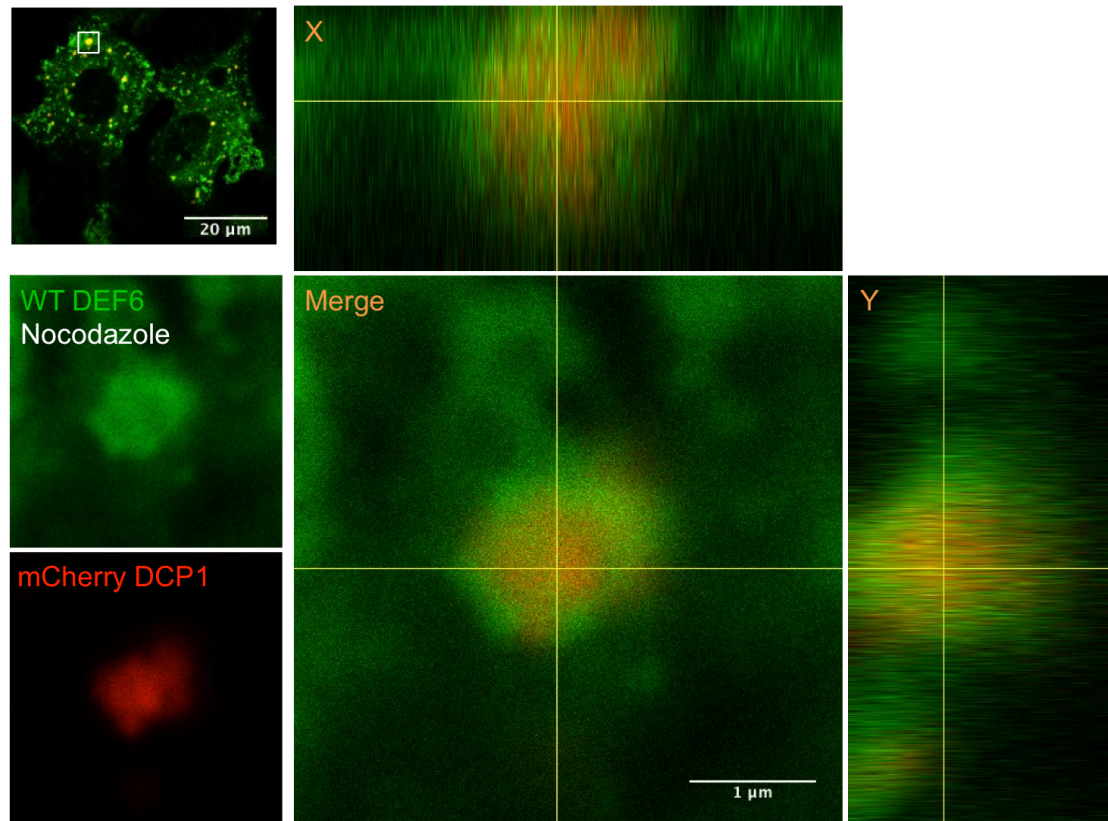


Fig. 3.9.0 Cellular stress induced through nocodazole treatment results in WT DEF6 colocalising with DCP1

Confocal analysis of COS7 cells expressing GFP-tagged wild type DEF6 and mCherry-tagged DCP1 after nocodazole treatment as described before. Merged images including vertical and side views (X and Y coordinates) shown on the right indicated colocalisation.

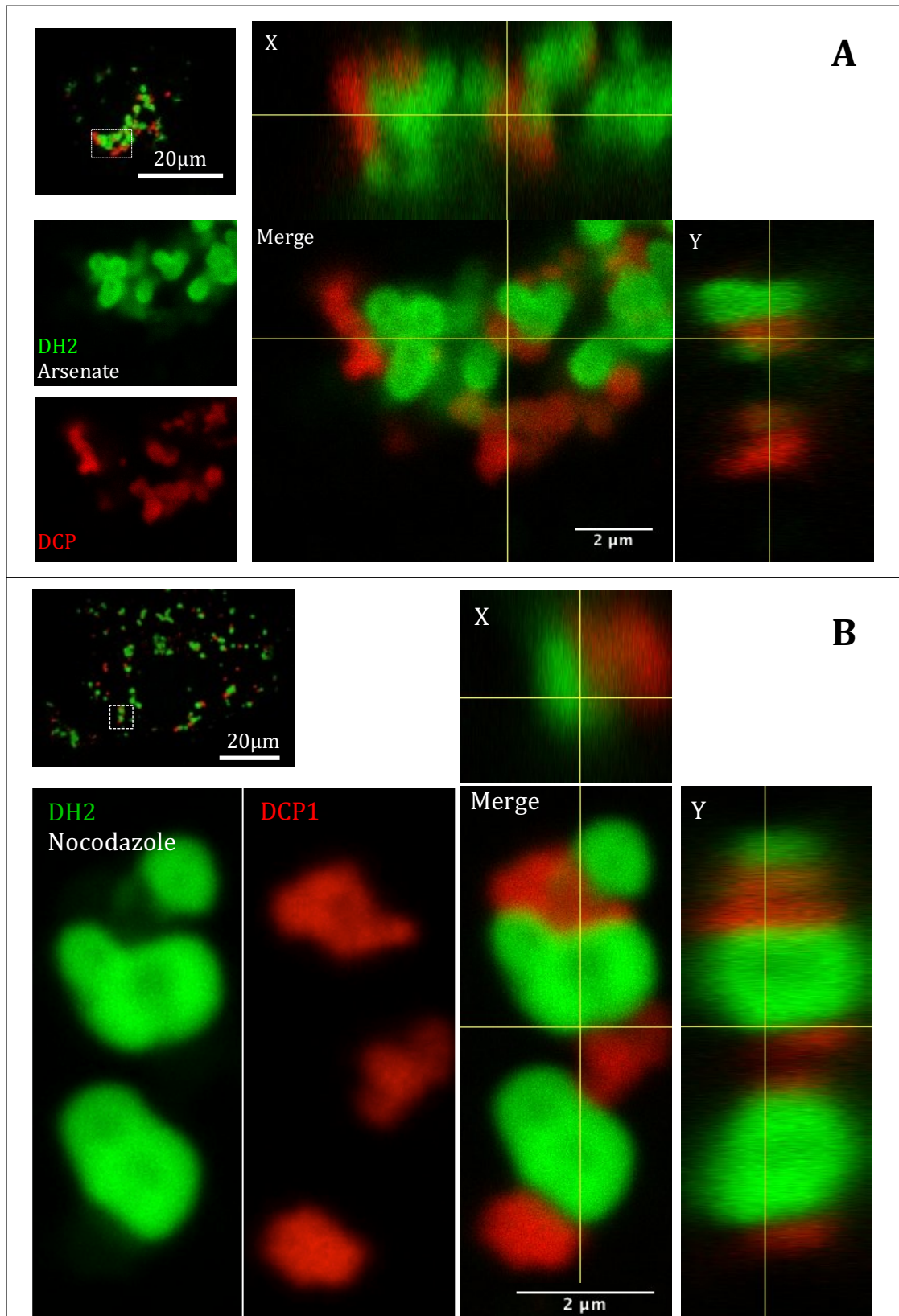


Fig. 3.10.1 Cellular stress had no effect on formation of vesicle-like structures of DH2 and their ability to 'trap' DCP1

Confocal analysis of COS7 cells expressing GFP-tagged DH2 and mCherry-tagged DCP1 after arsenate (A) or nocodazole (B) treatment as described before.

Merged images including vertical and side views (X and Y coordinates) shown on the right indicated large vesicle-like structures of DH2 adjacent to DCP1.

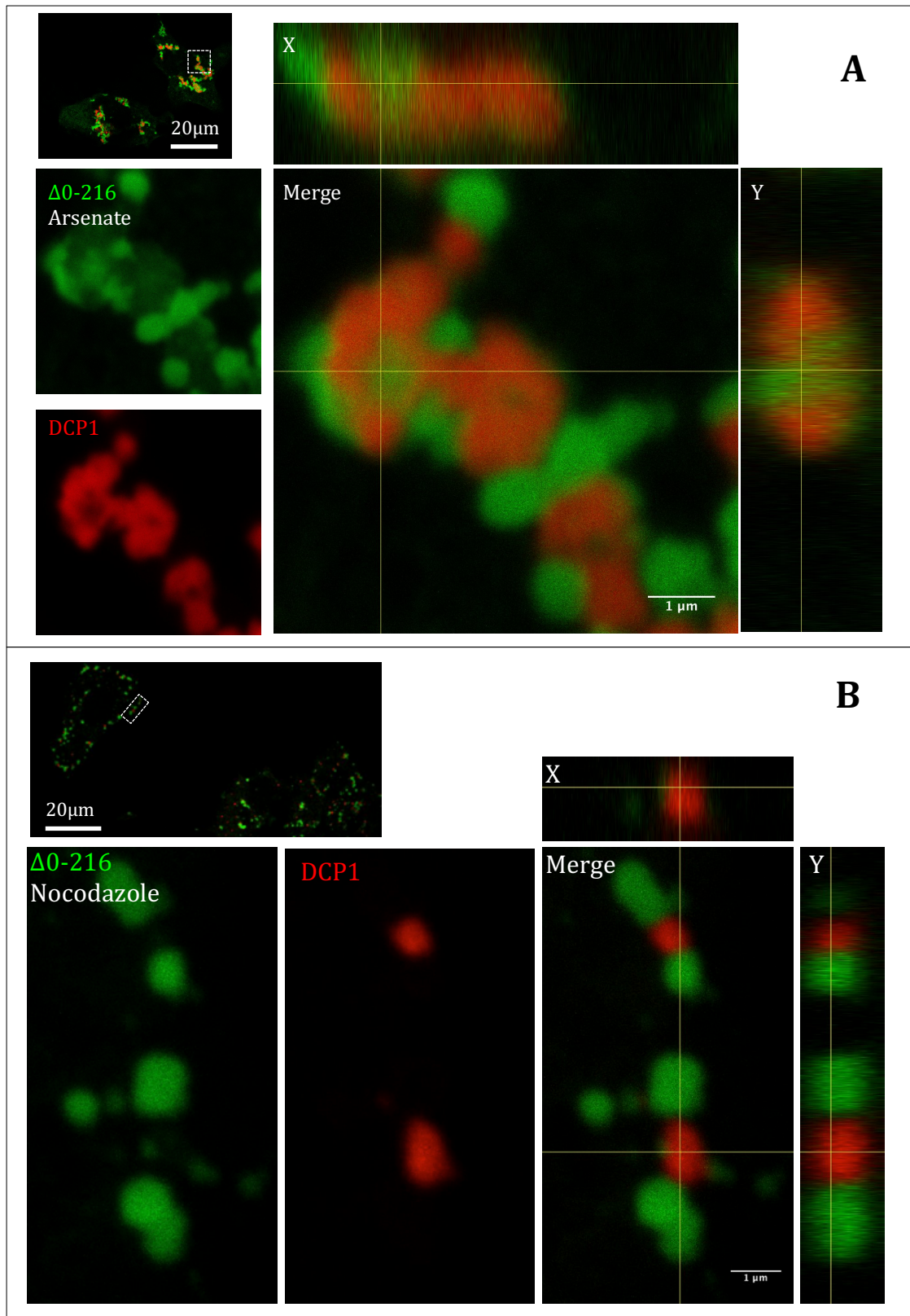


Fig. 3.10.2 Cellular stress had no effect on formation of large structures of $\Delta 0-216$ and their ability to 'trap' DCP1

Confocal analysis of COS7 cells expressing GFP-tagged $\Delta 0-216$ and mCherry-tagged DCP1 after arsenate (A) or nocodazole (B) treatment as described before.

Merged images including vertical and side views (X and Y coordinates) shown on the right indicated large structures of $\Delta 0-216$ adjacent to DCP1.

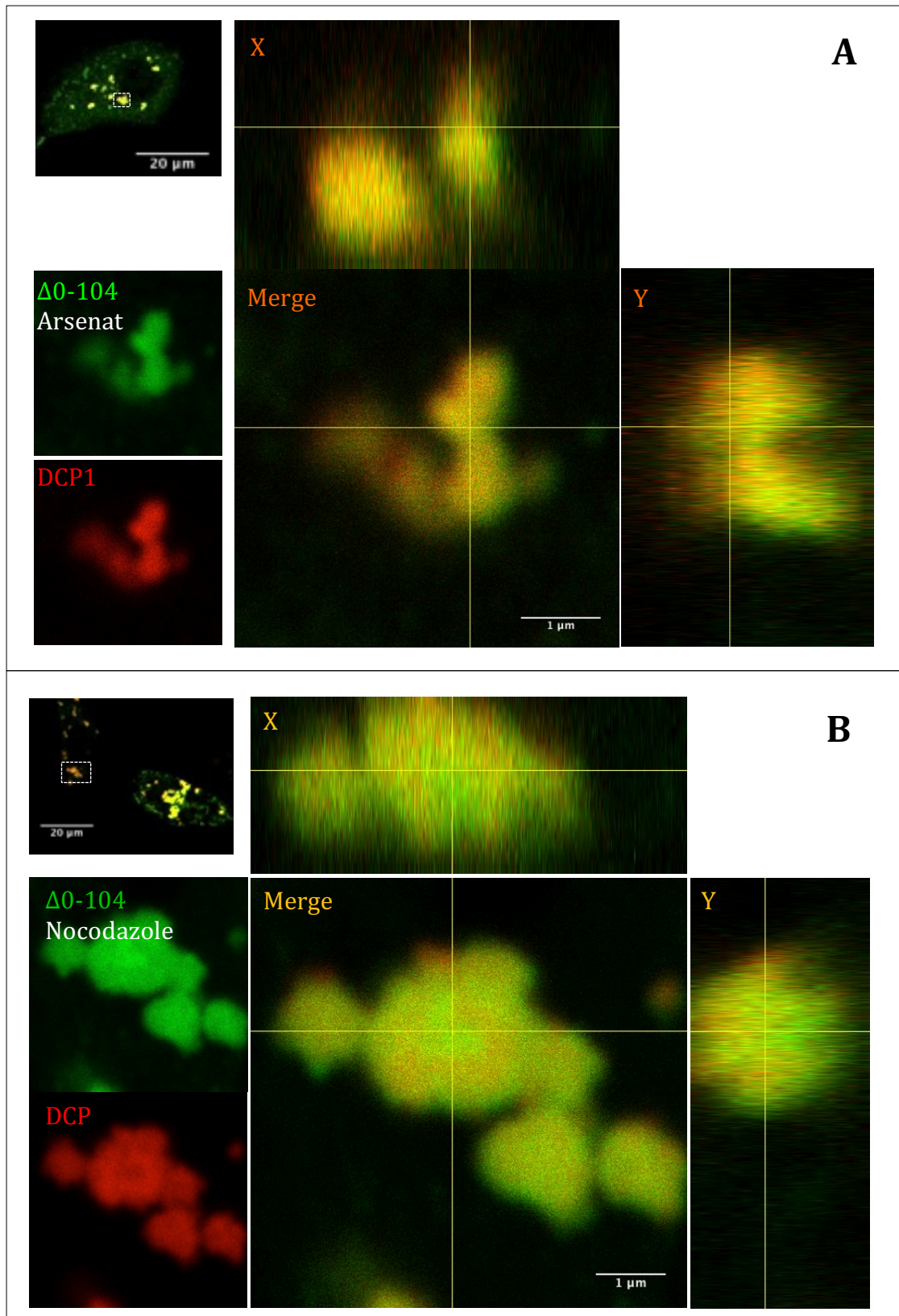


Fig. 3.10.3 Cellular stress results in complete colocalisation of $\Delta 0-104$ structures with DCP1

Confocal analysis of COS7 cells expressing GFP-tagged $\Delta 0-104$ (representing group 3 mutants) and mCherry-tagged DCP1 after arsenate (A) or nocodazole (B) treatment as described before.

Merged images including vertical and side views (X and Y coordinates) shown on the right indicated that large structures of $\Delta 0-104$ completely overlapped with DCP1.

3.8.2 ITAM and coiled coil domains are both required for colocalisation with P-bodies under cellular stress conditions

To further dissect the functional properties of the ITAM and the coiled coil domains, cellular localisation of a mutant protein just containing the ITAM domain and the All-10 mutant was tested after cellular stress. As shown in Figure 3.10.4, neither arsenate nor nocodazol treatment resulted in aggregates; rather both mutant proteins remained diffuse in the cytoplasm as in untreated cells similar to the GFP control. As shown before, wild type on the other hand did form granules colocalising with DCP1 after nocodazol treatment (Fig. 3.9.0).

Together these results suggest that neither domain alone (ITAM or coiled coil) respond to cellular stress but in combination they do as shown above resulting in colocalisation with DCP1.

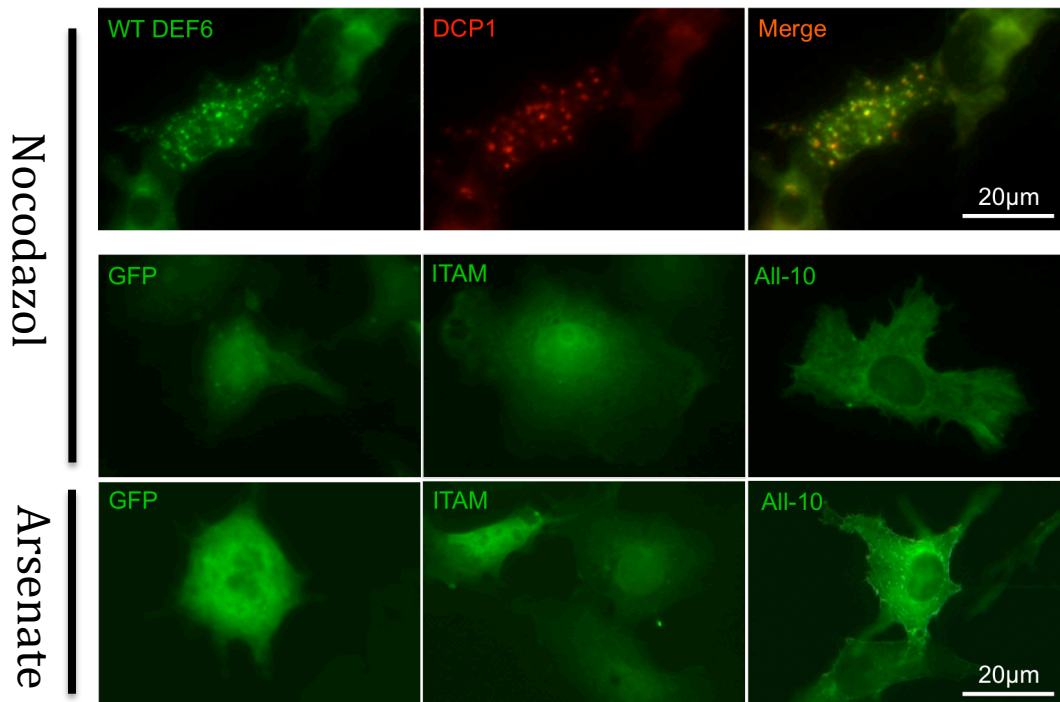


Fig. 3.10.4 Cellular stress did not alter localisation of the ITAM or All-10 mutants

Nocodazole (upper panels) or arsenate (bottom panel) treatment of COS7 cells transfected with GFP-tagged ITAM or All-10 mutants did not result in formation of aggregates. In comparison, wild type DEF6 did form granules that colocalised with DCP1 after treatment of transfected COS7 cells with nocodazol (upper panel).

3.8.3 Introduction of Y210/222E or Y210/222F mutations into $\Delta 0$ -104 did not alter the morphology of aggregates but prevented the mutant proteins completely colocalising with P-bodies under cellular stress condition.

In the context of the full-length wild type DEF6 protein introduction of the phosphomimic Y210/222E mutations resulted in spontaneous granule formation and colocalisation with DCP1 (Hey *et al.*, 2012) due to its unmasking effect on the N-terminal domain as shown above (Fig. 3.5.1 and Fig 3.5.1). It was therefore not surprising that introduction of the same Y210/222E phosphomimic mutations into the $\Delta 0$ -104 mutant lacking the N-terminal 104 amino acids did have no effect on the formation of aggregates that partially overlapped with DCP1 in untreated cells (Fig. 3.11.1). Similarly, the equivalent Y210/222F mutations introduced into $\Delta 0$ -104 that prevent potential phosphorylation on Tyr 210 and 222 also did not show an effect (Fig. 3.11.1). However, in contrast to $\Delta 0$ -104, introduction of either Y210/222E or Y210/222F into $\Delta 0$ -104 prevented complete colocalisation with DCP1 after nocodazol treatment (Fig. 3.11.2). These results suggest that alteration in the ITAM (Y210E/F) and PH domain (Y222E/F) influence the structural conformation independent of the phosphorylation status that alters the response of $\Delta 0$ -104 to cellular stress.

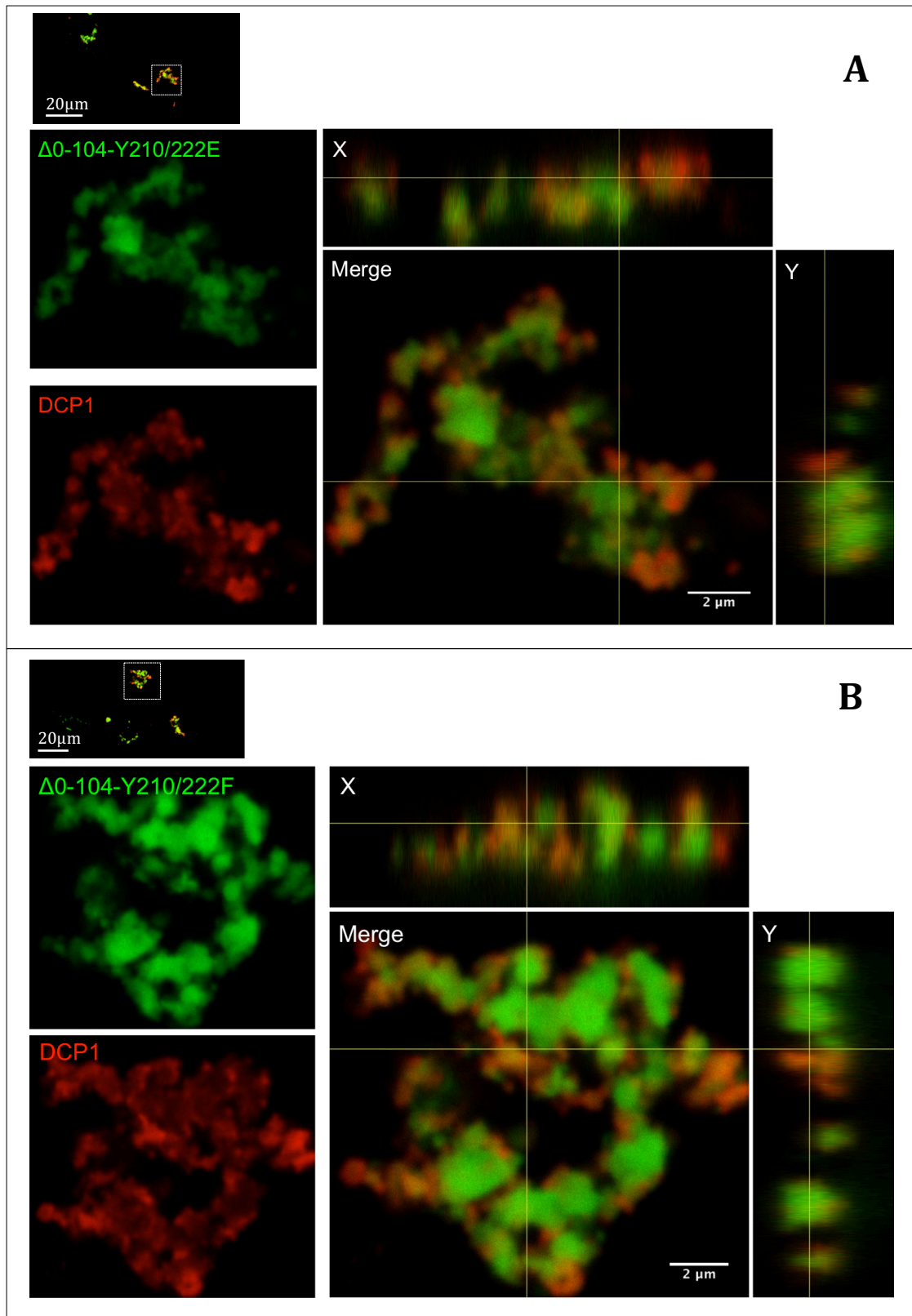


Fig. 3.11.1 Introduction of Y210/222E or Y210/222F mutations into $\Delta 0-104$ did not alter the morphology of aggregates that still partially overlapped with DCP1

Confocal analysis of COS7 cells expressing GFP-tagged $\Delta 0-104-Y210/222E$ (**A**) or $\Delta 0-104-Y210/222F$ (**B**) and mCherry-tagged DCP1 as described before. Merged images including vertical and side views (X and Y coordinates) shown on the right indicated that both mutant proteins formed large structures partially overlapped with DCP1.

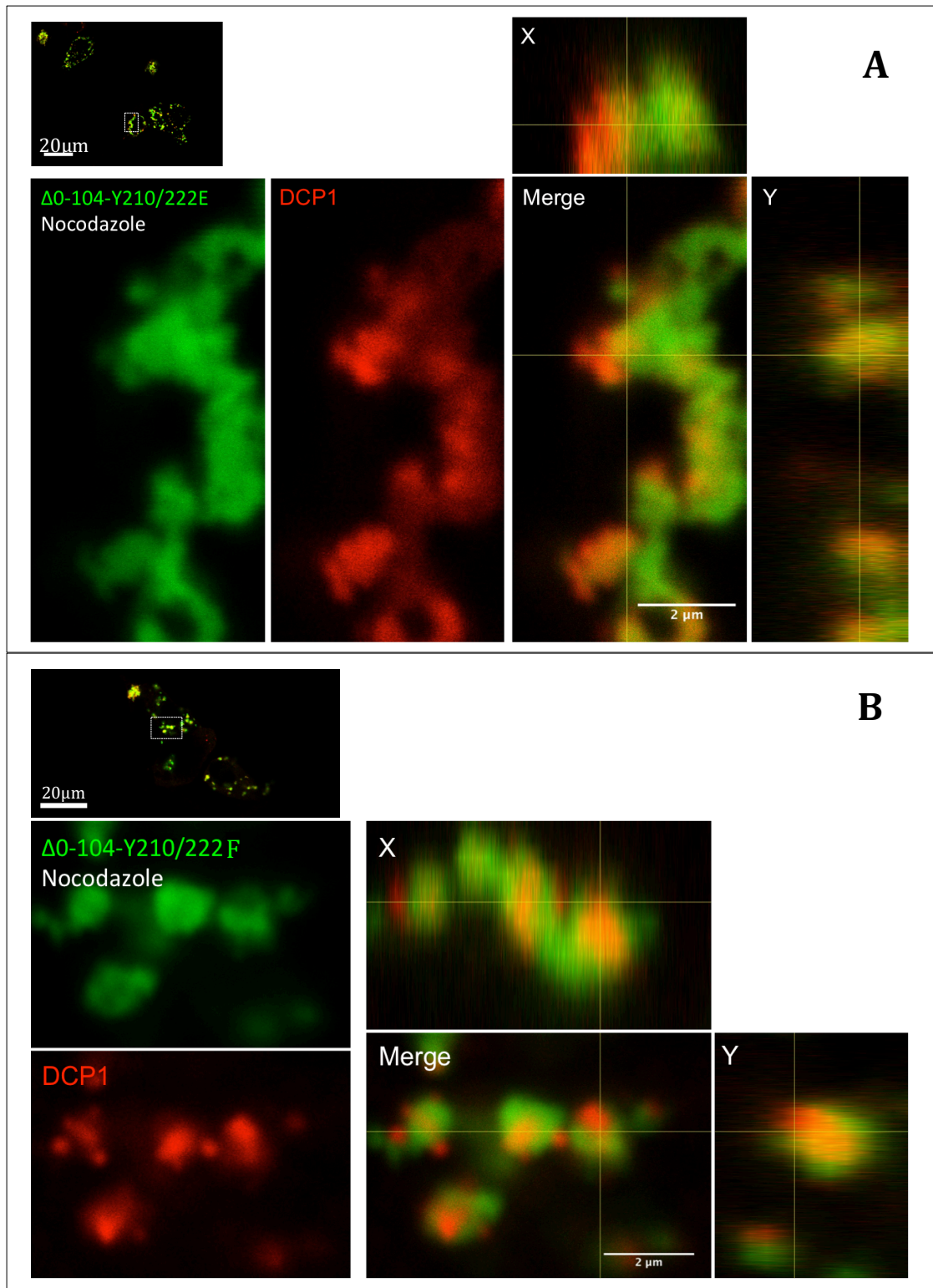


Fig. 3.11.2 Introduction of Y210/222E or Y210/222F mutations into $\Delta 0-104$ prevented complete overlap with DCP1 under cellular stress conditions

Confocal analysis of COS7 cells expressing GFP-tagged $\Delta 0-104-Y210/222E$ (**A**) or $\Delta 0-104-Y210/222F$ (**B**) and mCherry-tagged DCP1 after nocodazole treatment as described before.

Merged images including vertical and side views (X and Y coordinates) shown on the right indicated that both mutant proteins formed large structures partially overlapped with DCP1 which differs from $\Delta 0-104$ that completely overlapped with DCP1 under stress conditions (see Figure 3.10.3).

3.9 The N- and C-terminal of DEF6 mediate interactions

As described above, in isolation, both the N-terminal end as well as the coiled coil domain of DEF6 forms spontaneously either granules or aggregates indicating that both N- and C-terminal parts of DEF6 are capable of oligomerisation. Full-length wild type DEF6 protein on the other hand is mainly diffuse in the cytoplasm when overexpressed in COS7 cells. However, endogenous DEF6 in Jurkat T cells does form granules that overlap with DCP1 (Remon, 2016) suggesting that also the wild type DEF6 protein can oligomerise. To test this directly, a mCherry-tagged wild type DEF6 protein was also tagged with a SV40 nuclear localisation signal (NLS) (mCherry-NLS-DEF6; Appendix 8.1, Fig. 8.1.2 and Appendix 8.3, Fig. 8.3.2). Although DEF6 contains a functional NLS (amino acid positions 330-341), as verified by the fact the PH2 mutant including the NLS is located exclusively in the nucleus (Fig. 3.7.2b), the NLS is masked in the full length DEF6 protein which is largely absent from the nucleus (Fig. 3.3.0). mCherry-NLS-DEF6 however is exclusively found in the nucleus (Fig. 3.12.0 upper panel).

If full length wild type DEF6 dimerises or oligomerises then cotransfection of GFP-DEF6 with mCherry-NLS-DEF6 could result in the retention of mCherry-NLS-DEF6 in the cytoplasm or the import of GFP-DEF6 into the nucleus.

As shown Fig. 3.12.0 (lower panel), cotransfection of GFP-DEF6 with mCherry-NLS-DEF6 resulted in a clearly visible localisation of GFP-DEF6 in the nucleus completely overlapping with mCherry-NLS-DEF6. This is the first direct evidence that full length wild type DEF6 dimerises and/or oligomerises.

To test whether the observed interaction is mediated through the coiled coil domain, mCherry-NLS-DEF6 was cotransfected with mutant proteins N-590, DH1 and DH2. Similar to full length wild type DEF6, mCherry-NLS-DEF6 dragged some of the mutant N-590, DH1 and in part DH2 proteins into the nucleus (Fig. 3.12.0). However, DH2 aggregates in the cytoplasm trapped some mCherry-NLS-DEF6 protein preventing it from entering the nucleus (Fig. 3.12.0). Confocal analysis revealed that mCherry-NLS-DEF6 retained in the cytoplasm was within the vesicle-like tubes formed by DH2 aggregates (Fig. 3.12.1). Furthermore, mutant proteins Q371P-A374P, L442P-E445P, All-10 all disrupting the coiled coil domain, as well as DHL-N which contains only a part of the coiled coil domain did not interact with mCherry-NLS-DEF6.

Together these data suggest that oligomerisation of DEF6 is indeed mediated through the coiled coil domain. However, when mCherry-NLS-DEF6 was cotransfected with N-108 lacking the coiled coil domain, mCherry-NLS-DEF6 was also partially retained in the cytoplasm colocalising with N-108 granules (Fig. 3.12.1). Importantly, phosphomimic mutant Y210/222E that spontaneously colocalises with DCP1 also retained mCherry-NLS-DEF6 in the cytoplasm (Fig. 3.12.0) suggesting that DEF6 is capable of dimer formation and/or oligomerisation in P-bodies. A summary of the data is collated in Table 7.

DEF6/Mutants	Phenotypes		Molecule Features	
	Colocalised in nucleus	Colocalised in granules		
WT DEF6	✓	/		Contain N-terminal and full or part of coiled coil domain
DH1	✓	/		
DH2	✓	✓		
N-590	✓	✓	Contain N-terminal domain	
Y210/222E	✗	✓		
N-108	✗	✓		
DHL-N	✗	/	No full coiled coil domain or coiled coil structure is disrupted	
Q371P-A374P	✗	/		
L442P-E445P All-10				

Table 7: Cellular localisation of wild type and mutant DEF6 proteins coexpressed with mCherry-NLS-DEF6

Import of wild type or mutant proteins into the nucleus as well as retention of mCherry-NLS-DEF6 in the cytoplasm indicates interaction through dimerization and or oligomerisation. ✓: Yes, ✗: No, /: Not done

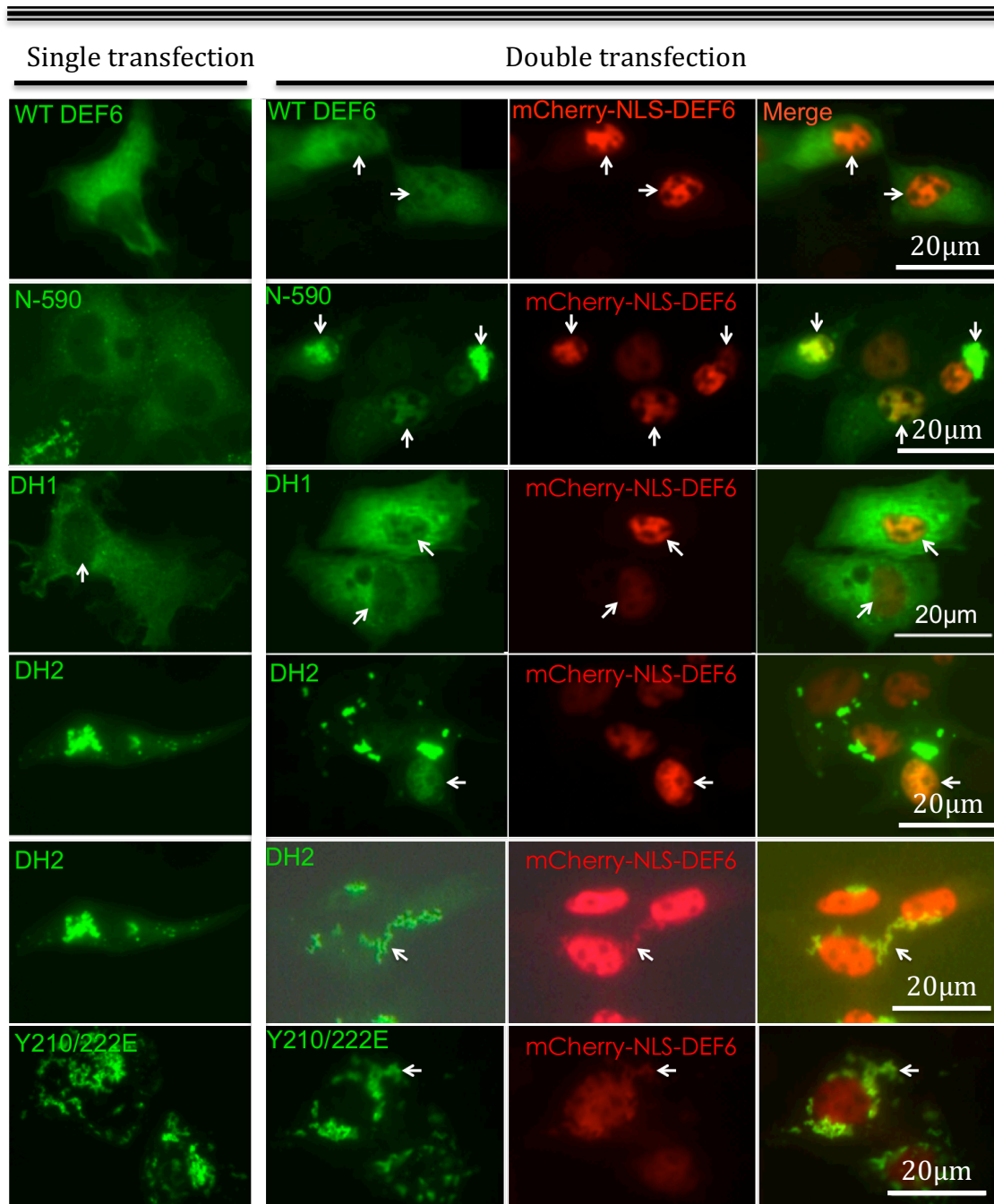
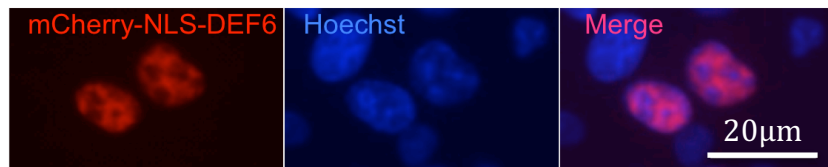


Fig. 3.12.0 Interaction of DEF6 molecules through dimerisation and or oligomerisation

Upper Panel: **mCherry-NLS-DEF6** localised exclusively to the nucleus that was stained with Hoechst.

Lower Panel: **WT DEF6**, **N-590**, **DH1** and **DH2** that on their own were localised in the cytoplasm (left column) as shown before, cotransfection with **mCherry-NLS-DEF6** resulted in clear nuclear import of these mutants (merged images in the right column). In addition, **DH2** and **Y210/222E** aggregations (lower two rows) retained some **mCherry-NLS-DEF6** in the cytoplasm.

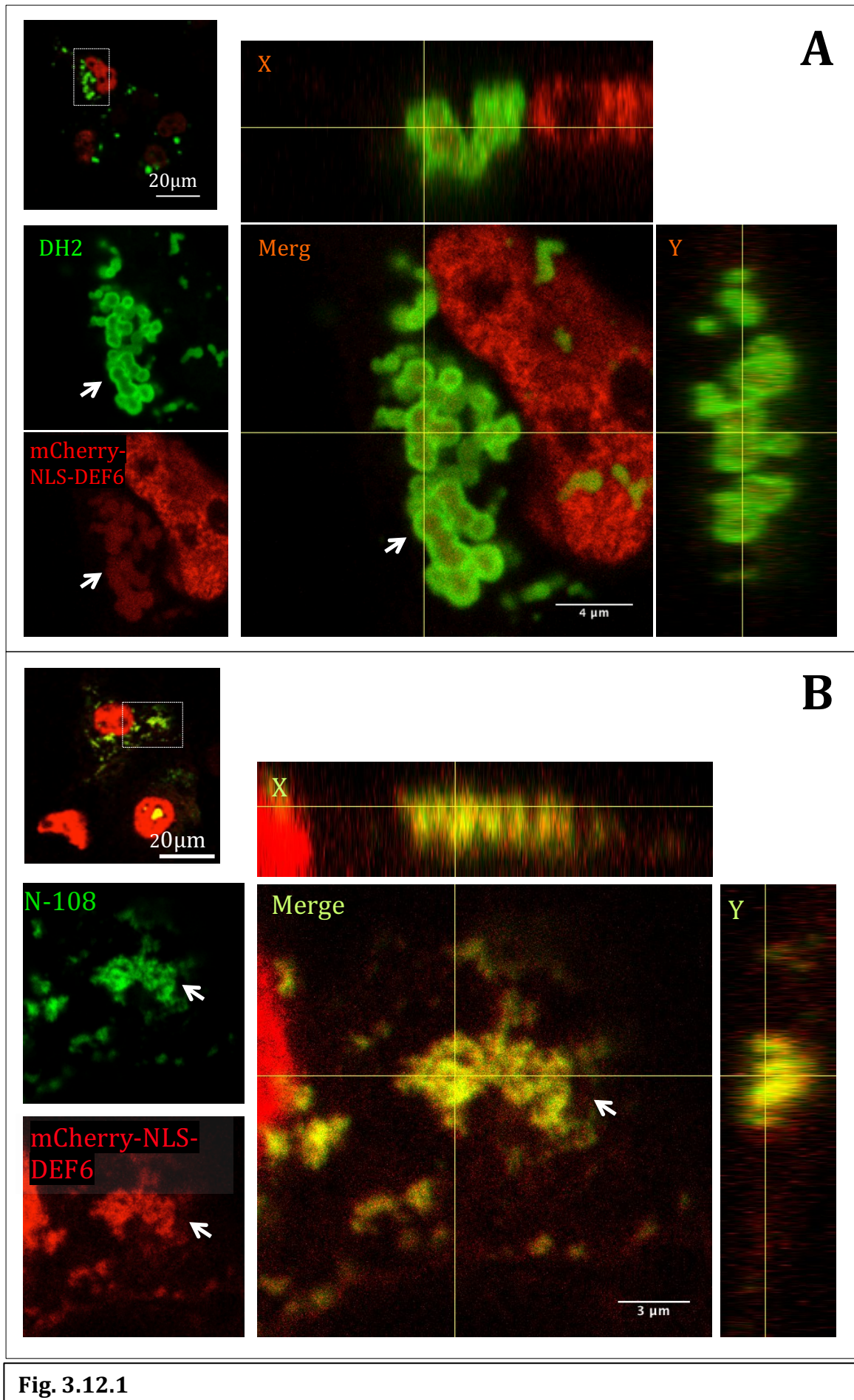


Fig. 3.12.1 Dimerisation and or oligomerisation of DEF6 can also be mediated through its N-terminal 108 amino acids

Confocal analysis of COS7 cells cotransfected with mCherry-NLS-DEF6 and either DH2 **(A)** or N-108 **(B)** as described before.

Merged images on the right including vertical and side views (X and Y coordinates) show that DH2 vesicle-like structures retain some mCherry-NLS-DEF6 in the cytoplasm by 'trapping' it within the vesicle-like structures.

N-108 also formed cytoplasmic aggregations that retained some mCherry-NLS-DEF6 in the cytoplasm indicating the the N-terminal 108 amino acids of DEF6 can also facilitate interaction resulting demerisation and or oligomerisation.

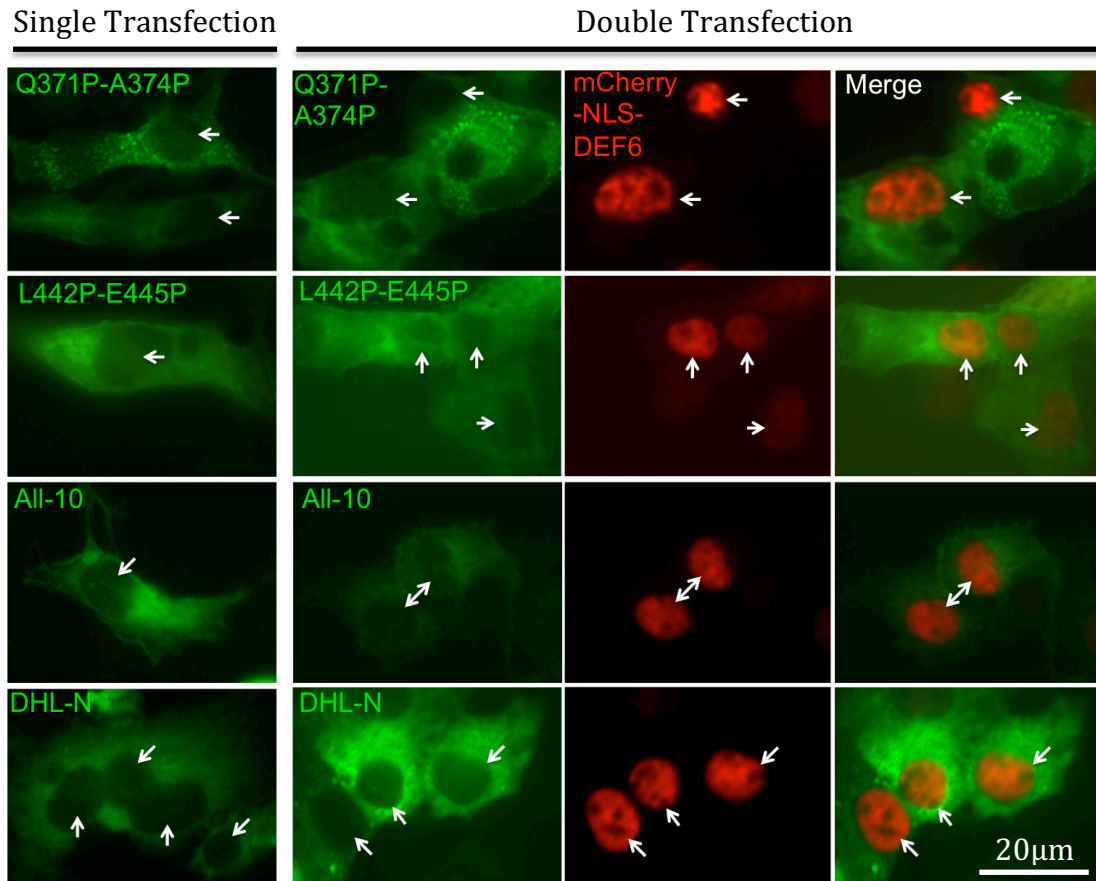


Fig. 3.13.0 DEF6 mutants Q371P-A374P, L442P-E445P, All-10 and DHL-N did not interact with mCherry-NLS-DEF6

Comparison of single transfection (left column) and cotransfection of Q371P-A374P, L442P-E445P, All-10 and DHL-N mutants with mCherry-NLS-DEF6 (right three columns). Merged images on the right show that mutants with disrupted coiled coil and/or partial coiled coil domain failed to interact with mCherry-NLS-DEF6.

3.10 LCK phosphomimic mutant Y133-144D forms aggregates that interact with DEF6 N-terminal truncated mutants

It had been reported that the LCK phosphorylation of DEF6 is required for DEF6 to locate to the IS and that phosphomimic mutant Y133/144D spontaneously localised to the IS (Gupta *et al.*, 2003b and Bécart *et al.*, 2008). However, expression of Y133/144D in COS7 cells resulted in aggregate formation that partially overlapped with DCP1 (Fig. 3.14.0). This phenotype is reminiscent of the one observed with DEF6 N-terminal truncated mutants such as $\Delta 0-104$ (section 3.8). However, unlike to $\Delta 0-104$ (Fig. 3.10.3), nocodazole treatment had no effect with Y133/144D still only partially overlapping with DCP1 (Fig. 3.14.0). mCherry-tagged Y133/144D aggregates did however fully colocalise with aggregates formed by DH2, $\Delta 0-216$ and $\Delta 0-104$ (Fig. 3.15.0).

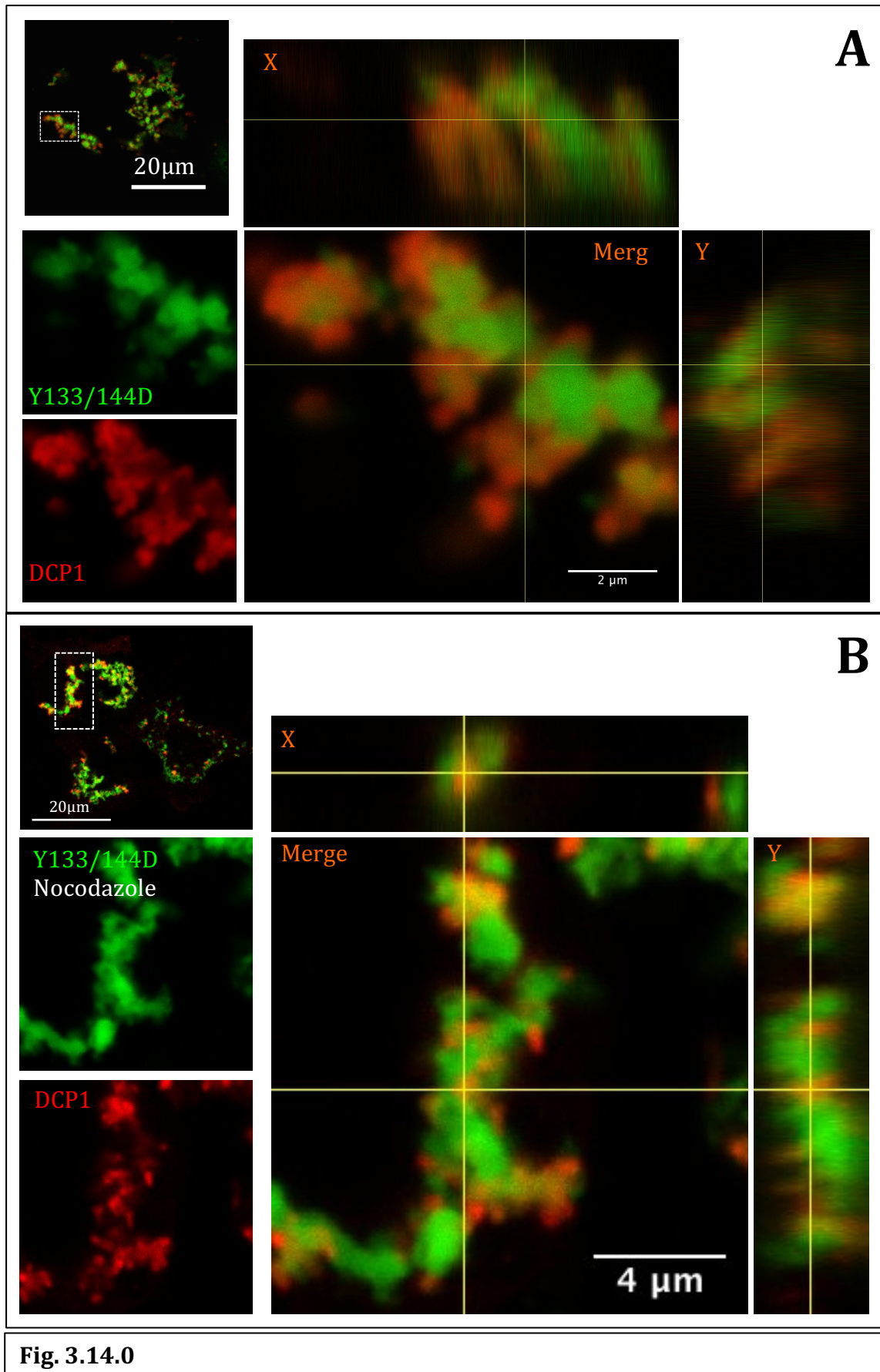


Fig. 3.14.0 LCK phosphomimic mutant Y133/144D formed aggregates that partially overlapped with DCP1 in untreated and nocodazole treated cells

Confocal analysis of COS7 cells cotransfected with GFP-tagged Y133/144D and mCherry-tagged DCP1 in untreated cells **(A)** and after nocodazole treatment **(B)**. Boxed area in the upper left images are enlarged in the lower left and further enlarged in the merged images on the right. Vertical and side views (X and Y coordinates) are also shown on the right. DCP1 is trapped by Y133/144D aggregates resulting in partial overlap in untreated and nocodazole treated cells.

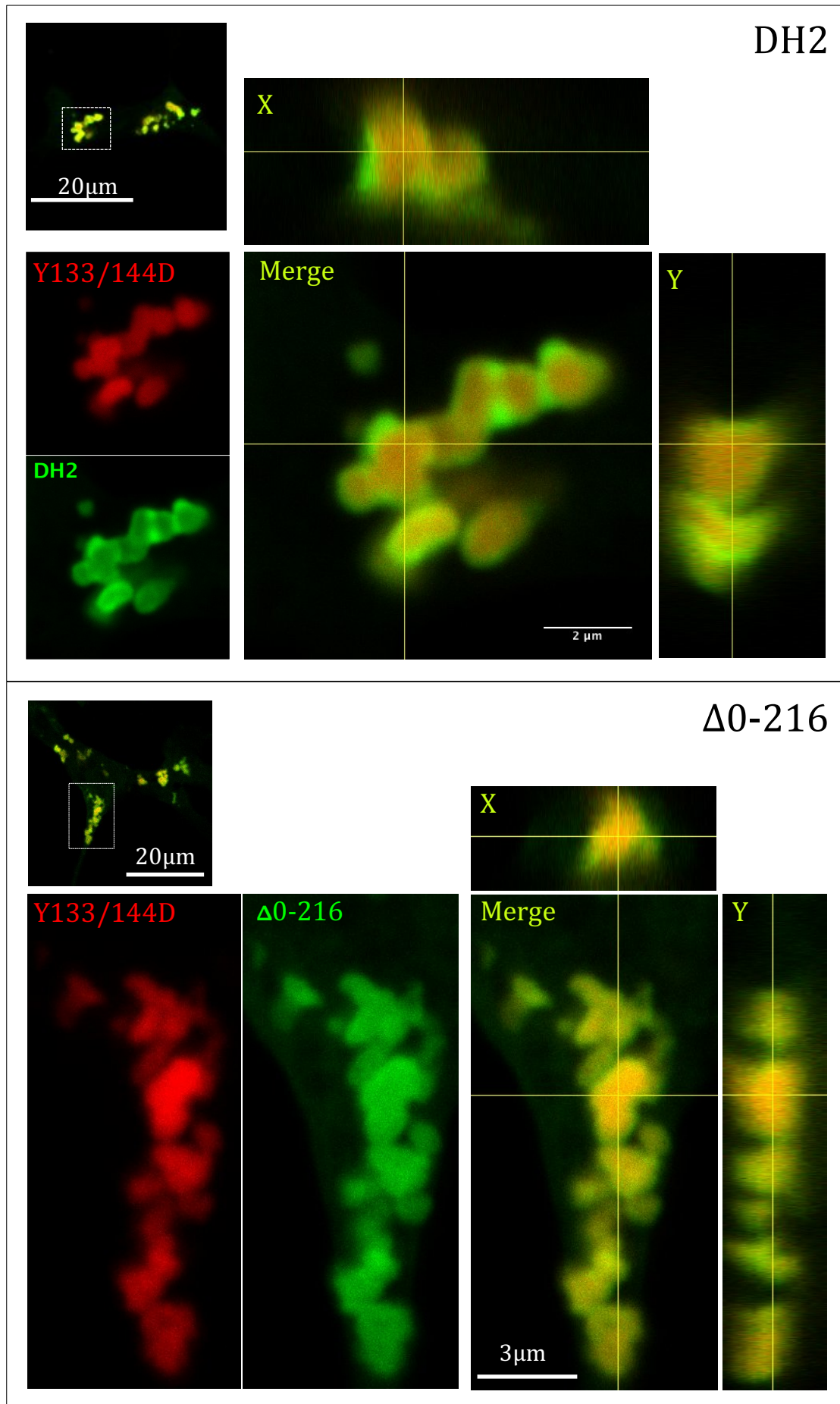


Fig. 3.15.0

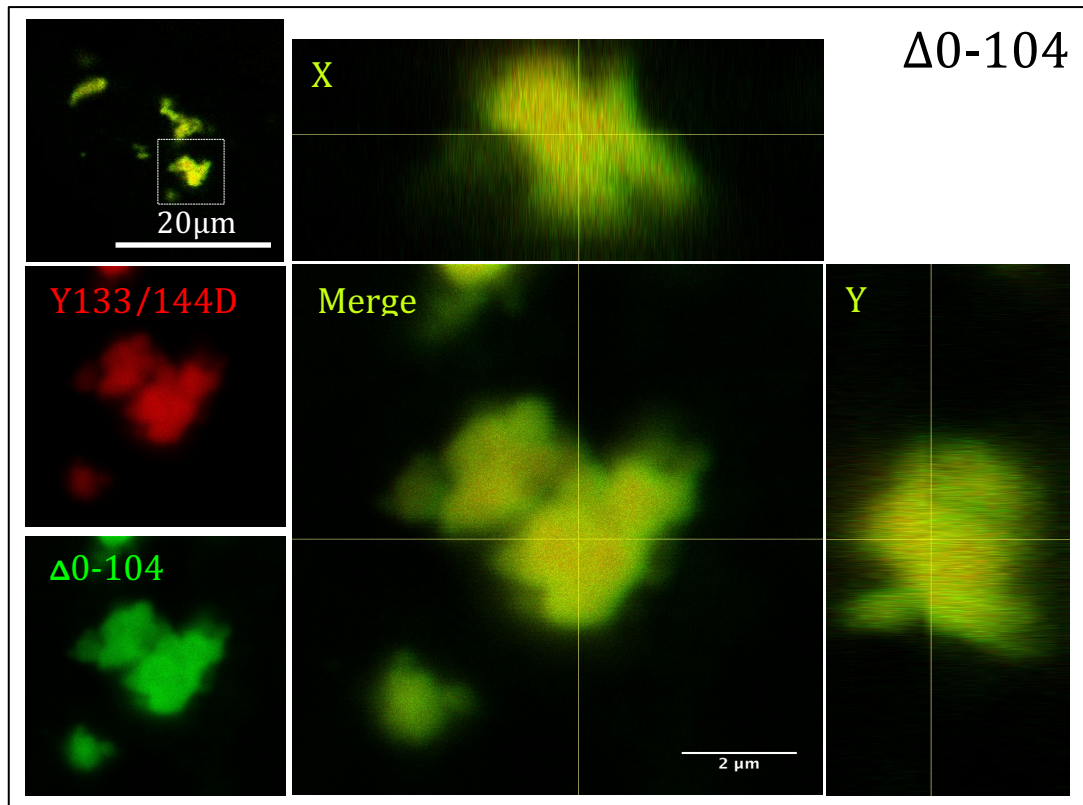


Fig. 3.15.0 Aggregates formed by the LCK phosphomimic mutant Y133/144D interact with DH2, $\Delta 0$ -216 and $\Delta 0$ -104

Confocal analysis of COS7 cells cotransfected with mCherry-tagged Y133/144D (red) and either GFP-tagged DH2 (upper panel), $\Delta 0$ -216 (middle panel) or $\Delta 0$ -104 (lower panel; green). Boxed area in the upper left images are enlarged in the lower left and further enlarged in the merged images on the right. Vertical and side views (X and Y coordinates) are also shown on the right in each panel. Complete overlap of aggregates formed indicate that Y133/144D mutant aggregates are mediated through the coiled coil domain.

3.11 Summary of main findings

- **The coiled coil domain is dispensable for DEF6 granule formation and colocalisation with P-bodies**
- **The N-terminal 45 amino acids of DEF6 are necessary and sufficient to spontaneously colocalise with P-bodies**
- **Phosphorylation of DEF6 by ITK at Y210 and Y220 releases the N-terminal end rather than the C-terminal coiled coil domain resulting in colocalisation with P-bodies**
- **The C-terminal coiled coil domain of DEF6 facilitates formation of aggregates that form large structures within the cytoplasm**
- **Coiled coil-mediated aggregates of DEF6 'trap' DCP1 suggesting a strong interaction between both proteins**
- **Both, N-terminal end and the coiled coil domain are mediating dimerisation and or oligomerisation of DEF6**
- **LCK phosphomimic mutant Y133/144D forms aggregates that interact with N-terminal truncation mutants**
- **Cellular stress induced through nocodazole treatment results in wild type DEF6 colocalising with P-bodies**
- **Differential response of DEF6 aggregates to cellular stress**
- **Nocodazole or arsenate treatment revealed a cooperation between ITAM domain and the coiled coil structure that facilitates colocalisation with P-bodies**

Chapter 4

Mapping the GEF function of DEF6

4.1 Molecular organisation of actin assembly

4.1.1 F-actin polymerisation

F-actin is a filamentous structure, which is assembled by monomer actins called globular actin or G-actin (Fig. 4.1.0). The two ends of actin filaments are distinct in that G-actin is assembled at one end called “barbed” end and disassembled at the other end called “pointed” end. The actin polymerisation undergoes two steps, nucleation and elongation. G-actin molecules form dimer or trimer that cause more G-actins to assemble at the barbed end (Pollard *et al.*, 2000, Blanchoin *et al.*, 2014).

Although F-actin elongation could happen spontaneously, the concentration of G-actins in the cytoplasm is not sufficiently high enough for this to happen *in vivo*. In fact, numerous molecules are involved in the polymerisation of F-actin. A group of proteins called formins are required for F-actin elongation. They contain formin homology (FH) domains 1 and 2 and usually form dimers mediated through their FH2 domains. Formin dimers bind to F-actin barbed end catalysing G-actin assembly mediated through the FH1 domains. In addition, G-actin binds to either ATP or ADP. ATP-bound G-actin is assembled at the barbed end but ATP is hydrolysed at actin molecules towards the pointed end and G-actin binding GDP are released from the pointed end. As ADP is exchanged with ATP in the cytoplasm, ATP-bound G-actin gains the ability to polymerise again (Fig. 4.1.0). In addition, elongation of actin polymerisation can be limited by cap proteins binding to the barbed end preventing addition of new G-actins. Arp 2/3 are another major protein complex for actin assembly, which binds to an actin filament acting as a nucleus to recruit new G-actins forming a 70° side F-actin chain. Finally, cofilin severs F-actin and promoting actin depolymerisation

(Pollard *et al.*, 2000; Campellone and Welch 2010; Blanchoin *et al.*, 2014) (Fig. 4.1.0).

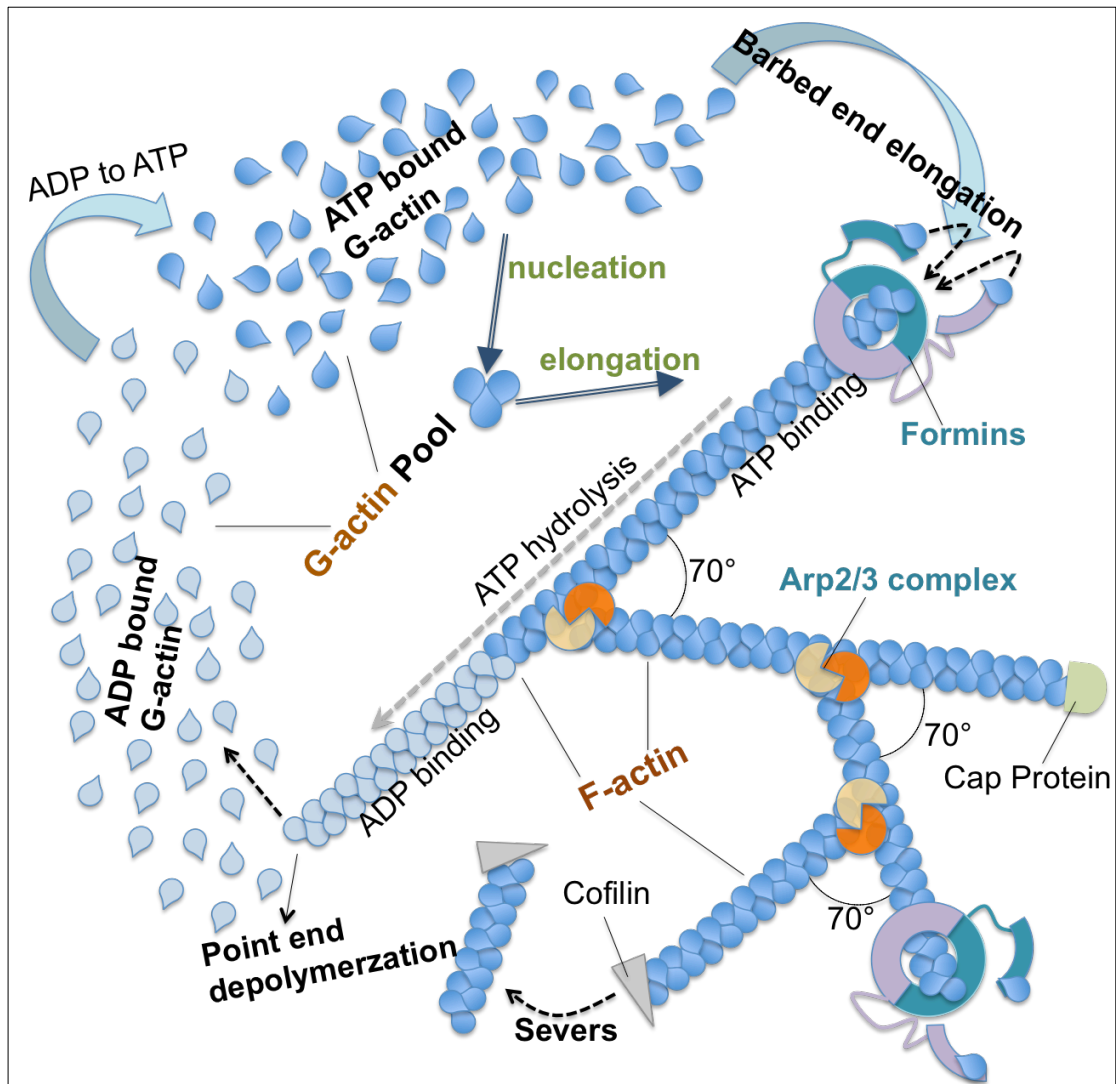


Fig. 4.1.0 Schematic of actin polymerisation

Monomer actins (G-actin) undergo nucleation to form dimers or trimers enabling G-actins to be added to the barbed end of the nucleus to elongate the actin filament (F-actin). G-actins bind ATP that is hydrolysed to ADP and Pi in the F-actin phase releasing G-actins bound to ADP at the pointed end. The depolymerised ADP bound actins exchange their ADP to ATP in the cytoplasm to obtain the ability to elongate F-actin again. Molecules that contribute to the actin dynamic are: formins that catalyse the elongation to add new G-actins on the barbed end, Arp2/3 protein complexes that bind to an actin filament as a nucleus to form a 70° angle at actin branch chains, cap proteins that limit binding of G-actins to the barbed ends thus limiting elongation, and cofilin that severs F-actin into fragments thereby promoting F-actin depolymerisation (Figure is based on information obtained from references cited in the text).

4.1.2 The signalling network of CDC42, Rac1 and RhoA

Cytoskeleton dynamics is partly regulated by the Rho GTPases CDC42, Rac1 and RhoA. They regulate F-actin polymerisation promoting the formation of lamellipodia, filopodia, invadosome and stress fibre/focal adhesion (Fig. 4.2.0). Rho GTPases function in an interacting network: Rac1 can be activated by CDC42 and CDC42 and RhoA can activate each other while RhoA inhibits the activity of Rac1. Rho GTPases also activate formins, such as mDia1-3, which through F-actin elongation regulates cytoskeleton dynamics. Furthermore, Rac1 and CDC42 respectively activate WAVE and WASP, which results in Arp2/3 complexes to promote F-actin side chain formation in lamellipodia, filopodia and invadosome. In addition, myosin II (MyoII) is a feature component of stress fibre/focal adhesion and invadosome. CDC42 and RhoA activate MyoII via MRCK and ROCK, respectively. Moreover, the activation of ROCK will activate formins. Finally, Rac1 and CDC42 can activate PAK, which in turn activates LIMK and inhibits cofilin. As described above, cofilin functions to sever actin filaments, hence the inhibition of cofilin increases the stability of F-actin. PAK activates MyoII and ROCK can promote LIMK (Goeckeler *et al.*, 2000; Brzeska *et al.*, 2004; Korobova and Svitkina, 2008; Linder, 2009; Tybulewicz and Henderson, 2009; Rottner and Stradal, 2011; Li *et al.*, 2011; Danielle and Courtneidge, 2011; Shinohara *et al.*, 2011; Jaiswal *et al.*, 2013; Ouderkirk and Krendel, 2014).

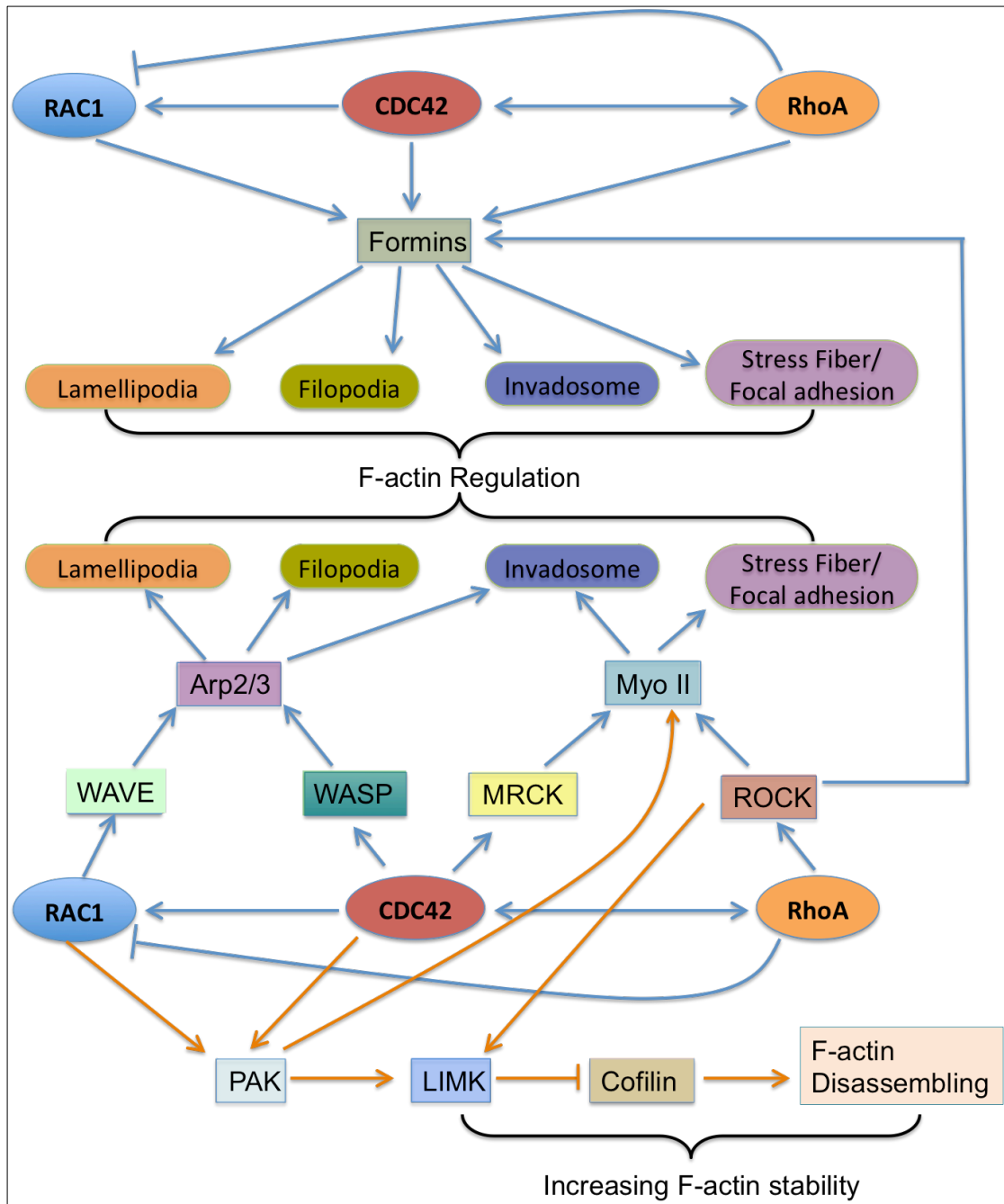


Fig. 4.2.0 Schematic of RAC1, CDC42 and RhoA interacting network

CDC42 can activate RAC1 and RhoA; RhoA can activate CDC42 but inhibits RAC1. Formins are common downstream targets of these three Rho GTPases contributing to F-actin elongation and regulating cytoskeleton dynamics. RAC1 and Cdc42 activate Arp2/3 to form branch actin filament in lamellipodia, filopodia and invadosome via WAVE and WASP. Myo II is activated by CDC42 and RhoA via MRCK and ROCK contributing to invadosome and stress fibre/focal adhesion formation. Activated ROCK can also activate formins. RAC1 and CDC42 activate PAK, which in turn activates LIMK and inhibits cofilin. Cofilin severs actin filament and inhibition of cofilin increases the stability of F-actin. (Figure is based on information obtained from references cited in the text).

4.1.3 Lamellipodia, Filopodia, Invadosome and Stress fibre

Even though lamellipodia, filopodia, invadosome and stress fibre are distinct structures, they are formed through actin polymerisation and contain a wide range of common components.

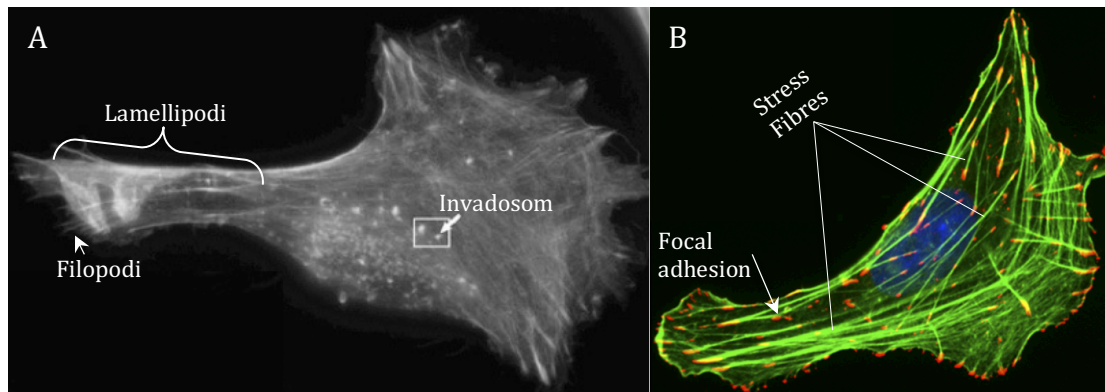


Fig. 4.3.0 F-actin dynamics

(A) Examples of lamellipodia, filopodia and invadosome (adopted from Baldassarre *et al.*, 2006)

(B) Examples of stress fibres and focal adhesion (adopted from Burridge and Wittchen, 2013).

Lamellipodia are broad but thin ($\sim 0.2\mu\text{m}$) protrusive structures at the leading edge of a spreading and migrating cell, which is filled with branched network actin (Fig. 4.3.0 A). When lamellipodia curl upwards they form membrane ruffles. In contrast, filopodia are thin ($0.1\text{-}0.3\mu\text{m}$) finger-like structures that extends from cell plasma membrane to explore extracellular environment. Filopodia are filled with tight parallel bundles of F-actin filaments and often form at the leading edge of migrating cells (Small *et al.*, 2002; Mattila and Lappalainen, 2008; nature. n.d. a) (Fig. 4.3.0 A). Stress fibres are more abundant, stable and thicker in non-motile cells. They are large filamentous F-actin bundles that extend across much of a cell and usually are anchored by focal adhesions at one or both of their ends. Stress fibres are made of antiparallel actin filaments and contain MyoII, which

endow stress fibres an ability of contraction (Tojkander *et al.*, 2012; Burridge and Wittchen, 2013) (Fig. 4.3.0 B). Focal adhesions are clustered transmembrane integrins and other associated proteins, which provide adhesive contacts between cells and extracellular matrix and mediate both mechanical and biochemical signalling (Smilenov *et al.*, 1999 and Nature; n.d. b) (Fig. 4.3.0 B). Invadosomes contain two types of very similar F-actin foci, podosome and invadopodia. They are both 0.5-2 μm diameter actin rich cellular protrusions that extend to extracellular matrix performing degradation of the matrix. While podosomes are present in normal cells, invadosome are found in cancer cells and are involved in cell invasion. Both also differ in length and have somewhat different components (Fig. 4.3.0 A) (Linder 2009; Rottner and Stradal, 2011; Murphy and Courtneidge, 2011 and nature n.d. c and d).

4.2 Proline mutations on several *a/d* positions within the coiled coil domain of DEF6 resulted in colocalisation with F-actin

As mentioned in Chapter 3 (3.3), cellular localisation of the proline mutants Q371P-A374P, R407P-M410P, I428P-L431P and K491P-494P was mainly diffuse within the cytoplasm. In contrast, mutant proteins L442P-E445P, L463P-E466P, L470P-L473P, L505P-A508P, L512P-V515P and L533P-A536P widely (>90%) colocalised with F-actin in lamellipodia, filopodia suggesting that disruption of the coiled coil domain at these *a/d* positions released GEF activity of DEF6. To further verify this interpretation, the latter proline mutations were introduced into the former to establish compound mutants Q371P-A374P-L505P-A508P, R407P-M410P-L505P-A508P, I428P-L431P-L505P-A508P as well as a mutant containing prolines at 10 *a/d* positions (All-10 mutant). As shown in (Fig. 4.4.0 and Appendix 8.4, Fig. 8.8.4 to Fig. 8.8.8) all of the compound mutants colocalised widely (>90%) with F-actin. These results suggest that the coiled coil domain itself is unlikely to be important for the colocalisation of DEF6 with F-actin. Rather they suggest, that disruption of the coiled coil domain results in conformational change resulting in F-actin-binding of DEF6.

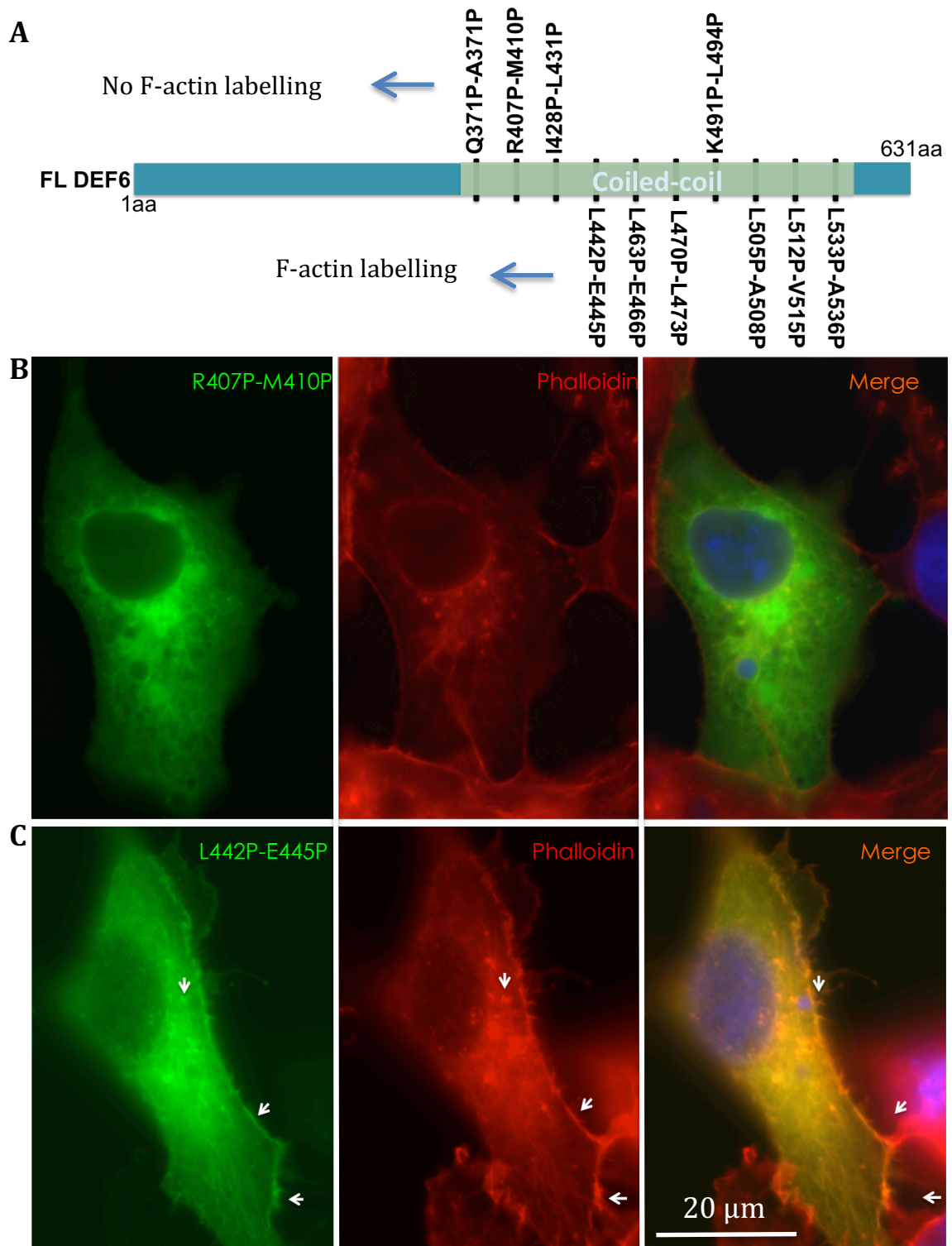


Fig. 4.4.0

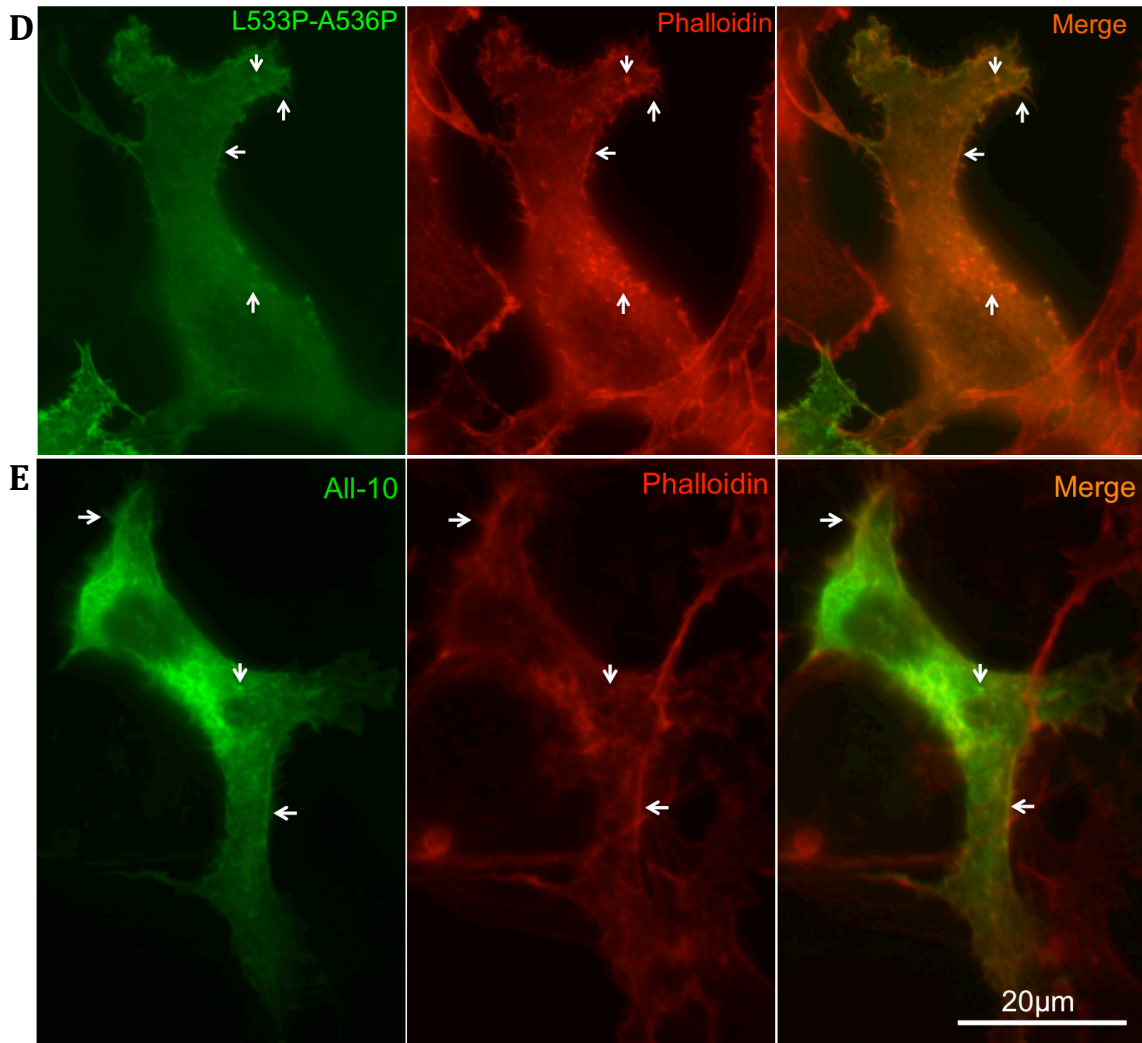


Fig. 4.4.0 Disruption of the coiled coil domain results in conformational change and colocalisation of some proline mutants with F-actin

(A); Schematic representation of the proline mutants that did or did not colocalise with F-actin.

(B): GFP tagged R407P-M410P (green) represents the proline mutants that were diffused in cytoplasm and did not colocalise with F-actin stained with phalloidin (red). (Q371P-A374P, R407P-M410P, I428P-L491P and K491P-L494P mutants also did not colocalise with F-actin; not shown).

(C): L442P-E445P, L533P-A536P **(D)** and All-10 mutants **(E)** do colocalise with F-actin (like L463P-E466P, L470P-L494P, L505P-A508P, L512P-V515P; not shown) labelling lamellipodia, filopodia and invadosome (arrows).

Merged images on the right show overlapping of green and red (yellow) indicating colocalisation. Images of COS7 cells were taken 24 hrs after transfection. Scale bar 20µm as indicated.

4.3 Truncation mutants containing amino acids 537 to 590 of DEF6 are sufficient to label F-actin

Initial work by Mavrakis *et al.* (2004) indicated that the C-terminal end of DEF6 (DH1: amino acids 355 to 631) exhibited constitutive GEF activity colocalising with F-actin. Hey *et al.* (2012) demonstrated that a portion of the C-terminal end (DHL-C: amino acids 476 to 590) was sufficient to label F-actin. Transfection of COS7 cells with DH1 and DHL-C confirmed these results (Fig. 4.5.0). These results together with those describe earlier (Fig. 4.4.0) suggested that the ability of DEF6 to colocalise with F-actin was likely to be mediated through the protein region encoded by amino acids 537 to 590. Hence, A GFP-tagged DEF6 mutant was established only containing amino acids 537 to 590. As shown in Fig. 4.5.0, expression of this region of the DEF6 protein was sufficient for colocalisation with F-actin in almost 100% of the transfected cells.

To further dissect the ability of DEF6 to colocalise with F-actin, mutants were established that either expressed amino acids 537 to 550 or 551 to 590 as GFP fusion proteins. Both mutants appeared to overlap with F-actin (Fig. 4.5.0) but were also distributed diffusely in the cytoplasm, which might indicate that both sub-regions are still able to bind F-actin albeit to a lesser extent compared to the combined region from amino acid 537 to 590.

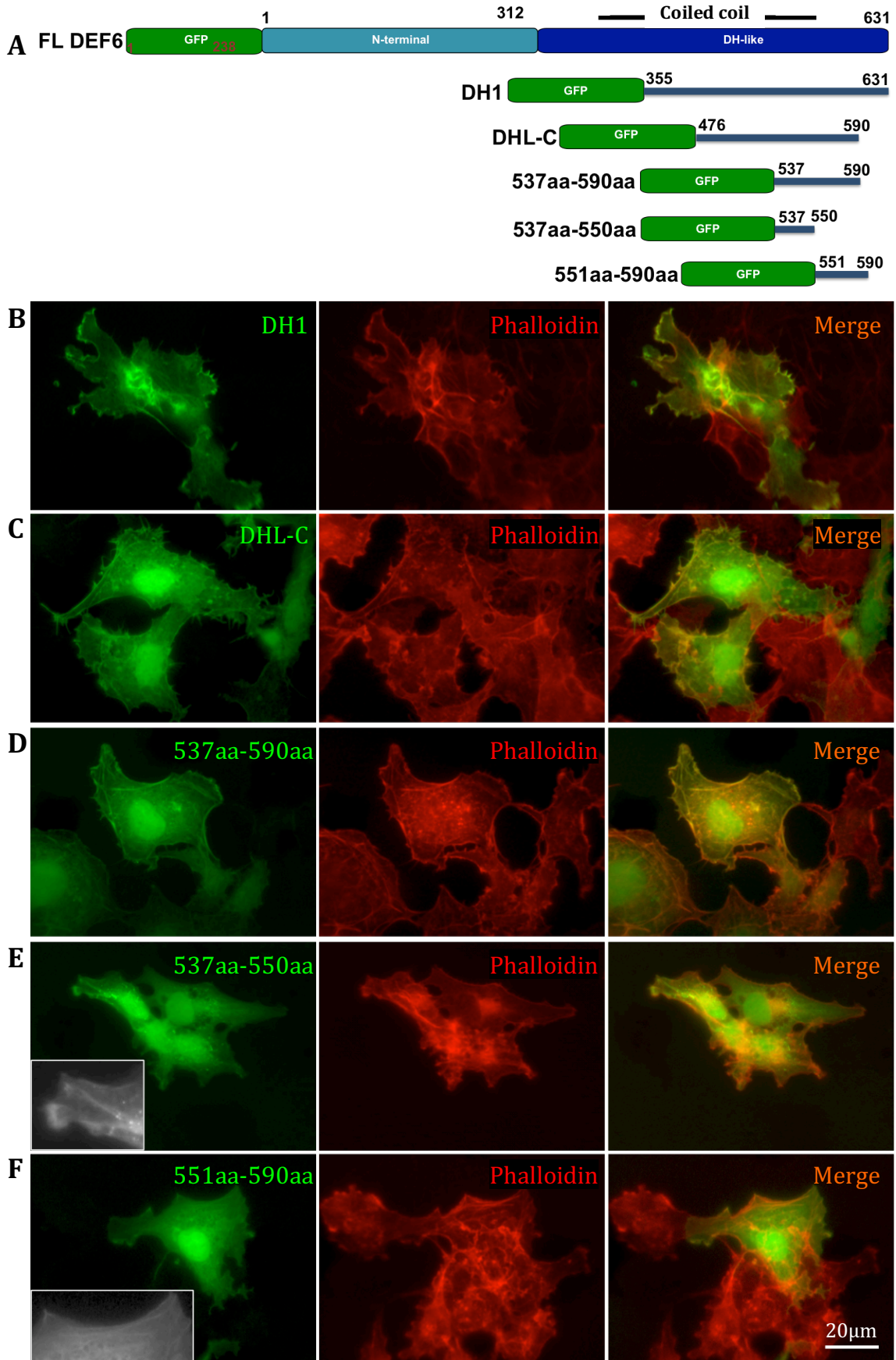


Fig. 4.5.0

Fig. 4.5.0 Amino acids 537 to 590 of DEF6 colocalise with F-actin

(A): Schematic depiction of GFP-DEF6 mutants DH1, DHL-C, amino acids 537 to 590aa, 537 to 550 and 551 to 590.

Expression of GFP-tagged DH1 **(B)**, DHL-C **(C)** and 537 to 590 **(D)**; green) overlapped with F-actin stained with phalloidin (Red).

In contrast, 537 to 550 **(E)** and 551 to 590 **(F)** did exhibit some F-actin labeling but this was less intense and somewhat blurry (white arrows). In addition, these mutants localized diffuse in the cytoplasm and exhibited some cytoplasmic granules (pink arrows) in about 37% of the transfected cells.

4.3.1 F-actin colocalisation is dependent on the coiled coil domain suggesting that oligomerisation is required for F-actin binding

SWAP70 forms oligomers via their coiled coil region, which is necessary for its F-actin labelling function (Chacón-Martínez *et al.*, 2013). To test whether the region of DEF6 that colocalised with F-actin (amino acids 537 to 590) was able to facilitate oligomerisation, the following experiment was performed. mCherry-Y133/144D mutant spontaneously aggregates (Fig. 3.14.0) and this aggregation is likely mediated through the coiled coil domain. Therefore mCherry-Y133/144D was cotransfected with GFP-tagged mutant 537 to 590. As shown in Fig. 4.6.0, in the presence of mCherry-Y133/144D aggregates, GFP-tagged mutant 537 to 590 protein colocalised with mCherry-Y133/144D aggregates. Similarly, when mCherry-Y133/144D was cotransfected with GFP-tagged 537 to 550, both colocalised in aggregates (Fig. 4.6.0). In contrast, GFP-tagged 551 to 590 did not colocalise with mCherry-Y133/144D aggregates (Fig. 4.6.0). It seems therefore that Y133/144D mutant that spontaneously aggregates can trigger aggregations of 537-590 and 537-550 that is presumably mediated through the coiled coil domain. If so, it suggests that the mutant Y133/144 acts like a prion: forcing other proteins to aggregate that on their own do not aggregate. Given that 537-590 localised with F-actin (Fig. 4.5.0), it suggests that the coiled coil domain facilitates oligomerisation and this oligomerisation is resulting in F-actin colocalisation and presumably binding.

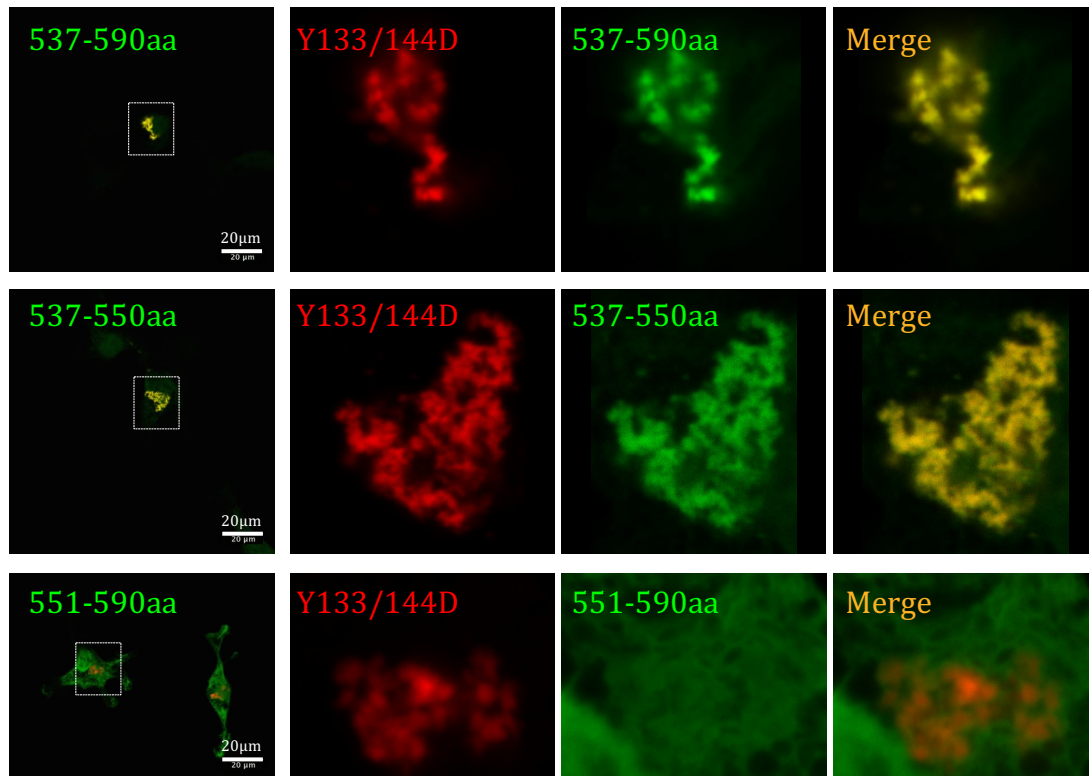


Fig. 4.6.0 Y133/144D aggregates enforce aggregation of mutant proteins 537 to 590 and 537-550

GFP-tagged DEF6 mutants 537 to 590, 537 to 550 and 551 to 590 were coexpressed with mCherry-tagged DEF6 Y133/144D mutant, as indicated. While 537 to 590 and 537 to 550 were captured by Y133/144D aggregates as seen in the merged images on the right, mutant 551 to 590 did not overlap with mCherry-tagged DEF6 Y133/144D aggregates.

4.4 Coiled coil-mediated aggregation prevents DEF6 from colocalising with F-actin

N-terminal truncated mutants that contain the entire coiled coil region such as DH2, $\Delta 0-104$ and $\Delta 0-216$ spontaneously aggregated in COS7 cell cytoplasm (Fig. 3.7.1). All these mutant proteins contain the amino acids 537 to 590 that were sufficient to colocalise with F-actin as shown above. Nevertheless, as shown in Fig. 4.7.0, formation of aggregates by the mutant proteins prevented colocalisation with F-actin again indicating that F-actin binding and presumably GEF activity of DEF6 is masked in aggregates. Interestingly, LCK was shown to phosphorylate DEF6 at residues Tyr 210, 133 and 144 apparently liberating the GEF activity of DEF6 (Gupta *et al.*, 2003b and Bécart *et al.*, 2008). However, the LCK phosphomimic mutant, Y133/144D, spontaneously aggregates in the cytoplasm and did not exhibit any visible filament-like distribution as previously shown (Fig. 3.17.0 and Fig. 4.7.0).

Together these results suggest that DEF6 can adopt multiple conformations that either result in diffuse distribution, coiled coil-mediated oligomerisation resulting in F-actin colocalisation and presumably GEF activity, N-45-mediated P-body colocalisation and coiled coil-mediated aggregation.

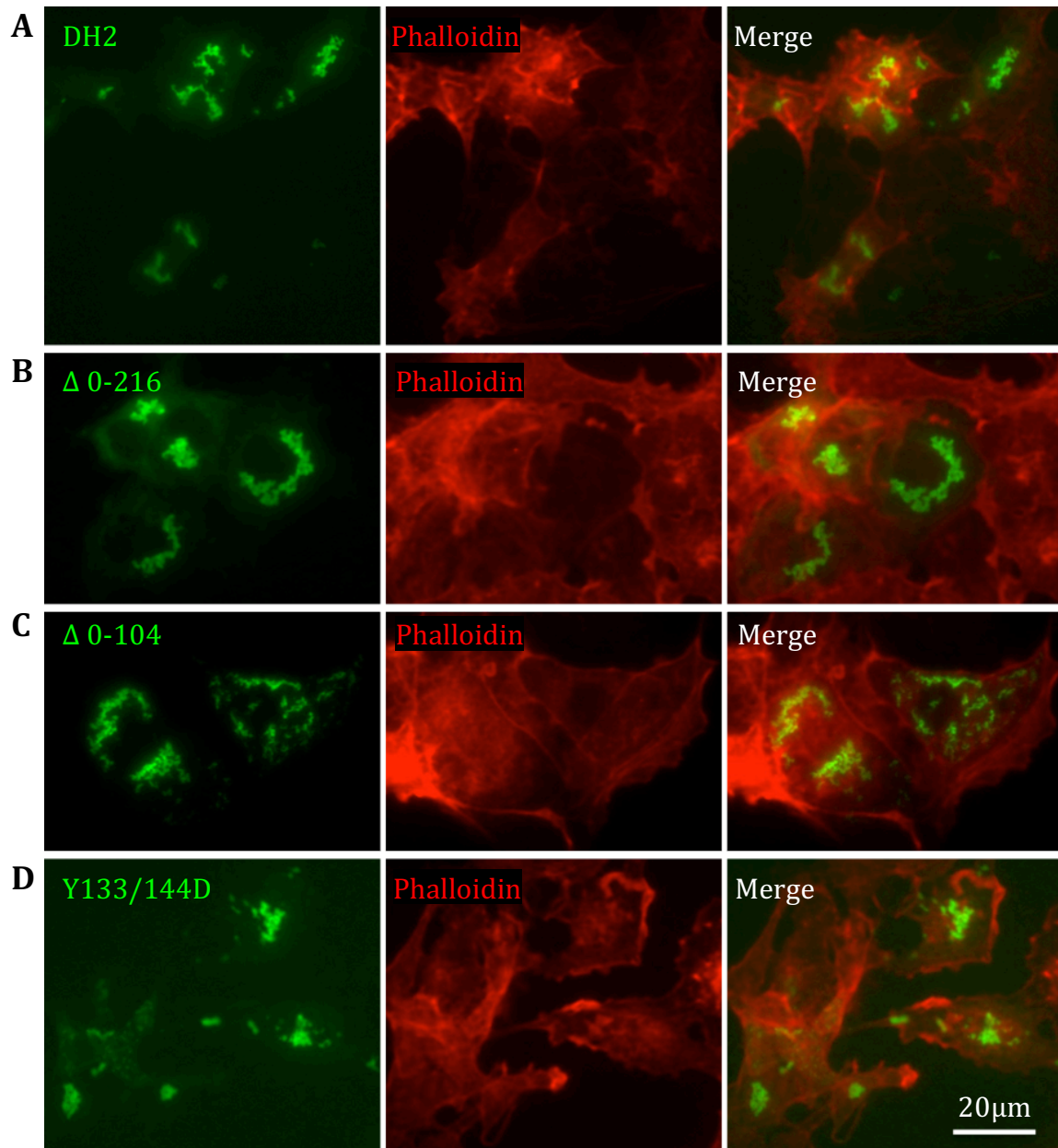


Fig. 4.7.0 Coiled coil-mediated aggregation prevents colocalisation of mutant proteins with F-actin

GFP-tagged DH2 (A), $\Delta 0-216$ (B), and $\Delta 0-104$ (C) Y133/144D (D) (green) spontaneously aggregate as shown before (Section 3.8). As can be seen in the merged images, these aggregates are not colocalising with F-actin (stained with phalloidin; red).

4.5 H₂O₂ treatment inducing PI3K activation resulted in DEF6/mutants labelling F-actin.

Mavrakis *et al* (2004) reported that either H₂O₂ treatment of, or PDGF-BB addition to COS7 cells transfected with GFP-tagged DEF6 resulted in relocalisation of the fusion protein and formation of lamellipodia and filopodia suggesting that DEF6 GEF activity is regulated via the PI3K pathway. To test whether mutant DEF6 proteins that spontaneously aggregate can still be induced via the PI3K pathway, transfected COS7 cells with selected mutants were treated with H₂O₂ (1 mM, 15mins) and the data summarised in Fig. 4.8.1, -2 and -3.

4.5.1 H₂O₂ treatment altered WT DEF6 and Δ 0-104 to overlap with F-actin

H₂O₂ treatment had no effect on the cellular localisation of GFP alone and as expected almost 100% WT DEF6 expressed COS7 cells showed colocalisation with F-actin. In addition, about 39% of transfected cells also contained cytoplasmic foci / small granules, and these granules did not overlap with F-actin (Fig. 4.8.1). N-terminal truncated mutants, such as DH2 and Δ 0-216 (3.7) still formed aggregates in cytoplasm indicating that H₂O₂ treatment could not override aggregation (Fig. 4.8.1). However, some mutants represented by Δ 0-104 (3.7), relocalised and overlapped with F-actin in lamellipodia, filopodia and invadosome in almost 100% of the transfected cells, even though aggregations were still widely present (in 28% of the transfected cells) (Fig. 4.8.1).

Taken together, it seems that the coiled coil domain can form stable aggregates and larger structure but also mediate oligomerisation facilitating F-actin colocalisation and presumably GEF activity.

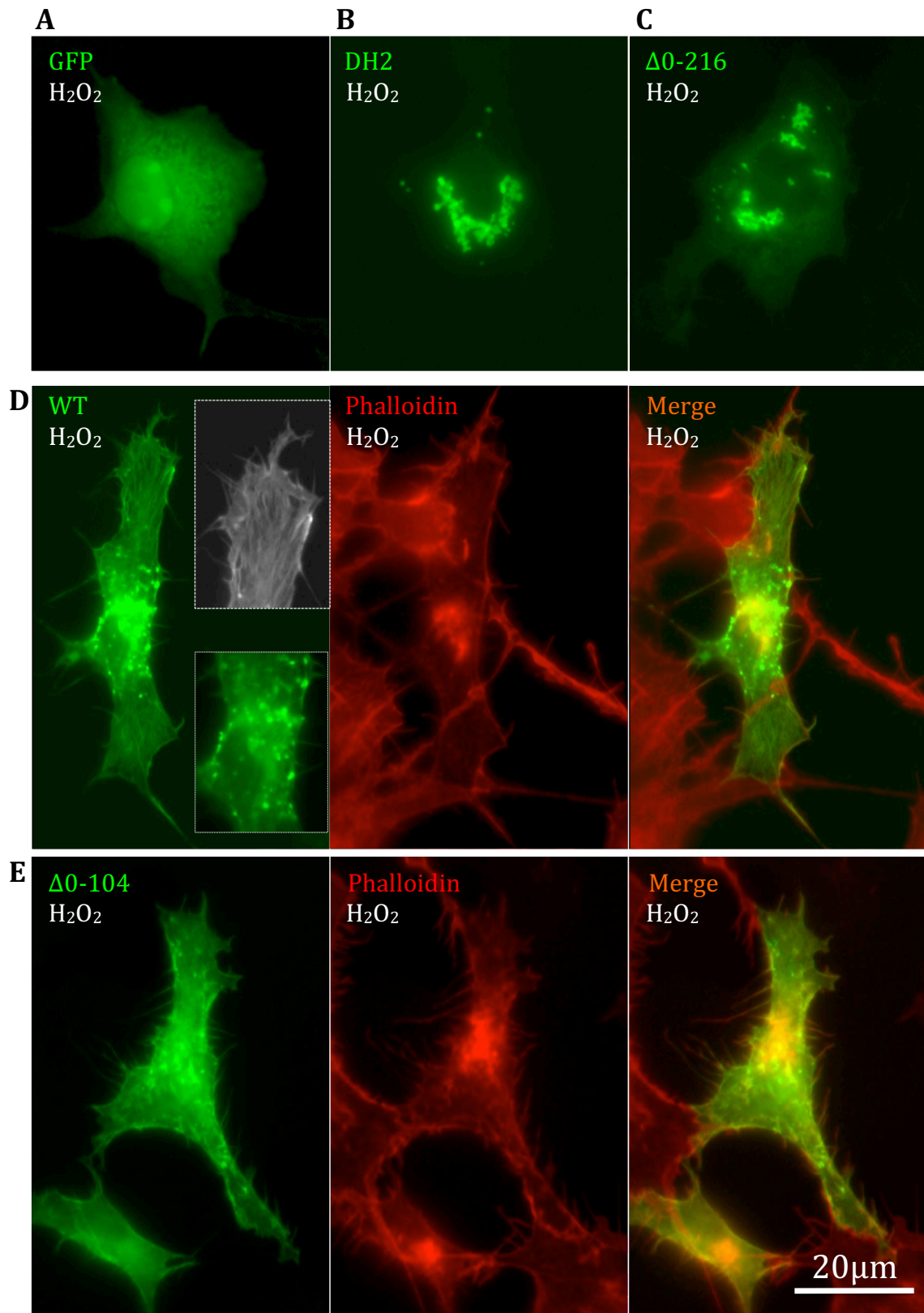


Fig. 4.8.1

Fig. 4.8.1 H₂O₂ treatment alleviates Δ 0-104 aggregates

COS7 cells transfected with GFP or GFP-tagged wild type DEF6 or mutants DH2, Δ 0-216 and Δ 0-104 were treated with 1 mM H₂O₂ for 15mins.

Localisation of GFP **(A)**, and aggregates of DH2 **(B)** and Δ 0-216 **(C)** did not change upon treatment.

Wild type (WT) DEF6 **(D)** colocalised with F-actin (stained with phalloidin; red) indicating GEF activity. H₂O₂ treatment also resulted in WT DEF6 forming granules in about 39% of transfected cells.

Δ 0-104 **(E)** also colocalised with F-actin in nearly 100% of the transfected cells and only about 29% of them exhibited still aggregations.

4.5.2 Conformation of phosphomimic DEF6 mutants are resistant to H₂O₂-mediated protein modifications

As shown above, DH2 and Δ 0-216 aggregates, which lack ITAM and PH domains, were resistant to H₂O₂-mediated protein modifications. Phosphomimic mutants Y133/144D that aggregates or Y210/222E that localises to P-bodies and the corresponding neutral mutants Y133/144F, Y210/222F were tested next. As shown in Fig. 4.8.2, Y133/144D and Y210/222E aggregates were also resistant to H₂O₂ treatment. Phosphomimic mutant Y210/220E in the context of Δ 0-104 (Y210/222E- Δ 0-104) again formed aggregates that were resistant to H₂O₂ treatment suggesting that the conformation of these aggregates is stable compared to those formed by Δ 0-104 (see Fig. 4.8.1). Y133/144F and Y210/222F formed aggregates but also colocalised with F-actin in few cells after the treatment (these rare cells depicted in Fig.4.8.2). These data suggest that modifications of ITAM and PH domains of DEF6 through phosphorylation determine conformation and function preventing colocalisation with F-actin.

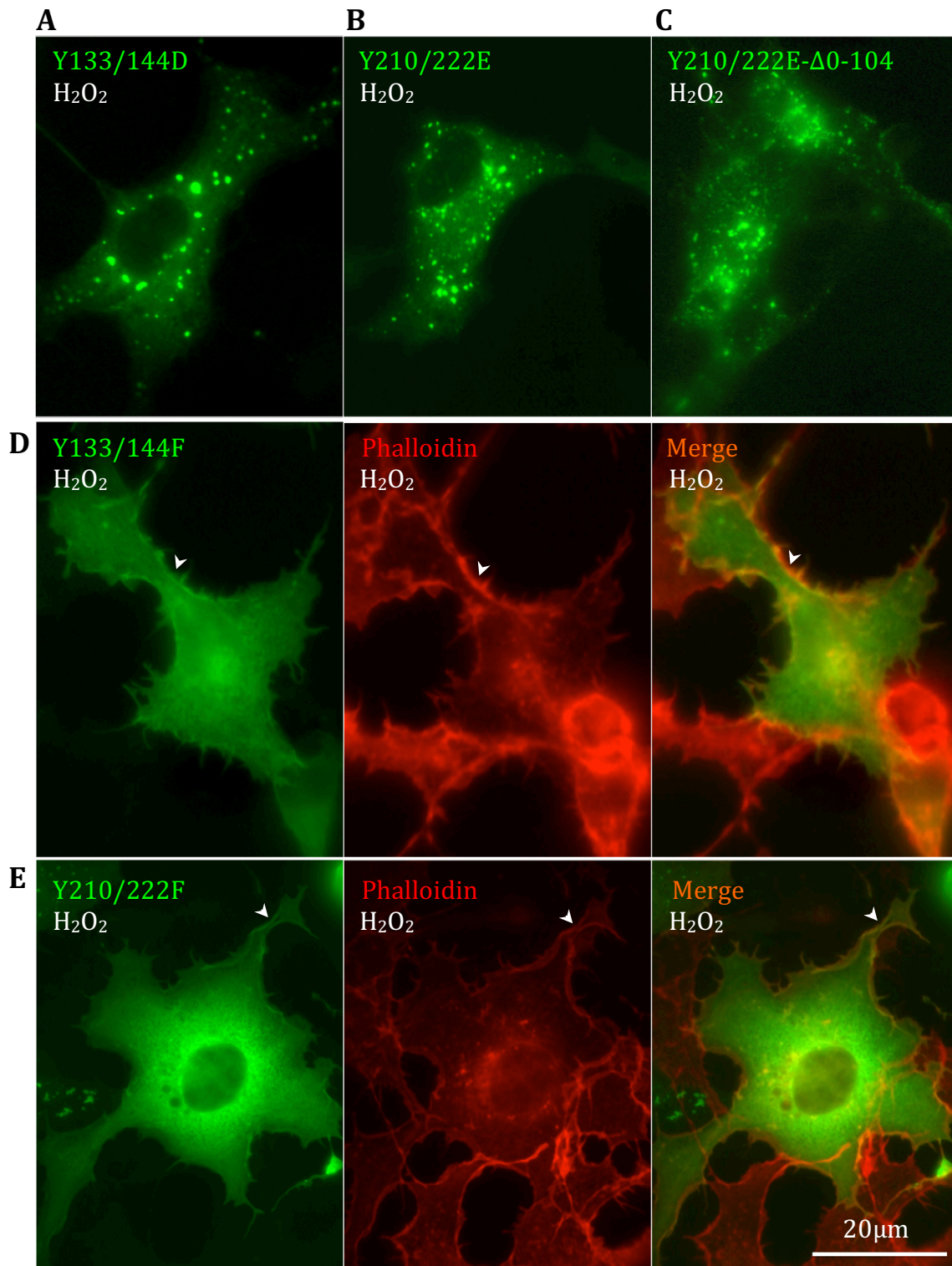


Fig. 4.8.2 Conformation of phosphomimetic DEF6 mutants are resistant to H₂O₂-mediated protein modifications

H₂O₂ treatment (1mM, 15mins) of COS7 cells transfected with GFP-tagged phosphomimetic mutants Y133/144D (A), Y210/222E (B) and Y210/222E-Δ0-104 (C) did not alter formation of aggregates observed in 68%, 68.5% and 88% of the transfected cells, respectively.

Expression of GFP-tagged Y133/144F (D) and Y210/222F (E) resulted in aggregates in 27.2% and 43.8% of the transfected cells and only few cells exhibited overlap with F-actin depicted here.

4.5.3 Conformation of proline mutants Q407P-M410P and I428P-L431P are resistant to H₂O₂-mediated protein modifications but localisation of Q371P-A374P and K491P-L494P was altered

As shown in Chapter 3 (3.3), Q371P-A374P, Q407P-M410P, I428P-L431P and K491P-L494P localised diffuse in the cytoplasm without any obvious overlap with F-actin (Fig. 3.3.0). As shown in Fig. 4.8.3, Q371P-A374P colocalised with F-actin in almost 100% of the transfected cells. In contrast, R407P-M410P and I428P-L431P were more diffuse in cytoplasm and rarely colocalised with F-actin. Surprisingly, 81% of cells transfected with K491P-L494P exhibited granules in the cytoplasm that did not seem to colocalise with F-actin but were frequently observed alongside F-actin.

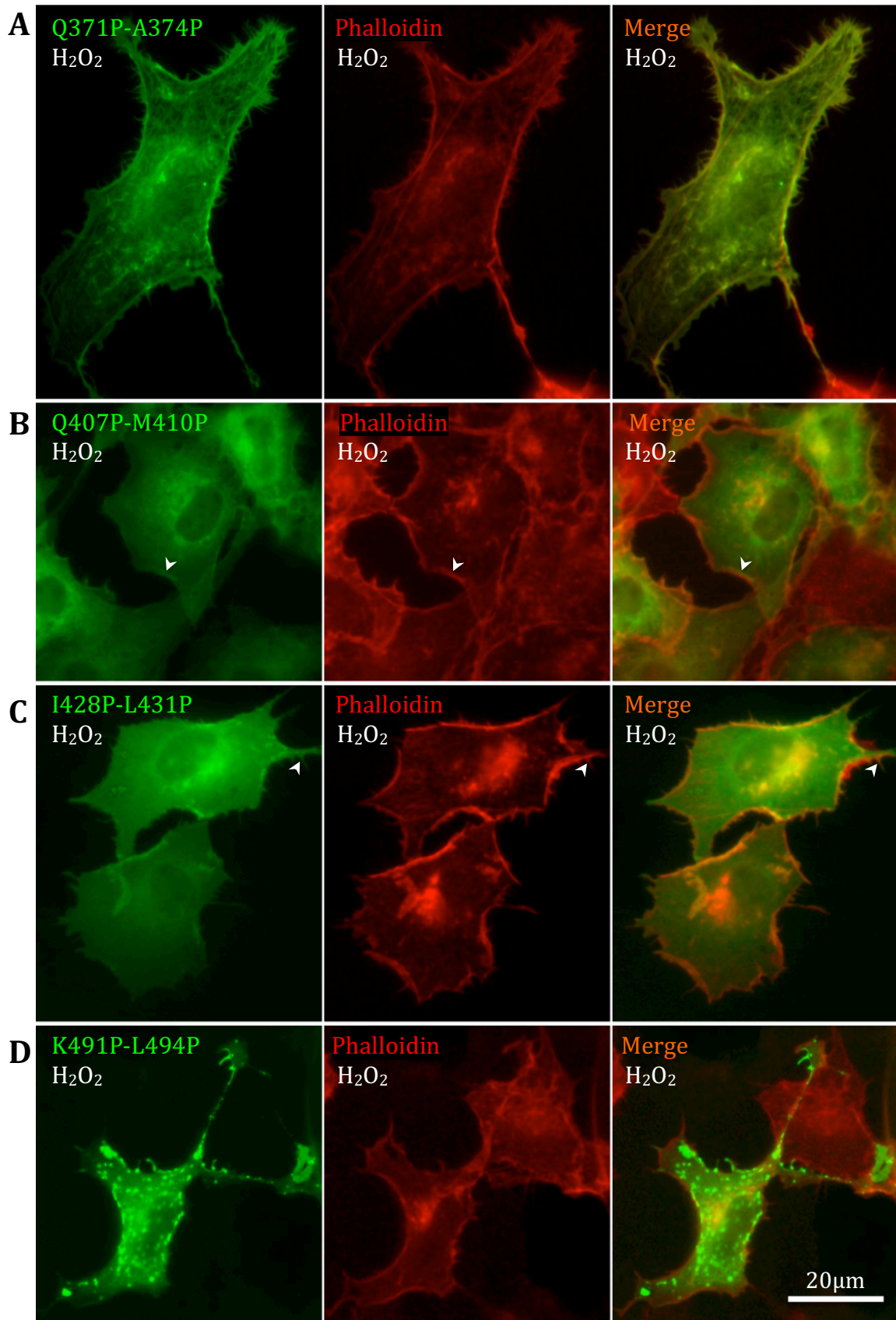


Fig. 4.8.3

Fig. 4.8.3 Proline mutants that exhibited a diffuse localisation in the cytoplasm react differently to H₂O₂-mediated protein modifications

(A) GFP-tagged Q371P-A374P colocalised with F-actin in 100% of the transfected cells. Q407P-M410P **(B)** and I428P-L431P **(C)** were diffuse in the cytoplasm and only rarely overlapped with F-actin. K491P-L494P **(D)** formed granules in 81% of the transfected cells that seemed to localise alongside F-actin.

4.6 Summary of main finding

- **Disruption of the coiled coil domain results in conformational change and colocalisation of some proline mutants with F-actin**
- **Truncation mutants containing amino acids 537 to 590 of DEF6 are sufficient to label F-actin**
- **F-actin colocalisation of DEF6 is dependent on the coiled coil domain suggesting that oligomerisation is required for F-actin binding**
- **Coiled coil-mediated aggregation prevents DEF6 from colocalising with F-actin**
- **Wild type and mutant DEF6 proteins react differentially to H₂O₂ - mediated protein modifications**

Chapter 5

DEF6 function in T cells

5.1 GEFs and F-actin are important for immunological synapse formation and function

T cell activation starts when T cell receptor (TCR) binds to major histocompatibility complex proteins (MHCs) of antigen presenting cells (APCs). This interaction initiates immunological synapse (IS) formation at the junction between T cells and APCs and triggers a series of reactions, such as TCR ζ chain phosphorylation and ZAP70 activation. Initiation of IS formation is accompanied by F-actin polymerisation which is an essential step and either enhanced or reduced F-actin stability disrupts this reaction. Therefore, balanced F-actin polymerisation is crucial for IS formation (Billadeau *et al.*, 2007; Alarcón *et al.*, 2011; Yu *et al.*, 2013). Once formed, the IS exhibits a spatial segmented supermolecular organisation, and has diverse patterns in different immune cell types (Davis and Dustin, 2004). As described in Chapter 1, upon TCR activation, DEF6 localised into IS in CD4 T cells (Bécart *et al.*, 2008 and Gupta *et al.*, 2004b). In CD4 T cells, supermolecular segregation results in a “bull’s eye” pattern with three distinct concentric domains that have been termed as supramolecular activation clusters (SMAC) (Fig. 5.1.0). The central domain (cSMAC) is characterised by abundance of TCRs and bound MHCs. cSMAC is directly surrounded by a ring structure that has been named peripheral SMAC (pSMAC). LFA-1 is concentrated in this domain where it binds to ICAM-1 expressed by APCs. The outer layer of the synapse is a ring domain called distal SMAC (dSMAC), which is full of F-actin (Fig. 5.1.0 B and C). IS formation is a dynamic process resulting in this asymmetric distribution of TCRs and F-actin. Once IS has started to form, TCR gradually concentrates in the center of the synapse, in contrast, actin distributes to a ring that surrounds the TCR center (Yu *et al.*,

2013).

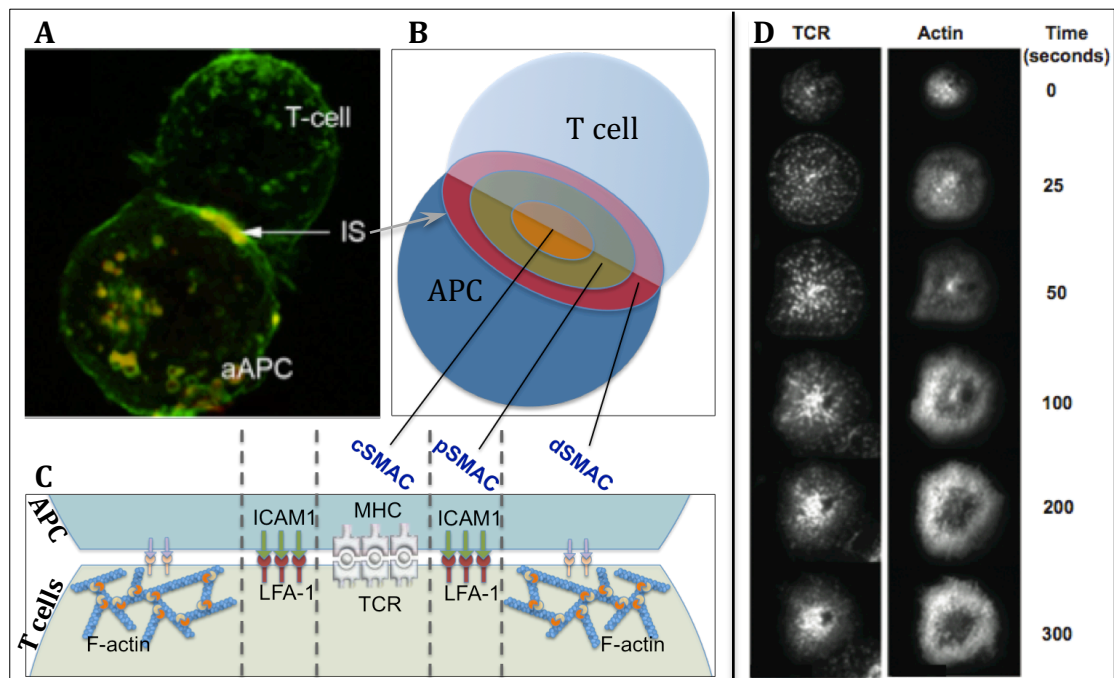


Fig. 5.1.0 Immunological synapse (IS) and its “bull’s eye” pattern

(A) IS formation at the junction of T cell and APC as indicated (Biggs *et al.*, 2011).

(B) and **(C)** Schematic representation of IS “bull’s eye” concentric domain pattern. The centre is termed central supramolecular activation cluster (cSMAC) with abundant TCRs and their bound MHCs. Next to the cSMAC is the peripheral SMAC (pSMAC) with LFA-1 and its bound ICAM1. The distal domain (dSMAC) is characterised by the abundance of F-actin.

(D) Dynamic of IS formation. TCRs gradually concentrate in the cSMAC while F-actin forms a ring structure in the dSMAC (Yu *et al.*, 2013).

F-actin plays multiple roles in IS formation and function. It provides a scaffold that stabilises the IS, and the F-actin ring in dSMAC seals the contact between two cells, which prevents leaking of cytokines during their transport between T and antigen presenting cells (Yu *et al.*, 2013). In addition, the dynamics of F-actin produces power to spatially segregate various molecules in the IS crucial for immune functions (Hartman *et al.*, 2009; Yu *et al.*, 2010 and Yu *et al.*, 2013). Finally, F-actin is also directly involved in the passage of T cell signalling, such as integrin activation (Kinashi, 2005).

F-actin dynamics are controlled by Rho GTPases that in turn are activated through GEFs. In T cells the vav family have been extensively analysed and are believed to be the main GEFs downstream of TCR-mediated signalling (Tybulewicz 2005). However, DEF6 is also recruited to the IS and functions as a GEF for Rho GTPases and lack of DEF6 results in impaired T cell function and autoimmunity (Gupta *et al.*, 2003b; Bécart *et al.*, 2008; Fanzo *et al.*, 2006). To further characterise DEF6 function in T cells, GFP-tagged WT and selected mutants were expressed in Jurkat T cells to determine their localisation before and after IS formation mediated through conjugation with APCs (Raji B cell preloaded with staphylococcal enterotoxin A/B).

5.2 WT DEF6, L533P-A536P, All-10 and Δ 0-216-All-10 labelled F-actin in Jurkat T cells.

In resting Jurkat cells, GFP on its own was present throughout the cells without any specific localisation (Fig. 5.2.1). In contrast, GFP-tagged WT DEF6 was mainly localised in lamellipodia- and filopodia-like cell protrusions, overlapping with F-actin. This is consistent with the report from Hey (2011, PhD thesis) that DEF6 localised in cell membrane of Jurkat cells, and might suggest that DEF6 exhibits GEF activity in resting cells independent of TCR-mediated activation. It seems therefore that DEF6 can be modified in resting T cells by mechanisms other than LCK phosphorylation (Bécart *et al.*, 2008 and Gupta *et al.*, 2004b) to liberate its GEF activity suggesting DEF6 plays multiple roles in T cells. However, while endogenous DEF6 can form granules (Remon, PhD thesis 2017) overexpressed DEF6 did not exhibit detectable granule formation (Fig. 5.2.1).

To test whether DEF6 mutants that spontaneously colocalised with F-actin in COS7 cells would also do so in Jurkat cells, GFP-tagged L533P-A536P, All-10 and Δ 0-216-All-10 were selected. As shown in Fig. 5.2.2, all three mutant proteins exhibited similar cellular distribution as overexpressed WT DEF6, colocalising with F-actin in cell protrusions in resting Jurkat cells.

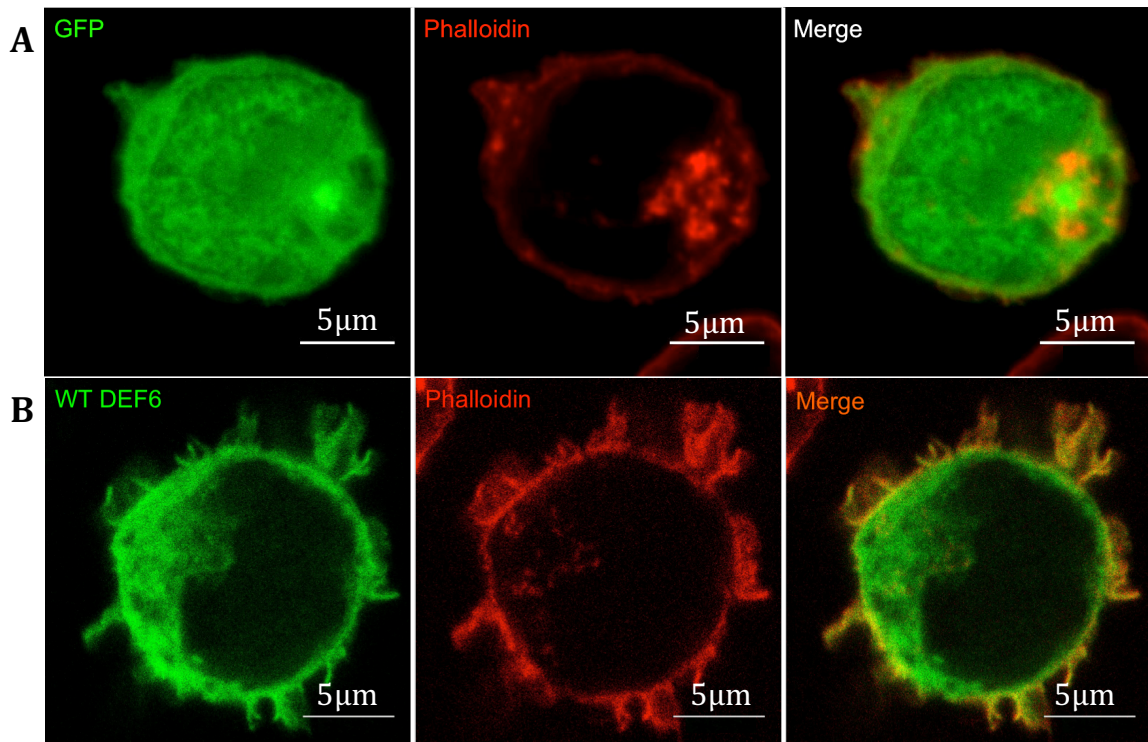


Fig. 5.2.1 GFP-tagged wild type DEF6 colocalises with F-actin in resting Jurkat T cells

While GFP alone (A) was diffused throughout the cells (as seen in COS7 cells), GFP-tagged WT DEF6 (B) localised to the cell membrane and protrusions colocalising with F-actin that was stained with phalloidin (red).

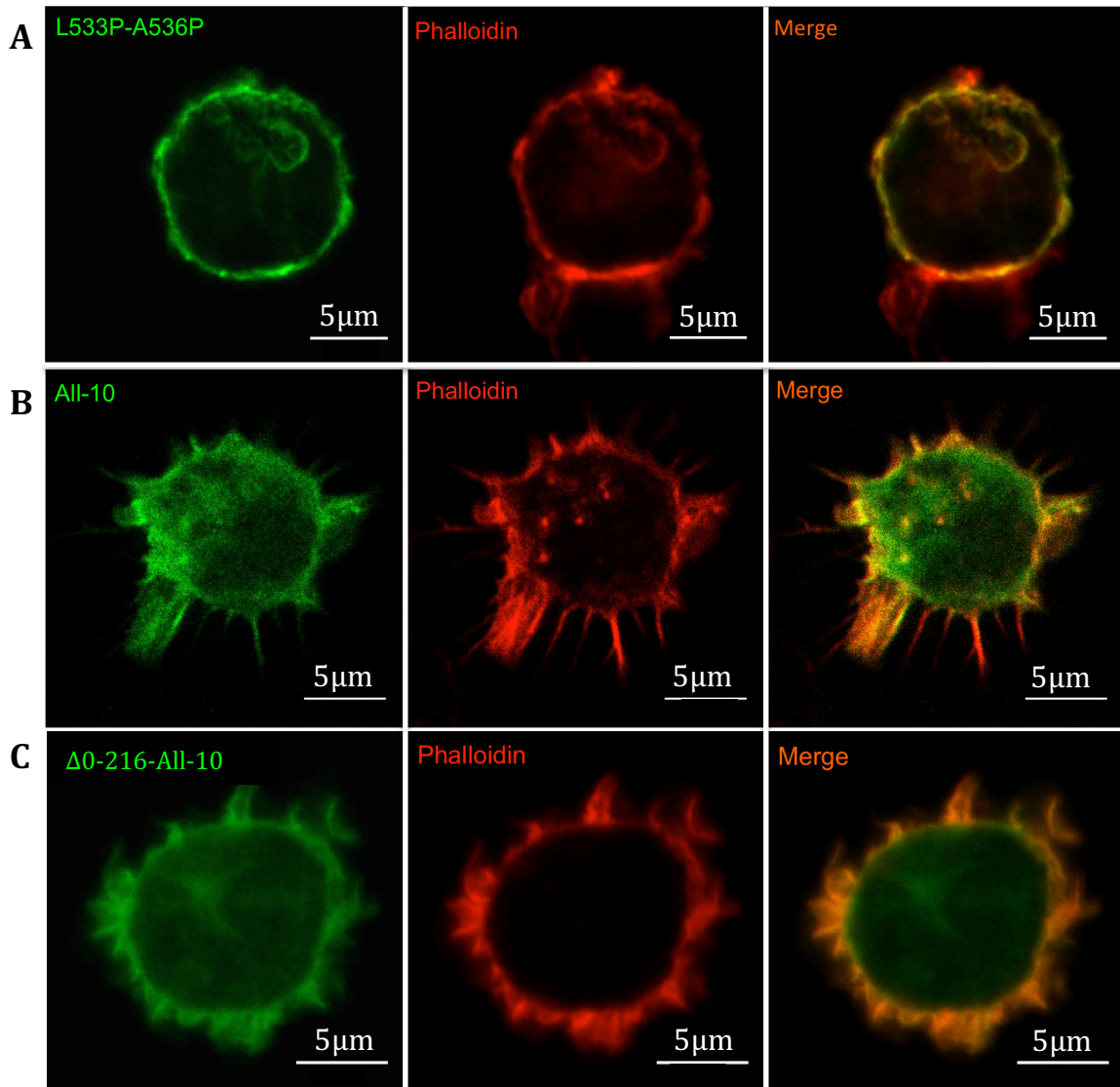


Fig. 5.2.2 GFP-tagged DEF6 mutants L533P-A536P, All-10 and Δ0-216-All-10 colocalised with F-actin in resting Jurkat T cells
GFP-tagged L533P-A536P (A), All-10 (B) and Δ0-216-All-10 (C) colocalised with phalloidin stained F-actin (red) in cell membrane and protrusions.

5.3 $\Delta 0$ -104, $\Delta 0$ -216, DH2 and Y133/144D exhibited diverse phenotypes in Jurkat T cells.

GFP-tagged DEF6 N-terminal truncated mutants $\Delta 0$ -104, $\Delta 0$ -216, the LCK phosphomimic mutant, Y133D/Y144D and DH2 formed aggregates in COS7 cells (Fig. 3.7.1 and Fig. 3.17.0). However, in Jurkat T cells, they exhibited more diverse phenotypes. As for $\Delta 0$ -104, only less than 2% of transfected cells (Appendix 8.4, Fig. 8.9.0) clearly contained aggregates whereas most cells exhibited colocalisation of $\Delta 0$ -104 with F-actin in cell protrusions. $\Delta 0$ -216 expressing cells did not exhibit any aggregates. Instead, $\Delta 0$ -216 localisation was more diffuse in the cytoplasm and weakly localised in cells protrusions overlapping with F-actin (Fig. 5.2.3). DH2 formed vesicular-like aggregates in about 60% of the transfected Jurkat cells that looked similar in morphology to those observed in COS7 cells. In about 40% Jurkat cells, DH2 was localised throughout the cytoplasm including cell protrusions overlapping with F-actin (Fig. 5.2.3). Occasionally, both DH2 phenotypes were observed in single cells. DEF6 mutant Y133D/Y144D that mimic LCK phosphorylation had been previously reported to translocate to immunological synapse (Bécart *et al.*, 2008). However, this mutant was barely detectable in Jurkat cells suggesting toxicity when overexpressed. The image shown in Fig. 5.2.4 was the only case detected showing Y133D/Y144D aggregates similar to its behaviour in COS7 cells.

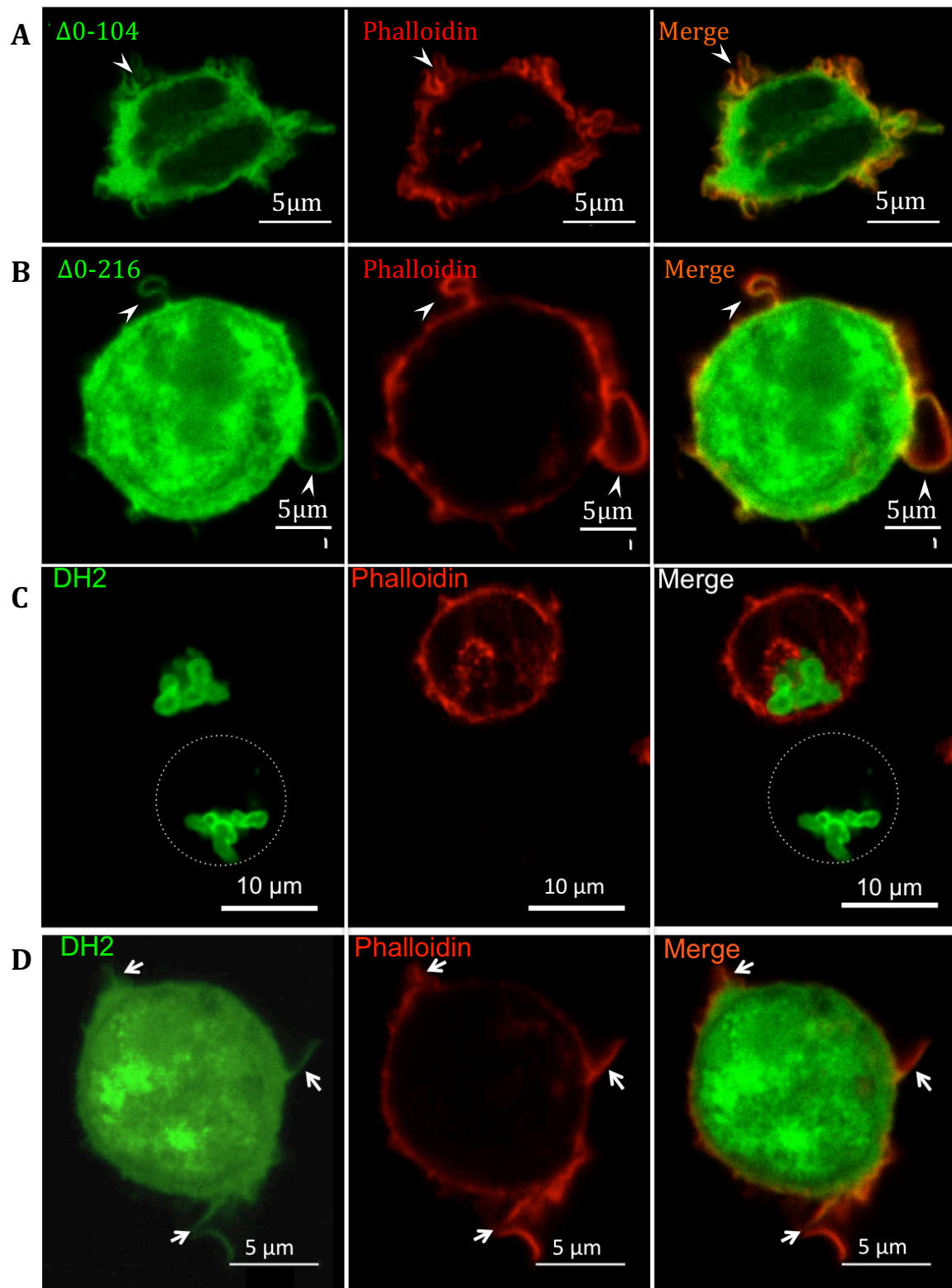


Fig. 5.2.3

Fig. 5.2.3 Cellular localisation of GFP-tagged $\Delta 0$ -104, $\Delta 0$ -216 and DH2 mutants in resting Jurkat T cells

The N-terminal truncation mutant $\Delta 0$ -104 **(A)** clearly overlapped with F-actin in cells protrusions and only rarely (2% of transfected cells) contained granules which is strikingly different from its phenotype in COS7 cells. $\Delta 0$ -216 **(B)** was diffuse in the cytoplasm and overlapped with F-actin. DH2 **(C)** formed vesicle-like aggregates in 60% of transfected cells like in COS7. In ~40% of the cells, DH2 **(D)** was diffuse and weakly overlapped with F-actin in cell protrusions.

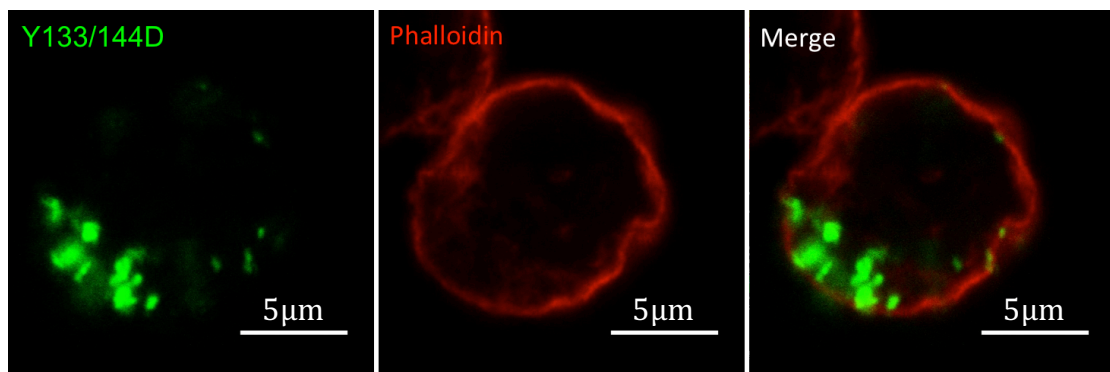


Fig. 5.2.4 GFP-tagged Y133D/Y144D formed aggregates in Jurkat T cells

Due to very low transfection efficiency that might suggest toxicity of Y133D/Y144D in Jurkat T cells, only a single transfected cell was detected that exhibited aggregation of Y133D/Y144D mutant protein.

5.4 The ITK phosphomimic mutant Y210E/Y222E formed granules co-localising with P-bodies but also appeared diffuse overlapping with F-actin.

As previously shown, ITK phosphomimic mutant Y210E/Y222E spontaneously aggregates and colocalises with P-bodies (Hey *et al*; 2012; Mollett; 2014, PhD thesis; Alsayegh, in preparation; Fig. 3.14.0). However, in about half of the transfected Jurkat cells, Y210E/Y222E was also diffuse overlapping with F-actin in cell protrusions (Fig. 5.2.5).

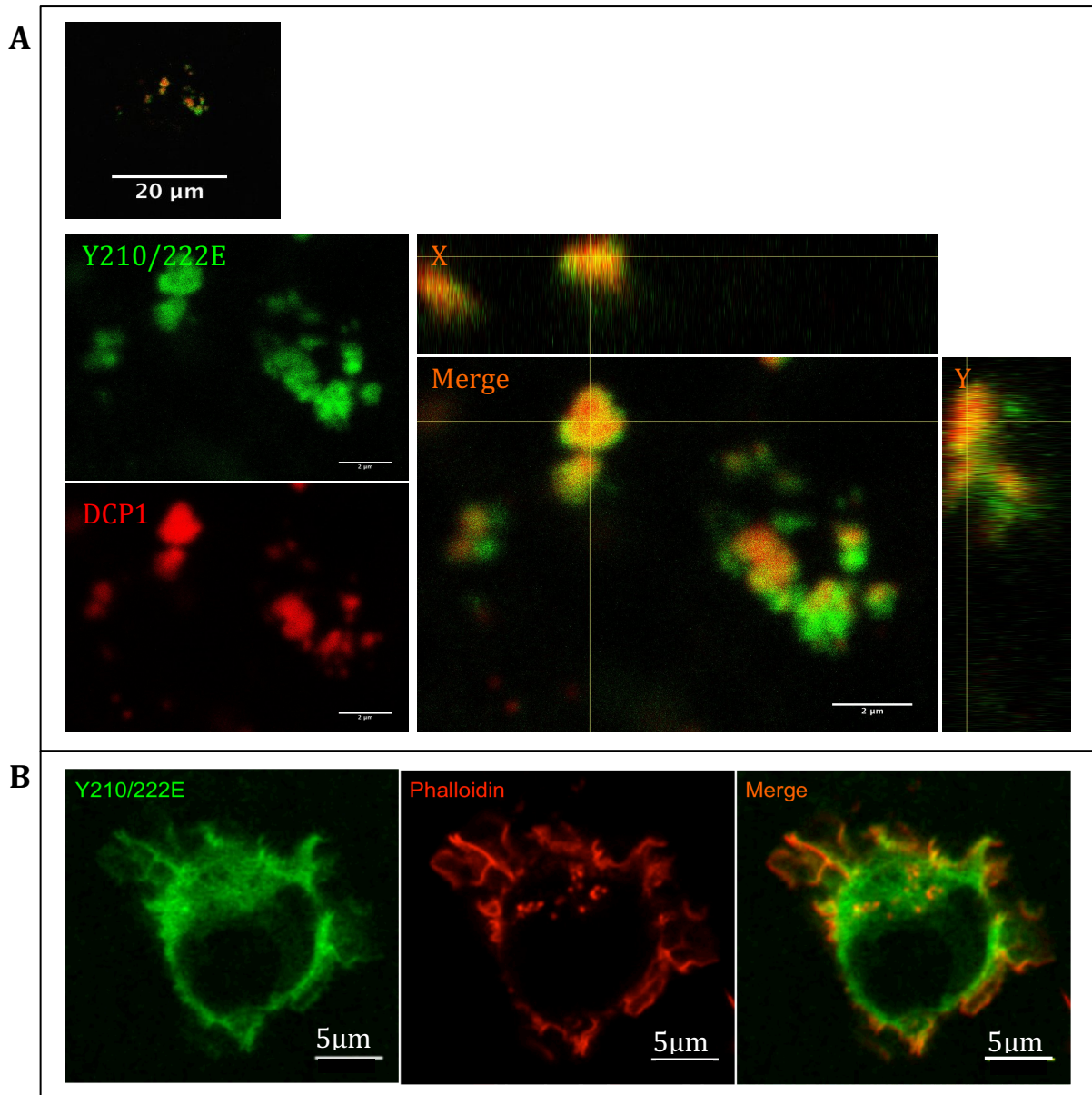


Fig. 5.2.5 ITK phosphomimic mutant Y2210E/Y222E colocalises with DCP1 but also colocalised with F-actin in cell protrusions

(A) Confocal analysis of Jurkat cells cotransfected with GFP-tagged Y210E/Y222E and mCherry-tagged DCP1. Enlarged region in the merged images including vertical and side views indicate colocalisation of the two proteins.

(B) Diffuse localisation of Y210E/Y222E and overlap with F-actin in cell protrusions was observed in about 50% of transfected cells.

5.5 Upon TCR-mediated activation, WT DEF6 is recruited to the IS concentrating in cSMAC

Upon TCR stimulation, DEF6 relocates to the IS, possibly depending on: a) F-actin interactions, and b) interaction with Rap1 linking DEF6 to LFA-1 that binds ICAM (Gupta *et al.*, 2003b and Côte *et al.*, 2015). To further characterise recruitment and localisation of WT and mutant DEF6, Jurkat T cells were transfected and subsequently incubated with Raji B cells pre-loaded with enterotoxin A/B to trigger TCR-mediated activation and IS formation (Marrack and Kappler, 1990). Using confocal microscopy allowed detailed analysis of the IS by zooming up the vertical and side view (Z-stack imaging and then x and y side views). As shown in Fig. 5.3.1, F-actin localised mainly to the outer layer of the IS forming a ring structure and was less abundant in the center. This was consistent with the “bull’s eye” pattern of IS structure shown in Figure 5.1.0. GFP as negative control was diffuse and did not exhibit any specific localisation (Fig. 5.3.1). In contrast, GFP-tagged WT DEF6 was clearly recruited to the IS as expected. From the side view, it is apparent that DEF6 is overlapping with F-actin in the outer layer, but it is much more concentrated in cSMAC, where F-actin is less abundant (Fig. 5.3.1). This result is consistent with previous data by Singleton *et al* (2011) as well as with unpublished data by fellow PhD students Alsayegh and Akdeniz who showed that endogenous DEF6 is also more concentrated in the center of IS.

5.6 All-10, Δ 0-216-All-10, L533P-A536P, DH2 and Δ 0-216 mutants translocate to the IS but don't concentrate in cSMAC

As shown above (Fig. 5.2.1 and -2), All-10, Δ 0-216-All-10 and L533P-A536P mutants localised in cell protrusion and overlapping with F-actin in resting Jurkat T cells similar to WT DEF6. Strikingly, all three mutants translocated to the IS, however, unlike WT DEF6, they did not concentrate in the cSMAC but overlapped with F-actin in the outer ring (Fig. 5.3.2). While All-10, Δ 0-216-All-10 were essentially absent from the cSMAC, L533P-A536P was also present here (Fig. 5.3.2). Interestingly, in the presence of L533P-A536P, F-actin did not exhibit the “bull’s eye” character but was also abundant in cSMAC (Fig. 5.3.2). This data is however preliminary and needs confirmation.

DH2 and Δ 0-216 were also recruited to the synapse and localised to the outer ring overlapping with F-actin (Fig. 5.3.3). Although DH2 also still formed aggregates, it is rather striking that some mutant DH2 protein was recruited to the IS suggesting that during T cell activation the vesicle-like structures formed by DH2 (Fig. 5.2.3) can be disrupted presumably through phosphorylation or other protein modifications.

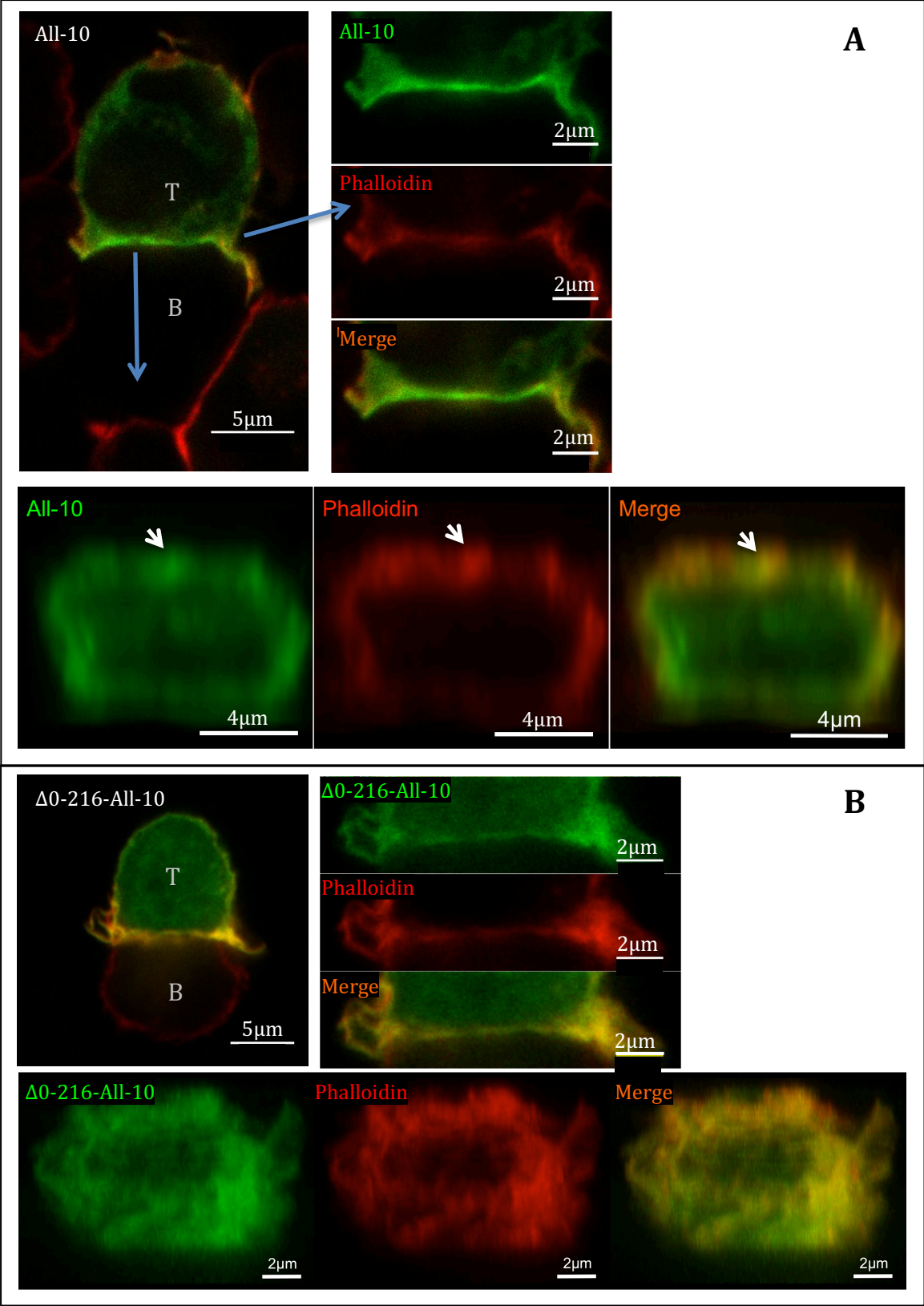


Fig. 5.3.2

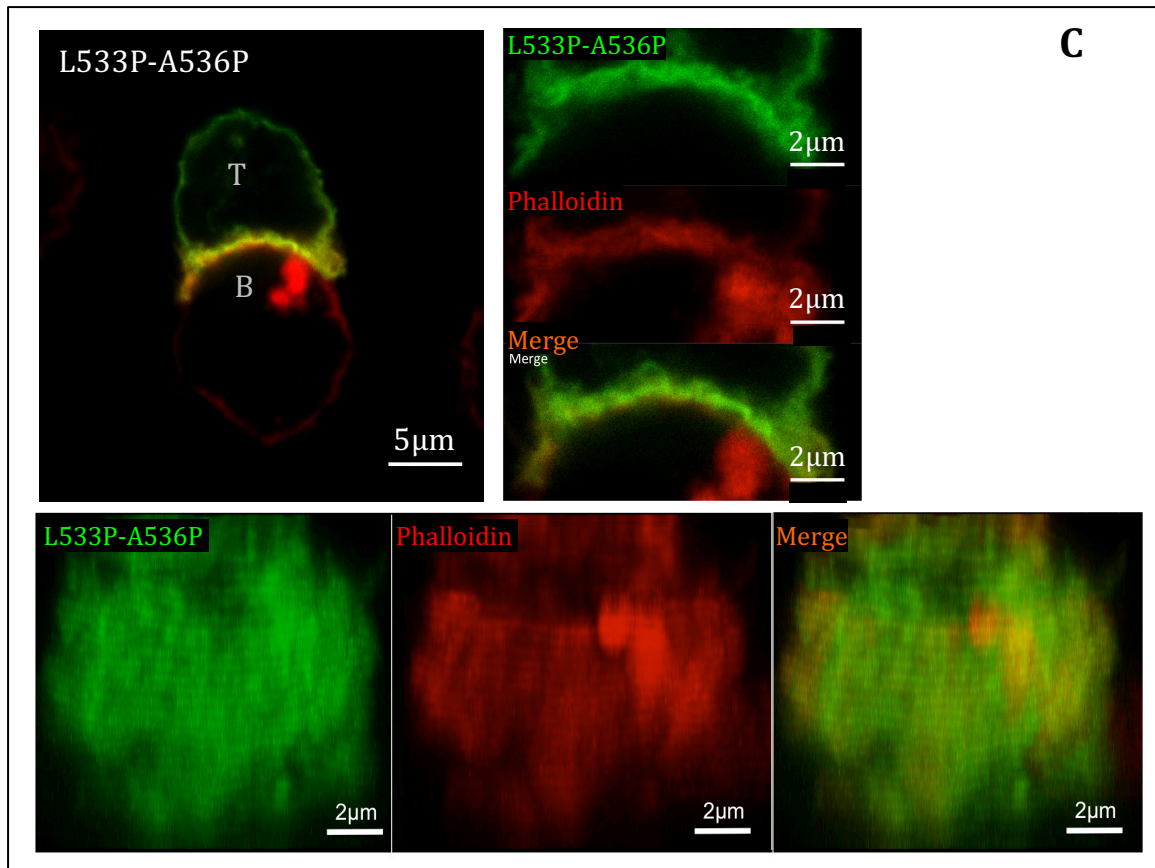


Fig. 5.3.2 Selected DEF6 mutants are recruited to the IS but their localisation is distinct from WT DEF6

Proline mutants All-10 (A), the N-terminal truncated proline mutant Δ 0-216-All-10 (B) and L533P-A536P (C) were recruited to the IS. Confocal microscopy analysis revealed that All-10 and Δ 0-216-All-10 localised in the pSMAC overlapping with the F-actin ring. L533P-A536P localised in both pSMAC and cSMAC altering F-actin localisation that was also present in cSMAC.

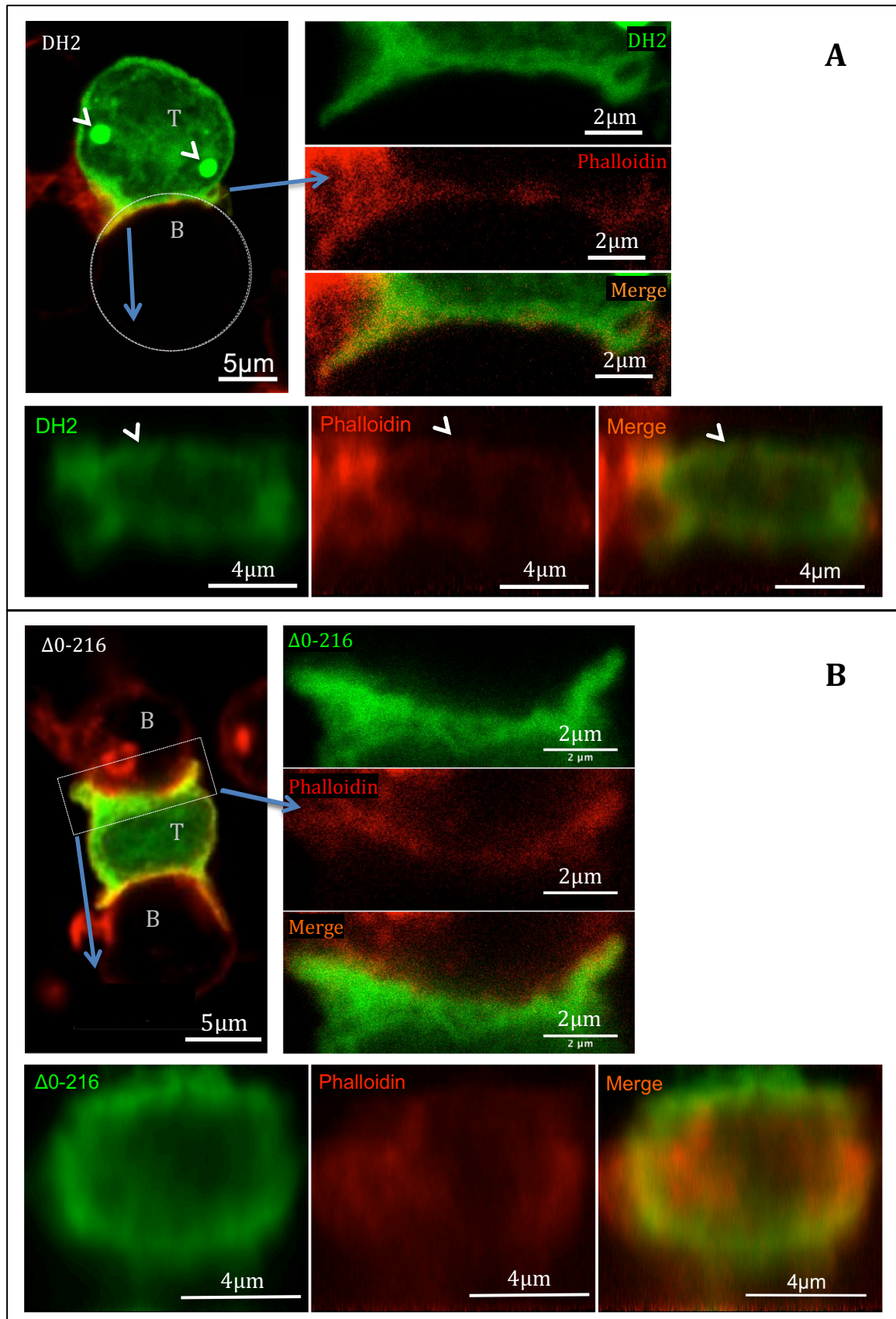


Fig. 5.3.3 DEF6 mutants DH2 and $\Delta 0-216$ are recruited to the IS but their localisation is distinct from WT DEF6

DH2 **(A)** and $\Delta 0-216$ **(B)** were recruited to the IS localising in the pSMAC. In addition, the vesicular-like aggregations of DH2 were still present. (The aggregates are over exposure to highlight IS translocation.)

5.7 WT DEF6 seems to be recruited to the IS through cell protrusion ruffling

Previous research (Ritter *et al.*, 2015) indicated that the interactions between B and T cell protrusions initiate conjugation and IS formation. Given that WT DEF6 was observed in cell protrusions in resting Jurkat cells, live cells imaging was applied to see whether DEF6 is recruited to the IS through cell protrusion ruffling. As shown in Fig. 5.4.0, GFP-tagged WT DEF6 localised in protrusions with ruffling but upon interaction between Jurkat cell protrusions and Raji B cells the IS is formed in seconds translocating DEF6 rapidly to the junction. It seems therefore that DEF6 is indeed translocated to the IS with the movement of cell protrusions.

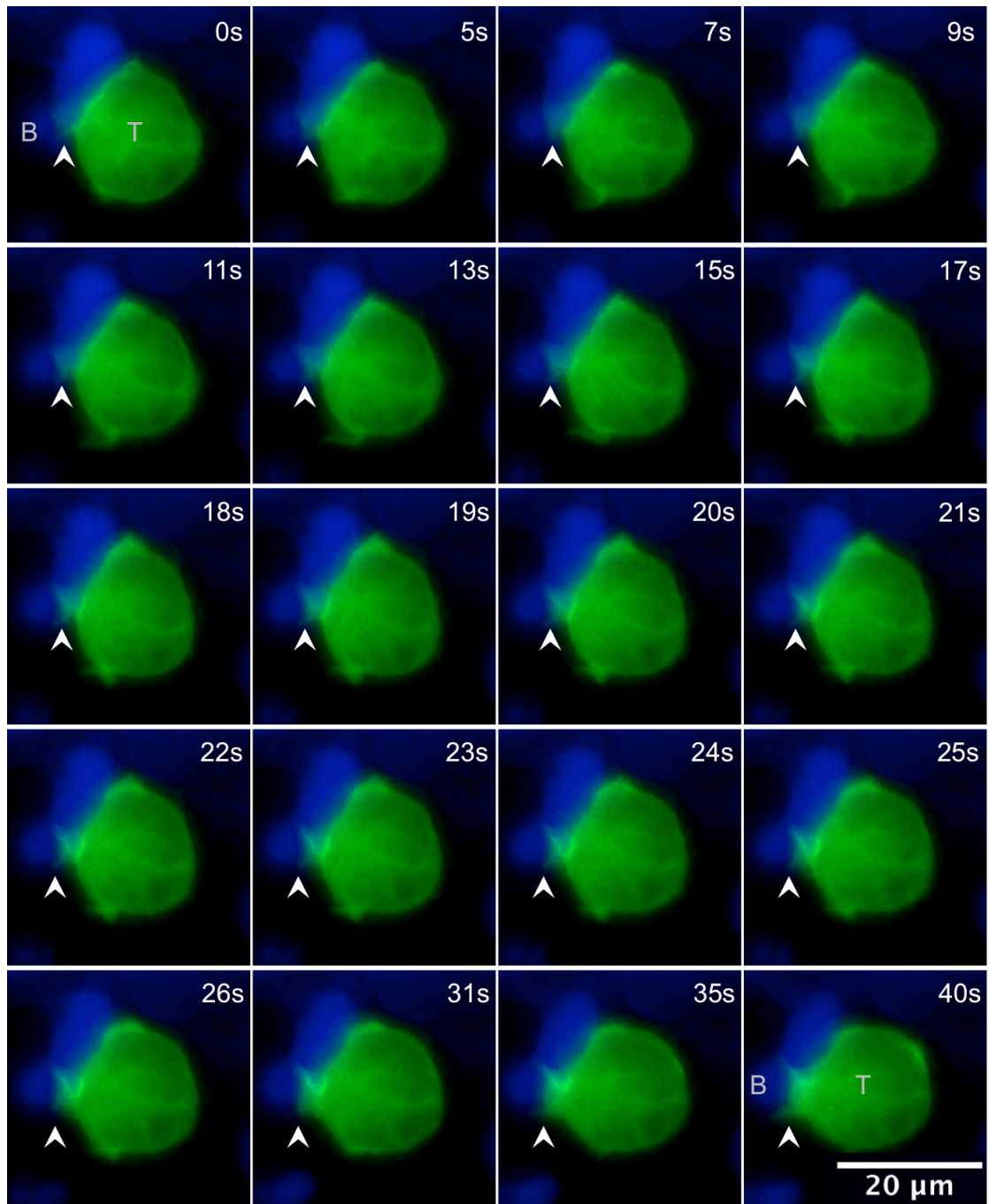


Fig. 5.4.0 Dynamic of WT DEF6 in Jurkat T cells forming conjugations with Raji B cells

Time lapse analysis of IS formation from 0 to 40 secs as indicated. GFP-tagged DEF6 localised in cell membrane and protrusions that seem to sense Raji B cells (arrow head) and subsequently, DEF6 is recruited to the synapse in seconds. Raji B cells are stained with Calcein Blue.

5.8 Spontaneous granule formation and colocalisation of Y210E/Y222E with P-bodies in resting T cells seems reversed in activated T cells

As shown in Fig. 5.2.5, the ITK phosphomimic mutant Y210E/Y222E formed spontaneous granules that colocalised with P-bodies in about 50% of the transfected Jurkat cells. However, after conjugation with Raji B cells, Y210E/Y222E was diffuse in activated Jurkat T cells and no granule formation was detected despite the presence of P-bodies (Fig.5-5-0). Given that Y210E/Y222E did not form granules in all of the transfected cells, this observation could be due to chance. However, if further experiments would confirm the result shown in Figure 5.5.0, then it might imply a link between T cells activation and DEF6 function in RNA metabolism.

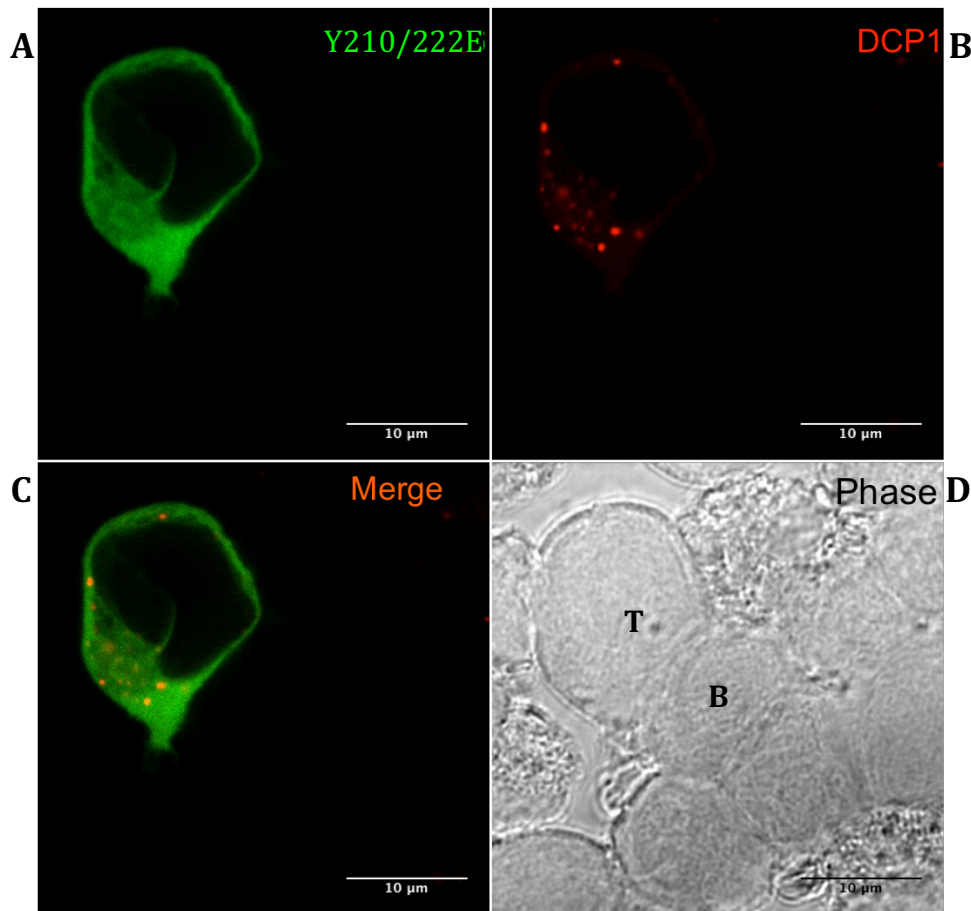


Fig. 5.5.0 Spontaneous granule formation and colocalisation with P-bodies of Y210E/Y222E in resting Jurkat T cells is reversed upon activation

Cotransfection of Jurkat T cells with GFP-tagged Y210E/Y222E and mCherry-tagged DCP1 conjugated with Raji B cells. While mCherry-tagged DCP1 exhibited its typical localisation for P-bodies **(B)**, GFP-tagged Y210E/Y222E was diffuse in the cytoplasm **(A)** not colocalising with DCP1 **(C)**. This would suggest that T cell activation results in conformational change of GFP-tagged Y210E/Y222E preventing granule formation and colocalisation with P-bodies. **(D)** Phase image showing T and B cell conjugation as indicated.

5.9 Summary of main finding

- In resting Jurkat T cells, GFP-tagged wild type DEF6 localised in cell membrane and protrusions overlapping with F-actin.
- N-terminal truncation mutants that formed aggregates in COS7 cells localised in cell membrane and protrusions in resting Jurkat T cells overlapping with F-actin.
- DH2 formed vesicle-like aggregates in resting Jurkat T cells but upon activation was mainly diffuse in the cytoplasm including the IS.
- Low transfection efficiency of the LCK phosphomimic mutant Y133/144D suggests toxicity in Jurkat cells.
- In resting Jurkat cells, ITK phosphomimic mutant Y210/222E formed granules that colocalised with P-bodies but equally appeared diffuse labelling F-actin in cell protrusions. Upon activation, Y210/222E was diffuse no longer colocalising with P-bodies.
- Upon TCR-mediated activation, wild type DEF6 was recruited to the IS concentrating in the cSMAC. A feature that was distinct from some proline mutants that were also recruited to the IS but exhibited a different localisation within the IS.
- Wild type DEF6 seems to translocate to the IS within cell protrusions contacting the APC.

Chapter 6

Discussion

6.1 Coiled coil-mediated aggregation

PairCoil2 analysis predicted a coiled coil domain in the glutamine (Q)-rich C-terminal part of DEF6 (between amino acids 330 and 550; Hey *et al.*, 2012; Figures 3.1.2 and 3.2.2). Q or hydrophobic amino acids occur frequently at the “*a*” and “*d*” position of the heptad repeats (*a-g*) of the predicted coiled coil region. Coiled coil domains can interact with other coiled coil domains resulting in right-handed supercoil structures that contain two to seven coiled coil domains (Liu *et al.*, 2006).

Given that wild type DEF6 tagged with GFP and overexpressed in COS7 cells localised diffuse in the cytoplasm, it is likely that the conformation of DEF6 is such that the coiled coil domain is masked to control its ability to interact with other coiled coil domains. However, several mutant versions of DEF6 (e.g. DH2, Y133/144D, Δ 104, Δ 216) formed aggregates in COS7 cells suggesting a conformational change unmasking the coiled coil domain. Some aggregates formed large structures that in the extreme were vesicle-like (mutant DH2; Figure 3.8.0). It seems therefore that the coiled coil domain of DEF6 can interact with itself and if uncontrolled, this interaction results in large aggregates. Cotransfection of mutant Y133/144D with either DH2, Δ 104 or Δ 216 confirmed this interpretation: aggregates formed were completely overlapping indicating that DEF6 molecules can interact with each other via the coiled coil domain (Figures 3.15.0).

6.2 Coiled coil-mediated interaction of wild type DEF6

To test whether wild type DEF6 molecules can also interact with each other, mCherry-NLS-DEF6 was cotransfected with GFP-tagged DEF6. Insertion of the NLS into mCherry-tagged wild type DEF6 resulted in nuclear localisation (see 3.9). As shown in Figure 3.12.0, some GFP-tagged DEF6 was colocalising with mCherry-NLS-DEF6 in the nucleus indicating that also wild type DEF6 molecules can interact with each other. This interaction is likely mediated through the coiled coil domain because mutant DEF6 proteins were either also dragged into the nucleus when cotransfected with mCherry-NLS-DEF6 (N590; DH1; Figure 3.12.0), or mCherry-NLS-DEF6 was retained in the cytoplasm (DH2; Y210/222E; Figure 3.12.0). In addition, proline mutants (e.g. All-10 disrupting the coiled coil domain did not interact with mCherry-NLS-DEF6 (Figure 3.13.0) indicating that the interactions observed are indeed coiled coil-mediated.

It seems therefore that unmasking of the coiled coil domain through conformational change facilitates interactions of DEF6 molecules that either result in 'controlled' dimer or oligomer formation or when 'uncontrolled' in aggregates that can assemble to large structures within the cytoplasm.

6.3 Coiled coil-mediated trapping or enforced conformational change

The experiments described above also showed that mutant DEF6 proteins forming coiled coil-mediated aggregates (DH2; Y210/222E) can alter the behaviour of wild type DEF6 that now also formed aggregates colocalising with the mutant protein (Figure 3.12.0). Either the coiled coil domains of the mutant

proteins in the aggregates are able to interact with the coiled coil domain of wild type DEF6 trapping it in the aggregates or the mutant protein enforced a conformational change that resulted in aggregation of the wild type protein. The latter interpretation would mean that mutant DEF6 can act prion-like, a notion that is supported by the finding that Y133/144D mutant that spontaneously aggregates can trigger aggregations of other proteins (537-590 and 537-550) that on their own do not aggregate (Figure 4.6.0). However, some aggregates formed by mutant proteins trapped mCherry-tagged DCP1 that no longer exhibited its normal cytoplasmic distribution when cotransfected (e.g. DH2 and Δ 216; Figure 3.8.0; Y133/144D; Figure 3.14.0). DCP1 does not contain a coiled coil domain but many P-body components do and it remains to be seen whether DCP1 on its own was trapped by the aggregates or whether localisation of entire P-bodies was altered.

6.4 The coiled coil domain is dispensable for both granule formation and P-body localisation

To test whether the coiled coil domain is required for granule formation and P-body localisation proline residues were introduced in highly conserved *a/d* positions of the heptad repeats to disrupt the coiled coil domain (Figure 3.2.2). Proline mutants did not form granules under cellular stress conditions (Figure 3.4.0) but introduction of Y210/222E into proline mutants resulted in spontaneous granule formation colocalising with DCP1 (Figure 3.5.0). This suggested that the coiled coil domain is dispensable for both granule formation and P-body localisation.

6.5 The N-terminal 45 amino acids of DEF6 are sufficient for spontaneous P-bodies colocalisation

Hey *et al.* (2012) demonstrated that tyrosine (Y) residues 210 and 222 of DEF6 are phosphorylated by ITK in Jurkat T cells and that phosphomimic mutant Y210/222E spontaneously formed cytoplasmic granules that colocalised with P-body marker DCP1. In addition, they showed that treatment of COS7 cells expressing GFP-tagged wild type DEF6 with sodium arsenate resulted in the formation of DEF6 granules colocalising with DCP1. Although COS7 cells do not express ITK, these data suggested that arsenate treatment resulted in modification of DEF6 (perhaps through phosphorylation by an unknown kinase) causing a conformational change that unmasked a region within DEF6 mediating P-body colocalisation. Several C-terminal truncation mutants were generated and tested whether they colocalise with DCP1 when coexpressed in COS7 cells. As shown in Figures 3.6.0 and 3.6.1, several C-terminal truncated mutants fused to GFP spontaneously formed cytoplasmic granules that colocalised with DCP1 in COS7 cells. Indeed, the N-terminal 45 amino acids were sufficient to target P-bodies whereas localisation of N-terminal 30 amino acids fused to GFP was diffuse in the cytoplasm (N-45; N-30; Figures 3.6.0; 3.6.1). The N-terminal end of DEF6 contains two Ca²⁺-binding EF hand motifs (Fos *et al.*, 2014) that are both present in N-45 but only one is left in N-30 and it is not known whether Ca²⁺-binding is required for P-body colocalisation. This observation suggests that phosphorylation of Y210 and 222 results in conformational change liberating the N-terminal end and P-body colocalisation.

6.6 ITAM, PH and/or coiled coil domains facilitate cellular stress-induced P-body colocalisation

While the N-terminal 45 amino acids are sufficient, the first 104 amino acids are not required for P-body colocalisation. $\Delta 0-104$ lacking the first 104 amino acids but containing ITAM, PH and the coiled coil domain (Figure 3.7.1a), formed coiled coil-mediated aggregates that trapped DCP1 in untreated COS7 cells (3.8.0), but formed granules that completely overlapped with DCP1 in arsenate or nocodazole treated cells (Figure 3.10.3) indicating that stress induced modifications of $\Delta 0-104$ results in conformational change unmasking parts of DEF6 within ITAM, PH and/or coiled coil domains that facilitates P-body colocalisation. However, neither domain on its own colocalised with P-bodies. ITAM and PH1 localised diffuse in the cytoplasm and nucleus and DH2 containing the coiled coil domain formed aggregates (Figure 3.7.2b) suggesting that the stress-induced conformation of $\Delta 0-104$ is required for P-body localisation. Indeed, introduction of Y210/222E into $\Delta 0-104$ did not change aggregate formation in untreated cells but prevented complete overlap with DCP1 in stressed cells (Figure 3.11.2). This might suggest that ITK phosphomimic mutant in the context of the N-terminal truncation mutant $\Delta 0-104$ 'fixed' its conformation preventing stress-induced modifications. Overall, these results suggest that ITAM, PH and coiled coil can cooperate in a stress-induced conformation that facilitates P-body localisation independent of the N-terminal end.

6.7 Both, N-terminal end and the coiled coil domain are mediating dimerisation and/ or oligomerisation of DEF6

As discussed above (6.2), controlled unmasking of the coiled coil domain facilitates dimerisation and/or oligomerisation of wild type DEF6. Coexpression of GFP-tagged N-108 with mCherry-NLS-DEF6 revealed that N-108 retained some mCherry-NLS-DEF6 in the cytoplasm indicating that the N-terminal 108 amino acids interact with wild type DEF6 (Figure 3.12.1). Similarly, Y210/222E that colocalises with DCP1 also retained some mCherry-NLS-DEF6 in the cytoplasm when coexpressed (Figure 3.12.0) suggesting that DEF6 dimerisation and/or oligomerisation can occur in P-bodies.

6.8 F-actin labelling of DEF6 is regulated through the coiled coil domain

GFP-tagged wild type DEF6 is localised diffuse in the cytoplasm of COS7 cells not overlapping with F-actin indicating that its GEF activity is masked. Treatment of transfected cells with H₂O₂ that triggers PI3K activity resulted in DEF6 translocation to lamellipodia, filopodia and stress fibres colocalising with F-actin (Mavrakis *et al.*, 2004). Expression of proline mutants including the All-10 mutant revealed that disruption of the coiled coil domain could lead to colocalisation with F-actin in cell protrusions like lamellipodia and filopodia (Figure 4.4.0) suggesting that the coiled coil domain is controlling GEF activity of DEF6. However, amino acids 355 to 631 of DEF6 (DH1; Figure 4.5.0) containing the coiled coil domain exhibited a constitutive GEF activity (Mavrakis *et al.*, 2004) suggesting that unmasking of the coiled coil domain is required for GEF activity. However, mutant DEF6 proteins that formed coiled coil domain-

mediated aggregates never colocalised with F-actin (Figure 4.7.0) again emphasising the importance of controlled unmasking of the coiled coil domain.

6.9 Amino acids 537 to 590 of DEF6 are sufficient to label F-actin in cell protrusions

To further pinpoint the region that confers GEF activity, several mutant proteins containing parts of the C-terminal end of DEF6 were tested for their ability to colocalise with F-actin (Figure 4.5.0). GFP-tagged 537-590 overlapped with F-actin in 100% of the transfected cells while sub-regions 537-550 and 551-590 were still labelling F-actin but to a lesser extent than 537-590 (Figure 4.5.0). Amino acids 537-550 are the C-terminal end of the coiled coil domain and it is feasible that this part is still capable to facilitate dimerisation. To test this, mCherry-tagged Y133/144D was coexpressed with either GFP-tagged 537-590, 537-550 or 551-590. While 537-590 and 537-550 colocalised with Y133/144D aggregates, 551-590 did not (Figure 4.6.0) indicating that amino acids 537 to 550 can indeed still facilitate interaction with coiled coil-mediated aggregates. It is plausible therefore, that the C-terminal end of the coiled coil domain is required for GEF activity perhaps through the facilitation of dimer formation similar to SWAP70 (Chacón-Martinez *et al.*, 2013).

6.10 How is the GEF activity of DEF6 controlled?

H₂O₂ treatment induced GEF activity of GFP-tagged wild type DEF6 suggesting that PI3K signalling might trigger GEF activity (Mavrakis *et al.*, 2004). Indeed, inhibition of the PI3K signalling pathway with wortmannin almost completely abolished DEF6-mediated filopodia formation (Mavrakis *et al.*, 2004). PI3K

signalling is also indispensable for DEF6 to translocate to the IS (Gupta *et al.*, 2003b) as discussed later in more detail. PI3K signals through PIP3 and it was shown that the PH domain of DEF6 binds PIP3 (Gupta *et al.*, 2003b and Bécart *et al.*, 2008). Therefore, it is tempting to speculate that PIP3 binding results in a conformational change that liberates the coiled coil domain allowing dimerisation that in turn results in GEF activity.

6.11 Overexpressed DEF6 in resting Jurkat T cells localises in cell protrusions

As discussed above, localisation of GFP-tagged DEF6 in COS7 cells is diffuse in the cytoplasm not exhibiting any colocalisation with F-actin but its GEF activity can be induced through H₂O₂ treatment of the cells. Overexpression of GFP-tagged DEF6 in Jurkat T cells resulted in clear colocalisation of DEF6 with F-actin in lamellipodia and filopodia (Figure 5.2.1) suggesting GEF activity of DEF6 in resting Jurkat cells. Mutants All-10 and Δ 0-216-All-10 also colocalised with F-actin (Figure 5.2.2) indicating that neither the N-terminal EF-hands nor the ITAM motif and therefore LCK phosphorylation of Y133 and Y144 are required and suggests that the proline residues in 10 *a/d* positions so not interfere with dimer formation of DEF6. Δ 0-216-All10 contains the PH domain and could potentially bind PIP3 but it also contains Y222 that is phosphorylated by ITK.

6.12 ITK phosphomimic mutant Y210/222E colocalises with P-bodies and F-actin in resting Jurkat cells

Mutant Y210/222E spontaneously colocalised with p-bodies in COS7 cells. Similarly, Y210/222E colocalised with DCP1 in transfected Jurkat cells (Figure 5.2.5). However, it equally colocalised with F-actin (Figure 5.2.5) suggesting that

Y210/222E is shuttling between P-bodies and F-actin. In addition, upon TCR-mediated activation, Y210/222E neither formed granules nor was it colocalising with F-actin (Figure 5.5.0) perhaps indicating that modifications of Y210/222E or PIP3-binding determines its location and function.

6.13 LCK phosphomimic mutant Y133/144D forms aggregates in Jurkat T cells

Transfection of Jurkat cells with mCherry-tagged Y133/144D was very difficult despite the fact that COS7 cells could be readily transfected. This might suggest that expression of mCherry-tagged Y133/144D is toxic to Jurkat T cells but this was not further investigated. Nevertheless, a single transfected Jurkat cell was observed that exhibited large aggregates (Figure 5.2.4). If representative, this result would contrast the one described by Bécart *et al.* (2008) who showed that Y133/144D mutant can be expressed in DEF6-deficient T cells and that it is recruited to the IS upon TCR activation.

6.14 The coiled coil domain is important for DEF6 localisation in the cSMAC of the IS

Upon TCR-mediated activation of Jurkat cells, GFP-tagged DEF6 is recruited to the IS concentrating in cSMAC (Figure 5.3.1). This result is in line with those by Singleton *et al.* (2011) who showed that DEF6 recruitment to the cSMAC depends on ITK function. Localisation of DEF6 to the cSMAC was abolished in mutant proteins All-10 and Δ 0-216-All-10 that were recruited to the IS but localised throughout the outer ring of IS (Figure 5.3.2) suggesting that neither the N-terminal end nor the coiled coil domain is required for IS recruitment. However, it seems that the coiled coil domain is required for DEF6 to localise in

the cSMAC perhaps indicating that ITK phosphorylation of DEF6 liberates its coiled coil domain that then facilitates oligomerisation. Mutant L533P-A536P was also recruited to the IS and localised throughout. However, in this case, F-actin which is mainly present in the outer ring dSMAC, was colocalising with L533P-A536P in the entire IS (Figure 5.3.2) suggesting that this mutant binds F-actin and perhaps has GEF activity in the IS whereas wild type DEF6 does not bind F-actin nor has GEF activity.

6.15 Neither N-Terminus nor coiled coil domain is necessary for IS recruitment of DEF6

As discussed above, mutant DEF6 proteins like $\Delta 0-216$ -All-10 were recruited to the IS indicating that the N-terminal EF hands and ITAM motif are not required for recruitment. Strikingly, DH2 that aggregates and forms large vesicle-like structure was also recruited to the IS (Figure 5.3.3). Similarly, $\Delta 0-216$ was recruited to the IS (Figure 5.3.3) indicating that neither N-terminus nor the coiled coil domain is required for IS recruitment. However, like for other mutants, DH2 and $\Delta 0-216$ localisation was distinct from wild type DEF6 concentrating in pSMAC.

6.16 DEF6 recruitment to the IS appears to be mediated through cell protrusions initiated by APC conjugation with T cells

Preliminary data shown in Figure 5.4.0 seems to suggest that cell protrusions that are initiated through contact of APCs and T cells prior to IS formation contain DEF6. And that within seconds DEF6 localises with the IS (Figure 5.4.0). This process might be linked with DEF6 promoting Rap1-dependent LFA-1

activation and adhesion through interaction of its PH domain with Rap1 (Cote *et al.*, 2015).

Conclusion

Structure-function analysis dissected the role of DEF6 domains in cellular localisation and function. While dormant in its native stage, post-translational modifications of DEF6 such as phosphorylation result in conformational changes that determine DEF6's behaviour and function. Not only is DEF6 recruited to the IS in activated T cells, it is also present in cell protrusion overlapping with F-actin and can shuttle to P-bodies combining TCR-mediated signalling with F-actin organisation and control of mRNA metabolism in P-bodies.

Reference

- Abraham, A. G., & O'Neill, E. (2014). PI3K/Akt-mediated regulation of p53 in cancer. *Biochemical Society Transactions*, 42(4), 798–803. <http://doi.org/10.1042/BST20140070>
- Aizer, A., Brody, Y., Ler, L. W., Sonenberg, N., Singer, R. H., & Shav-Tal, and Y. (2008). The Dynamics of Mammalian P Body Transport, Assembly, and Disassembly In Vivo. *Molecular Biology of the Cell*, 19, 4154–4166. <http://doi.org/10.1091/mbc.E08>
- Aizer, A., Brody, Y., Ler, L. W., Sonenberg, N., Singer, R. H., & Shav-Tal, and Y. (2008). The Dynamics of Mammalian P Body Transport, Assembly, and Disassembly In Vivo. *Molecular Biology of the Cell*, 19, 4154–4166. <http://doi.org/10.1091/mbc.E08>
- Aizer, A., Brody, Y., Ler, L. W., Sonenberg, N., Singer, R. H., & Shav-Tal, and Y. (2008). The Dynamics of Mammalian P Body Transport, Assembly, and Disassembly In Vivo. *Molecular Biology of the Cell*, 19, 4154–4166. <http://doi.org/10.1091/mbc.E08>
- Aizer, A., Kalo, A., Kafri, P., Shraga, A., Ben-Yishay, R., Jacob, A., ... Shav-Tal, Y. (2014). Quantifying mRNA targeting to P bodies in living human cells reveals a dual role in mRNA decay and storage. *Journal of Cell Science*, 4443–4456. <http://doi.org/10.1242/jcs.152975>
- Alan, J. K., & Lundquist, E. A. (2013). Mutationally activated Rho GTPases in cancer. *Small GTPases*, 4(3), 159–163. <http://doi.org/10.4161/sgtp.26530>
- Alarcón, B., Mestre, D., & Martínez-Martín, N. (2011). The immunological synapse: A cause or consequence of T-cell receptor triggering? *Immunology*, 133(4), 420–425. <http://doi.org/10.1111/j.1365-2567.2011.03458.x>
- Altman, A., & Bécart, S. (2009). Does Def6 deficiency cause autoimmunity? *Immunity*, 31(1), 1–2; author reply 2–3. doi:10.1016/j.immuni.2009.06.013
- Anderson, P., & Kedersha, N (a). (2008). Stress granules: the Tao of RNA triage. *Trends in Biochemical Sciences*, 33(3), 141–150. doi:10.1016/j.tibs.2007.12.003
- Anderson, P., & Kedersha, N (b). (2009). Stress granules. *Current Biology*, 19(C), 397–398. doi:10.1016/j.cub.2009.03.013
- Anderson, P., & Kedersha, N. (2009). Stress granules Primer Inhibition in cortical circuits. *Current Biology*, 19(C), 397–398. <http://doi.org/10.1016/j.cub.2009.03.013>

- Anton, O. M., Andres-Delgado, L., Reglero-Real, N., Batista, A., & Alonso, M. A. (2011). MAL Protein Controls Protein Sorting at the Supramolecular Activation Cluster of Human T Lymphocytes. *The Journal of Immunology*, *186*(11), 6345–6356. <http://doi.org/10.4049/jimmunol.1003771>
- Astoul, E., Cantrell, D. A., Edmunds, C., & Ward, S. G. (2001). PI 3-K and T-cell activation: Limitations of T-leukemic cell lines as signaling models. *Trends in Immunology*. [http://doi.org/10.1016/S1471-4906\(01\)01973-1](http://doi.org/10.1016/S1471-4906(01)01973-1)
- Baek, J. H., Moon, C. H., Cha, S. J., Lee, H. S., Noh, E.-K., Kim, H., ... Min, Y. J. (2012). Arsenic trioxide induces depolymerization of microtubules in an acute promyelocytic leukemia cell line. *Korean Journal of Hematology*, *47*(2), 105–112. <http://doi.org/10.5045/kjh.2012.47.2.105>
- Baldassarre, M., Ayala, I., Beznoussenko, G., Giacchetti, G., Machesky, L. M., Luini, A., & Buccione, R. (2006). Actin dynamics at sites of extracellular matrix degradation. *European Journal of Cell Biology*, *85*(12), 1217–1231. <http://doi.org/10.1016/j.ejcb.2006.08.003>
- Bartles, J. R. (2000). Parallel actin bundles and their multiple actin-bundling proteins. *Current Opinion in Cell Biology*, *12*(1), 72–78. [http://doi.org/10.1016/S0955-0674\(99\)00059-9](http://doi.org/10.1016/S0955-0674(99)00059-9)
- Bécart, S., Balancio, A. J. C., Charvet, C., Feau, S., Sedwick, C. E., & Altman, A. (2008). Tyrosine-phosphorylation-dependent translocation of the SLAT protein to the immunological synapse is required for NFAT transcription factor activation. *Immunity*, *29*(5), 704–19. doi:10.1016/j.immuni.2008.08.015
- Bécart, S., Charvet, C., Balancio, A. J. C., Trez, C. De, Tanaka, Y., Duan, W., ... Altman, A. (2007). SLAT regulates Th1 and Th2 inflammatory response by controlling Ca²⁺/NFAT signaling. *The Journal of Clinical Investigation*, *117*(8). doi:10.1172/JCI31640DS1
- Bhattacharyya, S. N., Habermacher, R., Martine, U., Closs, E. I., & Filipowicz, W. (2006). Relief of microRNA-Mediated Translational Repression in Human Cells Subjected to Stress. *Cell*, *125*(6), 1111–1124. <http://doi.org/10.1016/j.cell.2006.04.031>
- Biggs, M. J. P., Milone, M. C., Santos, L. C., Gondarenko, a, & Wind, S. J. (2011). High-resolution imaging of the immunological synapse and T-cell receptor microclustering through microfabricated substrates. *Journal of the Royal Society, Interface / the Royal Society*, *8*(63), 1462–1471. <http://doi.org/10.1098/rsif.2011.0025>
- Billadeau, D. D., Nolz, J. C., & Gomez, T. S. (2007). Regulation of T-cell activation by the cytoskeleton. *Nature Reviews Immunology*, *7*(2), 131–143. <http://doi.org/10.1038/nri2021>

- Binder, N., Miller, C., Yoshida, M., Inoue, K., Nakano, S., Hu, X., ... Zhao, B. (2017). Def6 Restrains Osteoclastogenesis and Inflammatory Bone Resorption. *The Journal of Immunology*, 1601716. <http://doi.org/10.4049/jimmunol.1601716>
- Blanchoin, L., Boujemaa-Paterski, R., Sykes, C., & Plastino, J. (2014). Actin dynamics, Architecture, and Mechanics in cell Motility. *Physiol Rev*, 235–263. <http://doi.org/10.1152/physrev.00018.2013>
- Borggreffe, T., Wabl, M., Akhmedov, A. T., & Jessberger, R. (1998). A B-cell-specific DNA recombination complex. *Journal of Biological Chemistry*, 273(27), 17025–17035. <http://doi.org/10.1074/jbc.273.27.17025>
- Boundedjah, O., Desforges, B., Wu, T. Di, Pioche-Durieu, C., Marco, S., Hamon, L., ... Pastré, D. (2014). Free mRNA in excess upon polysome dissociation is a scaffold for protein multimerization to form stress granules. *Nucleic Acids Research*, 42(13), 8678–8691. <http://doi.org/10.1093/nar/gku582>
- Brengues, M. (2005). Movement of Eukaryotic mRNAs Between Polysomes and Cytoplasmic Processing Bodies. *Science*, 310(5747), 486–489. <http://doi.org/10.1126/science.1115791>
- Brown, D. L., Heimann, K., Lock, J., Kjer-Nielsen, L., van Vliet, C., Stow, J. L., & Gleeson, P. A. (2001). The GRIP Domain is a Specific Targeting Sequence for a Population of trans-Golgi Network Derived Tubulo-Vesicular Carriers. *Traffic*, 2(5), 336–344. <http://doi.org/10.1034/j.1600-0854.2001.002005336.x>
- Brownlie, R. J., & Zamoyska, R. (2013). T cell receptor signalling networks: branched, diversified and bounded. *Nature Reviews. Immunology*, 13(4), 257–69. <http://doi.org/10.1038/nri3403>
- Brüstle, A., Heink, S., Huber, M., Rosenplänter, C., Stadelmann, C., Yu, P., ... Lohoff, M. (2007). The development of inflammatory T(H)-17 cells requires interferon-regulatory factor 4. *Nature Immunology*, 8(9), 958–966. doi:10.1038/ni1500
- Burridge, K., & Wittchen, E. S. (2013). The tension mounts: Stress fibers as force-generating mechanotransducers. *Journal of Cell Biology*, 200(1), 9–19. <http://doi.org/10.1083/jcb.201210090>
- Campellone, K. G., & Welch, M. D. (2010). A nucleator arms race: cellular control of actin assembly. *Nature Reviews. Molecular Cell Biology*, 11(4), 237–51. <http://doi.org/10.1038/nrm2867>
- Canonigo-Balancio, A. J., Fos, C., Prod'homme, T., Bécart, S., & Altman, A. (2009). SLAT/Def6 plays a critical role in the development of Th17 cell-mediated experimental autoimmune encephalomyelitis. *Journal of Immunology (Baltimore, Md. : 1950)*, 183, 7259–7267. doi:10.4049/jimmunol.0902573

- Carbonaro, M., O'Brate, A., & Giannakakou, P. (2011). Microtubule disruption targets HIF-1 α mRNA to cytoplasmic P-bodies for translational repression. *Journal of Cell Biology*, 192(1), 83–99. <http://doi.org/10.1083/jcb.201004145>
- Chacón-Martínez, C. A., Kiessling, N., Winterhoff, M., Faix, J., Müller-Reichert, T., & Jessberger, R. (2013). The switch-associated protein 70 (SWAP-70) bundles actin filaments and contributes to the regulation of F-actin dynamics. *Journal of Biological Chemistry*, 288(40), 28687–28703. <http://doi.org/10.1074/jbc.M113.461277>
- Chan, D. C., Chutkowski, C. T., & Kim, P. S. (1998). Evidence that a prominent cavity in the coiled-coil of HIV type 1 gp41 is an attractive drug target. *Proceedings of the National Academy of Sciences of the United States of America*, 95(26), 15613–7.
- Chan, S., & Slack, F. J. (2006). microRNA-Mediated Silencing Inside P-Bodies. *RNA Biology*, 3(3), 97–100.
- Chang, C. Te, Bercovich, N., Loh, B., Jonas, S., & Izaurralde, E. (2014). The activation of the decapping enzyme DCP2 by DCP1 occurs on the EDC4 scaffold and involves a conserved loop in DCP1. *Nucleic Acids Research*, 42(8), 5217–5233. <http://doi.org/10.1093/nar/gku129>
- Chen, Q., Yang, W., Gupta, S., Biswas, P., Smith, P., Bhagat, G., & Pernis, A. B. (2008). IRF-4-Binding Protein Inhibits Interleukin-17 and Interleukin-21 Production by Controlling the Activity of IRF-4 Transcription Factor. *Immunity*, 29(6), 899–911. doi:10.1016/j.immuni.2008.10.011
- Chen, Q., Yang, W., Gupta, S., Biswas, P., Smith, P., Bhagat, G., & Pernis, A. B. (2009). Response to Letter from Altman and Bécart. *Immunity*, 31(1), 2–3. doi:10.1016/j.immuni.2009.06.012
- Chen, S., Han, Q., Wang, X., Yang, M., Zhang, Z., Li, P., ... Li, S. (2013). IBP-mediated suppression of autophagy promotes growth and metastasis of breast cancer cells via activating mTORC2/Akt/FOXO3a signaling pathway. *Cell Death & Disease*, 4, e842. <http://doi.org/10.1038/cddis.2013.380>
- Chichili, G. R., Cail, R. C., & Rodgers, W. (2012). Cytoskeletal modulation of lipid interactions regulates Ick kinase activity. *Journal of Biological Chemistry*, 287(29), 24186–24194. <http://doi.org/10.1074/jbc.M111.320747>
- Corda, D., Barretta, M. L., Cervigni, R. I., & Colanzi, A. (2012). Golgi complex fragmentation in G2/M transition: An organelle-based cell-cycle checkpoint. *IUBMB Life*, 64(8), 661–670. <http://doi.org/10.1002/iub.1054>
- Côte M., Fos C., Canonigo-Balancio A. J., Ley K., Bécart S., . Altman A. (2015). SLAT promotes TCR-mediated, Rap1-dependent LFA-1 activation and adhesion

- through interaction of its PH domain with Rap1. *JCS Advance Online Article*, 44(November), 4–8. doi:10.1242/jcs.179960
- Davis, D. M., & Dustin, M. L. (2004). What is the importance of the immunological synapse? *Trends in Immunology*, 25(6), 323–327. <http://doi.org/10.1016/j.it.2004.03.007>
- Davis, S. J., & van der Merwe, P. A. (2011). Lck and the nature of the T cell receptor trigger. *Trends in Immunology*, 32(1), 1–5. <http://doi.org/10.1016/j.it.2010.11.003>
- Davis, S. J., & van der Merwe, P. A. (2011). Lck and the nature of the T cell receptor trigger. *Trends in Immunology*, 32(1), 1–5. <http://doi.org/10.1016/j.it.2010.11.003>
- Deng, Y., Zheng, Q., Liu, J., Cheng, C., Kallenbach, N. R., & Lu, M. (2007). Self-assembly of coiled-coil tetramers in the 1.40 Å structure of a leucine-zipper mutant. *Protein Science: A Publication of the Protein Society*, 16(2), 323–8. <http://doi.org/10.1110/ps.062590807>
- Derby, M. C. (2004). Mammalian GRIP domain proteins differ in their membrane binding properties and are recruited to distinct domains of the TGN. *Journal of Cell Science*, 117(24), 5865–5874. <http://doi.org/10.1242/jcs.01497>
- Ding, L., Spencer, A., Morita, K., & Han, M. (2005). The developmental timing regulator AIN-1 interacts with miRISCs and may target the argonaute protein ALG-1 to cytoplasmic P bodies in *C. elegans*. *Molecular Cell*, 19(4), 437–447. <http://doi.org/10.1016/j.molcel.2005.07.013>
- Dong, G., Medkova, M., Novick, P., & Reinisch, K. M. (2007). A catalytic coiled coil: structural insights into the activation of the Rab GTPase Sec4p by Sec2p. *Molecular Cell*, 25(3), 455–62. <http://doi.org/10.1016/j.molcel.2007.01.013>
- Dustin, M. L., & Cooper, J. a. (2000). The immunological synapse and the actin cytoskeleton: molecular hardware for T cell signaling. *Nature Immunology*, 1(1), 23–29.
- Eckstein, N., Servan, K., Girard, L., Cai, D., von Jonquieres, G., Jaehde, U., ... Royer, H. (2008). Epidermal growth factor receptor pathway analysis identifies amphiregulin as a key factor for cisplatin resistance of human breast cancer cells. *The Journal of Biological Chemistry*, 283(2), 739–750. <http://doi.org/10.1074/jbc.M706287200>
- Eulalio, A., Behm-Ansmant, I., & Izaurralde, E. (2007). P bodies: at the crossroads of post-transcriptional pathways. *Nature Reviews Molecular Cell Biology*, 8(1), 9–22. <http://doi.org/10.1038/nrm2080>
- Fanzo, J. C., Yang, W., Jang, S. Y., Gupta, S., Chen, Q., Siddiq, A., ... Pernis, A. B. (2006). Loss of IRF-4-binding protein leads to the spontaneous

- development of systemic autoimmunity. *The Journal of Clinical Investigation*, 116(3), 703–741. doi:10.1172/JCI24096.skeletal
- Feau, S., Schoenberger, S. P., Altman, A., & Bécart, S. (2013). SLAT regulates CD8+ T cell clonal expansion in a Cdc42 and NFAT1 dependent manner. *J Immunol.*, 48(Suppl 2), 1–6. doi:10.1097/MPG.0b013e3181a15ae8.Screening
- Ferdinando Fiumara, Luana Fioriti, Eric R. Kandel, W. A. H. (2012). Essential role of coiled-coils for aggregation and activity of Q/N- rich prions and polyQ proteins, 143(7), 1121–1135. doi:10.1016/j.cell.2010.11.042.Essential
- Filipp, D., Ballek, O., & Manning, J. (2012). Lck, membrane microdomains, and TCR triggering machinery: Defining the new rules of engagement. *Frontiers in Immunology*, 3(JUN), 1–14. <http://doi.org/10.3389/fimmu.2012.00155>
- Fos, C., Becart, S., Balancio, A. J., Boehning, D., & Altman, A. (2014). Association of the EF-hand and PH domains of the guanine nucleotide exchange factor SLAT with IP3 receptor 1 promotes Ca²⁺ signaling in T cells. *Sci Signal*, 7(345), ra93. doi:10.1126/scisignal.2005565
- Fuchs, G., Voichek, Y., Benjamin, S., Gilad, S., Amit, I., & Oren, M. (2014). 4sUDRB-seq: measuring genomewide transcriptional elongation rates and initiation frequencies within cells. *Genome Biology*.
- Garneau, N. L., Wilusz, J., & Wilusz, C. J. (2007). The highways and byways of mRNA decay. *Nature Reviews. Molecular Cell Biology*, 8(2), 113–126. <http://doi.org/10.1038/nrm2104>
- Gasper, R., Thomas, C., Reza Ahmadian, M., & Wittinghofer, A. (2008). The Role of the Conserved Switch II Glutamate in Guanine Nucleotide Exchange Factor-Mediated Nucleotide Exchange of GTP-Binding Proteins. *Journal of Molecular Biology*, 379(1), 51–63. <http://doi.org/10.1016/j.jmb.2008.03.011>
- Gleeson, P. A., Lock, J. G., Luke, M. R., & Stow, J. L. (2004). Domains of the TGN: Coats, tethers and G proteins. *Traffic*, 5(5), 315–326. <http://doi.org/10.1111/j.1398-9219.2004.00182.x>
- Goeckeler, Z. M., Masaracchia, R. A., Zeng, Q., Chew, T., Gallagher, P., & Wysolmerski, R. B. (2000). Phosphorylation of Myosin Light Chain Kinase by p21-activated Kinase PAK2 *. *The Journal of Biological Chemistry*, 275(24), 18366–18374. <http://doi.org/10.1074/jbc.M001339200>
- Guo, Y., Sirkis, D. W., & Schekman, R. (2014). Protein Sorting at the *trans* -Golgi Network. *Annual Review of Cell and Developmental Biology*, 30(1), 169–206. <http://doi.org/10.1146/annurev-cellbio-100913-013012>

- Guo, Z., Hou, X., Goody, R. S., & Itzen, A. (2013). Intermediates in the guanine nucleotide exchange reaction of Rab8 protein catalyzed by guanine nucleotide exchange factors Rabin8 and GRAB. *Journal of Biological Chemistry*, 288(45), 32466–32474. <http://doi.org/10.1074/jbc.M113.498329>
- Gupta, S., Fanzo, J. C., Hu, C., Cox, D., Jang, S. Y., Lee, A. E., ... Pernis, A. B. (2003, b). T cell receptor engagement leads to the recruitment of IBP, a novel guanine nucleotide exchange factor, to the immunological synapse. *The Journal of Biological Chemistry*, 278(44), 43541–9. doi:10.1074/jbc.M308960200
- Gupta, S., Lee, A., Hu, C., Fanzo, J., Goldberg, I., Cattoretti, G., & Pernis, A. B. (2003, a). Molecular cloning of IBP, a SWAP-70 homologous GEF, which is highly expressed in the immune system. *Human Immunology*, 64(4), 389–401. doi:10.1016/S0198-8859(03)00024-7
- Hall, a, & Hall, a. (2005). Rho GTPases and the control of cell behaviour. *Biochemical Society Transactions*, 33(Pt 5), 891–5. <http://doi.org/10.1042/BST20050891>
- Hannon, G. J. (2002). RNA interference. *Nature*, 418, 24–26.
- Hartman, N. C., Nye, J. a, & Groves, J. T. (2009). Cluster size regulates protein sorting in the immunological synapse. *Proceedings of the National Academy of Sciences of the United States of America*, 106(31), 12729–12734. <http://doi.org/10.1073/pnas.0902621106>
- Hashimoto, M., Nagao, J., Ikezaki, S., Tasaki, S., Narita, Y., Cho, T., ... Tanaka, Y. (2017). Identification of a Novel Alternatively Spliced Form of Inflammatory Regulator SWAP-70-Like Adapter of T Cells, 2017.
- Hey, F. (2011) DEF6 is phosphorylated by the TEC-family kinase Itk and forms inducible cytoplasmic granules, *University of Nottingham*
- Hey, F., Czyzewicz, N., Jones, P., & Sablitzky, F. (2012). DEF6, a novel substrate for the Tec kinase ITK, contains a glutamine-rich aggregation-prone region and forms cytoplasmic granules that co-localize with P-bodies. *The Journal of Biological Chemistry*, 287(37), 31073–84. doi:10.1074/jbc.M112.346767
- Hirokawa, N., Noda, Y., Tanaka, Y., & Niwa, S. (2009). Kinesin superfamily motor proteins and intracellular transport. *Nature Reviews Molecular Cell Biology*, 10(10), 682–696. <http://doi.org/10.1038/nrm2774>
- Hogg, N., Henderson, R., Leitinger, B., McDowall, A., Porter, J., & Stanley, P. (2002). Mechanisms contributing to the activity of integrins on leukocytes. *Immunological Reviews*, 186(4), 164–71. <http://doi.org/10.1034/j.1600-065X.2002.18614.x>

- Hogg, N., Patzak, I., & Willenbrock, F. (2011). The insider's guide to leukocyte integrin signalling and function. *Nature Reviews Immunology*, *11*(6), 416–426. <http://doi.org/10.1038/nri2986>
- Hotfilder, M., Baxendale, S., Cross, M.A., Fred. S. (1999). Def-2, -3, -6 and -8, novel mouse genes differentially expressed in the haemopoietic system. *British Journal of Haematology*, *106*, 335–344.
- Huber, M., Brüstle, A., Reinhard, K., Guralnik, A., Walter, G., Mahiny, A., ... Lohoff, M. (2008). IRF4 is essential for IL-21-mediated induction, amplification, and stabilization of the Th17 phenotype. *Proceedings of the National Academy of Sciences of the United States of America*, *105*(52), 20846–20851. doi:10.1073/pnas.0809077106
- Ingolia, N. T., Lareau, L. F., & Weissman, J. S. (2011). Ribosome profiling of mouse embryonic stem cells reveals the complexity and dynamics of mammalian proteomes. *Cell*, *147*(4), 789–802. <http://doi.org/10.1016/j.cell.2011.10.002>
- Jackson, R. J., Hellen, C. U. T., & Pestova, T. V. (2010). The mechanism of eukaryotic translation initiation and principles of its regulation. *Nature Reviews. Molecular Cell Biology*, *11*(2), 113–127. doi:10.1038/nrm2838
- Jaiswal, R., Breitsprecher, D., Collins, A., Corrêa, I. R., Xu, M. Q., & Goode, B. L. (2013). The formin daam1 and fascin directly collaborate to promote filopodia formation. *Current Biology*, *23*(14), 1373–1379. <http://doi.org/10.1016/j.cub.2013.06.013>
- Jakymiw, A., Lian, S., Eystathioy, T., Li, S., Satoh, M., Hamel, J. C., ... Chan, E. K. L. (2005). Disruption of GW bodies impairs mammalian RNA interference. *Nature Cell Biology*, *7*(12), 1267–74. <http://doi.org/10.1038/ncb1334>
- Jian, C.-X., Yang, M.-Z., Li, P., Xiong, J., Zhang, Z.-J., Li, C.-J., ... Li, S.-H. (2012). Ectopically Expressed IBP Promotes Cell Proliferation in Oral Squamous Cell Carcinoma. *Cancer Investigation*, *30*(10), 748–756. <http://doi.org/10.3109/07357907.2012.734355>
- Kammerer, R. a, Schulthess, T., Landwehr, R., Lustig, a, Engel, J., Aebi, U., & Steinmetz, M. O. (1998). An autonomous folding unit mediates the assembly of two-stranded coiled coils. *Proceedings of the National Academy of Sciences of the United States of America*, *95*(23), 13419–24.
- Kapoor-Kaushik, N., Hinde, E., Compeer, E. B., Yamamoto, Y., Kraus, F., Yang, Z., ... Rossy, J. (2016). Distinct mechanisms regulate Lck spatial organization in activated T cells. *Frontiers in Immunology*, *7*(MAR), 1–12. <http://doi.org/10.3389/fimmu.2016.00083>

- Kedersha, N., & Anderson, P. (2007). Mammalian stress granules and processing bodies. *Methods in Enzymology*, 431(7), 61–81. [http://doi.org/10.1016/S0076-6879\(07\)31005-7](http://doi.org/10.1016/S0076-6879(07)31005-7)
- Khan, D., & Ahmed, S. A. (2015). Regulation of IL-17 in autoimmune diseases by transcriptional factors and microRNAs. *Frontiers in Genetics*, 6(JUL), 1–9. doi:10.3389/fgene.2015.00236
- Kilchert, C., Weidner, J., Prescianotto-Baschong, C., & Spang, A. (2010). Defects in the Secretory Pathway and High Ca²⁺ Induce Multiple P-bodies. *Molecular Biology of the Cell*, 21(24), 2642–2638. <http://doi.org/10.1091/mbc.E10>
- Kinashi, T. (2005). Intracellular signalling controlling integrin activation in lymphocytes. *Nature Reviews Immunology*, 5(7), 546–559. <http://doi.org/10.1038/nri1646>
- Kokona, B., Rosenthal, Z. P., & Fairman, R. (2014). Role of the coiled-coil structural motif in polyglutamine aggregation. *Biochemistry*, 53(43), 6738–6746. <http://doi.org/10.1021/bi500449a>
- Komiyama, Y., Nakae, S., Matsuki, T., Nambu, A., Ishigame, H., Kakuta, S., ... Iwakura, Y. (2006). IL-17 plays an important role in the development of experimental autoimmune encephalomyelitis. *J Immunol.*, 177(1), 566–73. doi:10.4049/jimmunol.177.1.566
- Korobova, F., & Svitkina, T. (2008). Arp2/3 Complex Is Important for Filopodia Formation, Growth Cone Motility, and Neuritogenesis in Neuronal Cells Farida. *Molecular Biology of the Cell*, 19, 1561–1574. <http://doi.org/10.1091/mbc.E07>
- Kroschwald, S., Maharana, S., Mateju, D., Malinowska, L., Nüske, E., Poser, I., ... Alberti, S. (2015). Promiscuous interactions and protein disaggregases determine the material state of stress-inducible RNP granules. *eLife*, 4(AUGUST2015), 3–5. <http://doi.org/10.7554/eLife.06807>
- Lee, M., Sadowska, A., Bekere, I., Ho, D., Gully, B. S., Lu, Y., ... Bond, C. S. (2015). The structure of human SFPQ reveals a coiled-coil mediated polymer essential for functional aggregation in gene regulation. *Nucleic Acids Research*, 43(7), 3826–3840. <http://doi.org/10.1093/nar/gkv156>
- Lee, S. H., & Dominguez, R. (2010). Regulation of Actin Cytoskeleton Dynamics in Cells. *Molecular Cell*. <http://doi.org/10.1038/jid.2014.371>
- Letort, G., Ennomani, H., Gressin, L., Theyry, M., & Blanchoin, L. (2015). Dynamic reorganization of the actin cytoskeleton [version 1; referees: 2 approved]. *F1000Research*.
- Li, P., Zhang, Z., Wang, Q., Li, S., Zhang, Y., Bian, X., ... Hu, C. (2009). The ectopic expression of IFN regulatory factor 4-binding protein is correlated with the

- malignant behavior of human breast cancer cells. *International Immunopharmacology*, 9(7–8), 1002–1009. <http://doi.org/10.1016/j.intimp.2009.04.008>
- Li, T., Fang, Y., Yang, G., Xu, J., Zhu, Y., & Liu, L. (2011). Effects of the balance in activity of RhoA and Rac1 on the shock-induced biphasic change of vascular reactivity in rats. *Ann Surg*, 253(1), 185–193. <http://doi.org/10.1097/SLA.0b013e3181f9b88b>
- Lian, S., Jakymiw, A., Eystathioy, T., Hamel, J. C., Fritzler, M. J., & K.L., C. E. (2006). GW Bodies, MicroRNAs and the Cell Cycle Shangli. *Cell Cycle*, 5(3), 1588–1599.
- Liew, P.-L., Fang, C.-Y., Lee, Y.-C., Lee, Y.-C., Chen, C.-L., & Chu, J.-S. (2016). DEF6 expression in ovarian carcinoma correlates with poor patient survival. *Diagnostic Pathology*, 11(1), 68. <http://doi.org/10.1186/s13000-016-0518-y>
- Linder, B., Fischer, U., & Gehring, N. H. (2015). mRNA metabolism and neuronal disease. *FEBS Letters*, 589(14), 1598–1606. <http://doi.org/10.1016/j.febslet.2015.04.052>
- Linder, S. (2009). Invadosomes at a glance. *Journal of Cell Science*, 122(Pt 17), 3009–3013. <http://doi.org/10.1242/jcs.032631>
- Liu, J (b)., Rivas, F. V., Wohlschlegel, J., Yates III, J. R., Parker, R., & Hannon, G. J. (2005). A role for the P-body component, GW182, in microRNA function. *Nature Cell Biology*, 4(3), 735–745. <http://doi.org/10.1038/jid.2014.371>
- Liu, J.-L., & Gall, J. G. (2007). U bodies are cytoplasmic structures that contain uridine-rich small nuclear ribonucleoproteins and associate with P bodies. *Proceedings of the National Academy of Sciences of the United States of America*, 104(28), 11655–9. <http://doi.org/10.1073/pnas.0704977104>
- Liu, J., Valencia-Sanchez, M. A., Hannon, G. J. H., & Parker, R. (2005). MicroRNA-dependent localization of targeted mRNAs to mammalian P-bodies. *Nature Cell Biology*, 100(2), 130–134. <http://doi.org/10.1016/j.pestbp.2011.02.012>. Investigations
- Liu, J., Zheng, Q., Deng, Y., Cheng, C., Kallenbach, N. R., & Lu, M. (2006). A seven-helix coiled coil. *PNAS*, 103(42).
- Loschi, M., Leishman, C. C., Berardone, N., & Boccaccio, G. L. (2009). Dynein and kinesin regulate stress-granule and P-body dynamics. *Journal of Cell Science*, 122(21), 3973–3982. <http://doi.org/10.1242/jcs.051383>
- Lucas, C. L., Chandra, A., Nejentsev, S., Condliffe, A. M., & Okkenhaug, K. (2016). PI3K δ and primary immunodeficiencies. *Nature Reviews Immunology*, 16(11), 702–714. <http://doi.org/10.1038/nri.2016.93>

- Luckheeram, R. V., Zhou, R., Verma, A. D., & Xia, B. (2012). CD4+T Cells: Differentiation and Functions. *Clinical and Developmental Immunology*, 2012, 1–12. doi:10.1155/2012/925135
- Luke, M. R., Houghton, F., Perugini, M. A., & Gleeson, P. A. (2005). The trans-Golgi network GRIP-domain proteins form α -helical homodimers. *The Biochemical Journal*, 388(Pt 3), 835–41. <http://doi.org/10.1042/BJ20041810>
- Luke, M. R., Kjer-Nielsen, L., Brown, D. L., Stow, J. L., & Gleeson, P. A. (2003). GRIP domain-mediated targeting of two new coiled-coil proteins, GCC88 and GCC185, to subcompartments of the trans-Golgi network. *Journal of Biological Chemistry*, 278(6), 4216–4226. <http://doi.org/10.1074/jbc.M210387200>
- Macian, F. (2005). NFAT proteins: key regulators of T-cell development and function. *Nature Reviews. Immunology*, 5(6), 472–84. doi:10.1038/nri1632
- Manni, M., Ricker, E., & Pernis, A. B. (2017). Regulation of systemic autoimmunity and CD11c + Tbet + B cells by SWEF proteins. *Cellular Immunology*, (April), 0–1. <http://doi.org/10.1016/j.cellimm.2017.05.010>
- Marrack, P., & Kappler, J. (1990). The staphylococcal enterotoxins and their relatives. *Science*, 248(4956), 705–711. <http://doi.org/10.1126/science.248.4959.1066-b>
- Martin, P. (2007). Analysis of Def6, a novel guanine nucleotide exchange factor showing dynamic regulation in vitro and playing an essential role in zebrafish development, *University of Nottingham*.
- Mattila, P. K., & Lappalainen, P. (2008). Filopodia: molecular architecture and cellular functions. *Nature Reviews Molecular Cell Biology*, 9(6), 446–454. <http://doi.org/10.1038/nrm2406>
- Mavrakis, K. J., McKinlay, K. J., Jones, P., & Sablitzky, F. (2004). DEF6, a novel PH-DH-like domain protein, is an upstream activator of the Rho GTPases Rac1, Cdc42, and RhoA. *Experimental Cell Research*, 294(2), 335–44. doi:10.1016/j.yexcr.2003.12.004
- McConville, M. J., Ilgoutz, S. C., Teasdale, R. D., Foth, B. J., Matthews, A., Mullin, K. a, & Gleeson, P. a. (2002). Targeting of the GRIP domain to the trans-Golgi network is conserved from protists to animals. *European Journal of Cell Biology*, 81(9), 485–95. Retrieved from <http://www.ncbi.nlm.nih.gov/pubmed/12416725>
- McEwen, E., Kedersha, N., Song, B., Scheuner, D., Gilks, N., Han, A., ... Kaufman, R. J. (2005). Heme-regulated inhibitor kinase-mediated phosphorylation of eukaryotic translation initiation factor 2 inhibits translation, induces stress granule formation, and mediates survival upon arsenite exposure. *Journal of*

- Biological Chemistry*, 280(17), 16925–16933.
<http://doi.org/10.1074/jbc.M412882200>
- Mollett, E (2014) A study of DEF6 granule formation using biophysical and cellular methods, *University of Nottingham*
- Munro, S. (2011). The golgin coiled-coil proteins of the Golgi apparatus. *Cold Spring Harbor Perspectives in Biology*, 3(6), 1–14.
<http://doi.org/10.1101/cshperspect.a005256>
- Munro, S., & Nichols, B. J. (1999). The GRIP domain – a novel Golgi-targeting domain found in several coiled-coil proteins. *Current Biology*, (v), 377–380.
- Murphy, D. A., & Courtneidge, S. A. (2011). The “ins” and “outs” of podosomes and invadopodia: characteristics, formation and function. *Nature Reviews. Molecular Cell Biology*, 12(7), 413–26. <http://doi.org/10.1038/nrm3141>
- Nature. (n.d.) a. Filopodia. Retrieved from <http://www.nature.com/subjects/filopodia> [Accessed 22 Mar.2018]
- Nature. (n.d.) b. Focal adhesion. Retrieved from <http://www.nature.com/subjects/focal-adhesion> [Accessed 22 Mar.2018]
- Nature. (n.d.) c. Focal adhesion. Retrieved from <http://www.nature.com/subjects/podosomes> [Accessed 22 Mar.2018]
- Nature. (n.d.) d. Focal adhesion. Retrieved from <http://www.nature.com/subjects/invadopodia> [Accessed 22 Mar.2018]
- Nika, K., Soldani, C., Salek, M., Paster, W., Gray, A., Etzensperger, R., ... Acuto, O. (2010). Constitutively active lck kinase in T cells drives antigen receptor signal transduction. *Immunity*, 32(6), 766–777.
<http://doi.org/10.1016/j.immuni.2010.05.011>
- Oh, J.-Y., Kwon, A., Jo, A., Kim, H., Goo, Y.-S., Lee, J.-A., & Kim, H. K. (2013). Activity-dependent synaptic localization of processing bodies and their role in dendritic structural plasticity. *Journal of Cell Science*, 126(9), 2114–2123.
<http://doi.org/10.1242/jcs.125690>
- Okkenhaug, K., & Vanhaesebroeck, B. (2003). PI3K in lymphocyte development, differentiation and activation. *Nature Reviews Immunology*, 3(4), 317–330.
<http://doi.org/10.1038/nri1056>
- Osugi, K., Suzuki, H., Nomura, T., Ariumi, Y., Shibata, H., & Maki, M. (2012). Identification of the P-body component PATL1 as a novel ALG-2-interacting protein by in silico and far-Western screening of proline-rich proteins. *Journal of Biochemistry*, 151(6), 657–666.
<http://doi.org/10.1093/jb/mvs029>

- Otsubo, T., Hida, Y., Ohga, N., Sato, H., Kai, T., Matsuki, Y., ... Hida, K. (2014). Identification of novel targets for antiangiogenic therapy by comparing the gene expressions of tumor and normal endothelial cells. *Cancer Science*, *105*(5), 560–567. <http://doi.org/10.1111/cas.12394>
- Ouderkirk, J. L., & Krendel, M. (2015). Myosin 1e is a component of the invadosome core that contributes to regulation of invadosome dynamics. *Exp Cell Res*. <http://doi.org/10.1016/j.pestbp.2011.02.012>. Investigations
- Panic, B., Perisic, O., Veprintsev, D. B., Williams, R. L., & Munro, S. (2003). Structural basis for Arl1-dependent targeting of homodimeric GRIP domains to the Golgi apparatus. *Molecular Cell*, *12*(4), 863–874. [http://doi.org/10.1016/S1097-2765\(03\)00356-3](http://doi.org/10.1016/S1097-2765(03)00356-3)
- Park, H., Li, Z., Yang, X. O., Chang, S. H., Nurieva, R., Wang, Y.-H., ... Dong, C. (2005). A distinct lineage of CD4 T cells regulates tissue inflammation by producing interleukin 17. *Nature Immunology*, *6*(11), 1133–41. doi:10.1038/ni1261
- Parker, R., & Sheth, U. (2007). P Bodies and the Control of mRNA Translation and Degradation. *Molecular Cell*, *25*(5), 635–646. doi:10.1016/j.molcel.2007.02.011
- Pillai, R. S., Bhattacharyya, S. N., Artus, C. G., Zoller, T., Cougot, N., Basyuk, E., ... Filipowicz, W. (2005). Inhibition of translational initiation by Let-7 MicroRNA in human cells. *Science*, *309*(5740), 1573–1576. <http://doi.org/10.1126/science.1115079>
- Pollard, T. D., Blanchoin, L., & Mullins, R. D. (2000). Molecular Mechanisms Controlling Actin Filament Dynamics in Nonmuscle Cells, 545–557.
- Reijns, M. A. M., Alexander, R. D., Spiller, M. P., & Beggs, J. D. (2009). A role for Q / N-rich aggregation-prone regions in P-body localization. *J Cell Sci*, *121*(Pt 15), 2463–2472. <http://doi.org/10.1242/jcs.024976.A>
- Remon K.L. (2016) DEF6 Aggregation is Linked to Active Translation and mRNA Turnover in T Cells, *University of Nottingham*
- Ridley, A. J. (2011). Life at the leading edge. *Cell*, *145*(7), 1012–1022. <http://doi.org/10.1016/j.cell.2011.06.010>
- Ripich, T., Chacón-Martínez, C. A., Fischer, L., Pernis, A., Kiessling, N., Garbe, A. I., & Jessberger, R. (2016). SWEF proteins distinctly control maintenance and differentiation of hematopoietic stem cells. *PLoS ONE*, *11*(8), 1–12. <http://doi.org/10.1371/journal.pone.0161060>
- Ritter, A. T., Asano, Y., Stinchcombe, J. C., Dieckmann, N. M. G., Chen, B. C., Gawden-Bone, C., ... Griffiths, G. M. (2015). Actin Depletion Initiates Events Leading to Granule Secretion at the Immunological Synapse. *Immunity*, *42*(5), 864–876. <http://doi.org/10.1016/j.immuni.2015.04.013>

- Roberts, A. J., Kon, T., Knight, P. J., Sutoh, K., & Burgess, S. A. (2013). Functions and mechanics of dynein motor proteins. *Nature Reviews Molecular Cell Biology*, *14*(11), 713–726. <http://doi.org/10.1038/nrm3667>
- Roh, K.-H., Lillemeier, B. F., Wang, F., & Davis, M. M. (2015). The coreceptor CD4 is expressed in distinct nanoclusters and does not colocalize with T-cell receptor and active protein tyrosine kinase p56lck. *Proceedings of the National Academy of Sciences*, *112*(13), E1604–E1613. <http://doi.org/10.1073/pnas.1503532112>
- Rossy, J., Owen, D. M., Williamson, D. J., Yang, Z., & Gaus, K. (2012). Conformational states of the kinase Lck regulate clustering in early T cell signaling. *Nature Immunology*, *14*(1), 82–89. <http://doi.org/10.1038/ni.2488>
- Rottner, K., & Stradal, T. E. B. (2011). Actin dynamics and turnover in cell motility. *Current Opinion in Cell Biology*, *23*(5), 569–578. <http://doi.org/10.1016/j.ceb.2011.07.003>
- Sato, Y., Fukai, S., Ishitani, R., & Nureki, O. (2007). Crystal structure of the Sec4p.Sec2p complex in the nucleotide exchanging intermediate state. *Proceedings of the National Academy of Sciences of the United States of America*, *104*(20), 8305–10. <http://doi.org/10.1073/pnas.0701550104>
- Seddon, B., & Zamoyska, R. (2002). TCR signals mediated by Src family kinases are essential for the survival of naive T cells. *Journal of Immunology (Baltimore, Md. : 1950)*, *169*(6), 2997–3005. <http://doi.org/10.4049/jimmunol.169.6.2997>
- Sen, G. L., & Blau, H. M. (2005). Argonaute 2/RISC resides in sites of mammalian mRNA decay known as cytoplasmic bodies. *Nature Cell Biology*, *7*(6), 633–636. <http://doi.org/10.1038/ncb1265>
- Sheth, U., & Parker, R. (2007). Decapping and Decay of Messenger RNA Occur in Cytoplasmic Processing Bodies. *Science*, *300*(5620), 805–808.
- Shinohara, R., Thumkeo, D., Kamijo, H., Kaneko, N., Sawamoto, K., Watanabe, K., ... Narumiya, S. (2012). A role for mDia, a Rho-regulated actin nucleator, in tangential migration of interneuron precursors. *Nature Neuroscience*, *15*(3), 373–80, S1-2. <http://doi.org/10.1038/nn.3020>
- Shuen, W. H. (2010) Molecular Evolution of the def6/swap70 Gene Family and Functional Analysis of swap70a in Zebrafish Embryogenesis, *The University of Nottingham*
- Singh, J., & Padgett, R. A. (2009). Rates of in situ transcription and splicing in large human genes. *Nature Structural & Molecular Biology*, *16*(11), 1128–1133. <http://doi.org/10.1038/nsmb.1666>

- Singleton, K. L., Gosh, M., Dandekar, R. D., Au-Yeung, B. B., Ksionda, O., Tybulewicz, V. L. J., ... Wülfing, C. (2011). Itk controls the spatiotemporal organization of T cell activation. *Science Signaling*, 4(193), ra66. <http://doi.org/10.1126/scisignal.2001821>
- Small, J. V., Stradal, T., Vignat, E., & Rottner, K. (2002). The lamellipodium: Where motility begins. *Trends in Cell Biology*, 12(3), 112–120. [http://doi.org/10.1016/S0962-8924\(01\)02237-1](http://doi.org/10.1016/S0962-8924(01)02237-1)
- Smilenov, L. B., Mikhailov, A., Pelham, R. J., Marcantonio, E. E., & Gundersen, G. G. (1999). Focal Adhesion Motility Revealed in Stationary Fibroblasts. *Science*, 286(5442), 1172–1174. <http://doi.org/10.1126/science.286.5442.1172>
- Stefanová, I., Dorfman, J. R., & Germain, R. N. (2002). Self-recognition promotes the foreign antigen sensitivity of naive T lymphocytes. *Nature*, 420(November), 429–434. <http://doi.org/10.1038/nature01146>
- Steinmetz, M. O., Jelesarov, I., Matousek, W. M., Honnappa, S., Jahnke, W., Missimer, J. H., ... Kammerer, R. A. (2007). Molecular basis of coiled-coil formation, 104(17).
- Steinmetz, M. O., Stock, A., Schulthess, T., Landwehr, R., Lustig, A., Faix, J., ... Kammerer, R. A. (1998). A distinct 14 residue site triggers coiled-coil formation in cortexillin I. *EMBO Journal*, 17(7), 1883–1891. <http://doi.org/10.1093/emboj/17.7.1883>
- Sun, C., Molineros, J. E., Looger, L. L., Zhou, X., Kim, K., Okada, Y., ... Nath, S. K. (2016). High-density genotyping of immune-related loci identifies new SLE risk variants in individuals with Asian ancestry. *Nature Genetics*, 48(January), 323–330. doi:10.1038/ng.3496
- Sweet, T. J., Boyer, B., Hu, W., Baker, K. E., & Collier, J. (2007). Microtubule disruption stimulates P-body formation. *Rna*, 13(4), 493–502. <http://doi.org/10.1261/rna.355807>
- Tabarkiewicz, J., Pogoda, K., Karczmarczyk, A., Pozarowski, P., & Giannopoulos, K. (2015). The Role of IL-17 and Th17 Lymphocytes in Autoimmune Diseases. *Archivum Immunologiae et Therapiae Experimentalis*, 63(6), 435–449. doi:10.1007/s00005-015-0344-z
- Takahama, Y. (2006). Journey through the thymus: stromal guides for T-cell development and selection. *Nature Reviews. Immunology*, 6(2), 127–35. doi:10.1038/nri1781
- Teixeira, D., Sheth, U., Valencia-sanchez, M. A., Brengues, M., & Parker, R. O. Y. (2005). Processing bodies require RNA for assembly and contain nontranslating mRNAs. *RNA*, 11, No. 4, 371–382. <http://doi.org/10.1261/rna.7258505.Experiments>

- Thomas, C., Fricke, I., Scrima, A., Berken, A., & Wittinghofer, A. (2007). Structural Evidence for a Common Intermediate in Small G Protein-GEF Reactions. *Molecular Cell*, 25(1), 141–149. <http://doi.org/10.1016/j.molcel.2006.11.023>
- Tojkander, S., Gateva, G., & Lappalainen, P. (2012). Actin stress fibers--assembly, dynamics and biological roles. *Journal of Cell Science*, 125(Pt 8), 1855–64. <http://doi.org/10.1242/jcs.098087>
- Tybulewicz, V. L. J. (2005). Vav-family proteins in T-cell signalling. *Current Opinion in Immunology*, 17(3), 267–274. <http://doi.org/10.1016/j.coi.2005.04.003>
- Tybulewicz, V. L. J., & Henderson, R. B. (2009). Rho family GTPases and their regulators in lymphocytes. *Nature Reviews. Immunology*, 9(9), 630–44. <http://doi.org/10.1038/nri2606>
- Ueno, T., Kaneko, K., Katano, H., Sato, Y., Mazitschek, R., Tanaka, K., ... Ogawa-Goto, K. (2010). Expansion of the trans-Golgi network following activated collagen secretion is supported by a coiled-coil microtubule-bundling protein, p180, on the ER. *Experimental Cell Research*, 316(3), 329–340. <http://doi.org/10.1016/j.yexcr.2009.11.009>
- Valencia-Sanchez, M. A., Liu, J., Hannon, G. J., & Parker, R. (2006). Control of translation and mRNA degradation by miRNAs and siRNAs. *Genes and Development*, 20(5), 515–524. <http://doi.org/10.1101/gad.1399806>
- Vetter, I. R., & Wittinghofer, a. (2001). The guanine nucleotide-binding switch in three dimensions. *Science (New York, N.Y.)*, 294(5545), 1299–304. <http://doi.org/10.1126/science.1062023>
- Vistica, B. P., Shi, G., Nugent, L., Tan, C., Altman, A., & Gery, I. (2012). SLAT/Def6 plays a critical role in the pathogenic process of experimental autoimmune uveitis (EAU). *Molecular Vision*, 18(February), 1858–64. Retrieved from <http://www.pubmedcentral.nih.gov/articlerender.fcgi?artid=3398495&tool=pmcentrez&rendertype=abstract>
- Watson, A. R. O., & Lee, W. T. (2004). Differences in signaling molecule organization between naive and memory CD4+ T lymphocytes. *Journal of Immunology (Baltimore, Md.: 1950)*, 173(1), 33–41. <http://doi.org/10.4049/jimmunol.173.1.33>
- Welch, E. Z., Anderson, K. L., & Feldman, S. R. (2015). Interleukin 17 deficiency and implications in cutaneous and systemic diseases. *Journal of Dermatology & Dermatologic Surgery*, 19(2), 73–79. doi:<http://dx.doi.org/10.1016/j.jdds.2015.03.004>

- Wu, M., Lu, L., Hong, W., & Song, H. (2004). Structural basis for recruitment of GRIP domain golgin-245 by small GTPase Arl1. *Nature Structural & Molecular Biology*, *11*(1), 86–94. <http://doi.org/10.1038/nsmb714>
- Yang, J., Sundrud, M. S., Skepner, J., & Yamagata, T. (2014). Targeting Th17 cells in autoimmune diseases. *Trends in Pharmacological Sciences*, *35*(10), 493–500. doi:10.1016/j.tips.2014.07.006
- Yang, M. Z., Yuan, F., Li, P., Chen, Z. J., Chen, A., Li, S. H., & Hu, C. M. (2012). Interferon regulatory factor 4 binding protein is a novel p53 target gene and suppresses cisplatin-induced apoptosis of breast cancer cells. *Molecular Cancer*, *11*, 1–13. <http://doi.org/10.1186/1476-4598-11-54>
- Yang, Z., Jakymiw, A., Wood, M. R., Eystathiou, T., Rubin, R. L., Fritzler, M. J., & Chan, E. K. L. (2004). GW182 is critical for the stability of GW bodies expressed during the cell cycle and cell proliferation. *Journal of Cell Science*, *117*(23), 5567–5578. <http://doi.org/10.1242/jcs.01477>
- Youn, B. U., Kim, K., Kim, J. H., Lee, J., Moon, J. B., Kim, I., ... Kim, N. (2013). SLAT negatively regulates RANKL-induced osteoclast differentiation. *Molecules and Cells*, *36*(3), 252–257. <http://doi.org/10.1007/s10059-013-0159-x>
- Yu Tanaka, Y., Bi, K., Kitamura, R., Hong, S., Altman, Y., Matsumoto, A., ... Altman, A. (2003). SWAP-70-like adapter of T cells, an adapter protein that regulates early TCR-initiated signaling in Th2 lineage cells. *Immunity*, *18*(3), 403–14. Retrieved from <http://www.ncbi.nlm.nih.gov/pubmed/12648457>
- Yu, C. han, Wu, H. J., Kaizuka, Y., Vale, R. D., & Groves, J. T. (2010). Altered actin centripetal retrograde flow in physically restricted immunological synapses. *PLoS ONE*, *5*(7), 1–9. <http://doi.org/10.1371/journal.pone.0011878>
- Yu, Y., Smoligovets, A. A., & Groves, J. T. (2013). Modulation of T cell signaling by the actin cytoskeleton. *Journal of Cell Science*, *126*(Pt 5), 1049–58. <http://doi.org/10.1242/jcs.098210>
- Zhang, Z., Wang, Q., Li, P., Zhou, Y., Li, S., Yi, W., ... Hu, C. (2009). Overexpression of the Interferon regulatory factor 4-binding protein in human colorectal cancer and its clinical significance. *Cancer Epidemiology*, *33*(2), 130–136. <http://doi.org/10.1016/j.canep.2009.05.004>
- Zhao, Y., Toselli, P., & Li, W. (2012). Microtubules as a critical target for arsenic toxicity in lung cells in vitro and in vivo. *International Journal of Environmental Research and Public Health*, *9*(2), 474–495. <http://doi.org/10.3390/ijerph9020474>
- Zhu, S., & Qian, Y. (2012). IL-17/IL-17 receptor system in autoimmune disease: mechanisms and therapeutic potential. *Clinical Science (London, England: 1979)*, *122*(11), 487–511. doi:10.1042/CS20110496

Zilfou, J. T., & Lowe, S. W. (2009). Tumor suppressive functions of p53. *Cold Spring Harbor Perspectives in Biology*, 1(5), 1–12.

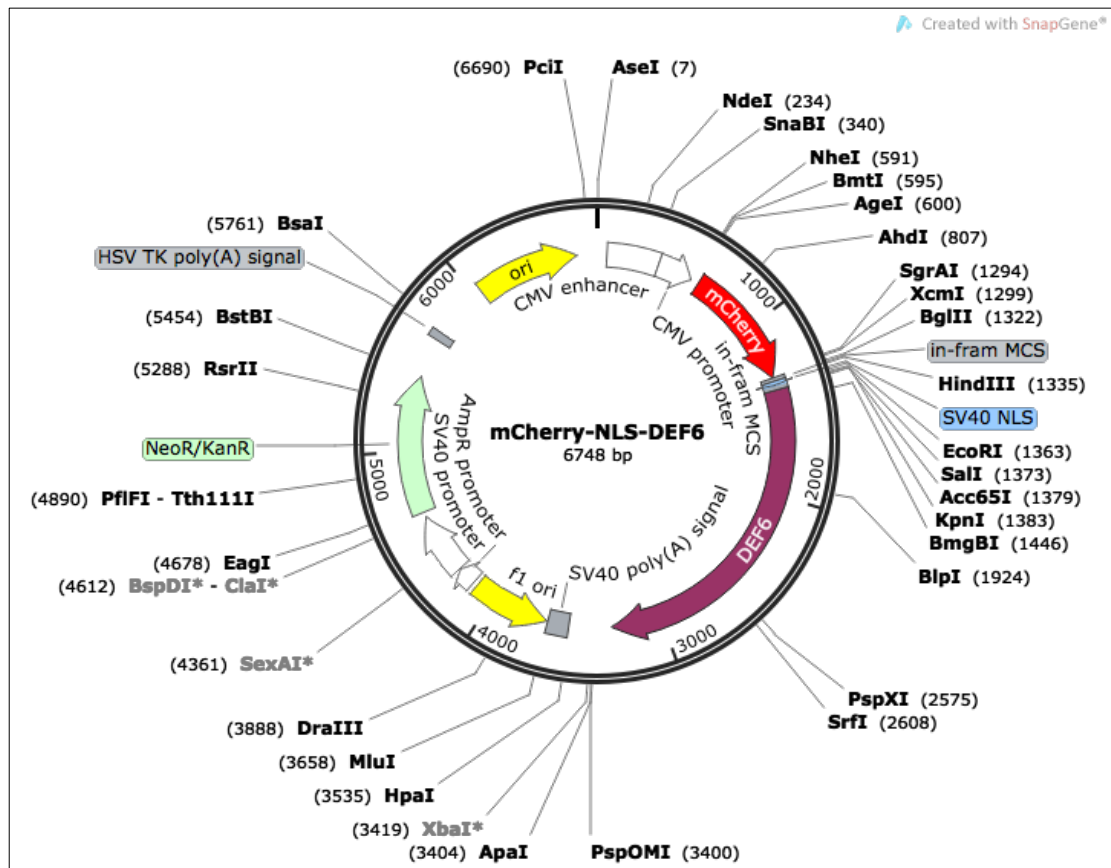


Fig. 8.1.2 Plasmid map of mCherry and SV40 NLS tagged DEF6

Plasmid type: Mammalian. Bacterial resistance: Kanamycin. Mammalian Selection: Neomycin. Map established by SnapGene Viewer.

8.2 Wild Type DEF6 Full Length sequence

```

ATG GCC CTG CGC AAG GAA CTG CTC AAG TCC ATC TGG TAC GCC TTT
                10
ACC GCG CTG GAC GTG GAG AAG AGT GGC AAA GTC TCC AAG TCC CAG
                20
                30
CTC AAG GTG CTG TCC CAC AAC CTG TAC ACG GTC CTG CAC ATC CCC
                40
                50
CAT GAC CCC GTG GCC CTG GAG GAA CAC TTC CGA GAT GAT GAT GAC
                60
                70
GGC CCT GTG TCC AGC CAG GGA TAC ATG CCC TAC CTC AAC AAG TAC
                80
                90
ATC CTG GAC AAG GTG GAG GAG GGG GCT TTT GTT AAA GAG CAC TTT
                100
GAT GAG CTG TGC TGG ACG CTG ACG GCC AAG AAG AAC TAT CGG GCA
                110
                120
GAT AGC AAC GGG AAC AGT ATG CTC TCC AAT CAG GAT GCC TTC CGC
                130
                140
CTC TGG TGC CTC TTC AAC TTC CTG TCT GAG GAC AAG TAC CCT CTG
                150
                160
ATC ATG GTT CCT GAT GAG GTG GAA TAC CTG CTG AAA AAG GTA CTC
                170
                180
AGC AGC ATG AGC TTG GAG GTG AGC TTG GGT GAG CTG GAG GAG CTT
                190
                200
CTG GCC CAG GAG GCC CAG GTG GCC CAG ACC ACC GGG GGG CTC AGC
                210
                220
GTC TGG CAG TTC CTG GAG CTC TTC AAT TCG GGC CGC TGC CTG CGG
                230
                240
GGC GTG GGC CGG GAC ACC CTC AGC ATG GCC ATC CAC GAG GTC TAC
                250
                260
CAG GAG CTC ATC CAA GAT GTC CTG AAG CAG GGC TAC CTG TGG AAG
                270
                280
CGA GGG CAC CTG AGA AGG AAC TGG GCC GAA CGC TGG TTC CAG CTG
                290
                300
CAG CCC AGC TGC CTC TGC TAC TTT GGG AGT GAA GAG TGC AAA GAG
                310
                320
AAA AGG GGC ATT ATC CCG CTG GAT GCA CAC TGC TGC GTG GAG GTG
                330
                340
CTG CCA GAC CGC GAC GGA AAG CGC TGC ATG TTC TGT GTG AAG ACA
                350

```

Fig. 8.2.0 DNA sequence of DEF6

The numbers in blue indicates the amino acids positions in DEF6 molecule.
Continued in next two pages.

GCC AAC CGC ACG	290	TAT GAG ATG AGC GCC TCA GAC ACG CGC CAG CGC	300
CAG GAG TGG ACA		GCT GCC ATC CAG ATG	310
GAG GGG AAG ACG	320	TCC CTA CAC AAG GAC CTG AAG CAG AAA CGG CGC	330
GAG CAG CGG GAG		CAG CGG GAG CGG CGC	340
GAG CTG CTG CGG	350	CTG CAG CAG CTG CAG GAG GAG AAG GAG CGG AAG	360
CTG CAG GAG CTG		GAG CTG CTG CAG GAG	370
CGG CTG CTG CAG	380	GAG GAG GAG GAA CGG CGC CGC AGC CAG CAC CGC	390
GAG CTG CAG CAG		GCG CTC GAG GGC CAA	400
GCC CGG GCC TCC	410	ATG CAG GCT GAG ATG GAG CTG AAG GAG GAG GAG	420
GCT GCC CGG CAG		CGG CAG CGC ATC AAG	430
CAG CGG TTG CAG	440	GAG GCC CTG CAA CTA GAG GTG AAA GCT CGG CGA	450
GAT GAA GAA TCT		GTG CGA ATC GCT CAG	460
GAG GAA GAG AAG	470	CTG AAG CAG TTG ATG CAG CTG AAG GAG GAG CAG	480
GAG CGC TAC ATC		GAA CGG GCG CAG CAG	490
CAG GAG ATG GCA	500	CAG CAG AGC CGC TCC CTG CAG CAG GCC CAG CAG	510
CAG CTG GAG GAG		GTG CGG CAG AAC CGG	520
GTG GAG GCT GCC	530	CAG AGA AAA CTG CGC CAG GCC AGC ACC AAC GTG	540
AAA CAC TGG AAT		GTC CAG ATG AAC CGG	550
CCT GGA GAT AAG	560	CGT CCG GTC ACC AGC AGC TCC TTC TCA GGC TTC	570

Fig. 8.2.0 DNA sequence of DEF6.

The numbers in blue indicates the amino acids positions in DEF6 molecule.
Continued in next page.

```
CAG CCC CCT CTG CTT GCC CAC CGT GAC TCC TCC CTA AAG CGC CTG
ACC CGC TGG GGA TCC CAG GGC AAC AGG ACC CCC TCG CCC AAC AGC
AAT GAG CAG CAG AAG TCC CTC AAT GGT GGG GAT GAG GCT CCT GCC
CCG GCT TCC ACC CCT CAG GAA GAT AAA CTG GAT CCA GCA CCA GAA
AAT
```

Fig. 8.2.0 DNA sequence of DEF6.

The numbers in blue indicates the amino acids positions in DEF6 molecule.

8.3 DNA sequencing results of DEF6 mutants

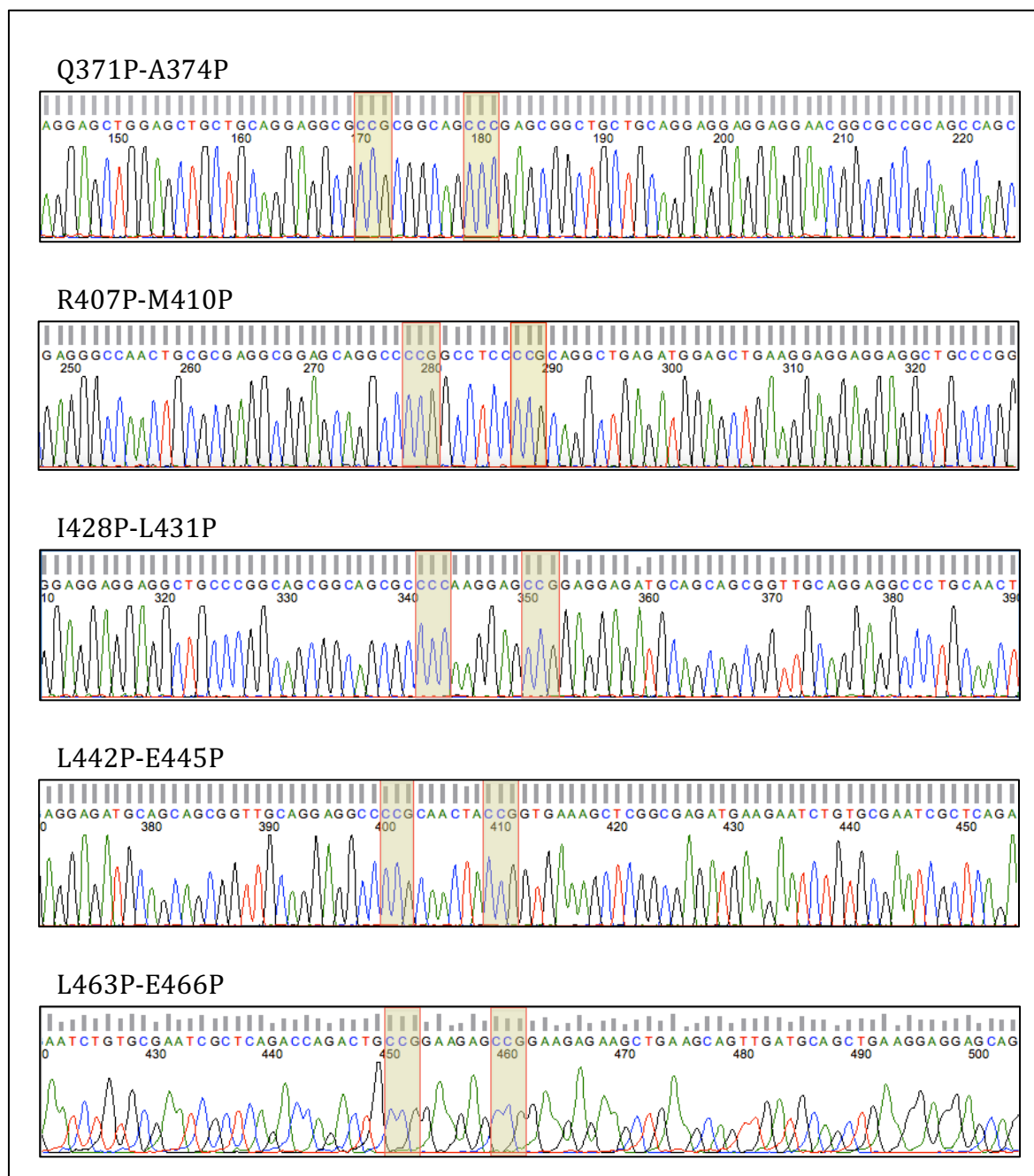


Fig. 8.3.1 DNA Sequencing results of DEF6 Proline mutants

The mutated positions are highlighted by coloured boxes. Continued in next three pages.

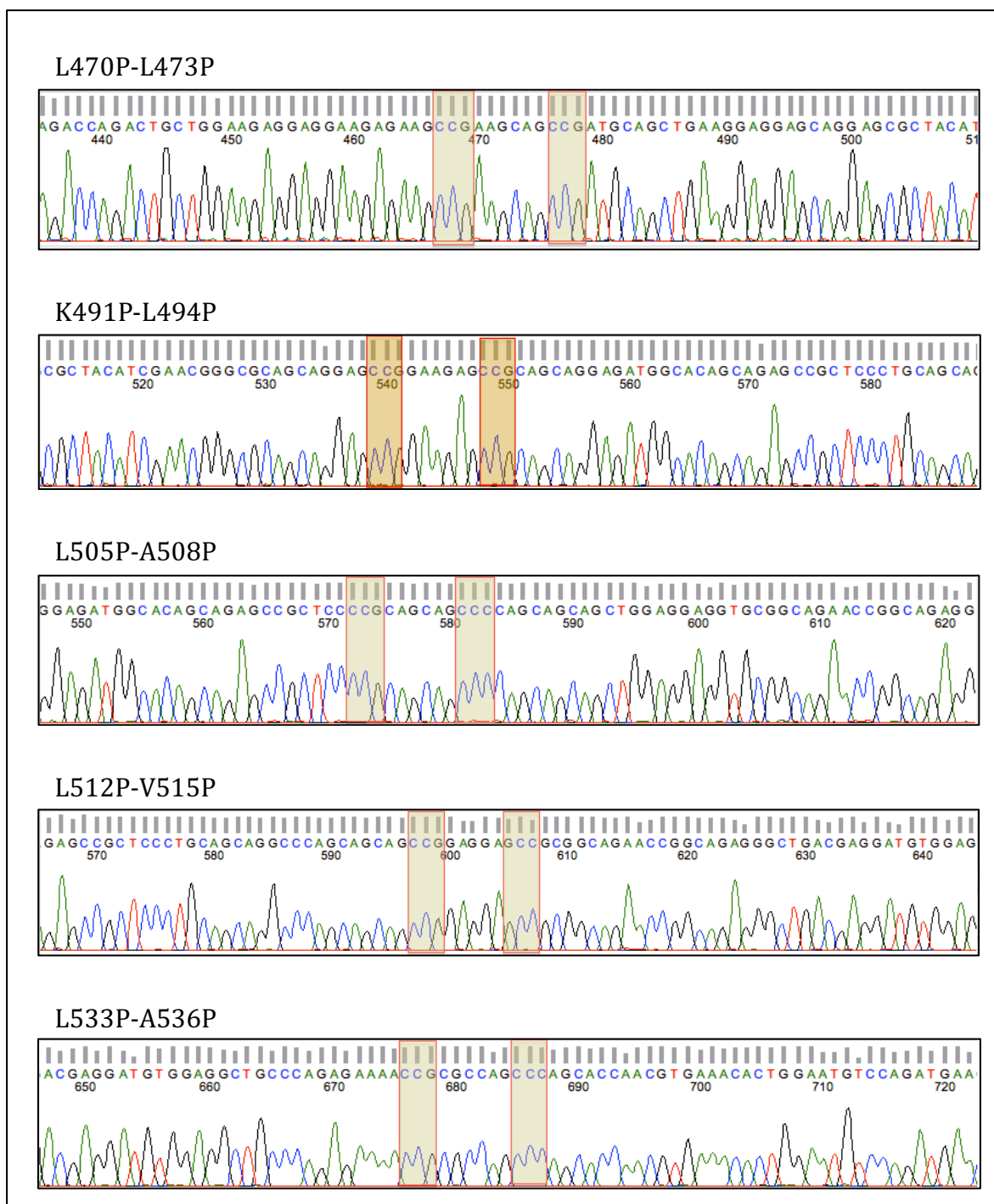
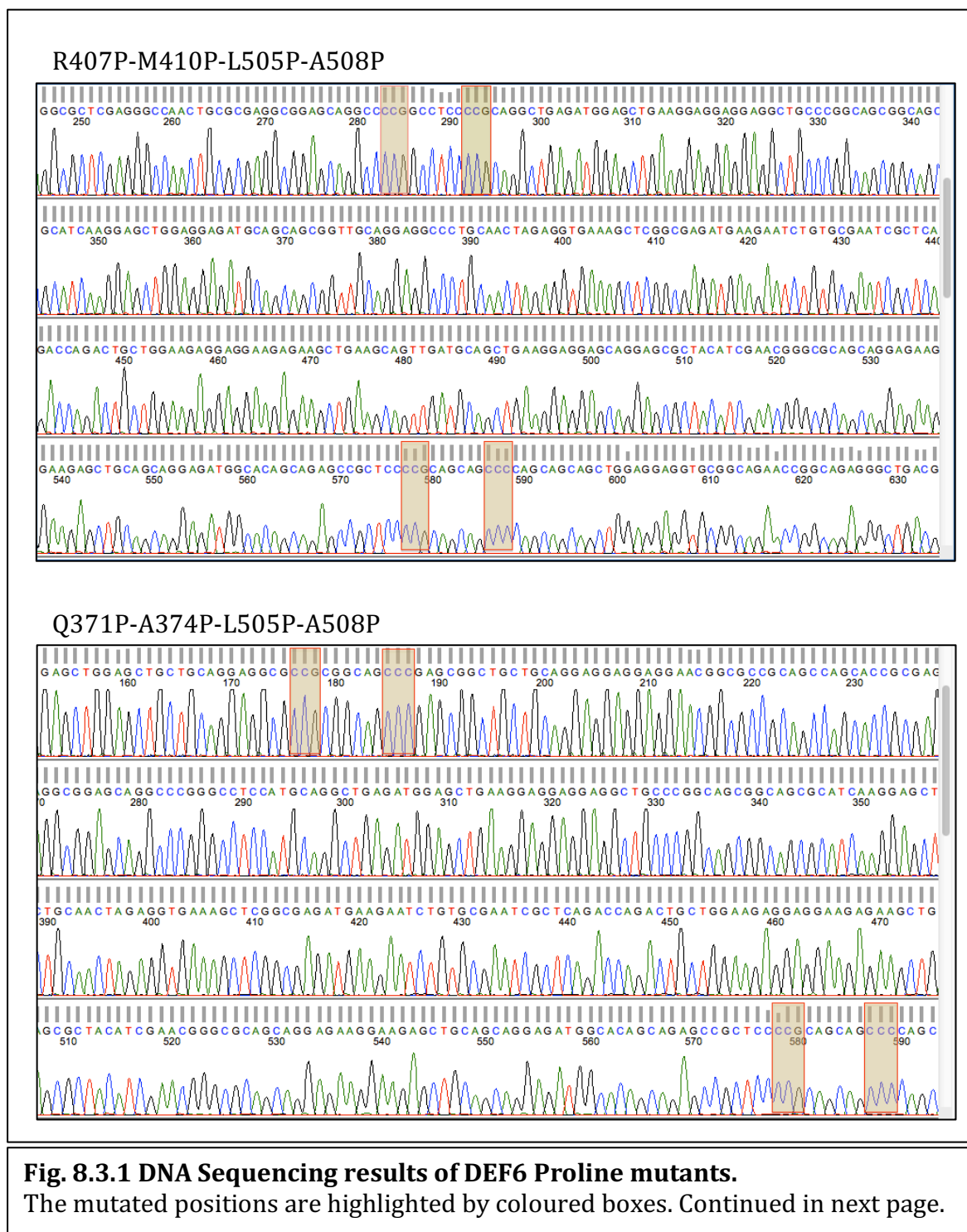
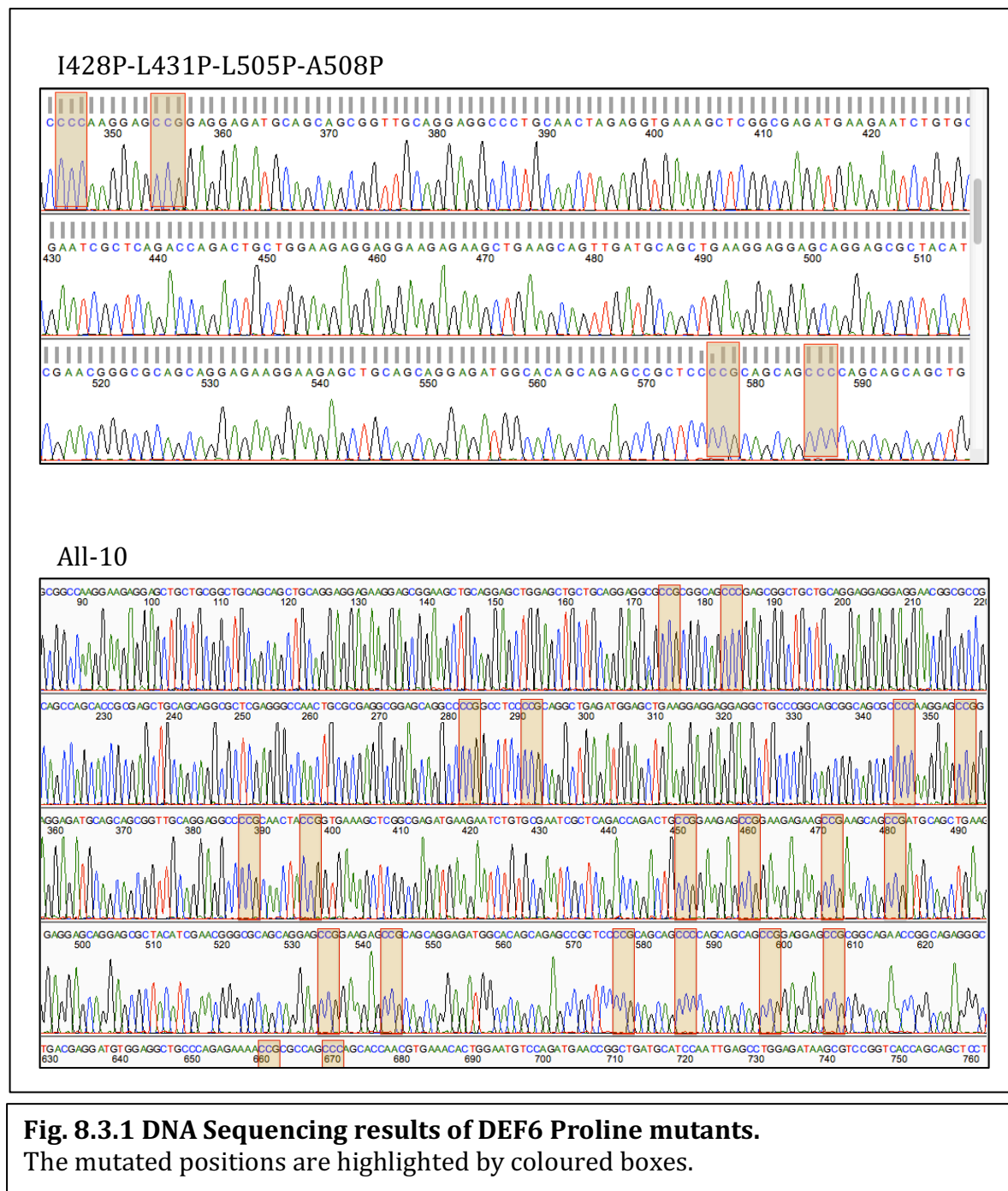


Fig. 8.3.1 DNA Sequencing results of DEF6 Proline mutants.

The mutated positions are highlighted by coloured boxes. Continued in next two pages.





mCherry-NLS-DEF6

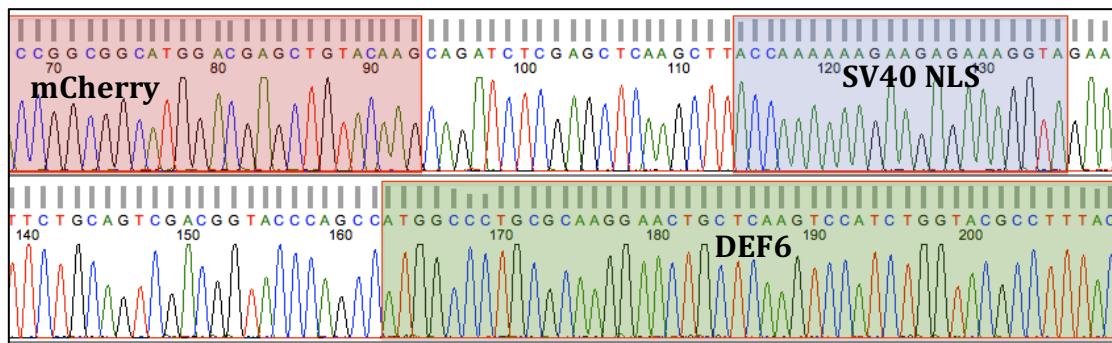


Fig. 8.3.2 DNA sequencing result of mCherry-NLS-DEF6

mCherry and DEF6 are respectively indicated in red and green; SV40 nuclear localization sequence (NLS) is indicated in purple that is localized between mCherry and DEF6.

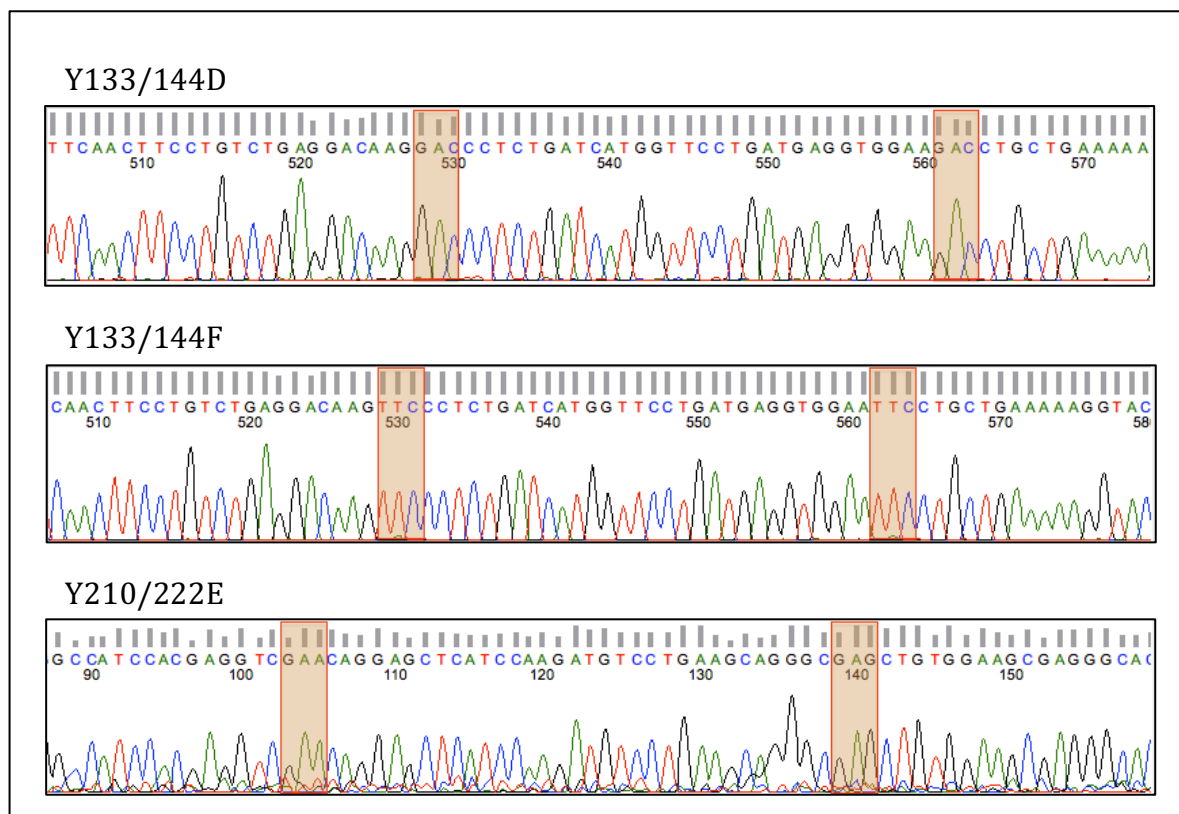
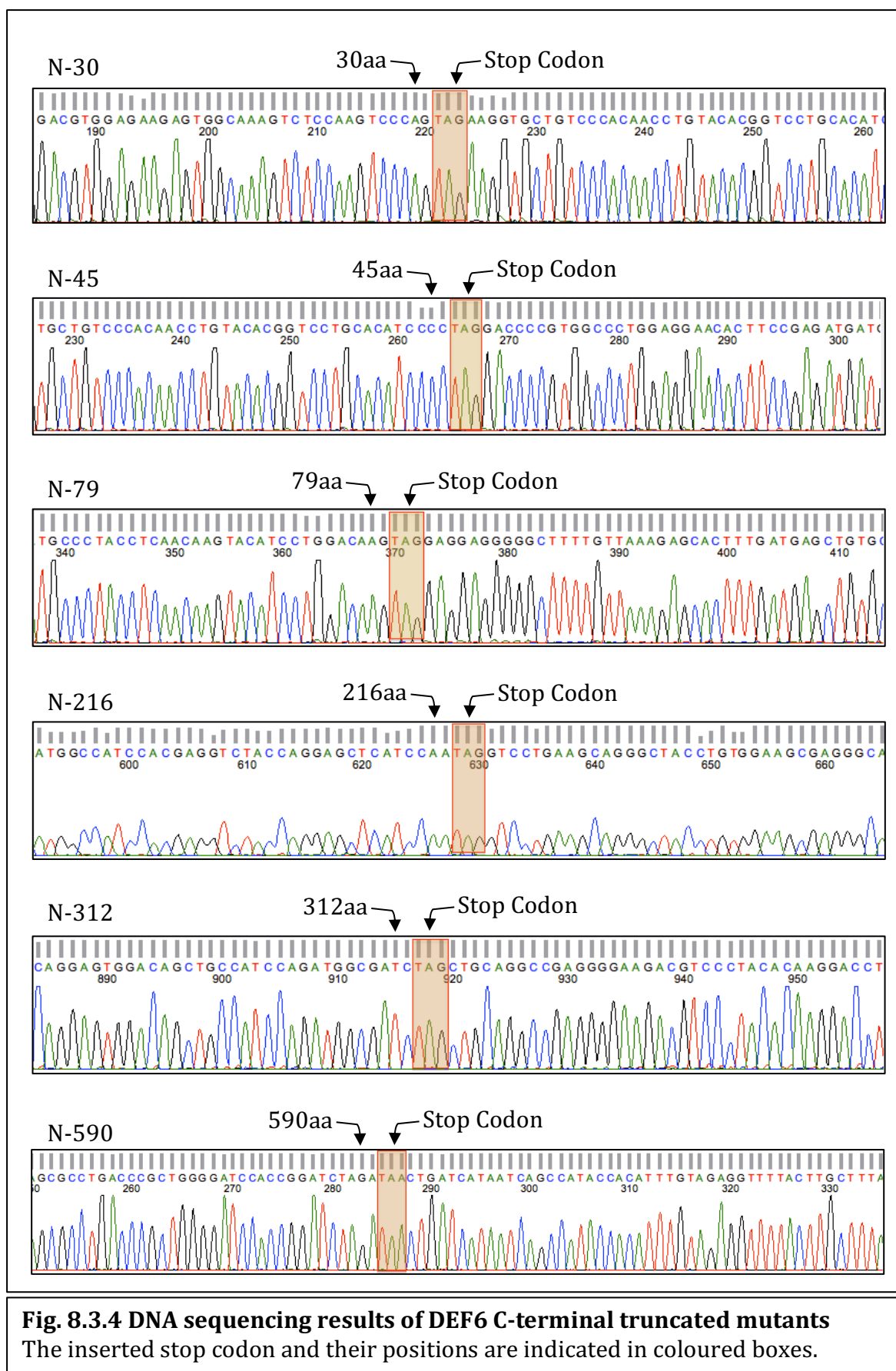


Fig. 8.3.3 DNA sequencing results of DEF6 phosphomimetic and phosphor preventing mutants

The mutated positions are indicated by coloured boxes.



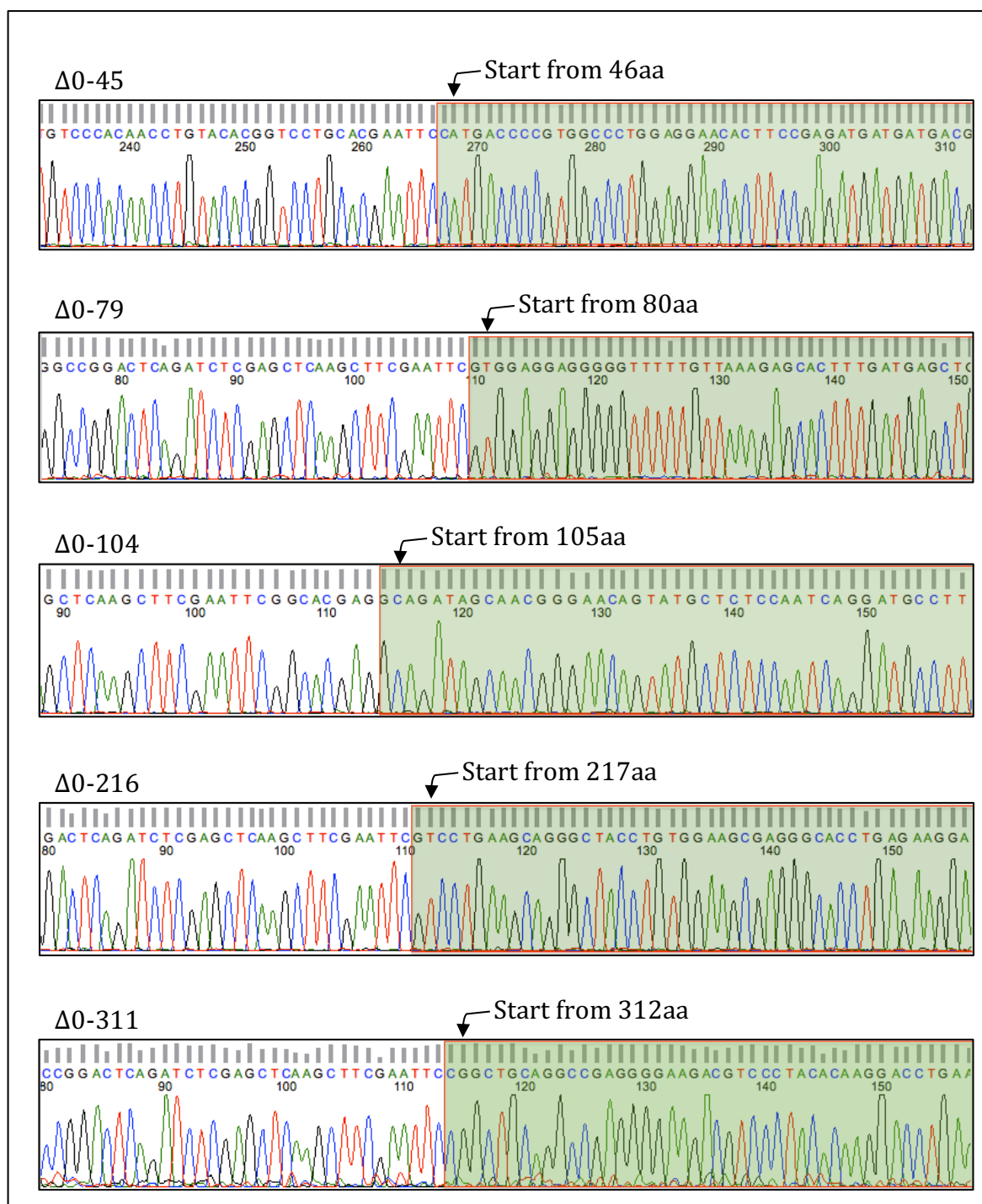


Fig. 8.3.5 DNA sequencing results of DEF6 N-terminal truncated mutants
Green colour and arrow indicates the start amino acids of these mutants.

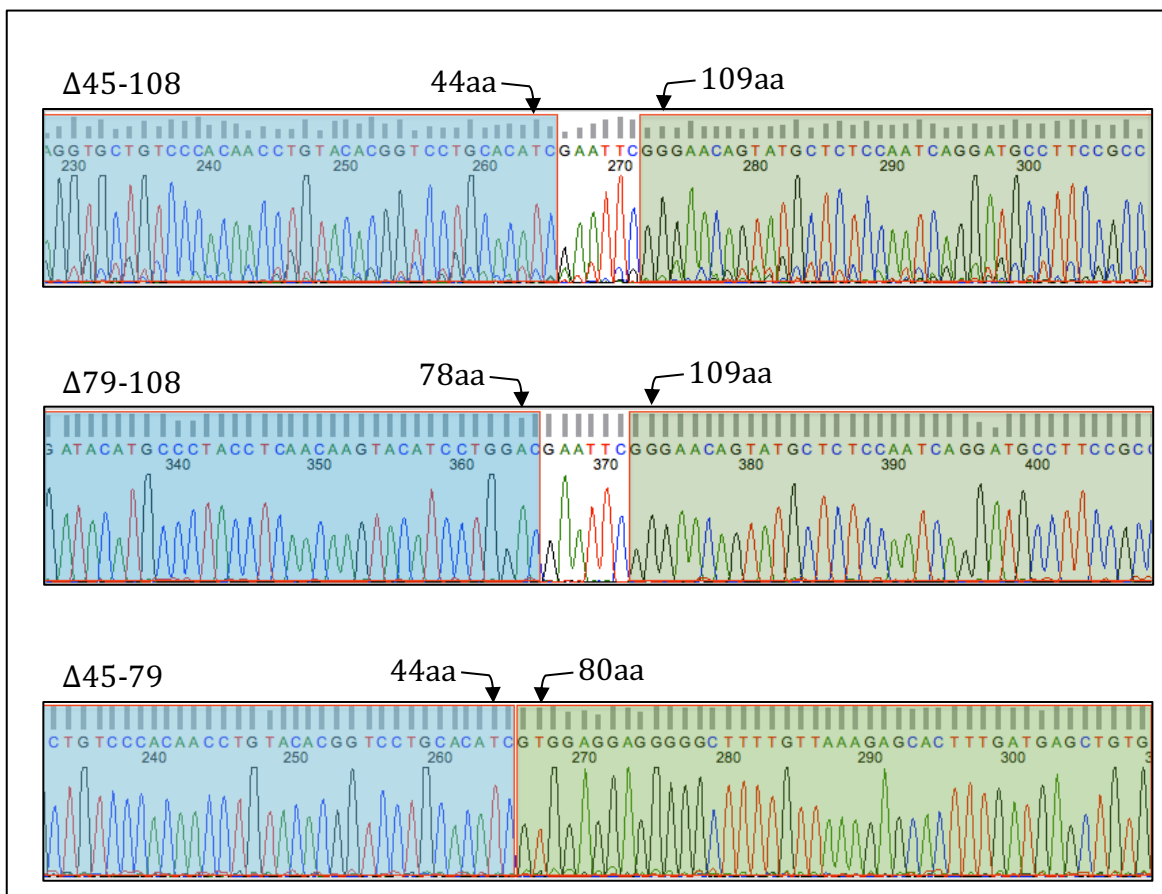


Fig. 8.3.6 DNA sequencing results of $\Delta 45-108$, $\Delta 79-108$ and $\Delta 45-79$

The introduced EcoRI digesting sites were remaining in $\Delta 45-108$ and $\Delta 79-108$; only $\Delta 45-79$ has been completely removed this site.

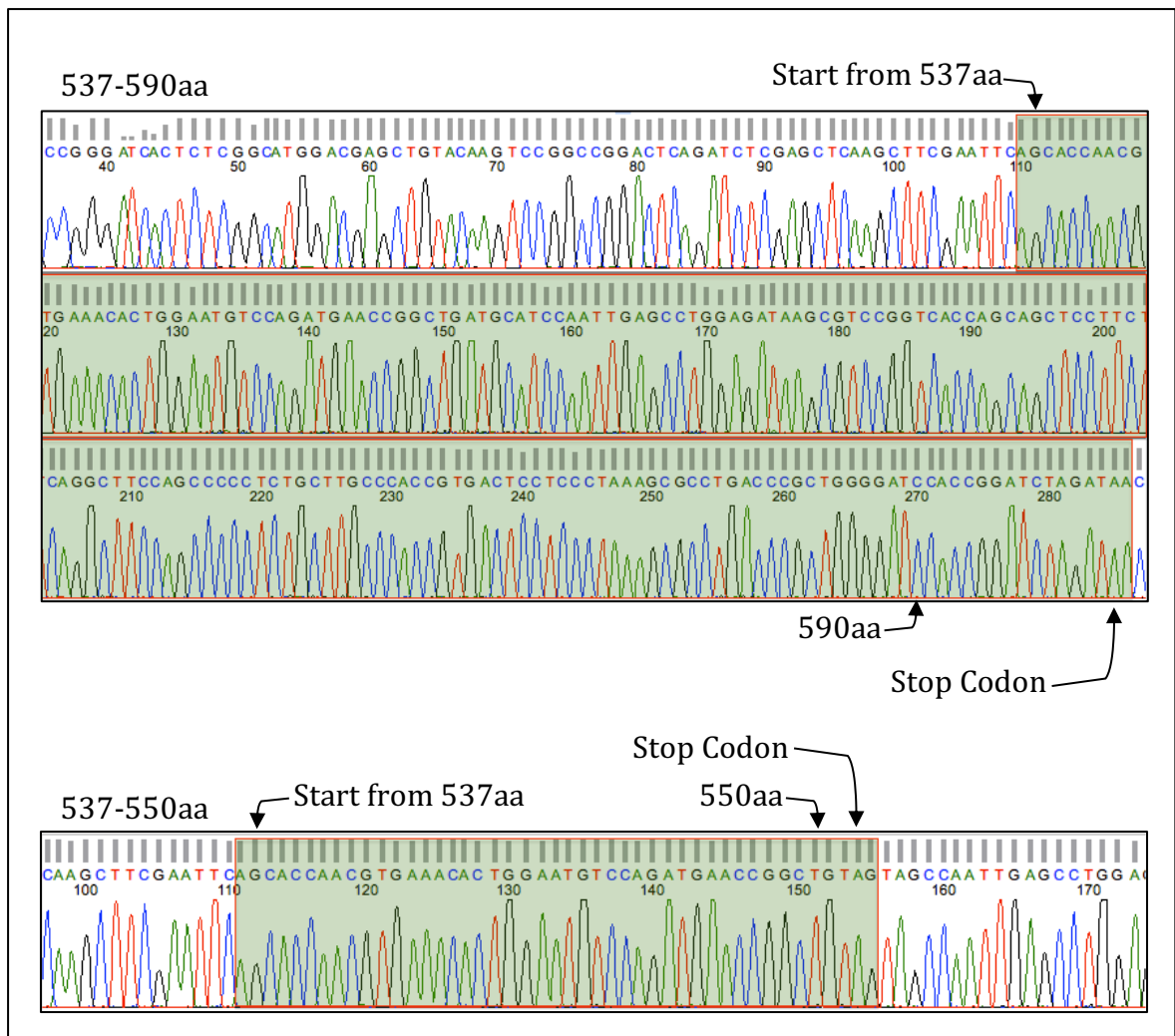


Fig. 8.3.7a DNA sequencing result of DEF6 mutants 537-590aa, 537-550aa
The molecules are indicated in green with arrows to indicate start and stop positions.

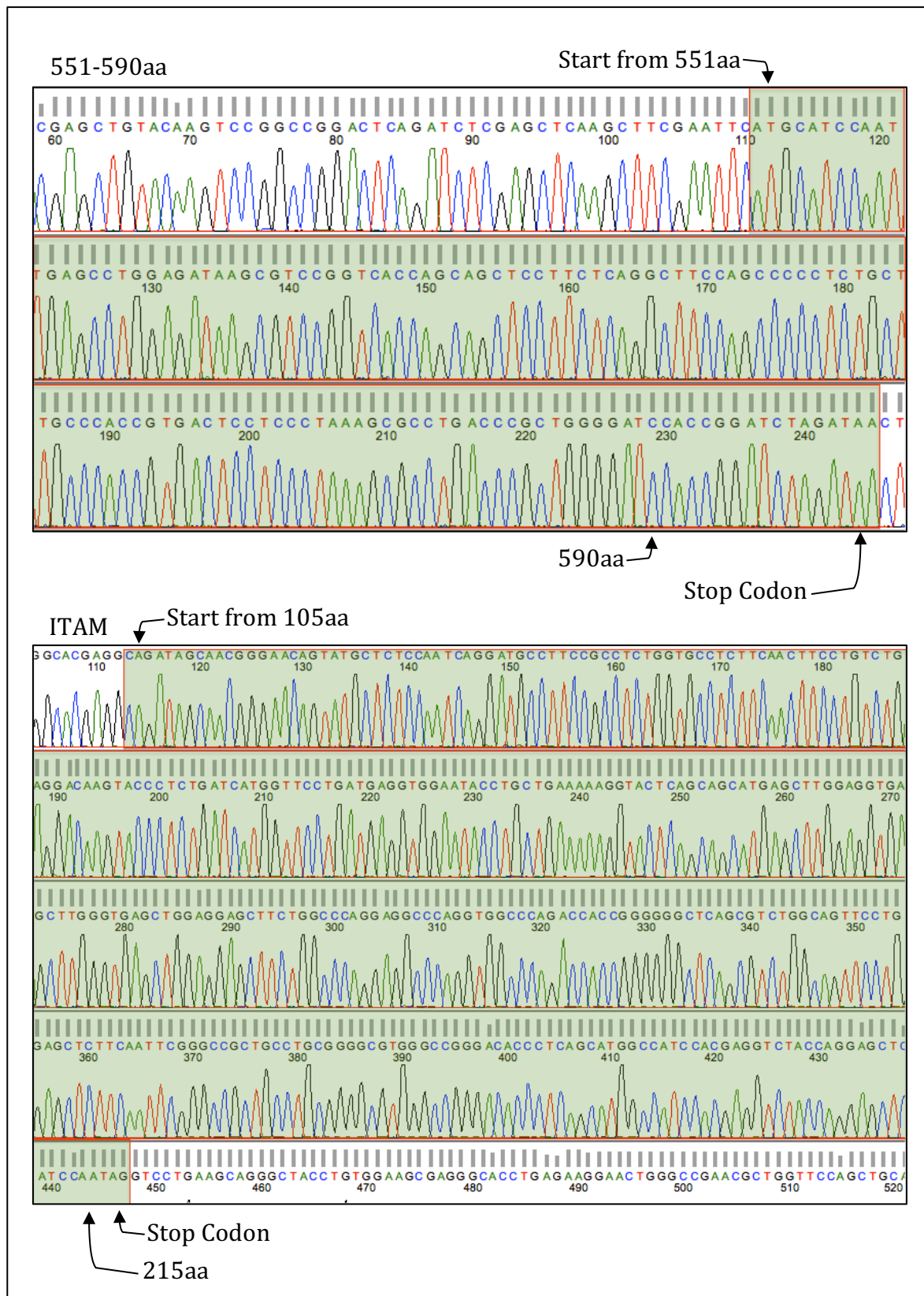


Fig. 8.3.7b DNA sequencing result of DEF6 mutants 551-590aa and ITAM (105-215aa)

The molecules are indicated in green with arrows to indicate start and stop positions.

8.4 Additional images

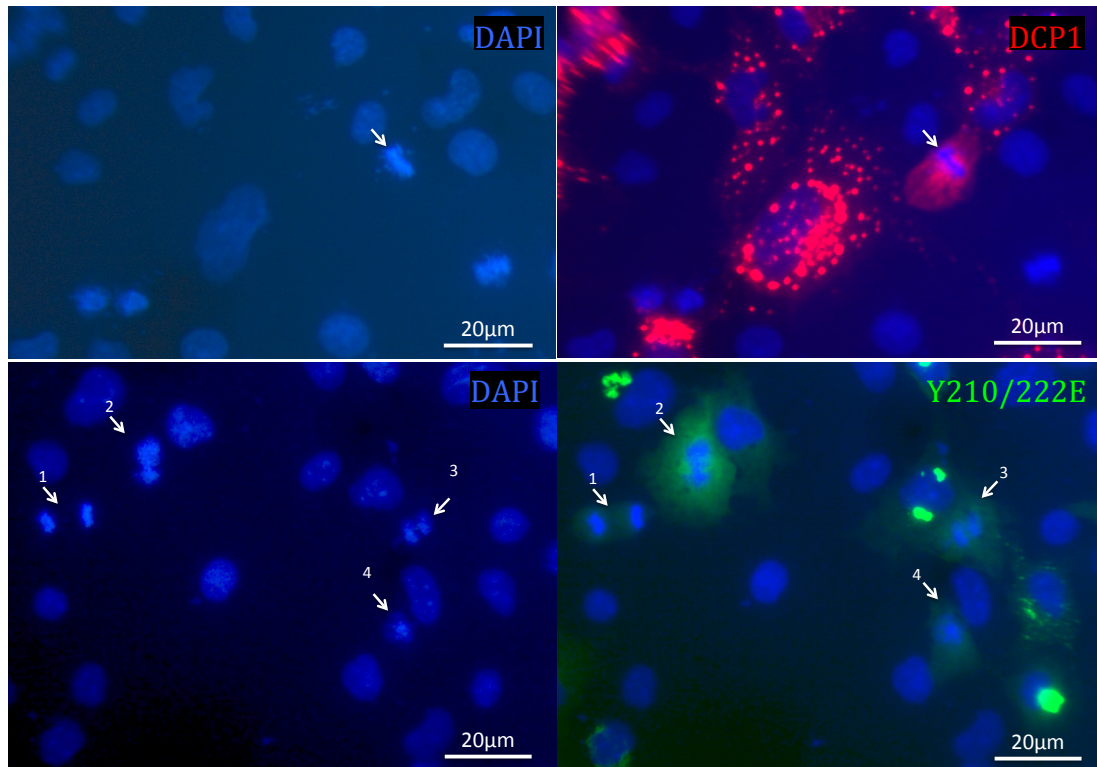


Fig. 8.4.0 DCP1 and DEF6 Y210/222E did not form granules in COS7 cells mitosis phase

DAPI staining indicated chromosome situations and mitotic cells (arrows). Both DCP1 and DEF6 Y210/222E did not demonstrated visible granules in these cells.

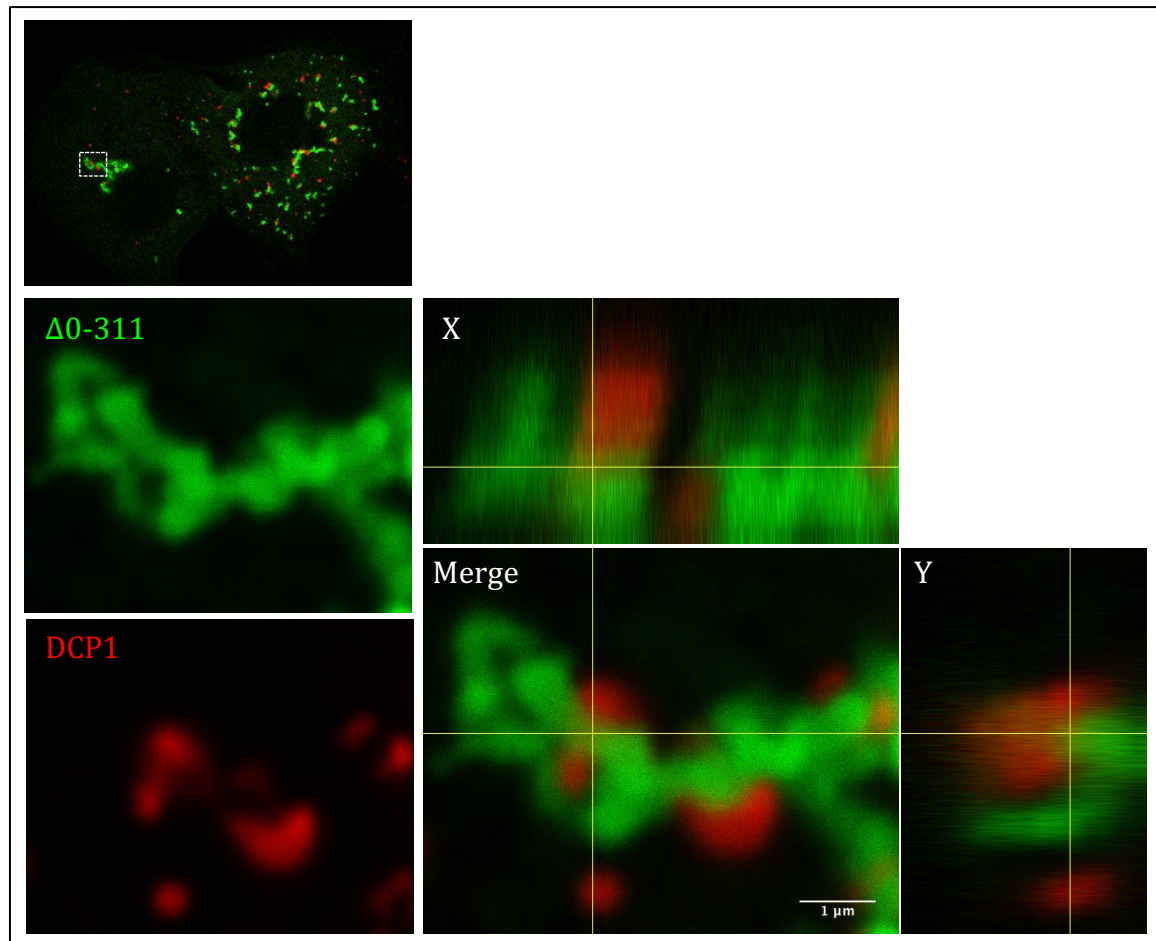


Fig. 8.5.1 Coiled coil-mediated aggregates ($\Delta 0-311$) of DEF6 form large structure that 'trap' DCP1

Confocal analysis of transfected COS7 cells as described before. GFP-tagged $\Delta 0-311$ aggregates also formed large structures but these did not appear vesicle-like. However, these structures also altered the localisation of DCP1 that was always associated with DEF6 structures (see merged images on the right)

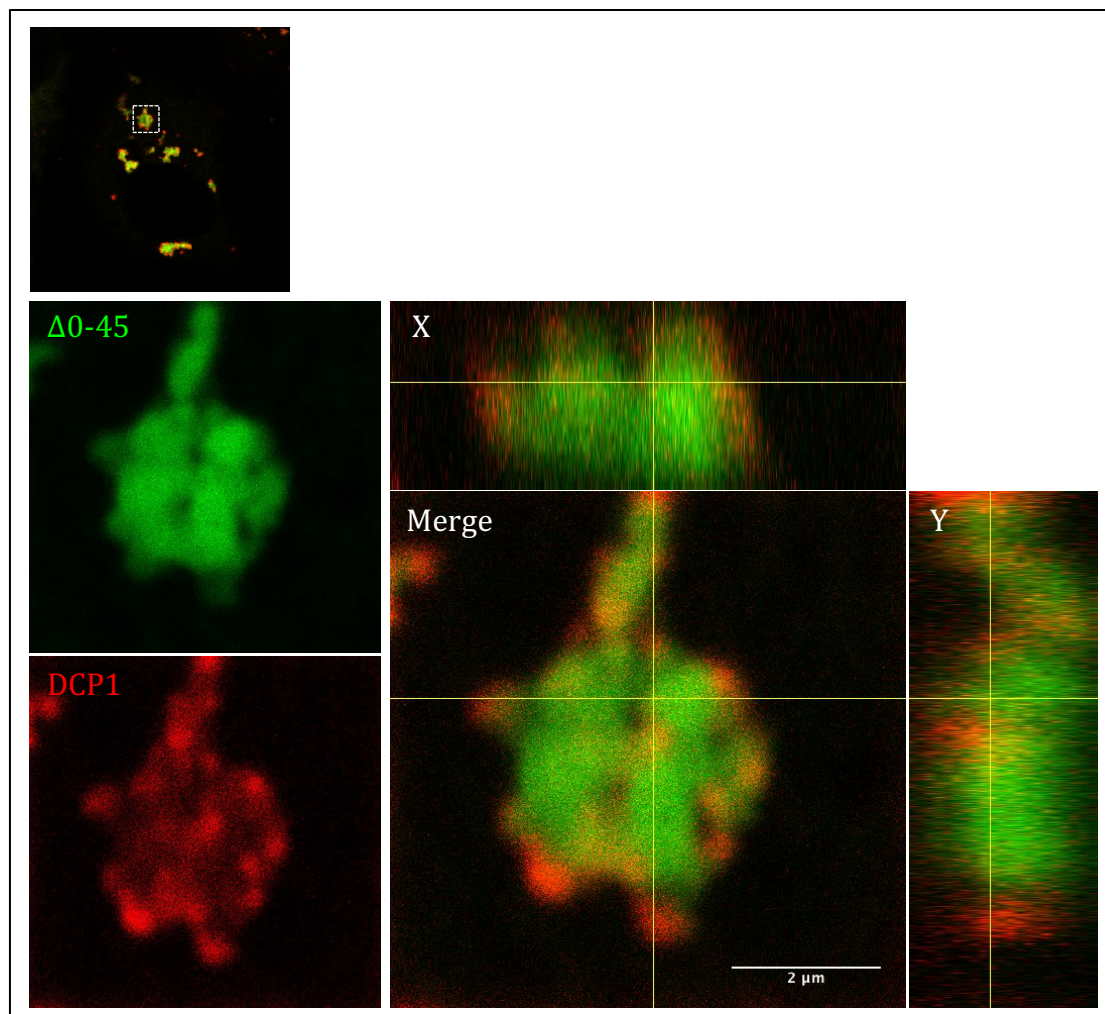


Fig. 8.5.2 Coiled coil-mediated aggregates ($\Delta 0-45$) of DEF6 form large structure that 'trap' DCP1

Confocal analysis of transfected COS7 cells as described before. GFP-tagged $\Delta 0-45$ formed aggregates and larger structures but in this case these structures partially overlapped with DCP1; again altering the normal cellular localisation of DCP1 (see merged images on the right).

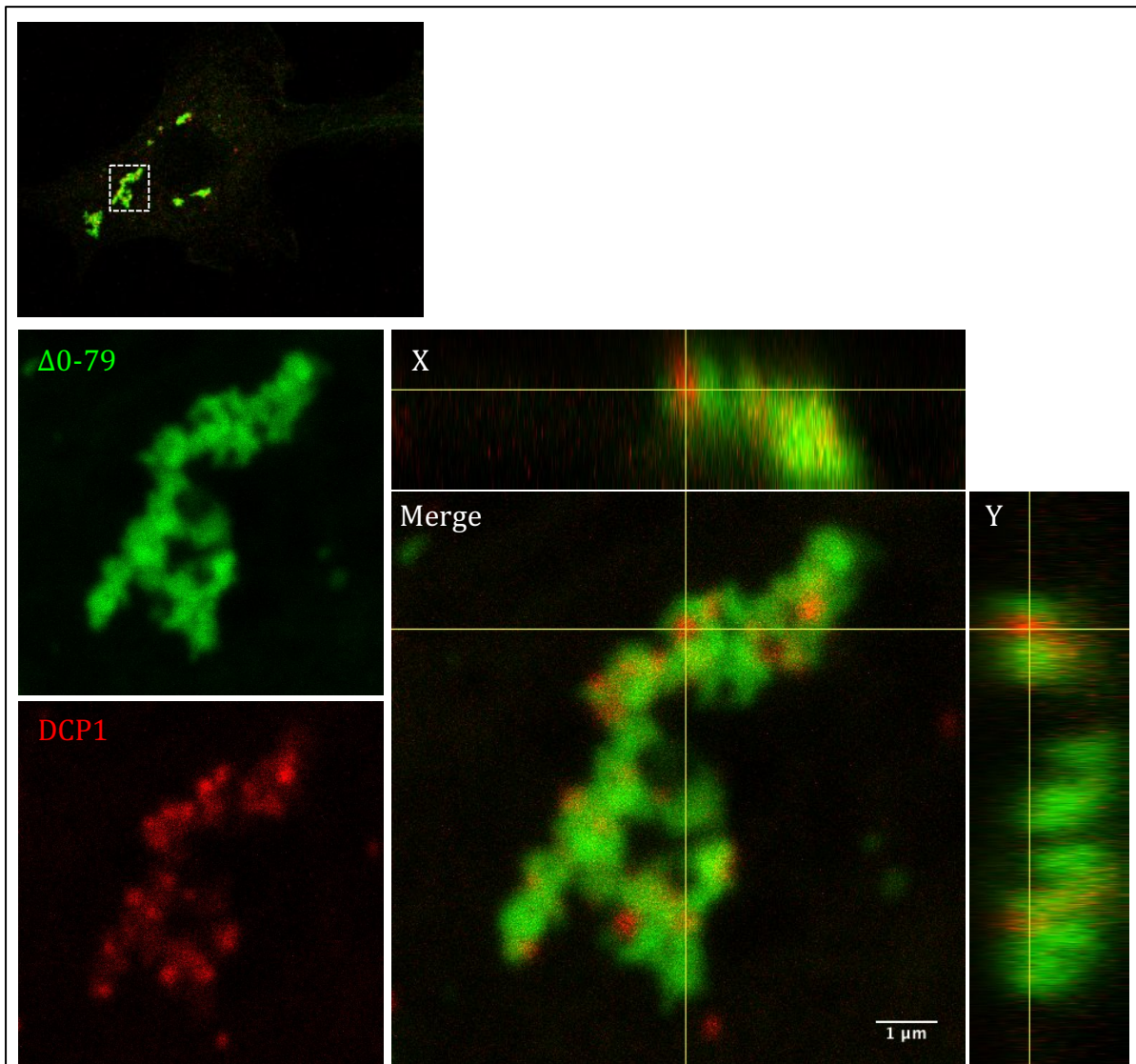


Fig. 8.5.3 Coiled coil-mediated aggregates ($\Delta 0-79$) of DEF6 form large structure that 'trap' DCP1

Confocal analysis of transfected COS7 cells as described before. GFP-tagged $\Delta 0-79$ formed aggregates and larger structures but in this case these structures partially overlapped with DCP1; again altering the normal cellular localisation of DCP1 (see merged images on the right).

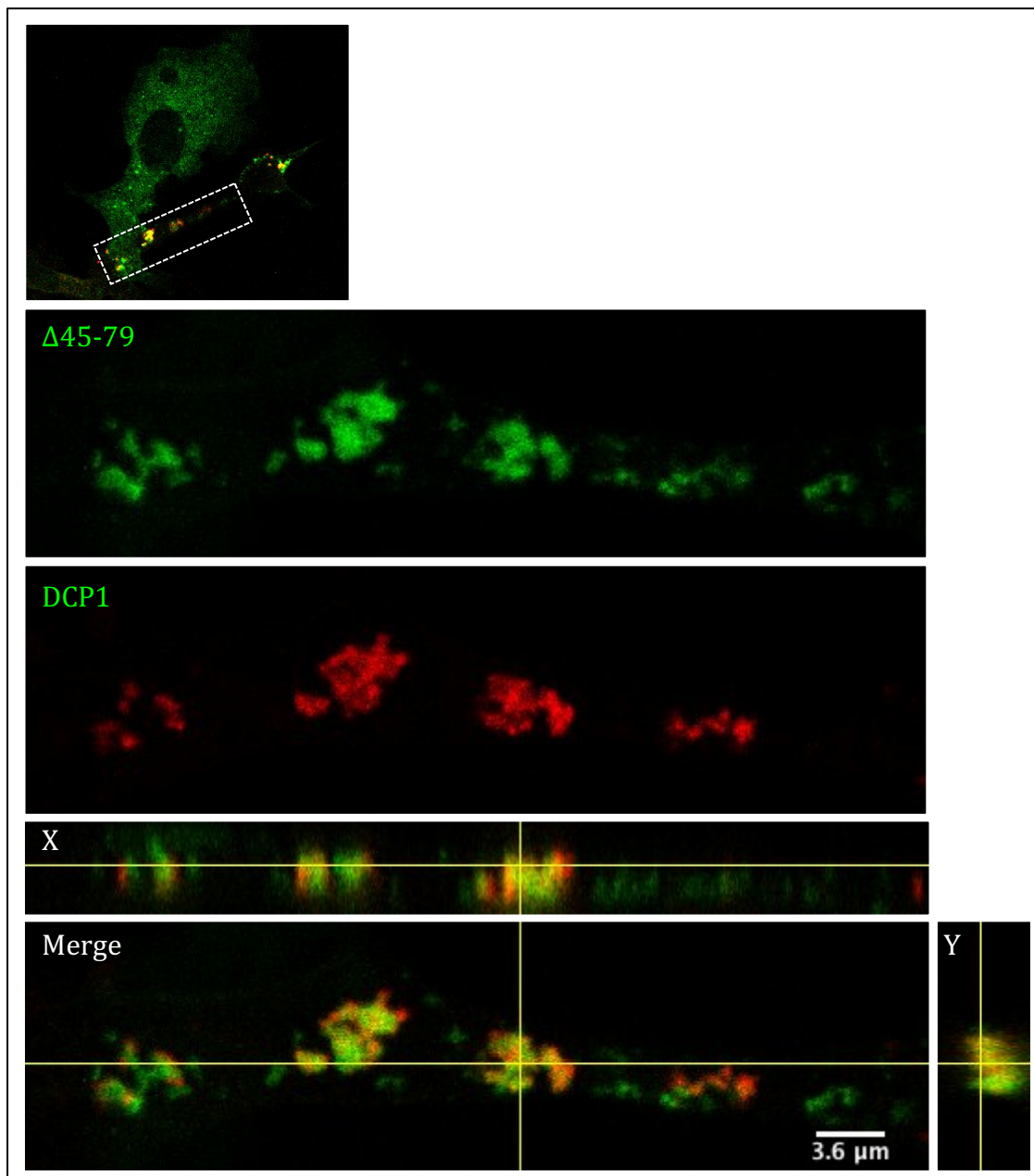


Fig. 8.5.4 Coiled coil-mediated aggregates ($\Delta 45-79$) of DEF6 form large structure that 'trap' DCP1

Confocal analysis of transfected COS7 cells as described before. GFP-tagged $\Delta 45-79$ formed aggregates and larger structures but in this case these structures partially overlapped with DCP1; again altering the normal cellular localisation of DCP1 (see merged images on the right).

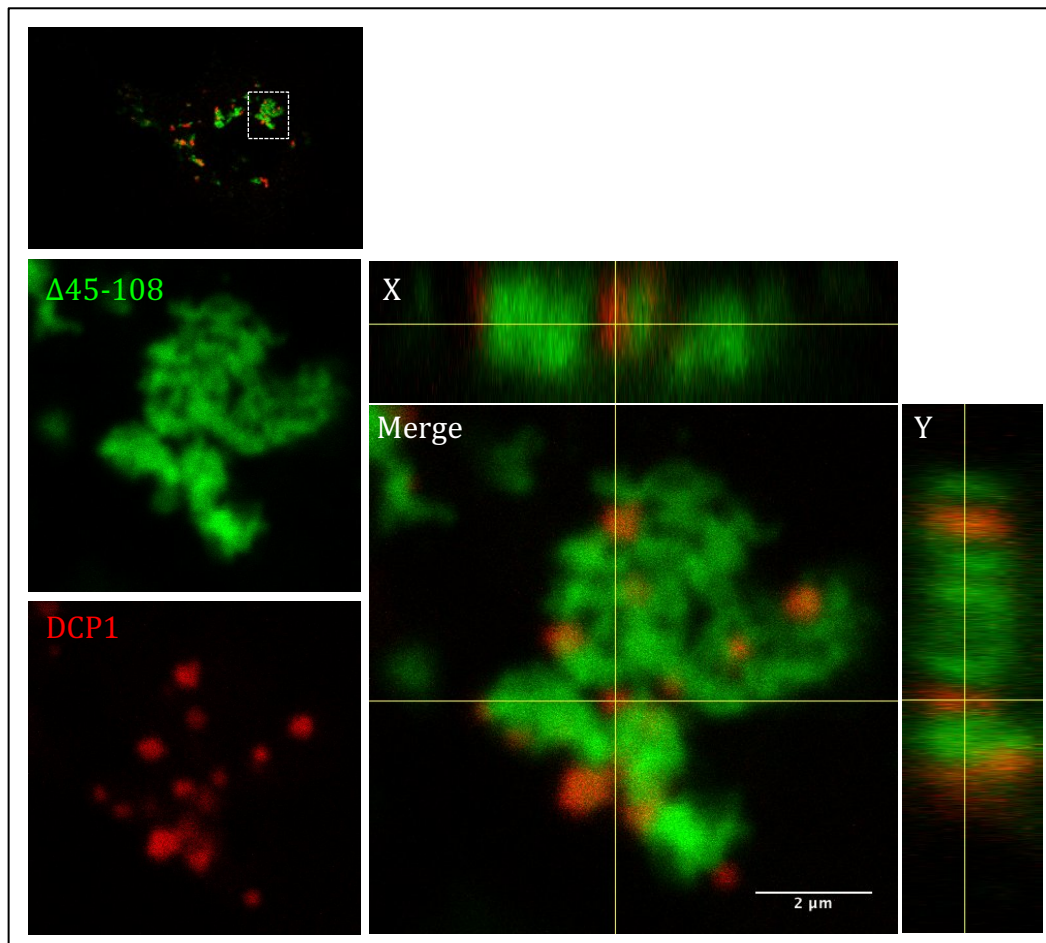


Fig. 8.5.5 Coiled coil-mediated aggregates ($\Delta 45-108$) of DEF6 form large structure that 'trap' DCP1

Confocal analysis of transfected COS7 cells as described before. GFP-tagged $\Delta 45-108$ formed aggregates and larger structures but in this case these structures partially overlapped with DCP1; again altering the normal cellular localisation of DCP1 (see merged images on the right).

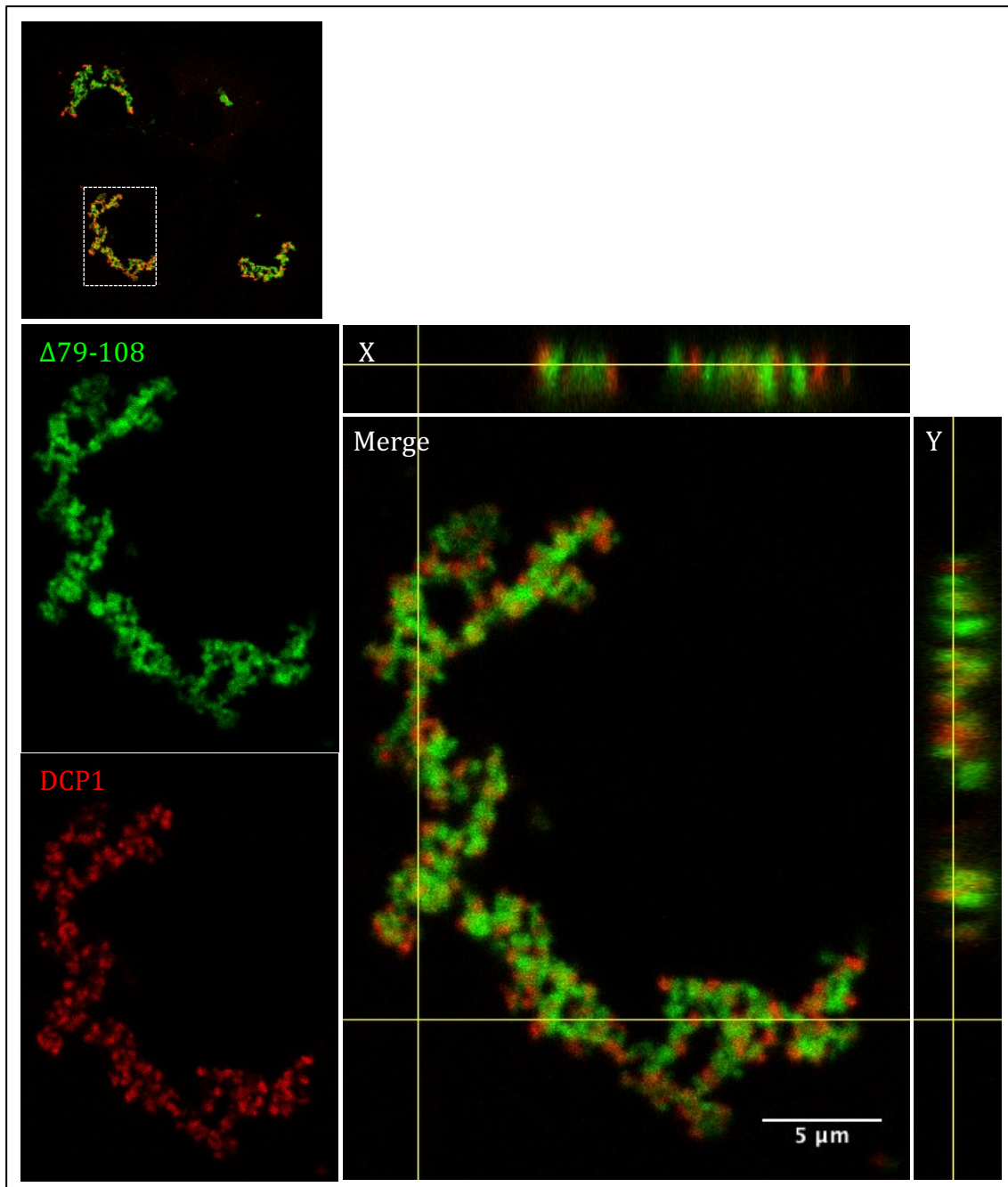


Fig. 8.5.6 Coiled coil-mediated aggregates ($\Delta 79-108$) of DEF6 form large structure that 'trap' DCP1

Confocal analysis of transfected COS7 cells as described before. GFP-tagged $\Delta 79-108$ formed aggregates and larger structures but in this case these structures partially overlapped with DCP1; again altering the normal cellular localisation of DCP1 (see merged images on the right).

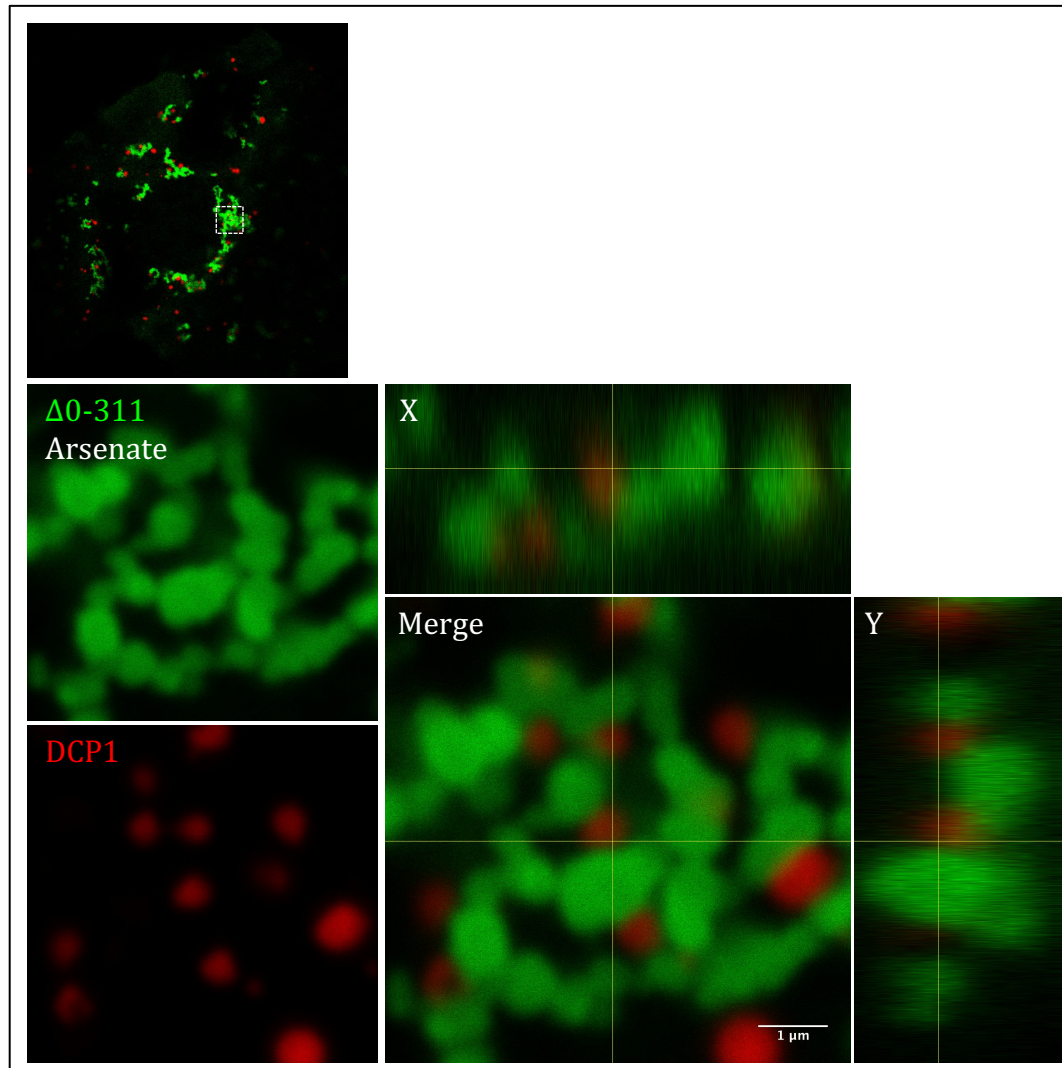


Fig. 8.6.1 Cellular stress (Arsenate) had no effect on formation of large structures of $\Delta 0-311$ and their ability to 'trap' DCP1 

Confocal analysis of COS7 cells expressing GFP-tagged $\Delta 0-311$ and mCherry- tagged DCP1 after arsenate treatment as described before. Merged images including vertical and side views (X and Y coordinates) shown on the right indicated large structures of $\Delta 0-311$ adjacent to DCP1

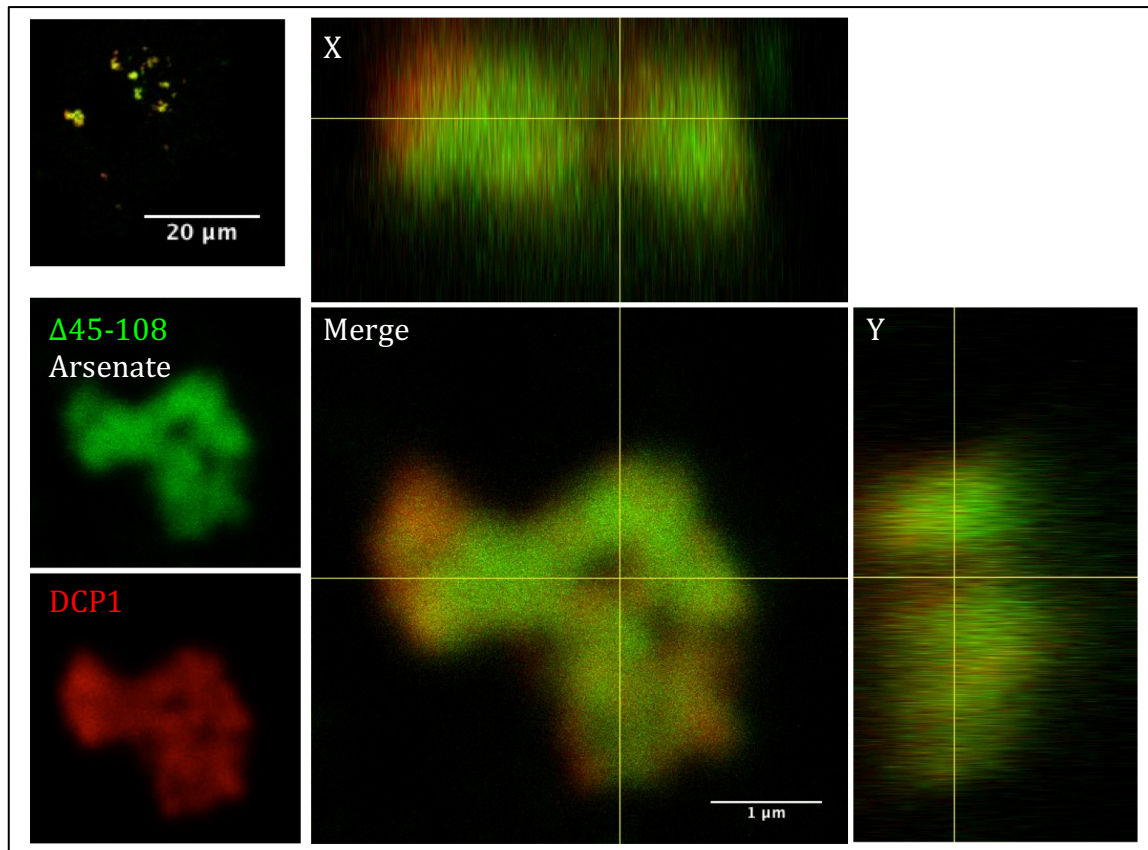


Fig. 8.6.2 Cellular stress (Arsenate) results in complete colocalisation of $\Delta 45-108$ structures with DCP1

Confocal analysis of COS7 cells expressing GFP-tagged $\Delta 45-108$ (representing group 3 mutants) and mCherry-tagged DCP1 after arsenate treatment as described before.

Merged images including vertical and side views (X and Y coordinates) shown on the right indicated that large structures of $\Delta 45-108$ completely overlapped with DCP1.

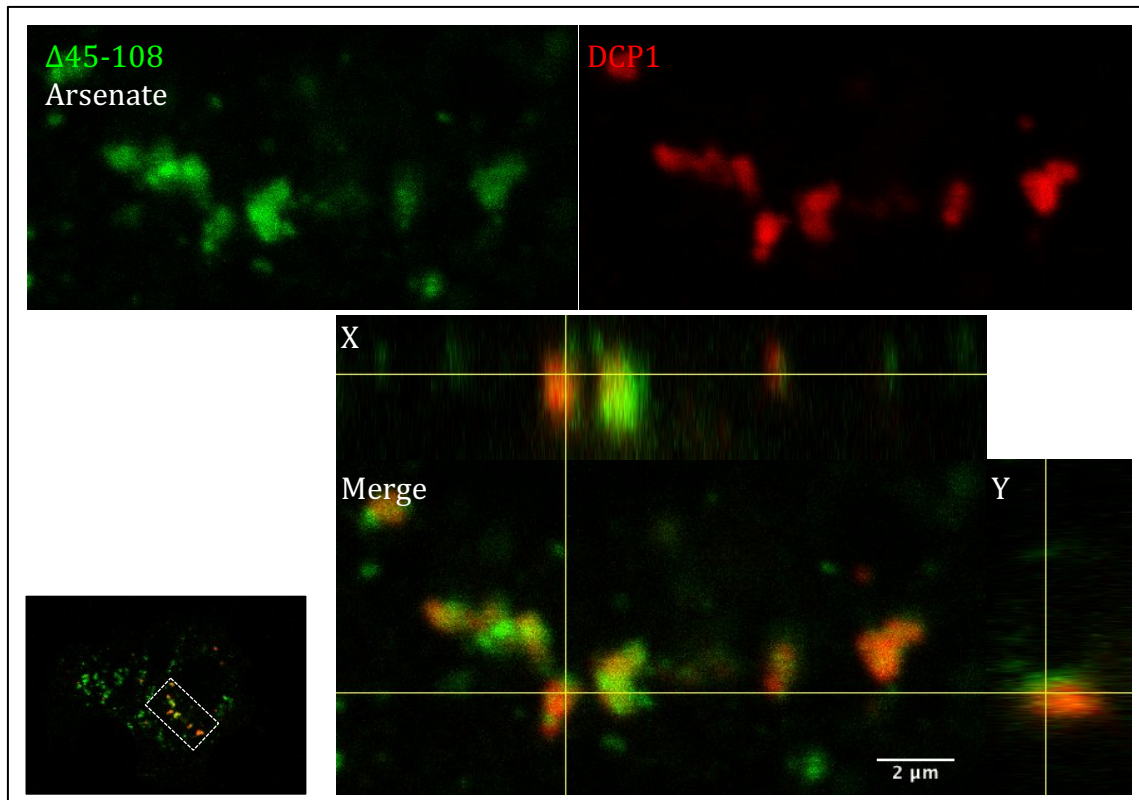


Fig. 8.6.3 After arsenate treatment, few samples of $\Delta 45-108$ remained in partially overlapping with DCP1 [?]

Confocal analysis of COS7 cells expressing GFP-tagged $\Delta 45-108$ (representing group 3 mutants) and mCherry-tagged DCP1 after arsenate treatment as described before.

Merged images including vertical and side views (X and Y coordinates) shown on the right indicated that few large structures of $\Delta 45-108$ remained in partially overlapped with DCP1.

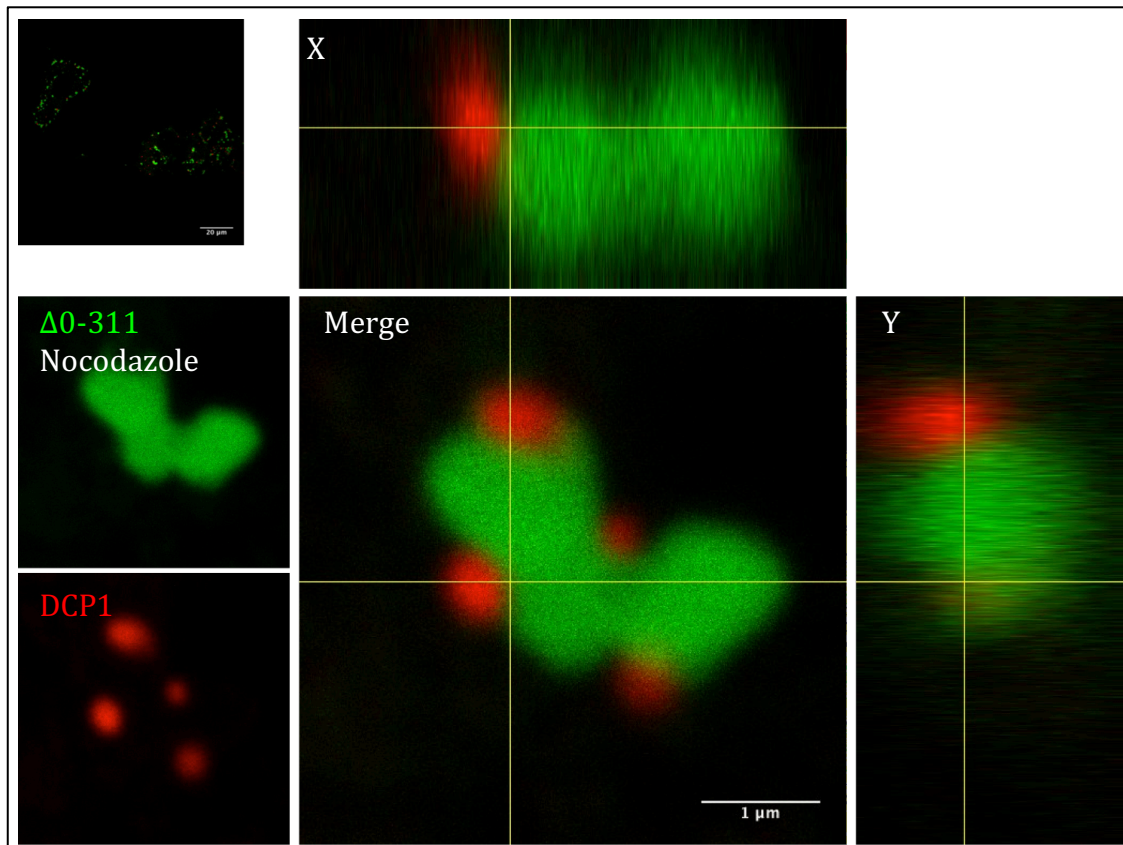


Fig. 8.7.1 Cellular stress (Nocodazole) had no effect on formation of large structures of $\Delta 0-311$ and their ability to 'trap' DCP1

Confocal analysis of COS7 cells expressing GFP-tagged $\Delta 0-311$ and mCherry-tagged DCP1 after arsenate treatment as described before. Merged images including vertical and side views (X and Y coordinates) shown on the right indicated large structures of $\Delta 0-311$ adjacent to DCP1

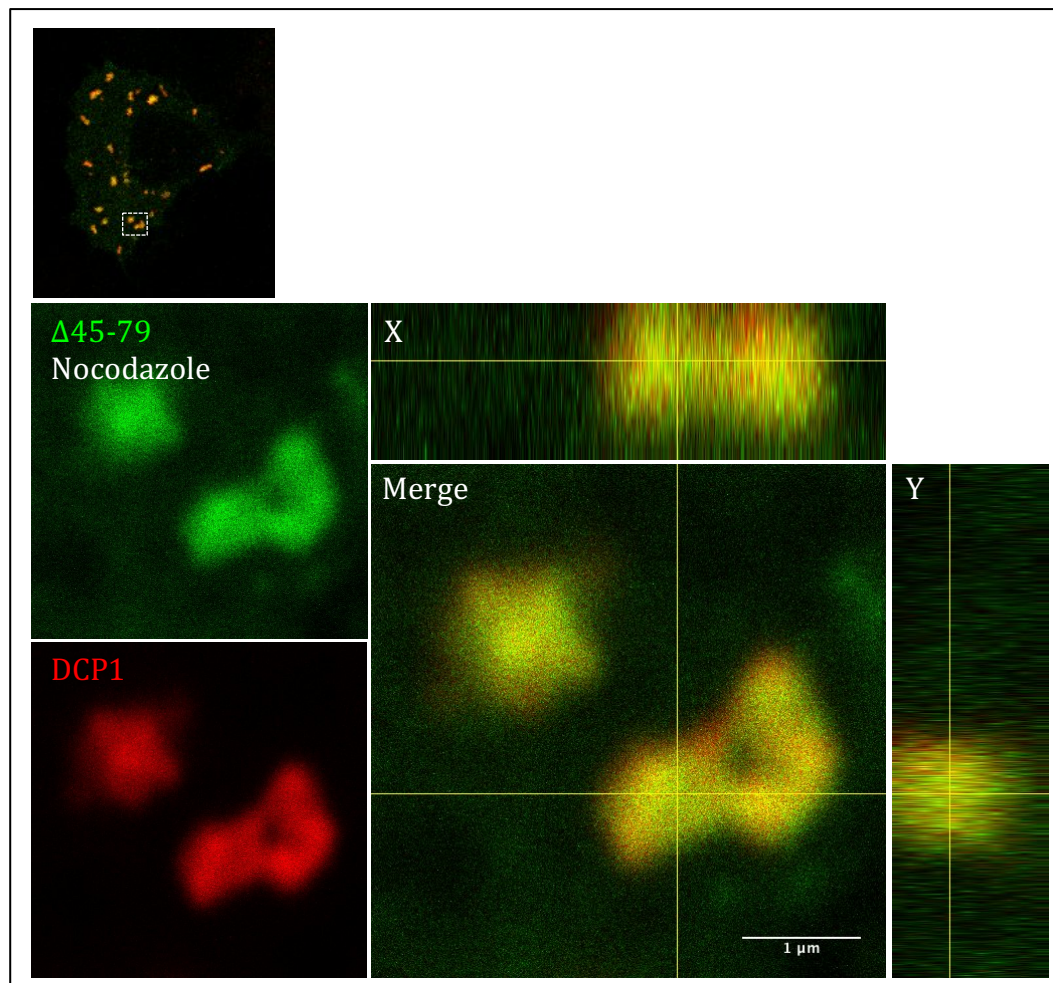


Fig. 8.7.2 Cellular stress (Nocodazole) results in complete colocalisation of $\Delta 45-79$ structures with DCP1

Confocal analysis of COS7 cells expressing GFP-tagged $\Delta 45-79$ (representing group 3 mutants) and mCherry-tagged DCP1 after arsenate treatment as described before.

Merged images including vertical and side views (X and Y coordinates) shown on the right indicated that large structures of $\Delta 45-79$ completely overlapped with DCP1.

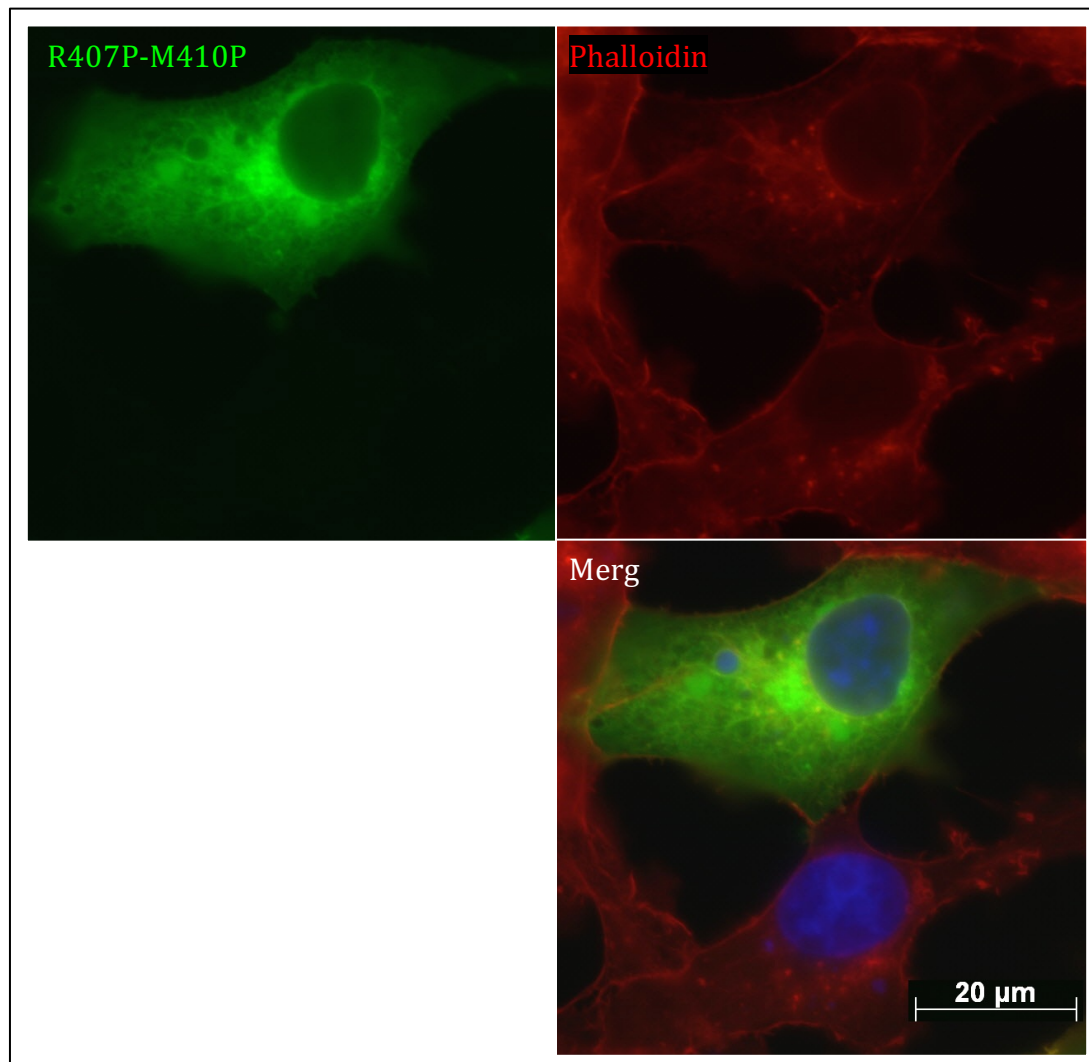


Fig. 8.8.1 Disruption of the coiled coil domain of R407P-M410P did not results in colocalisation with F-actin

GFP tagged R407P-M410P (green) represents the proline mutants that were diffused in cytoplasm and did not colocalise with F-actin stained with phalloidin (red).

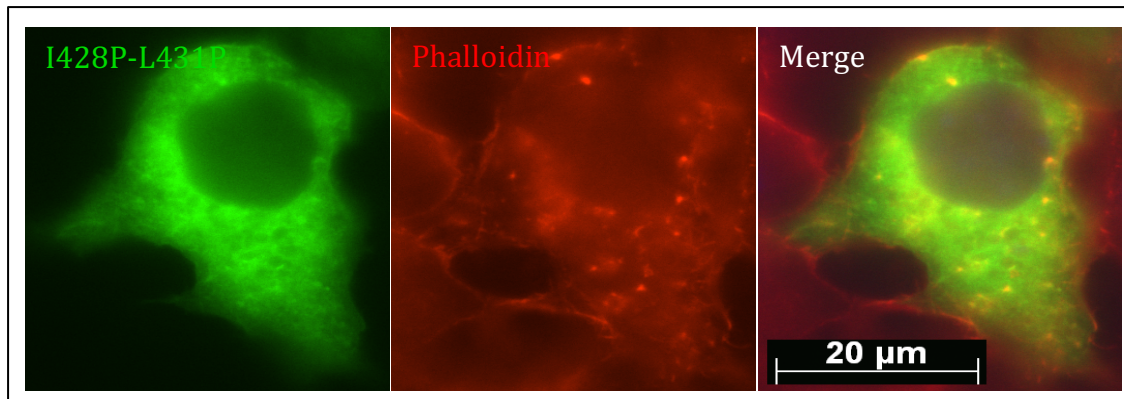


Fig. 8.8.2 Disruption of the coiled coil domain of I428P-L431P did not results in colocalisation with F-actin

GFP tagged I428P-L431P (green) represents the proline mutants that were diffused in cytoplasm and did not colocalise with F-actin stained with phalloidin (red).

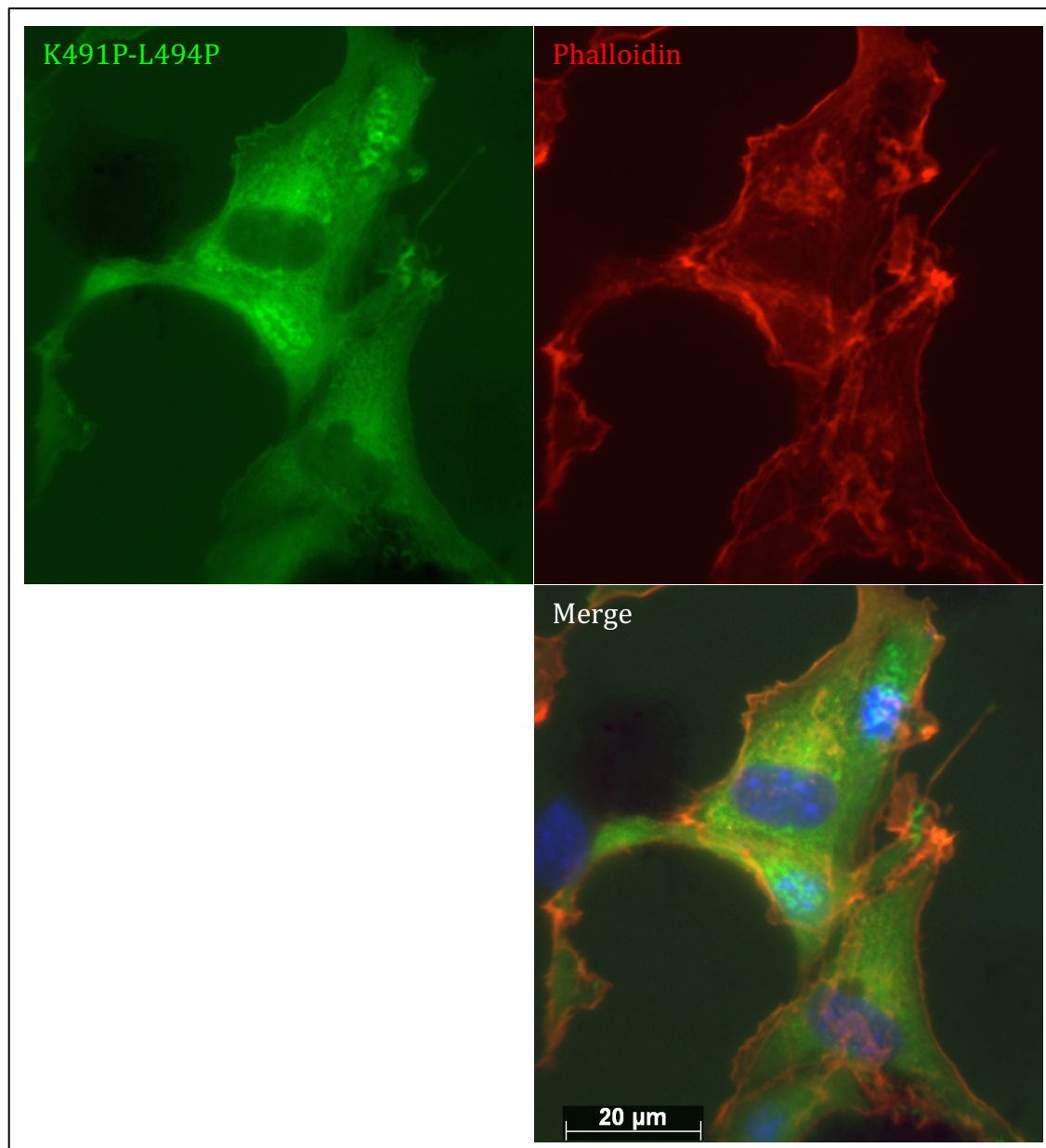


Fig. 8.8.3 Disruption of the coiled coil domain of K491P-L494P did not results in colocalisation with F-actin

GFP tagged K491P-L494P (green) represents the proline mutants that were diffused in cytoplasm and did not colocalise with F-actin stained with phalloidin (red).

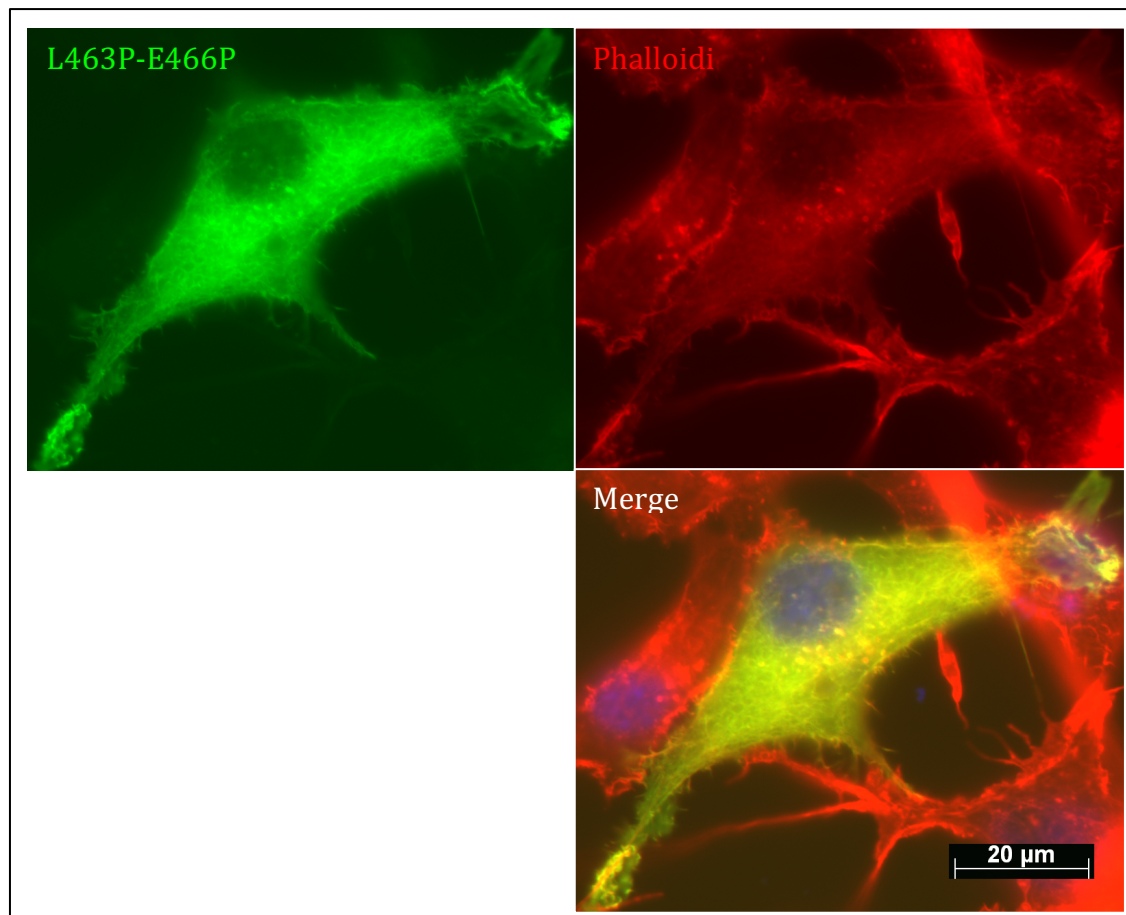


Fig. 8.8.4 Disruption of the coiled coil domain of L463P-E466P results in conformational change and colocalisation with F-actin

L463P-E466P colocalise with F-actin labelling lamellipodia, filopodia and invadosome. Merged images on the right show overlapping of green and red (yellow) indicating colocalisation. Images of COS7 cells were taken 24 hrs after transfection. Scale bar 20 μm as indicated.

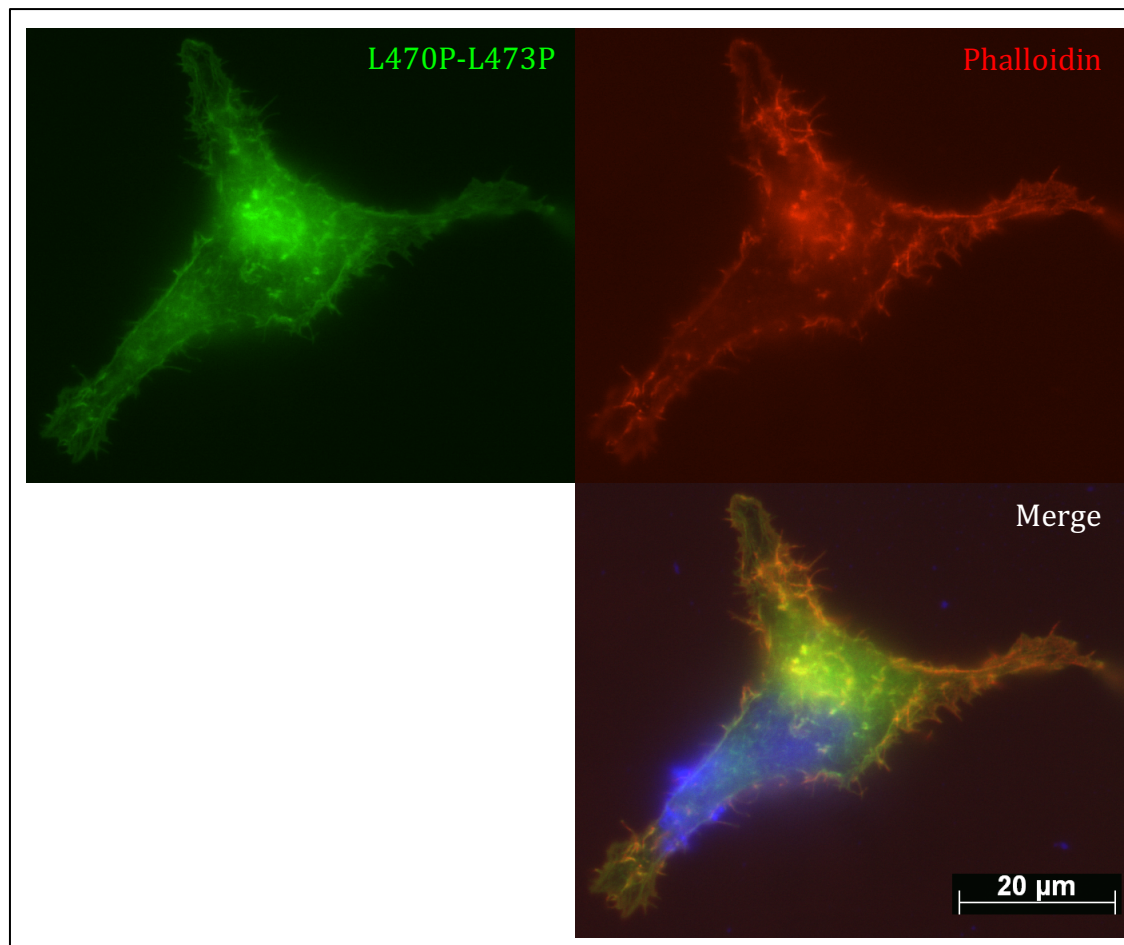


Fig. 8.8.5 Disruption of the coiled coil domain of L470P-E473P results in conformational change and colocalisation with F-actin

L470P-E473P colocalise with F-actin labelling lamellipodia, filopodia and invadosome. Merged images on the right show overlapping of green and red (yellow) indicating colocalisation. Images of COS7 cells were taken 24 hrs after transfection. Scale bar 20 μm as indicated.

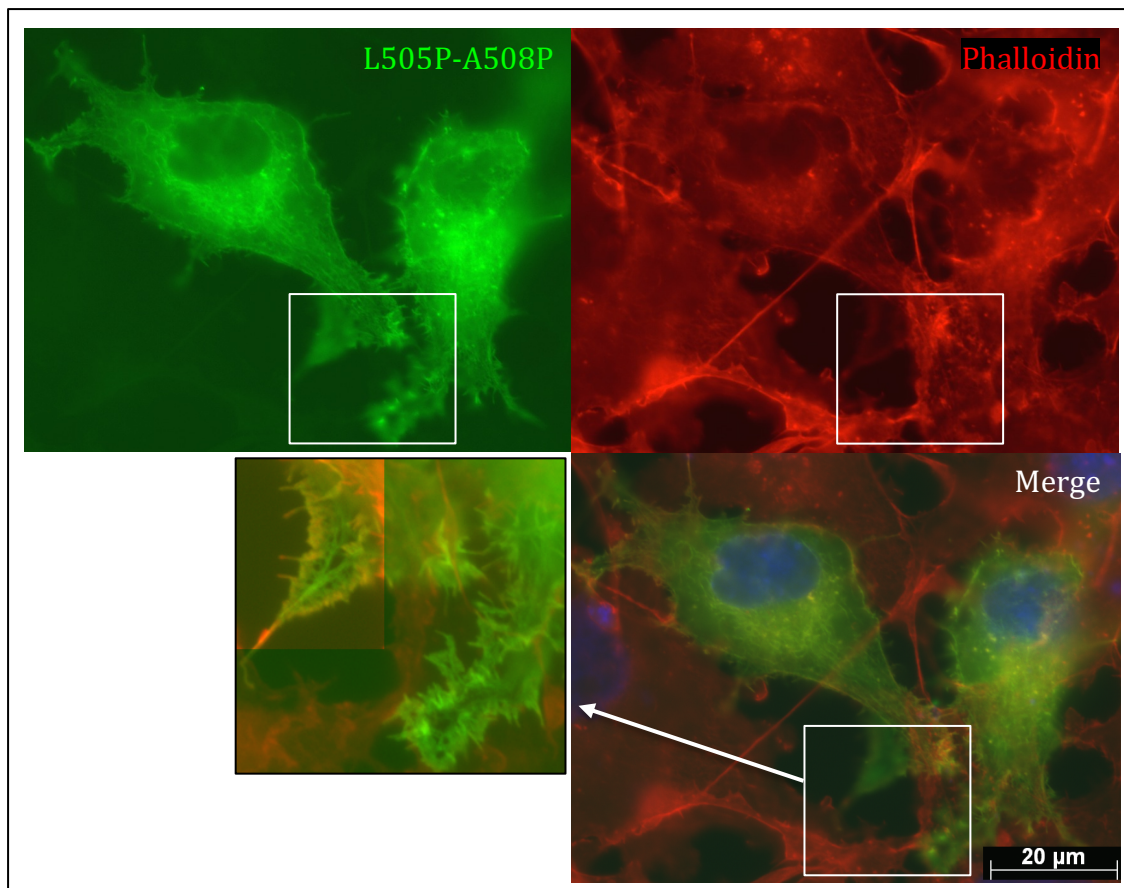


Fig. 8.8.6 Disruption of the coiled coil domain of L505P-A508P results in conformational change and colocalisation with F-actin

L505P-E508P colocalise with F-actin labelling lamellipodia, filopodia and invadosome. Merged images on the right show overlapping of green and red (yellow) indicating colocalisation. Images of COS7 cells were taken 24 hrs after transfection. Scale bar 20 μm as indicated.

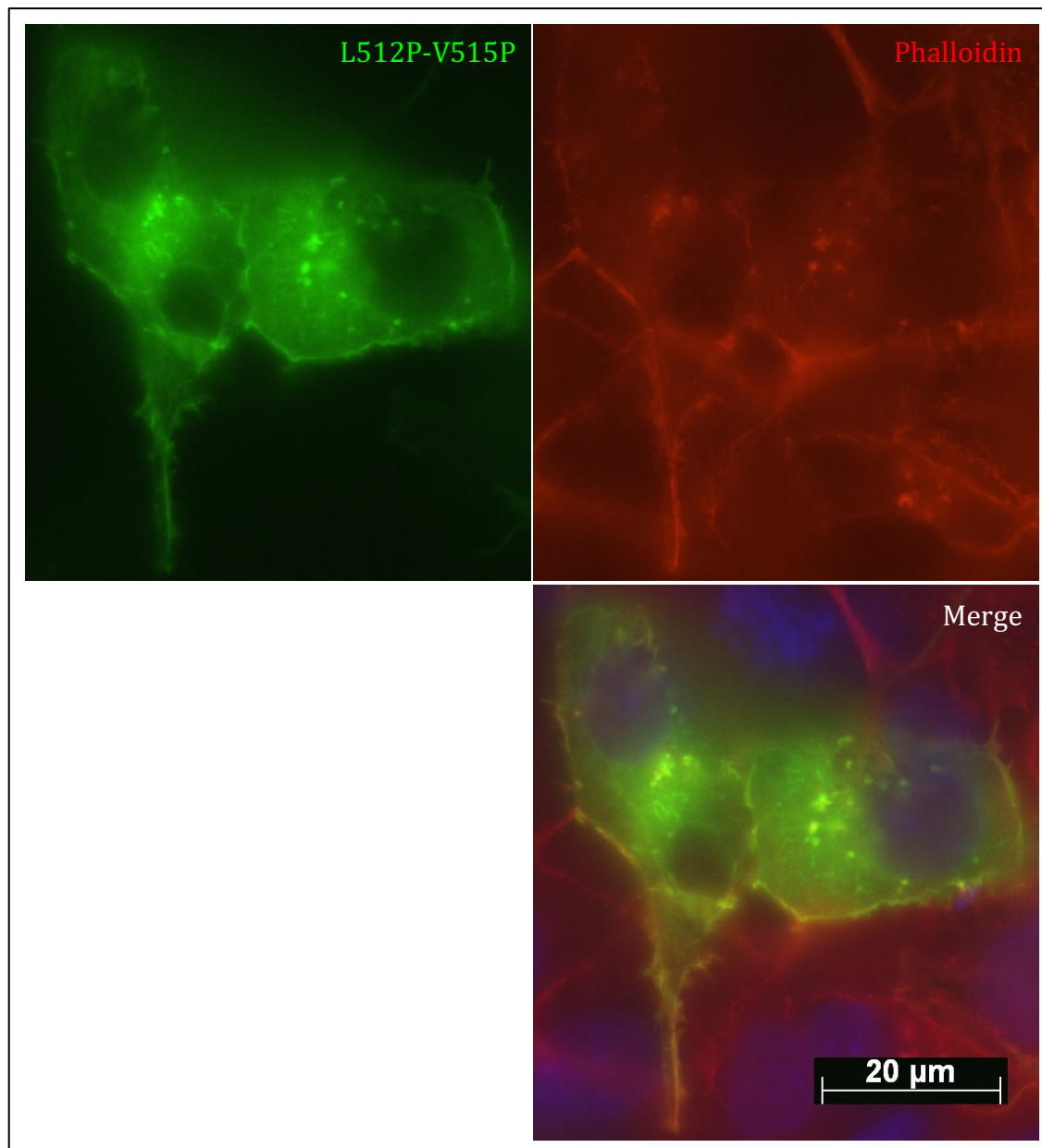


Fig. 8.8.7 Disruption of the coiled coil domain of L512P-V515P results in conformational change and colocalisation with F-actin

L512P-E515P colocalise with F-actin labelling lamellipodia, filopodia and invadosome. Merged images on the right show overlapping of green and red (yellow) indicating colocalisation. Images of COS7 cells were taken 24 hrs after transfection. Scale bar 20 μm as indicated.

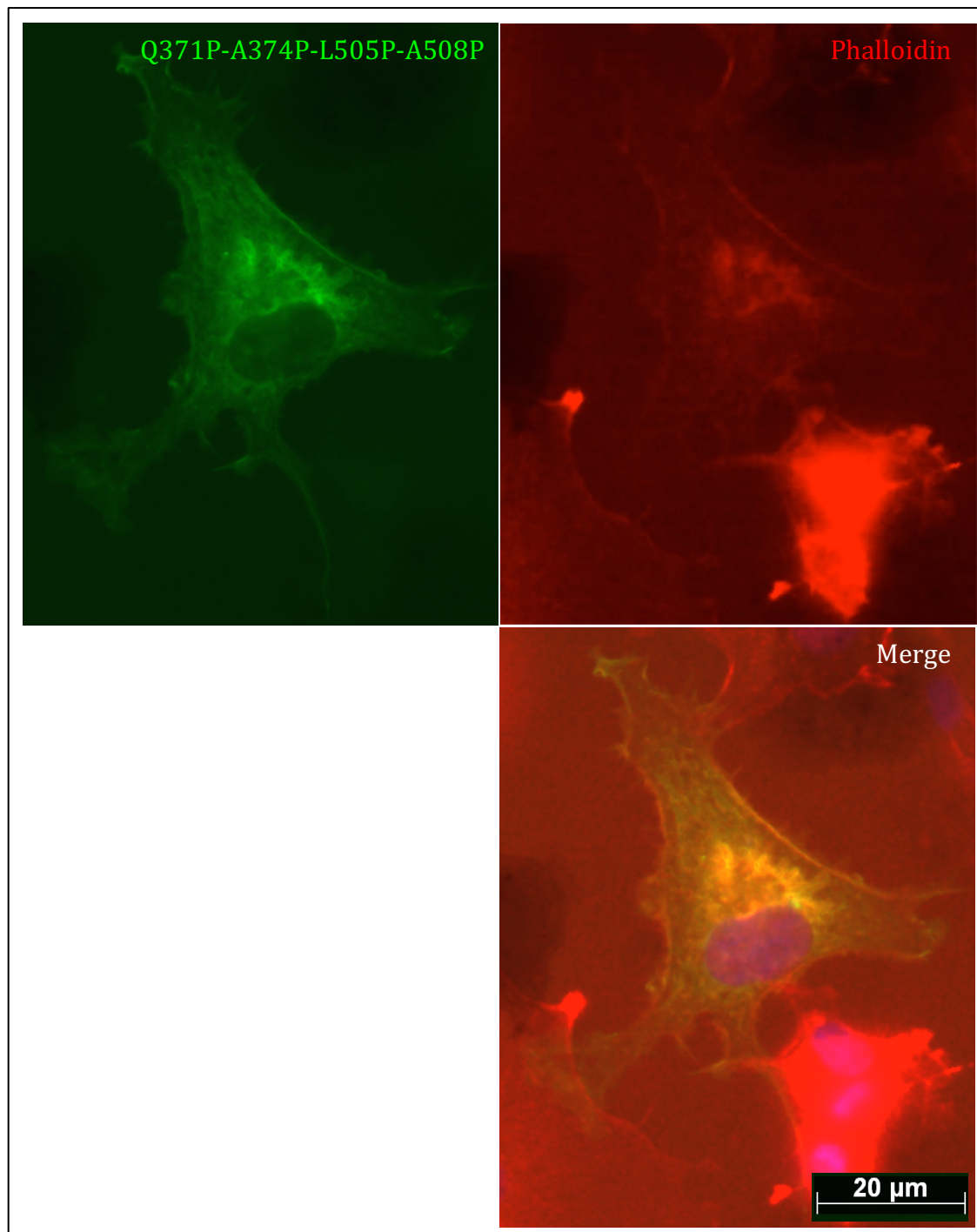


Fig. 8.8.8 Disruption of the coiled coil domain of Q371P-A374P-L505P-A508P results in conformational change and colocalisation with F-actin
Q371P-A374P-L505P-A508P colocalise with F-actin labelling lamellipodia, filopodia and invadosome. Merged images on the right show overlapping of green and red (yellow) indicating colocalisation. Images of COS7 cells were taken 24 hrs after transfection. Scale bar 20 μm as indicated.

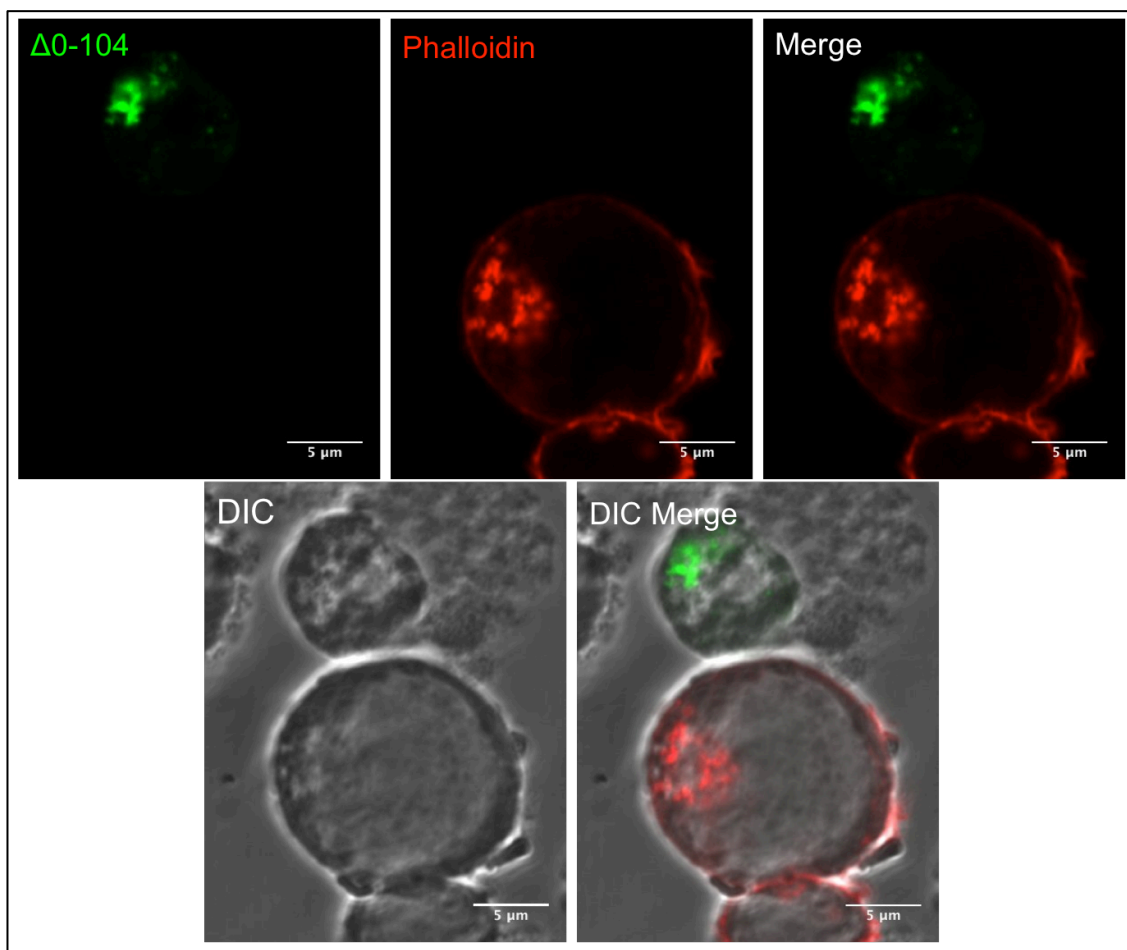
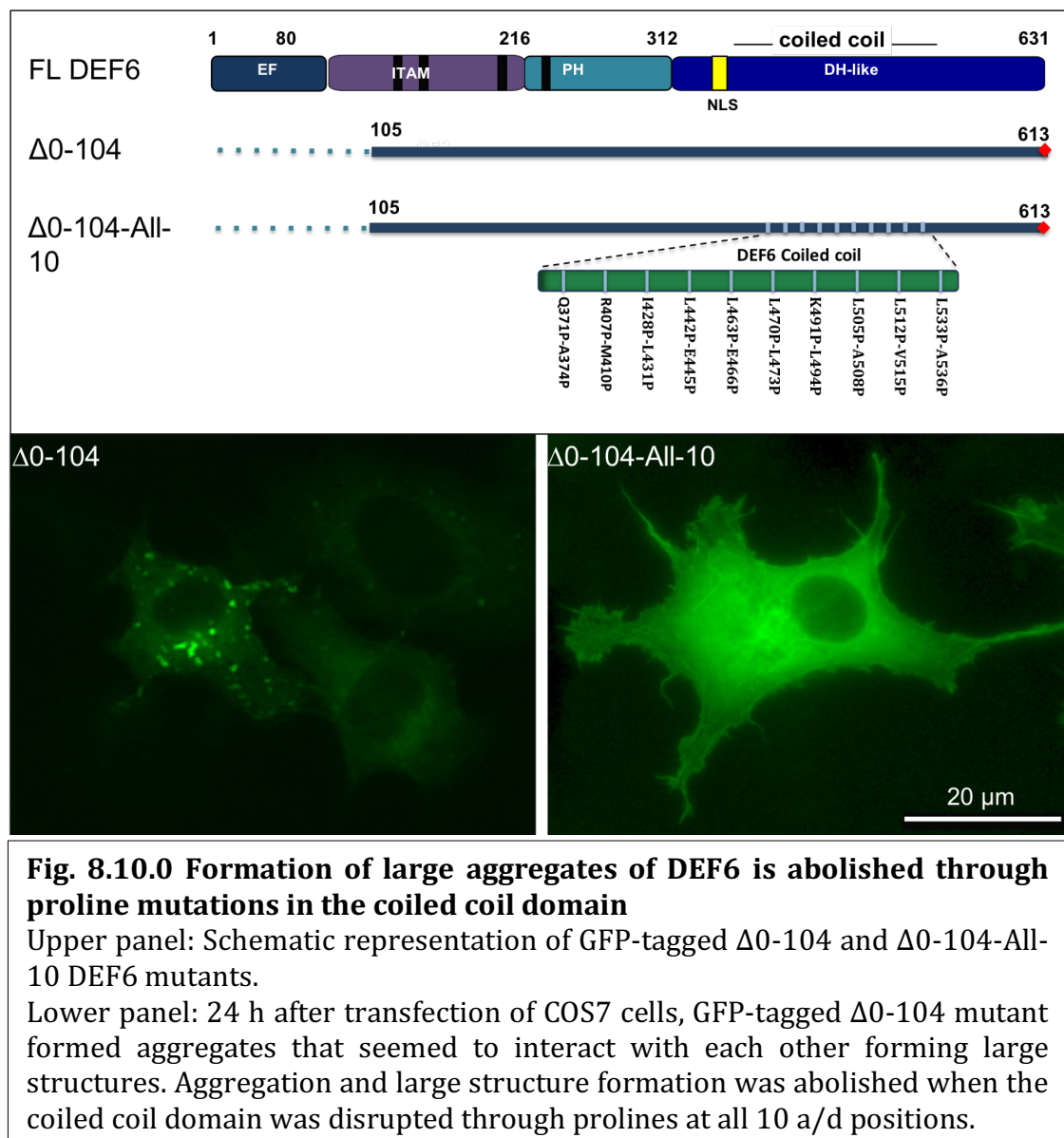


Fig. 8.9.0 Δ0-104 formed aggregations in less than 2% transfected Jurkat T cells



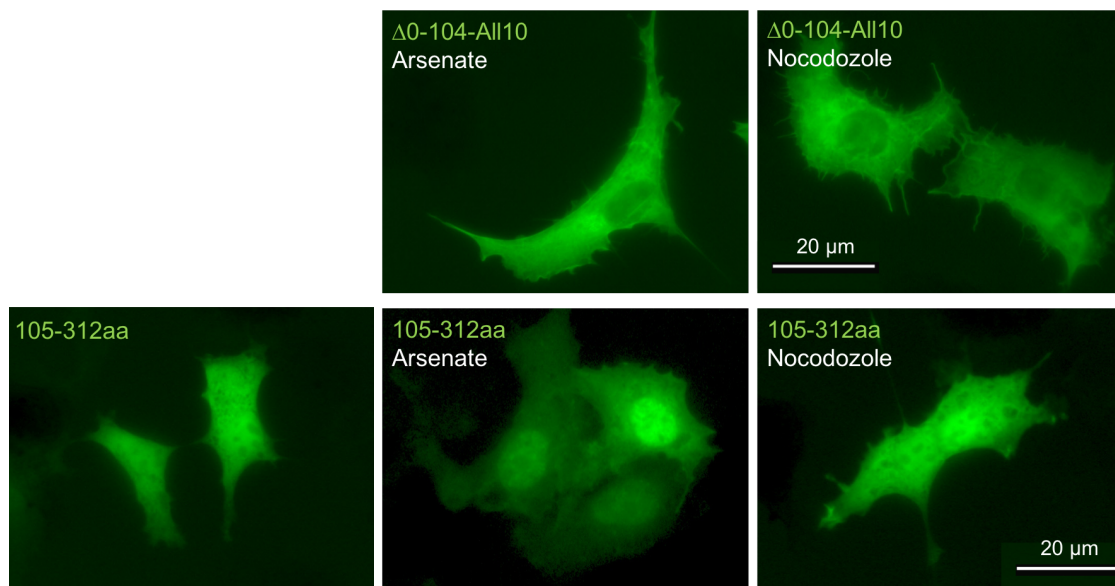


Fig. 8.11.0 Cellular stress did not alter localisation of the 105-312aa or $\Delta 0-104$ -All-10 mutants

GFP-tagged DEF6 mutant 105-312aa that only contains amino acids from 105 to 312 was diffuse in cytoplasm and nucleus (left panel).

Arsenate (middle panel) or nocodazole (right panel) treatment of COS7 cells transfected with GFP-tagged DEF6 105-312aa or $\Delta 0-104$ -All-10 mutants did not result in formation of aggregates.

8.5 Summary of DEF6/Mutants phenotypes

Table 8: DEF6/Mutants in COS7 cells

DEF6/Mutants	Treatments	Phenotypes in COS7 cells					Figure
		Diffused	Aggregates	P-bodies colocalisation	F-actin labelling	In nucleus	
GFP	/	✓	✗	✗	✗	✓	3.3.0
	Arsenate	✓	✗	✗	✗	✓	3.4.0
	H ₂ O ₂	✓	✗	✗	✗	✓	4.8.1
WT DEF6	/	✓	✗	✗	/	✗	3.3.0
	Arsenate	✓	✓	✓	✗	✗	3.4.0
	Nocodazole	✓	✓	✓	✗	✗	3.9.0
	H ₂ O ₂	✗	✓	/	✓	✗	4.8.1
Q371P-A374P	/	✓	✓	✗	✓	✗	3.3.0, 3.3.1
	Arsenate	✗	✗	✗	✗	✗	3.3.0
	H ₂ O ₂	✗	✗	✗	✓	✗	4.8.3
R407P-M410P I428P-L431P L442P-E449P	/	✓	✗	✗	✗	✗	3.3.0
	Arsenate	✓	✗	✗	✗	✗	3.4.0
	H ₂ O ₂	?	✗	✗	?	✗	4.8.3

DEF6/Mutants	Treatments	Phenotypes in COS7 cells					Figure
		Diffused	Aggregates	P-bodies colocalisation	F-actin labelling	In nucleus	
K491P-L494P	/	✓	✗	✗	✗	✗	3.3.0
	Arsenate	✓	✓	/	✗	✗	3.4.0
	H ₂ O ₂	✓	✓	/	?	✗	4.8.3
L463P-E466P	/	✗	✗	✗	✓	✗	3.3.0
L470P-L473P	Arsenate	✗	✗	✗	✓	✗	3.4.0
L505P-A508P							
L512P-V515P							
L533P-A536P							
R407P-M410P-							
L505P-A508P							
I428P-L431P-							
L505P-A508P							
Q371P-A374P-							
L505P-A508P							
All-10							
Δ0-216-All-10							

DEF6/Mutants	Treatments	Phenotypes in COS7 cells					Figure
		Diffused	Aggregates	P-bodies colocalisation	F-actin labelling	In nucleus	
Y210/222E- Q371P-A374P Y210/222E- I428P-L431P Y210/222E- L505P-A508P Y210/222E- Q371P-A374P- L505P-A508P Y210/222E- I428P-L431P- L505P-A508P Y210/222E-All- 10	/	x	✓	✓	/	x	3.5.0 3.5.1
N-30	/	✓	x	x	x	✓	3.6.0

DEF6/Mutants	Treatments	Phenotypes in COS7 cells					Figure
		Diffused	Aggregates	P-bodies colocalisation	F-actin labelling	In nucleus	
N-45 N-79	/	✗	✓	✓	✓	?	3.6.0 3.6.1
DH2	/	✓	✓ (Vesicle-like)	✗ (Adjacent)	✗	✗	3.7.1, 3.8.0
	Arsenate	✓	✓ (Vesicle-like)	✗ (Adjacent)	✗	✗	3.10.1
	Nocodazole	✓	✓ (Vesicle-like)	✗ (Adjacent)	✗	✗	3.10.1
	H ₂ O ₂	✓	✓ (Vesicle-like)	✗ (Adjacent)	✗	✗	4.8.1
Δ0-311 Δ0-216	/	✓	✓	✗ (Adjacent)	✗	✗	3.7.1, 3.8.0
	Arsenate	✓	✓	✗ (Adjacent)	✗	✗	3.10.2
	Nocodazole	✓	✓	✗ (Adjacent)	✗	✗	3.10.2
	H ₂ O ₂	✓	✓	✗ (Adjacent)	✗	✗	4.8.1
Δ0-104 Δ0-79 Δ0-45 Δ45-79 Δ79-108 Δ45-108	/	✓	✓	✗ (Partially overlap)	✗	✗	3.7.1, 3.8.0
	Arsenate	✓	✓	✓	✗	✗	3.10.2
	Nocodazole	✓	✓	✓	✗	✗	3.10.2
	H ₂ O ₂	✓	✓	/	✓	✗	4.8.1

DEF6/Mutants	Treatments	Phenotypes in COS7 cells					Figure
		Diffused	Aggregates	P-bodies colocalisation	F-actin labelling	In nucleus	
DHL-N	/	✓	✓	✗	✗	✗	3.7.2b
DH1	/	✗	✗	✗	✓	✗	3.7.2b
DHL-C	/	✗	✗	✗	✓	✓	3.7.2b
ITAM PH1	/	✓	✗	✗	✗	✓	3.7.2b
ITAM	Nocodazole	✓	✗	✗	✗	✓	3.10.4
PH2	/	✗	✗	✗	✗	✓	3.7.2b
Δ0-216-All-10	/	✗	✗	✗	✓	✗	3.7.3
All-10	Nocodazole	✗	✗	✗	✓	✗	3.10.4
Δ0-104-Y210/222E	/	✓	✓	✗ (Partially overlap)	✗	✗	3.11.1, 3.11.2
	Nocodazole	✓	✓	✗ (Partially overlap)	✗	✗	3.11.1, 3.11.2
Δ0-104-Y210/222F	/	✓	✓	✗ (Partially overlap)	✗	✗	3.11.1, 3.11.2
	Nocodazole	✓	✓	✗ (Partially overlap)	✗	✗	3.11.1, 3.11.2
Y133/144F	H ₂ O ₂	/	✓	/	?	✗	4.8.2
Y210/222F	H ₂ O ₂	/	✓	/	?	✗	4.8.2

DEF6/Mutants	Treatments	Phenotypes in COS7 cells					Figure
		Diffused	Aggregates	P-bodies colocalisation	F-actin labelling	In nucleus	
Y133/144D	/	✓	✓	X (Partially overlap)	X	X	3.14.0
	Nocodazole	✓	✓	X (Partially overlap)	X	X	3.14.0
	H ₂ O ₂	✓	✓	X (Partially overlap)	X	X	4.8.2
537-590aa	/	X	X	X	✓	✓	4.5.0
537-550aa	/	✓	X	X	?	✓	4.5.0
551-590aa	/	✓	X	X	?	✓	4.5.0

Table 9: Cellular localisation of wild type and mutant DEF6 proteins coexpressed with mCherry-NLS-DEF6

DEF6/Mutants	Phenotypes		Molecule Features		Figure
	Colocalised in nucleus	Colocalised in granules			
WT DEF6	✓	/	Contain N-terminal domain	Contain N-terminal and full or part of coiled coil domain	3.12.0
DH1	✓	/			3.12.0
DH2	✓	✓			3.12.0
N-590	✓	✓			3.12.0
Y210/222E	✗	✓			3.12.0, 3.12.1
N-108	✗	✓			3.12.1
DHL-N	✗	/	No full coiled coil domain or coiled coil structure is disrupted	3.13.0	
Q371P-A374P L442P-E445P All-10	✗	/		3.13.0	

Table 10: mCherry-Y133/144D coexpression with DEF6 mutants

Mutants	Colocalised in granules	Figure
DH2	✓	3.15.0
$\Delta 0-216$	✓	3.15.0
$\Delta 0-104$	✓	3.15.0
537-590aa	✓	4.6.0
537-550aa	✓	4.6.0
551-590aa	✗	4.6.0

Table 11: DEF6/Mutants in resting Jurkat T cells

DEF6/Mutants	Phenotypes in resting Jurkat T cells				Figure
	Diffused	Aggregates	P-bodies colocalisation	F-actin labelling	
GFP	✓	✗	✗	✗	5.2.1
WT DEF6	✗	✗	✗	✓	5.2.1
L533P-A536P	✗	✗	✗	✓	5.2.2
All-10	✗	✗	✗	✓	5.2.2
Δ0-216-All-10	✗	✗	✗	✓	5.2.2
Δ0-104	✗	✗	✗	✓	5.2.3
Δ0-216	✓	✗	✗	✓	5.2.3
DH2	✓	✓	✓	✓	5.2.3
Y133/144D	?	✓	?	?	5.2.4
Y210/222E	✗	✓	✓	✓	5.2.5

Table 12: DEF6/Mutants in conjugated Jurkat T cells

DEF6/Mutants	Phenotypes in conjugated Jurkat T cells				Figure
	Diffused	Aggregates	F-actin labelling	IS (cSMAC or pSMAC)	
GFP	✓	✗	✗	✗	5.3.1
WT DEF6	✗	✗	✓	✓cSMAC	5.3.1
All-10	✗	✗	✓	✓pSMAC	5.3.2
Δ0-216-All-10	✗	✗	✓	✓pSMAC	5.3.2
L533P-A536P	✗	✗	✓	✓ cSMAC and pSMAC	5.3.2
DH2	✓	✓	✓	✓ pSMAC	5.3.3
Δ0-216	/	✗	✓	✓ pSMAC	5.3.3